Towards a gene regulatory network for the regeneration of the adult skeleton in the brittle star *Amphiura filiformis*

Anna Czarkwiani

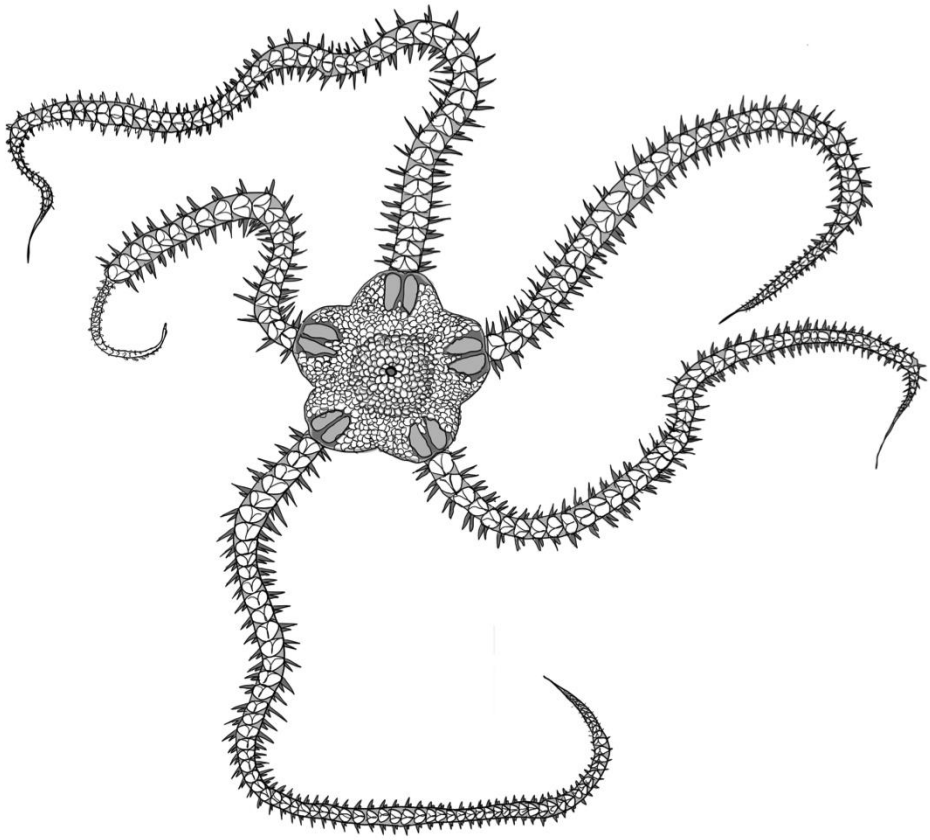

Research Department of Genetics, Evolution and Environment
University College London

Submitted for the Degree of Doctor of Philosophy

February 2017

Declaration of ownership

I, Anna Czarkwiani, confirm that the work presented in this thesis is my own. Where information has been derived from other sources, I confirm that this has been indicated in the thesis.

Abstract

The recent emergence of transcriptomic data available for echinoderms opened up the possibility of using this group of animals to study the molecular aspects underlying their extreme regenerative abilities. I use the brittle star *Amphiura filiformis* as a model to understand the cellular and molecular aspects of skeletogenesis during adult arm regeneration. This allowed me to begin compiling essential preparatory work for studying the gene regulatory network (GRN) underlying adult regeneration of the skeleton, which can be compared with the embryonic developmental program. I first studied the anatomy and morphogenesis of the skeleton during arm regeneration in *A. filiformis*, and defined a staging system relevant for the early developmental events occurring in the first 8 days post-amputation. I then established methods for spatio-temporal expression analysis and pharmacological treatments to characterise genes involved in adult arm regeneration in this brittle star. 18 genes expressed in embryonic skeletogenic cells (transcription factors, signalling receptors and downstream differentiation genes) were found to be expressed in the dermal layer of early stage regenerates, where skeletal spicules first form. This showed a very similar molecular signature of larval and regenerating arm skeletogenic cells. FGF signalling perturbation using the SU5402 inhibitor interfered with skeleton formation both in embryonic development and adult regeneration of the brittle star. A large-scale comparison revealed a conservation of a cohort of genes affected by SU5402 downstream of FGF signalling between those two developmental stages. In conclusion we found morphological and

molecular similarities underlying skeletogenesis during regeneration and embryonic development suggesting that the gene regulatory network driving skeletogenic cell specification and differentiation could be re-activated in adult arm regeneration.

Statement of impact

“The nature of discovery is that it is impossible to anticipate what you will find. That is discovery. Discovery-based research is most fruitful when new knowledge is sought for its own sake.”

- *Professor Sheila N. Patek*

The brittle star *Amphiura filiformis* possesses the spectacular ability to completely regenerate lost arms, which are composed of complex tissue structures such as muscles, nervous system and skeleton. Studying how this animal achieves this spectacular feat, and whether there are any similarities between skeleton regeneration and skeleton development during embryogenesis, has vast implications for our core understanding of this developmental process, the underlying molecular mechanisms at play and will contribute to our knowledge when considering the evolutionary pathways that lead to some animals being capable of regeneration and others not. This basic research contributes another small piece to our scientific understanding of the nature of our universe, which alone is the most important reason for conducting it.

Acknowledgements

There are many people that I would like to thank for making this work possible and making my time as a PhD student so incredibly enjoyable. First and foremost, I would like to thank my supervisor Paola Oliveri for so many things. I thank her for giving me the chance to work in her lab and for allowing me to come up with my own idea for this project, and developing it with me into something meaningful. For all the support, encouragement and inspiration during my PhD. For teaching me almost everything I know about how to do science and think scientifically, about the beauty of molecular biology and the wonderful diversity of animal life. She has shown me that you can be a fantastic teacher, a brilliant scientist and a mother, all at the same time, which is extraordinary. Working with her and learning from her over the past few years has given me the confidence to call myself a scientist and the drive to continue with this passion.

I thank the Wellcome Trust for funding and Claudio Stern for organizing the wonderful program that allowed me to carry out this project, attend many fascinating courses and conferences and learn incredibly valuable writing skills. I also want to thank my fellow WT companions: Isa Bahm, Ingrid Lekk and Laura Wagstaff for sharing the joys and the challenges of the program.

I would also like to show my deepest gratitude for all the amazing people I have encountered during my time as a PhD student. I would like to thank the past and present members of the Oliveri lab. I especially thank David Dylus, for being a great friend, for our excellent collaboration on the brittle star project, and for all the great times we've spent working like crazy at the

marine station in Sweden. I also thank Libero Petrone, Avi Lerner and Natalie Wood, as well as my collaborators from Italy - Cinzia Ferrario and Laura Pioviani, for making my time in the lab really fun, but also for fruitful scientific discussions and exchange of expertise. I also thank Olga Ortega-Martinez for introducing me to the basics of brittle star regeneration. Finally, I thank the members of Max Telford's lab including Anne Zakrzewski, Steven Müller and Helen Robertson for their company, scientific advice and friendship. Additionally, I would like to thank all of the undergraduate and masters students in our lab for teaching me how to be a teacher. I especially thank Prudence Lui for being the most hard-working, curious and motivated student I will likely ever have.

I am happy to take this opportunity to also thank my wonderful family for making all this possible in the first place. The constant support and encouragement of my parents throughout my life has allowed me to achieve my goals. They are a constant source of inspiration to me. I also thank my sister Olga for her faith in my sometimes-questionable abilities, and for always cheering me on no matter what I did.

Finally, I want to thank my extraordinary partner Johannes Girstmair for making these last, incredibly important, three years the happiest time in my life. Your curiosity and fascination with life, science and people has expanded my horizons and given me a whole new drive to explore the world around me. There are no words to express how grateful I am to have you in my life. Thank you.

Anna Czarkwiani

Dla moich wspaniałych Rodziców

Table of Contents

Declaration of ownership **2**

Abstract **3**

Statement of impact **5**

Acknowledgements **6**

List of figures and tables **13**

List of abbreviations **18**

Glossary **20**

1 Introduction **23**

1.1 Regeneration: definitions and mechanisms 23

1.2 Regeneration in echinoderms 30

1.2.1 Echinoids 34

1.2.2 Holothuroids 34

1.2.3 Asteroids 36

1.2.4 Crinoids 37

1.2.5 Ophiuroids 37

1.3 Skeletogenesis in echinoderms 39

1.4 Evolution of the larval skeleton 45

1.5 Model system: the brittle star *Amphiura filiformis* 48

1.6 Building a gene regulatory network model for regeneration 52

1.7 Aims and hypothesis 55

2 Materials and methods **58**

2.1 Adult animals and embryonic cultures 58

2.2 Calcein staining 59

2.3 Paraffin wax embedding and sectioning 59
2.4 Milligan's trichrome staining 60
2.5 EdU cell proliferation assay 60
2.6 Immunohistochemistry 61
2.7 Identification of candidate skeletogenesis genes 62
2.8 Total RNA extraction and cDNA synthesis 62
2.9 Primer design, PCR and cloning 64
2.10 *In vitro* antisense probe preparation 65
2.11 Whole mount *in situ* hybridization 66
2.12 Nanostring nCounter 67
2.13 Inhibitor treatments 68
2.14 EdU-labelled cell counting using Fiji 69
2.15 Microscopy techniques 70

3 Characterization of the morphological stages, internal anatomy, skeletogenesis and proliferation in the regenerating arm of *Amphiura filiformis* 71

3.1 Staging of early phases of regeneration based on morphological features 71
3.2 Skeletogenesis during early and late regeneration stages 82
3.3 *Afi-c-lectin* expression confirms molecular signature of skeletogenic cells in the dermal layer 86
3.4 Cell proliferation during arm regeneration in *A. filiformis* 89

4 Large-scale analysis of gene expression patterns in the regenerating arm of *A. filiformis* 100

4.1 Spatial expression of skeletogenic differentiation genes in regenerating arms 101

4.2 Expression of transcription factors previously implicated in embryonic skeletogenic gene regulatory networks 106
4.3 Expression of a set of neuronal genes during arm regeneration 114
4.4 Quantitative analysis of expressional profiles during regeneration gives insight into putative gene functions 117

5 Role of FGF and VEGF signalling pathways in skeleton regeneration of *A. filiformis* 124

5.1 Expression of FGF and VEGF signalling genes during arm regeneration 125
5.2 Inhibition of growth factor signalling pathways 129
5.3 Analysis of differentially expressed genes in regenerating arms treated with FGF and VEGF signalling inhibitors 135
5.4 Comparison of genes affected by SU5402 treatment in embryos and regenerating arms of the brittle star 136

6 Discussion 143

6.1 Redefining ophiuroid regeneration 143
6.1.1 Staging 143
6.1.2 Blastema 145
6.1.3 Distalization-intercalation mode of regeneration 148
6.2 Similarities and differences in skeleton regeneration and development 151
6.2.1 Morphological similarities of skeletogenic cells and spicules between the embryo and regenerating arm 151
6.2.2 Late differentiation and patterning of the skeleton 152
6.3 Molecular comparison of skeleton regeneration and development 154
6.3.1 Molecular signature and regulatory state conservation 154
6.3.2 Functionality of skeletogenic GRN downstream of FGF signalling is highly conserved between regeneration and embryonic development 157

6.4 New genes with unknown functions identified in the differential screen. 160

6.4.1 Transcription factors *Afi-egr* and *Afi-rreb1* 161

6.4.2 Potential taxonomically restricted genes *Afi-tr31926, Afi-tr35695, Afi-tr45279, Afi-6202* and *Afi-tr9107* 162

6.5 Evolutionary implications for skeletogenesis in deuterostomes 163

6.5.1 Implications for evolution of larval skeleton in echinoderms 164

6.5.2 Evolutionary similarities and differences in skeletogenesis among deuterostomes 167

6.6 Conclusive remarks 169

References 173

Appendix 207

List of figures and tables

Figure 1.1: Generalized process of regeneration.. 24

Figure 1.2: Recruitment of cells is essential for regeneration.. 26

Table 1.1: Summary of main functional assays performed in different echinoderm classes to date. 32

Figure 1.3: Images of representatives of five echinoderm classes and their phylogenetic position.. 33

Figure 1.4: Larval skeleton development in ophiuroids and echinoids.. 41

Figure 1.5: Comparison of sea urchin and brittle star skeletogenic gene regulatory networks.. 48

Figure 1.6: The brittle star *Amphiura filiformis*.. 51

Figure 1.7: Strategy for building a GRN. 55

Figure 2.1: Schematics showing method of regenerating arm sampling for RNA extraction at different time points.. 64

Figure 3.1: Staging of *A. filiformis* early arm regeneration based on morphological landmarks. 72

Figure 3.2: Early stages of arm regeneration in the brittle star *Amphiura filiformis*.. 74

Figure 3.3: Schematic representation of early arm regeneration stages showing two segments of the non-regenerating stump and the regenerating bud at its distal end as observed in sagittal sections. 75

Figure 3.4: Histological sections of the earliest stages of arm regeneration in the brittle star *Amphiura filiformis*.. 76

Figure 3.5: Histological sections of regenerating arms at stages 3, 4 and 5.. 78
Figure 3.6: Late stages of arm regeneration in *A. filiformis*. 81
Figure 3.7: Skeletogenesis during early regeneration stages.. 83
Figure 3.8: Skeletogenesis during late regeneration stages.. 85
Figure 3.9: *Afi-c-lectin* expression during early and late arm regeneration stages. 88
Figure 3.10: EdU labelling in non-regenerating arms.. 90
Figure 3.11: EdU labelling showing proliferation in non-regenerating arms and at stage 1 of regeneration at different time points post amputation. 91
Table 3.1: Manual scoring of confocal images of EdU and *Afi-c-lectin* double-labelled arms. 92
Figure 3.12: Confocal images showing EdU labelling of early stage regenerating arms counterstained with nuclear stain DAPI. 94
Figure 3.13: *Afi-c-lectin* expression combined with EdU labelling and counterstained with nuclear stain DAPI showing that skeletogenic cells do not proliferate.. 95
Figure 3.14: Cell proliferation-associated gene expression during arm regeneration in *A. filiformis*.. 98
Figure 3.15: Pulse and chase EdU experiments showing the contribution of proliferating cells in the adult to the regenerating arm. 99
Figure 4.1: Schematics of regenerating arms as orientated in WMISH experiments showing the main cellular territories.. 101

Figure 4.2: WMISH of differentiation genes in the early stages of arm regeneration. 103
Figure 4.3: WMISH showing expression of differentiation genes in the late stages of arm regeneration 105
Figure 4.4: WMISH showing expression of mesodermal transcription factors in the early stages of arm regeneration. 107
Figure 4.5: WMISH showing expression of transcription factors present in sea urchin skeletogenic GRN, which are not expressed in the mesodermal territory in the regenerating arm.. 110
Figure 4.6: WMISH showing expression of transcription factors in late stages of arm regeneration.. 111
Figure 4.7: Summary of expression patterns of skeletogenic genes in differentiating skeletal elements of late stage regenerating arms. 113
Figure 4.8: WMISH showing expression of neuronal genes in early and late stages of regeneration. 116
Figure 4.9: Genes expressed at low or undetectable levels in the adult brittle star arm..... 119
Figure 4.10: Comparison of potential stem cell related and final differentiation temporal gene expression patterns. 120
Figure 4.11: Dynamics of temporal gene expression patterns of differentiation genes and transcription factors detected using the Nanostring nCounter.. 123
Figure 5.1: WMISH of FGF and VEGF signalling components during early stages of regeneration.. 127

Figure 5.2: WMISH showing expression of FGF and VEGF signalling components during late stages of regeneration..... 128
Figure 5.3: Strategy for pharmacological treatments in regenerating arm explants of *A. filiformis*..... 130
Figure 5.4: SU5402 treatment in regenerating arm explants inhibits skeletal spicule formation.. 131
Figure 5.5: SU5402 treatment phenotypes after prolonged incubation..... 132
Figure 5.6: Axitinib treatment in regenerating arm explants does not significantly inhibit skeletal spicule formation.. 133
Figure 5.7: Embryo treatments with SU5402 and Axitinib.. 133
Figure 5.8: Comparison of differentially expressed genes in adult regenerating arms and embryos of *A. filiformis* treated with SU5402.. 137
Table 5.1: Five novel genes downregulated by FGF perturbation with unknown function.. 139
Figure 5.9: Spatio-temporal expression of novel FGF target genes during arm regeneration of the brittle star..... 141
Figure 5.10: WMISH showing expression of genes in regenerating arms and embryos treated with SU5402 compared with controls.. 142
Figure 6.1: Comparison of gene expression between early regenerating arm stages and early embryonic stages of the brittle star *A. filiformis*.. 156
Figure 6.2: Provisional gene regulatory network for the specification and differentiation of skeletogenic cells during arm regeneration in the brittle star.. 159
Table A.0.1: List of cloning primers for genes used in the thesis..... 207
Table A.0.2: Nanostring nCounter probe sequences..... 210

Table A.0.3: Adult arm gene expression time-courses heatmap.. 222

Table A.0.4: Embryonic gene expression time-courses heatmap.. 225

Table A.0.5: Summary of Nanostring experiments in embryos and regenerating adult arms of *A. filiformis* treated with SU5402 and Axitinib inhibitors.. 228

Table A.0.6: List of experiments performed in *A. filiformis* but not discussed in the thesis..... 231

Figure A.0.1: Summary of embryonic WMISH experiments in *A. filiformis*. 232

Figure A.0.2: WMISH on additional genes not discussed in thesis – *Afi-piwi, Afi-twist, Afi-otx* and *Afi-vegf2*. 233

Figure A.0.3: Preliminary data showing DiI labelling of cells in the radial water canal observed for eight days.. 234

List of abbreviations

ACC – aboral coelomic cavity

ACE – aboral coelomic epithelium

Afi – *Amphiura filiformis*

AS – aboral shield

ASW – artificial seawater

AV – aboral view

DAPI – 4,6-Diamidino-2-phenylindole

DI – differentiation index

DIC – differential interference contrast

Dist - distal

DMSO – dimethyl sulfoxide

Dpa – days post amputation

EdU – Ethynyl-2’-deoxyuridine

ES – epineural sinus

FSW – filtered seawater

GRN – gene regulatory network

HB – hybridization buffer

Hpa – hours post amputation

Hpf – hours post fertilization

Hpt – hours post treatment

HS – hyponeural sinus

ISH – *in situ* hybridization

LS – lateral shield

LV – lateral view

MABT – maleic acid buffer

NSM – non-skeletogenic cells

OS – oral shield

OV- oral view

PBS – phosphate buffer saline

PCR – polymerase chain reaction

PFA – paraformaldehyde

Prox – proximal

QPCR – quantitative polymerase chain reaction

RNC – radial nerve cord

RWC – radial water canal

S – spine

SM – skeletogenic cells

TF – transcription factor

V – vertebra

WMISH – whole mount *in situ* hybridization

Glossary

Aboral coelomic cavity – a narrow cavity outlined by a thick epithelium in the aboral part of the arms, located between the vertebral ossicles and the aboral and lateral arm shields, that contains the coelom.

Blastema - highly proliferative mass of undifferentiated, pluripotent cells, which forms at the wound site after injury or amputation and gives rise to regenerating structures.

Dermal layer (echinoderm) – layer of cells embedded in extracellular matrix containing skeletal ossicles in echinoderms, located just beneath the epidermis.

Eleutherozoa – Four members of the echinoderms, namely ophiuroids, asteroids, holothuroids and echinoids, excluding crinoids.

Ossicles (echinoderm) – calcareous elements embedded in the dermal layer in echinoderms. They include most of the structural skeletal elements, like shields and vertebrae, but exclude externally protruding skeletal elements like spines.

Podia – also referred to as tube feet, are externally protruding extensions of the radial water canal used for locomotion, feeding and sensing the environment.

Radial water canal – central canal of the water vascular system in ophiuroid arms, used for locomotion, water transport and respiration, also allowing contraction and extension of the connected podia.

Regulatory state – The sum of transcription factors co-expressed in a specific cell at the same time.

Skeleton (echinoderm) – in echinoderms the skeleton is covered by a thin epidermis and is thus an endoskeleton called the dermal skeleton. There are a variety of functionally different skeletal elements including shields, teeth, externally protruding spines. All these elements are composed of a single crystal of calcium carbonate.

Spicule – single unit of the calcitic skeleton of echinoderms, which, after growth, elongation and fusion with other units, will form the stereom structure of the skeleton. Spicules are often tri-radiated or tetra-radiated but can also be simply elongated rods.

Stereom – three-dimensional lattice networks of calcite microcrystals forming the porous echinoderm endoskeletal elements.

Stump – the remaining tissues protruding from the animal after some part of the limb has been amputated or autotomized. The new structure will regenerate from these remaining tissues.

Vertebrae (ophiuroid) – internal-most components of the ophiuroid arm skeleton composed of fused parallel ambulacral plates. There is one vertebra per each segment of the brittle star arm, which connect via ball-in-socket articulations and provide high flexibility of movement.

1 Introduction

1.1 Regeneration: definitions and mechanisms

The extraordinary ability to completely regenerate lost or injured body parts, although found amongst many metazoan phyla, is very limited in humans. Finding what gives other animals such an obvious advantage, on both a cellular and molecular level, has naturally fascinated scientists for centuries. This fascination began with ancient thinkers like Aristotle, who for the first time described lizard tail regeneration, through the naturalists of the eighteenth and nineteenth centuries like Spallanzani and Trembley who studied regeneration in a plethora of different animals, all the way to modern times starting with Morgan's "Regeneration" (Carlson, 2007). Here I provide a detailed background of classical studies summarizing the existing definitions of regeneration, different developmental modes that have been described for various animals and other key concepts of regenerative biology. Regeneration, in essence, is a post-embryonic developmental process occurring in an adult context and involves four major events: 1) wound healing characterized by re-epithelialization of the amputation site; 2) stump tissue remodelling and recruitment of cells, which could include pluripotent stem cells or dedifferentiated cells; 3) cell fate specification and differentiation and 4) re-establishment of the lost structure by growth, patterning and morphogenesis (Figure 1.1) (Sanchez Alvarado and Tsonis, 2006). Even though these steps are in common for most regenerative processes, the details of tissue remodelling and cell fate specification can vary among animals, which lead Morgan to subdivide regeneration into two

main modes – epimorphosis and morphallaxis. But even Morgan, who himself coined these definitions, mentions in his early work that these are not always strictly separated and there is a certain plasticity to regeneration, in that it may take on characteristics of either or both these two types.

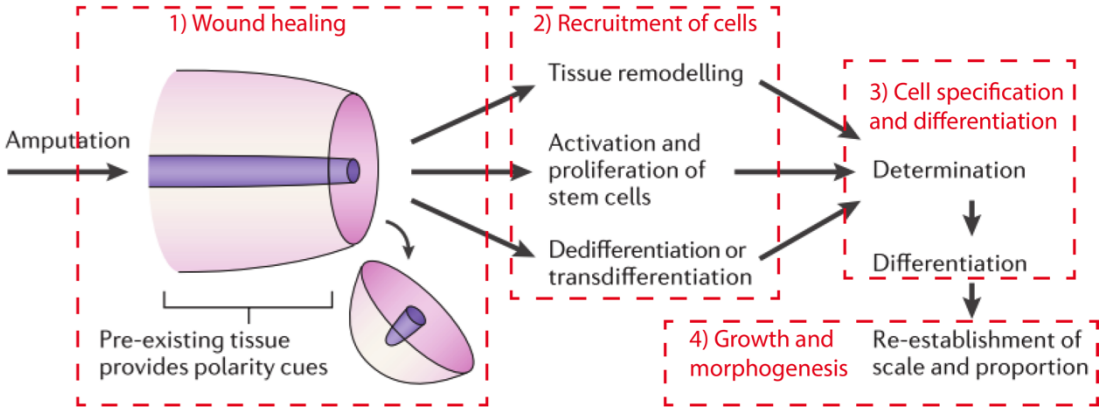

Figure 1.1: Generalized process of regeneration. 1) Wound healing and re-epithelialization. 2) Recruitment of cells and tissue remodelling. 3) Cell specification and dedifferentiation. 4) Growth and morphogenesis for the re-establishment of scale and proportion of lost or damaged tissues (adapted from Sanchez Alvarado and Tsonis, 2006).

Classically, epimorphosis is a mode of regeneration characterized primarily by the appearance (at the site of amputation) of a mass of proliferative, undifferentiated cells covered by an epidermis, which is often referred to as a blastema. Typical examples of regeneration through this mode include salamander limb regeneration (Young et al., 1983), arthropod leg regeneration (Hopkins, 2001; Konstantinides and Averof, 2014) or zebrafish and froglet tail regeneration (Poss et al., 2003; Suzuki et al., 2006). In contrast to epimorphosis, morphallaxis is defined as regeneration via extensive remodelling of stump tissue and a lower degree of proliferation at the site of injury. The most well-known example of morphallaxis-type regeneration is Hydra regeneration, whereby the pre-existing tissue in the

stump is directly rearranged to contribute to the newly forming structures and proliferation is not strictly required (Bosch, 2007; Cummings and Bode, 1984). Interestingly, cell proliferation has been shown to be regulated by apoptosis during Hydra head regeneration where cell proliferation contributes to the formation of new structures (Chera et al., 2009), thus showing that the regenerative process can rely on a combination of different mechanisms. In fact, numerous studies of various animal models prompted Agata and colleagues to propose a new unifying principle for animal regeneration via a combination of epimorphosis and morphallaxis-like processes. This principle, also known as the distalization-intercalation model of regeneration, states that in most non-vertebrate and vertebrate regenerating animals the distalmost part of the body is formed at the site of amputation immediately after wound healing (‘distalization’), and interaction of this distal part with the remaining proximal portion may induce intercalation of newly forming tissues according to positional information cues in-between the two ends of the regenerate (‘intercalation’) (Agata et al., 2003; Agata et al., 2007). A recent study by Roensch and colleagues suggested that limb regeneration in axolotls does not follow this mechanism, but rather that cell identities are progressively specified in a proximal-to-distal order similarly to development. This was revealed by blastemal cell transplantation experiments showing non-commitment to a distal fate (Roensch et al., 2013). In summary, various modes of regeneration are employed by different organisms and it is difficult to find a consensus mechanism.

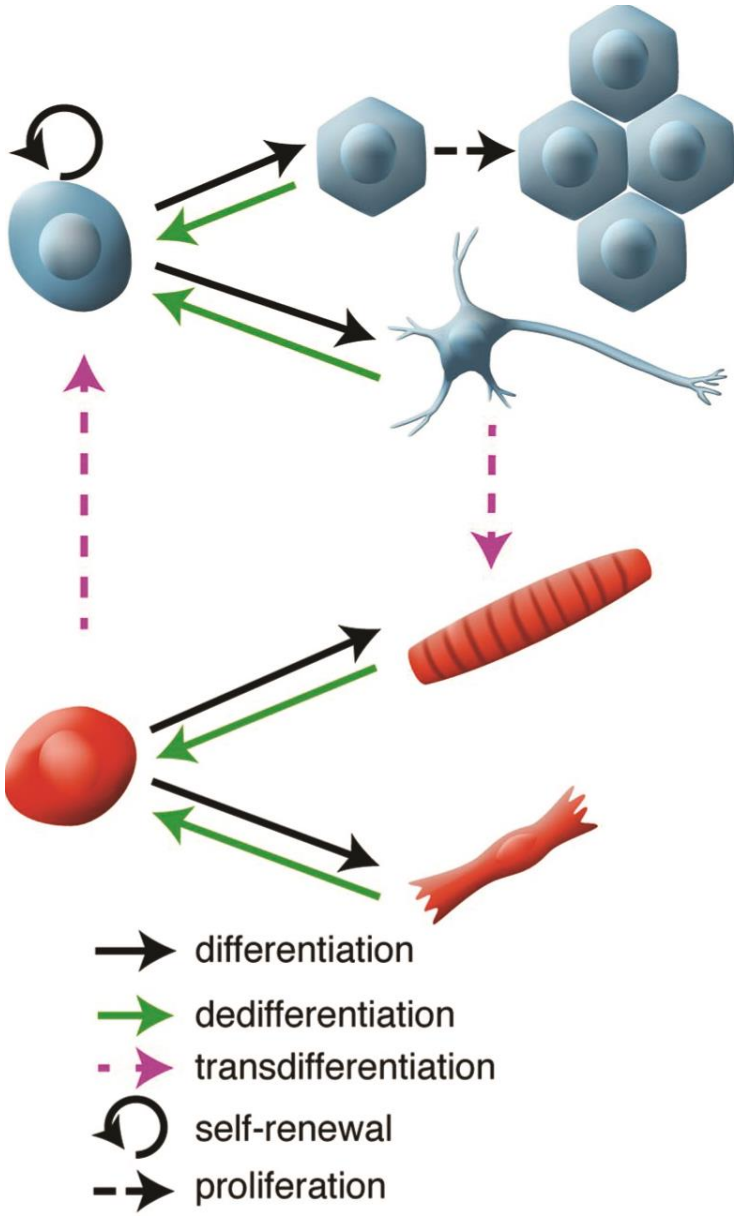

Figure 1.2: Recruitment of cells is essential for regeneration. These new cells can be derived from proliferation of resident pluripotent stem cells, proliferation of differentiated cells, from dedifferentiation of cells to a more primitive state and/or transdifferentiation of one cell type to another (adapted from King and Newmark, 2012).

In all cases of regeneration, wound healing is the initial step post damage or amputation. The initial response signals that induce regeneration following wound healing are not well known, however an involvement of thrombin (Tanaka et al., 1999) and various bioelectrical signals (Levin, 2009) have both been suggested as potential inputs. Importantly, the initial immune system response post-injury is crucial in the removal of damaged cells and as an antimicrobial defence, but has also been implicated directly in regulating important repair and regenerative mechanisms including cell migration, cell proliferation and degradation of the extracellular matrix (reviewed in Wenger et al., 2014). The cells and tissues then involved in reconstituting the lost structures vary between different animals (Figure 1.2). Planarians are unique in having a population of pluripotent and proliferative neoblast stem cells, which can reconstitute any lost tissue type (Montgomery and Coward, 1974; Newmark and Sánchez Alvarado, 2000; Reddien and Alvarado, 2004; Wagner et al., 2011). Hydra have three populations of stem cells, namely the ectodermal and endodermal epitheliomuscular cells and interstitial stem cells (David and Murphy, 1977; Wittlieb et al., 2006). Arthropods have recently been shown to employ lineage-restricted progenitor cells similarly to vertebrates (Konstantinides and Averof, 2014). In salamanders, both pre-existing cells retaining positional information, as well as multipotent stem cell populations are likely to contribute to regeneration (Kragl et al., 2009). Interestingly, it was recently demonstrated that in adult newts dedifferentiating myofibres contribute to newly regenerating muscle cells, whereas in neotenic axolotls and pre-metamorphosis newts muscles are regenerated using Pax7+ myogenic satellite cells (Sandoval-Guzmán et

al., 2014; Tanaka et al., 2016) demonstrating different regenerative strategies are employed during different life stages of the salamanders. Additional differences can be observed in heart regeneration in salamanders and zebrafish, whereby in the former dedifferentiated cardiomyocytes (Laube et al., 2006) and in the latter proliferating progenitor cells (Lepilina et al., 2006) are involved in regeneration. The employment of these different strategies, using either pluripotent progenitors or differentiated cells, which can re-enter the cell cycle and even transdifferentiate, could suggest independent evolutionary origins of regeneration. However, the variable distribution of this property in closely related phyla (closely related species often exhibiting loss or gain of this mechanism) complicates the understanding of the underlying evolutionary scenario (Brockes and Kumar, 2008; Grillo et al., 2016).

Although regeneration in all animals seems to require positional information and a signalling centre directing regeneration of new structures, such as the wound epithelium, or apical epithelial cap in limb regeneration in salamanders (Endo et al., 2004), not much is known about the molecular aspects underlying this highly complex developmental process. It has been speculated that perhaps embryonic developmental gene regulatory networks (GRNs) are re-used during regeneration of similar structures in the adult (see next section for detailed introduction into developmental gene regulatory networks) (Brockes and Kumar, 2008; Smith et al., 2011). A tempting theory for evolutionary origins of regeneration suggests it was selected as a secondary by-product of development and thus shares many similarities with embryogenesis (Brockes and Kumar, 2008; Morgan, 1901). Several

important differences are apparent between embryogenesis and regeneration: 1) nerve dependence in regeneration (Kumar and Brockes, 2012), 2) the obvious differences in overall scale and proportions of the organ/appendage of the embryo and the adult, and 3) the plasticity of differentiated cells (the ability to dedifferentiate and transdifferentiate) (Brockes, 2005). Nevertheless, it is quite conceivable that following the unique processes of regeneration (such as wound healing, dedifferentiation of cells or activation of progenitors), cell specification and differentiation occur just as they do during embryonic development. A molecular conservation of genes expressed during development and regeneration was previously demonstrated in the newt, where the sonic hedgehog gene recapitulated its role in developing limb buds during adult limb regeneration (Imokawa and Yoshizato, 1997); and during elbow joint regeneration in developing chick embryos (Özpolat et al., 2012). Although not through a direct comparison of the same animal during embryonic development and regeneration, developmental genes were often shown to be involved in adult regeneration. For example, in planarians many of the components of the genetic network underlying eye development (e.g.,*otx, six, opsin*) were shown to be expressed and functionally required during adult eye regeneration (Saló et al., 2002), though strikingly the conceived eye 'master regulatory' *pax6* plays no role in adult eye formation (Pineda et al., 2002). Although it is interesting that some potential eye development genes known from vertebrates are expressed in the planarian regenerating eye spots, only the comparison with embryonic formation of these structures in the same planarian species could yield a definitive proof of regeneration re-capitulating

embryonic development. For example, in salamanders, Meis genes under control of the retinoic acid signalling pathway have been shown to be involved in limb regeneration similarly to their role during embryonic limb development (Mercader et al., 2000; Mercader et al., 2005). Comparing the role of signalling pathways in embryogenesis and regeneration provides a compelling strategy to understand the extent of similarities in gene regulatory networks driving the two developmental processes. For example, the FGF signalling pathway plays important roles in both skeletal development and regeneration. Mutations in both ligands and receptors were found to cause a variety of congenital disorders including craniosyntoses, chondrodysplasia (Cunningham et al., 2007; Marie et al., 2005; Roscioli et al., 2000), and multiple types of gross skeletal development abnormalities in mouse models and humans (Teven et al., 2014). Similarly, multiple FGFs and FGFRs are expressed during fracture healing and bone regeneration (Schmid et al., 2009). Overall, regeneration in zebrafish, *Xenopus* and salamanders heavily relies on the expression of FGF genes in the blastema, and applying FGFR inhibitors results in regenerative defects (Lee et al., 2005; Lin and Slack, 2008; Makanae et al., 2014; Poss et al., 2000; Shibata et al., 2016). It would be interesting to determine if the role of this signalling pathway is homologous in these regenerative contexts, or can have varying contributions to the process. Unravelling the function of signalling pathways and transcription factors in development and regeneration can thus shed light on whether adult organisms with the capability of regeneration can re-use developmental gene regulatory networks.

1.2 Regeneration in echinoderms

A group of animals that has until recently been neglected in regeneration studies are the echinoderms, which in fact elegantly bridge the evolutionary gap between the commonly used vertebrate and non-vertebrate model systems (Dupont and Thorndyke, 2007). Echinoderms are non-vertebrate deuterostomes and constitute a strictly marine phylum of animals, which all possess extensive regenerative abilities in both adult and larval forms (reviewed in Candia Carnevali, 2006). Animals belonging to this phylum are characterized by 1) penta-radial symmetry, 2) large coelomic cavities, 3) a complex system of fluid-filled canals called the water vascular system, which is used for various aspects of animal life, 4) a well-developed nervous system, and 5) a calcareous endoskeleton (Brusca et al., 2016). The phylogeny of echinoderms has recently been clarified and the evolutionary relationships between the five extant classes are shown in Figure 1.3 (Cannon et al., 2014; Reich et al., 2015; Telford et al., 2014). The most early-branched are the crinoids (feather stars and sea lilies), followed by the four members of the Eleutherozoa: asteroids (sea stars), ophiuroids (brittle stars and basket stars), holothuroids (sea cucumbers) and echinoids (sea urchins).

Understanding how this group of animals regenerate entire body parts formed by different tissue types can provide valuable insight into our understanding of different mechanisms of animal regeneration and their evolutionary origin, and might help explain why not all animals possess this postembryonic developmental mode. Various instances of regeneration have been documented in the fossil record primarily for crinoids, ophiuroids and asteroids, suggesting this trait could be an ancient feature of echinoderms originating at the base of the phylum. This in turn suggests the

importance of this phenomenon in contributing to the evolutionary success of these animals (Oji, 2001). The extent of regenerative capabilities in echinoderms ranges from frequent reconstitutive regeneration of the brittle arms of ophiuroids and crinoids (Cardia and Daniela, 2006; Kondo and Akasaka, 2010), which are commonly subjected to predation or mutilations (either autotomy or traumatic amputations), all the way to the ability to reproduce asexually via regeneration of a complete specimen from a single arm as found in some sea stars (Rubilar et al., 2005). Additionally, many instances of larval regeneration can be found in the literature, where all four Eleutherozoa classes show some extent of asexual budding and regeneration (Balser, 1998; Eaves and Palmer, 2003; Oulhen et al., 2016). Interestingly, it appears that different species of the same phylum make use of different strategies to regenerate their appendages. Here, I will summarize the advances in understanding regeneration and functional assays in echinoderms showing possibilities and limitations of molecular studies (Table 1.1).

Table 1.1: Summary of main functional assays performed in different echinoderm classes to date.

Echinoderm	***Functional assays***	***Publications***
Echinoids	*In embryos:*	
	Morpholinos (MO),	(Coffman et al., 2004; Heyland et al., 2014) *and others*
	vivo MOs	
	CRISPR/CAS9	(Che-Yi Lin, 2015; Oulhen and Wessel, 2016)
	Inhibitors	(Adomako-Ankomah and Ettensohn, 2013; Cui et al., 2014) *and others*
	In adults: Inhibitors	(Reinardy et al., 2015)
Asteroids	*In embryos:* Morpholinos	(Cheatle Jarvela and Hinman, 2014; Yankura et al., 2013) *and others*
Holothuroids	*In embryo and adults:*	
	Morpholinos	(McCauley et al., 2012; Mashanov et al., 2015a)
Ophiuroids	*None*	*None*
Crinoids	*None*	*None*

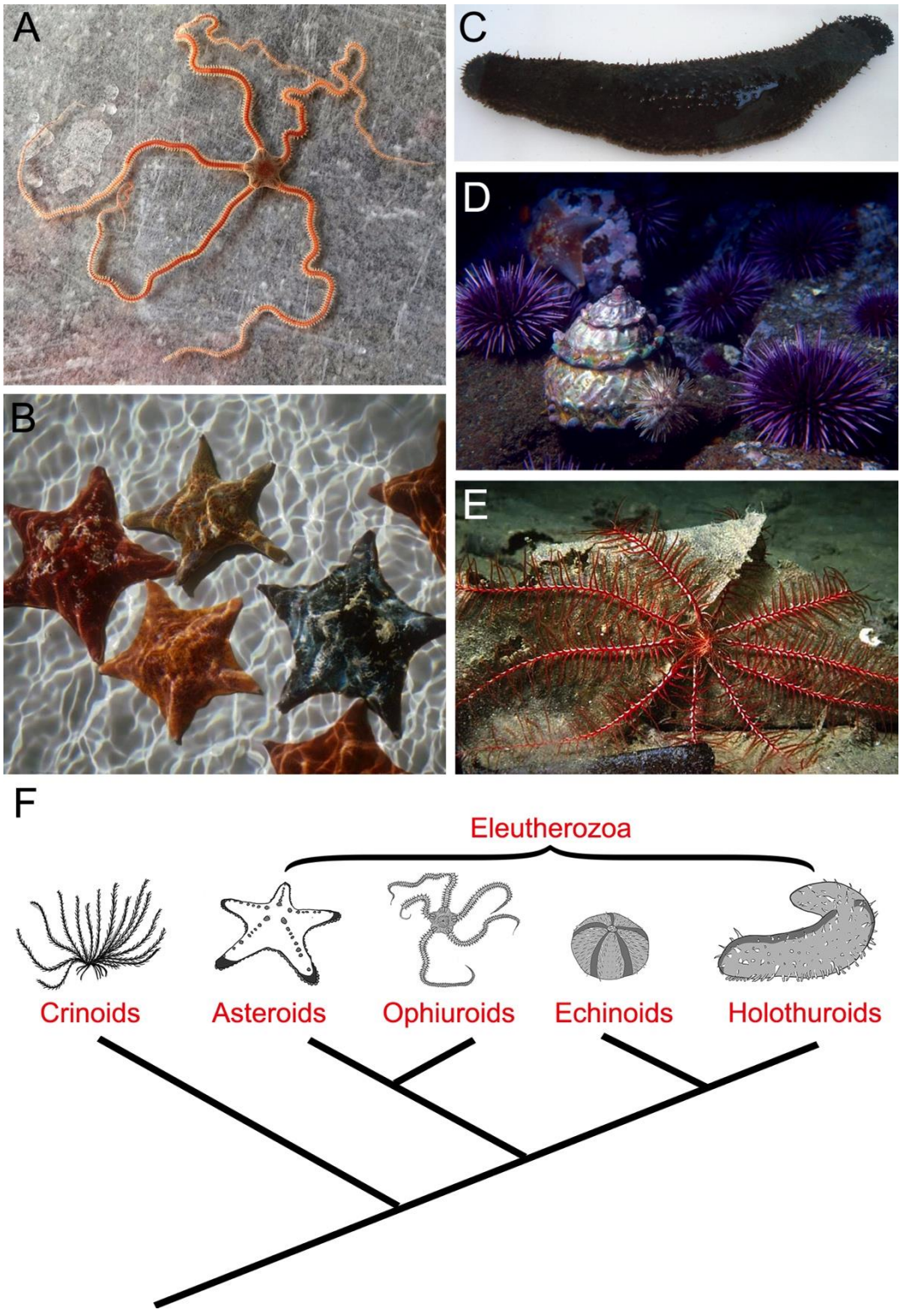

Figure 1.3: Images of representatives of five echinoderm classes and their phylogenetic position. A) Brittle star *A. filiformis*. B) Sea star *P. miniata* (https://montereybayaquarium.org). C) Sea cucumber *H. glaberrima* (Mashanov et al., 2014). D) Sea urchin *S. purpuratus* (http://calphotos.berkeley.edu). E) Crinoid *A. mediterranea* (http://umema.it). F) Phylogeny confirmed by molecular analyses (Cannon et al., 2014; Reich et al., 2015; Telford et al., 2014) showing the early-branched crinoids, then ophiuroids/asteroids grouping separately from echinoids/holothuroids.

1.2.1 Echinoids

Echinoids are known to regenerate external appendages such as the spines, pedicellaria and tube feet, as well as their skeletal plates (Bonasoro et al., 2004; Chadwick, 1929; Dubois and Ameye, 2001). The process of spine regeneration has been studied mostly in terms of ultrastructure and growth process of the tip of the spine. Stable ^{26}Mg isotope labelling and regular microscopic observations revealed that the spines first grow as conical micro-spines, which then fuse together to form the stereotypical mesh-like inner stereom later covered by layering of additional calcite deposits forming the outer stereom (Gorzelak et al., 2011; Heatfield and Travis, 1975). The cellular and molecular aspects of this regenerative process however are poorly understood. Only recently, a single study investigated the potential role of the Notch signalling pathway in sea urchin spine and tube feet regeneration (Reinardy et al., 2015), but without providing any insight into the cellular or molecular mechanisms underlying this process.

1.2.2 Holothuroids

Like echinoids, holothuroids can also regenerate the external appendages, but additionally can regenerate the whole visceral mass or individual internal organs including intestine, gut and radial nerve (García-arrarás and Greenberg, 2001; Mashanov and García-Arrarás, 2011; Mashanov et al., 2008). After evisceration, which is the ejection of the digestive tube, hemal system, and respiratory trees, the earliest response to

the injury is wound closure and reorganization of the remaining tissues, which involves extensive dedifferentiation of cells (Mashanov et al., 2005). This process triggers an increase of proliferation from normal physiological levels, which reaches its peak during the growth of the rudiments of the visceral mass (García-ArraráS et al., 1998). This early regenerative response is highly similar during radial nerve cord regeneration, which is also characterized by wound healing, remaining tissue reorganization and degeneration, and finally dedifferentiation of glial cells accompanied by cell proliferation (Mashanov et al., 2008). It has been shown that transdifferentiation of mesodermally-derived mesoepithelial cells is highly involved in reconstituting the regenerating digestive tube, however it is also possible that a population of resident stem cells could contribute to this regenerative process (Mashanov and García-Arrarás, 2011; Mashanov et al., 2005). In contrast to sea urchin regeneration, a series of papers has been published attempting to uncover the molecular mechanisms underlying sea cucumber regeneration of the radial nerve cord and the viscera. Large-scale transcriptomic studies were carried out to characterize the dynamic changes in gene expression during different stages of intestinal (Sun et al., 2013) and nervous system regeneration (Mashanov et al., 2014). For example, it has been shown specifically that *myc*, one of the Yamanaka pluripotency factors, was highly upregulated during regeneration of various sea cucumber tissue types (Mashanov et al., 2015b). RNA interference-mediated (RNAi) gene knockdown inhibits dedifferentiation of radial glia, confirming its' important role in regeneration (Mashanov et al., 2015a). Thus, regeneration of

holothurians has been the best studied among echinoderm regenerative processes to date.

1.2.3 Asteroids

Asteroids can regenerate both internal organs, including the cardiac stomach and the pyloric caeca, as well as their arms with all the complex structures they contain. Some species of sea stars can even regenerate the entire organism from a single arm demonstrating the most drastic regenerative ability in echinoderms (Ducati et al., 2004). Asteroid arm regeneration appears to differ significantly from crinoid and ophiuroid regeneration (see below) in that no discrete regenerative bud, acting as a centre of proliferation, is formed at the site of wound healing post-amputation. Rather, most cell cycle activity is localized at the epidermis and the epithelium of coelomic canals (Moss et al., 1998). During wound healing several different cell types can be observed at the site, including phagocytes and undifferentiated cells (Ben Khadra et al., 2015). Extensive dedifferentiation can also be observed and it has been shown that regeneration is nerve dependent in sea stars (Huet, 1975). Furthermore, sea star arms start to differentiate certain structures very early on (mainly the nervous system, muscles and skeleton) and only later in the advanced regenerative phase can obvious morphogenesis and re-growth of the regenerate be seen (Ben Khadra et al., 2015b). So far, little is known concerning the genes involved in sea star regeneration.

1.2.4 Crinoids

Crinoids exhibit extensive regenerative abilities both for the re-growth of external appendages such as the arms, cirri and pinnules as well as the internal organs such as the gonads, digestive tube or even the complete visceral mass as seen previously in holothuroids (Carnevali et al., 1993; Kondo and Akasaka, 2010; Mozzi et al., 2006). Arm regeneration has been the most thoroughly studied process in crinoid regeneration. It begins with typical wound healing and re-epithelialization, accompanied by tissue rearrangement and local repair of injured structures. A regenerative bud is then formed at the amputation site, and is characterized by high numbers of proliferating cells. The distal tip of the regenerate appears to maintain this high proliferative capacity throughout the advanced stages of regeneration when newly forming structures begin to differentiate (Candia Carnevali et al., 1997; Carnevali et al., 1993; Carnevali et al., 1998; Lucca et al., 1995). Coelomocytes and amoebocytes, which show a high degree of proliferation, have been suggested to act as potential stem cells or pluripotent cells. Although no molecular mechanisms have been studied as yet to support this claim, it has been shown that growth factor (TGFβ) and neuropeptide (SALMFamide) signalling is present during regeneration (Carnevali et al., 1998; Patruno et al., 2002).

1.2.5 Ophiuroids

Although ophiuroids have been shown to regenerate internal organs, arm regeneration is currently the most well understood in this class of

echinoderms (Cardia and Daniela, 2006; Charlina and Dolmatov, 2009). Ophiuroids exhibit high rates of arm regeneration due to the often-occurring breakage of arms and autotomy in response to predation. Arm regeneration in this class of echinoderms is usually rapid and can involve several arms at once. Because of this high rate of regeneration observed in the wild, various studies have focused on the physiological aspects of regeneration in these animals in response to changing environmental conditions (Clark and Souster, 2012; Hu et al., 2014; Nilsson and Sköld, 1996; Yokoyama and Amaral, 2010). In terms of cellular processes involved in arm regeneration in brittle stars, it has been previously described as closely resembling crinoid arm regeneration. Following wound healing and dedifferentiation processes a small regenerative bud can be observed protruding from the amputation site. This bud contains high levels of proliferating cells and histological analysis distinguished various cell types apparent in the early regenerate including coelomocytes, phagocytes, dedifferentiating myocytes and uncharacterized undifferentiated cells (Biressi et al., 2010; Thorndyke et al., 2001). During advanced regenerative stages extensive growth and differentiation can be observed and the new structure begins to closely resemble a miniature arm (Biressi et al., 2010; Dupont and Thorndyke, 2006). According to previous studies, while the proximal regions of the arm show advanced stages of differentiation of structures like the muscles, podia and the skeleton, the distal part remains undifferentiated and retains typical features of a blastema (Biressi et al., 2010). In recent years there has been an emergence of various molecular studies on ophiuroids including transcriptomic analyses (Burns et al., 2011; Burns et al., 2013; Delroisse et al., 2015; Delroisse et al.,

2016; Purushothaman et al., 2015; Vaughn et al., 2012) and investigation of individual gene expression during regeneration (Bannister et al., 2005; Bannister et al., 2008), which provides an excellent basis for further research on brittle star regeneration.

1.3 Skeletogenesis in echinoderms

One of the defining characters of echinoderms is their skeleton. Unlike any other non-vertebrate phyla, the echinoderms are unique in that instead of an exoskeleton they form an epithelium-covered endoskeleton. However, the many different skeletal elements including spines, teeth, tests, pedicellariae and shields are composed of calcium carbonate as opposed to calcium phosphate, which comprises the endoskeleton of chordates. The calcium carbonate is utilized as calcite, which is secreted in a process called biomineralization. 99% of the echinoderm endoskeleton is comprised of magnesium calcite (5% magnesium), while the remaining 1% contains primarily water-soluble matrix proteins amongst other components (reviewed in Killian and Wilt, 2008). Ossicles have a three-dimensional porous structure formed by crystals of calcite and associated proteins, also referred to as stereom, which provides light but sturdy endoskeletal support (Wilt et al., 2003). The molecular and cellular mechanisms of skeleton development have been extensively studied in sea urchin embryos (Oliveri et al., 2008; Rafiq et al., 2014; Wilt and Ettensohn, 2008) and they provide the basis for investigations on adult skeleton development, regeneration, and comparison with other classes. In postembryonic skeletogenesis, the formation of spicules and the participation of skeletogenic cells in echinoderm juveniles

has been previously described, and major morphological similarities between embryonic and juvenile skeletogenic cells have been observed (Yajima and Kiyomoto, 2006). Indeed, at both life stages the skeleton is formed by round-shaped mesenchymal cells with filopodia, capable of migrating to the location where new skeleton is deposited (Yajima and Kiyomoto, 2006). These morphological studies have been complemented by: 1) gene expression analyses, carried out in both sea urchin and sea stars, which show that many of the genes involved in sea urchin embryonic skeletogenesis are also expressed in juvenile skeletogenic centers (Gao and Davidson, 2008; Gao et al., 2015); and 2) proteomic studies that revealed an extensive similarity of the molecular make-up of embryonic and adult isolated skeletal elements (Mann et al., 2008a; Mann et al., 2008b; Mann et al., 2010). Nevertheless, the cellular and molecular aspects of skeletal regeneration have not been investigated in detail in any echinoderm clade.

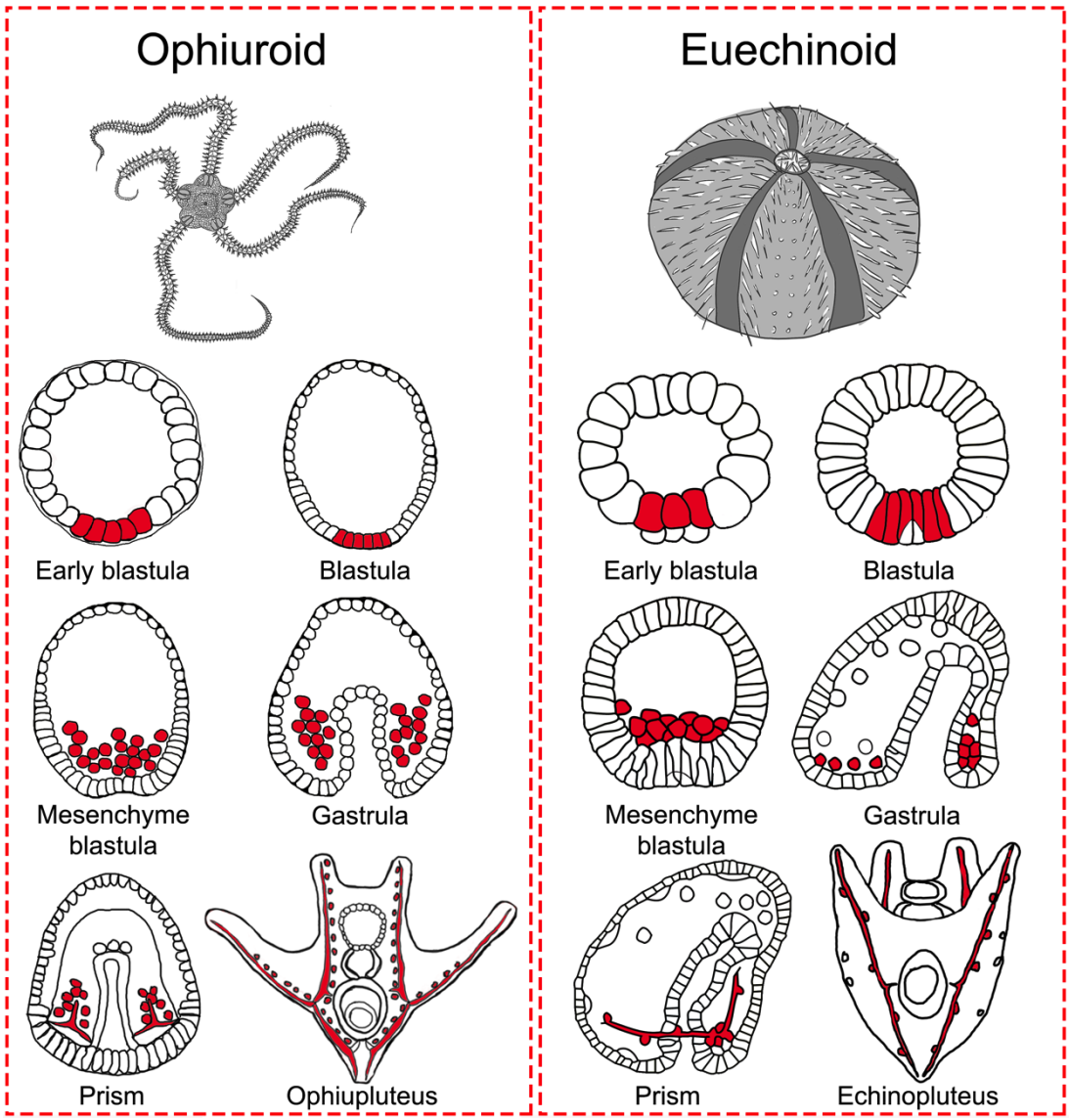

Figure 1.4: Larval skeleton development in ophiuroids and echinoids. Schematics show the development of the skeletogenic mesoderm and later skeletal spicules (both in red) in brittle stars and modern sea urchins. Schematics of sea urchin development adapted from (Davidson et al., 2002a).

Additionally to adult skeletal elements two of the echinoderm classes, ophiuroids and echinoids, also contain an extended larval skeleton, and the sea cucumber produces small larval spicules. How these two classes evolved this extended larval skeleton remains a controversial question (see section 1.4). The most extensive studies on echinoderm skeletogenesis have in fact been carried out in sea urchin embryos due to their accessibility, the availability of a genome and other important qualities of sea urchin as a model system (Sodergren et al., 2006). The larvae of sea urchins develop tri-partite spicules, which elongate to form their pluteus-type shaped endoskeleton (Figure 1.4). It has been shown that the embryonic domain which will give rise to skeleton-secreting cells is specified relatively early in euechinoid development; already the unequal 5th cleavage results in the separation of the four small micromeres and four large micromeres, from which the whole skeletogenic lineage is derived. The descendants of the large micromeres are the skeletogenic mesoderm (SM) cells, which ingress first (and therefore are also called primary mesenchyme cells) into the blastocoel of the embryo from the vegetal pole and accumulate at the ventrolateral clusters during gastrulation. Those cells will then form a syncytium, secrete the initial spicule, and migrate along the elongating spicules to continue skeleton deposition (Wilt and Ettensohn, 2008). Skeletogenic lineage cells are autonomously specified as shown by experiments whereby cultured SM cells can form skeletal elements *in vitro* without the need for signalling from other domains of the embryo (Okazaki, 1975; Decker, 1987). Cidaroids, the sister-group to all other extant groups of echinoids, also form a larval skeleton but their development differs

significantly from euechinoids (regular sea urchins including the most commonly studied species such as *S. purpuratus, L. variegatus* and *P. lividus*). There is no observable ingression of primary mesenchyme cells as observed in euechinoids and the ultimate skeletogenic cell descendants arise only after gastrulation has already started (Erkenbrack and Davidson, 2015; Yamazaki et al., 2014). In the brittle star embryo there is no unequal cell division, but skeletogenic mesenchymal cells do ingress into the blastocoel preceding gastrulation, then migrate into ventrolateral positions and deposit two bilaterally-arranged, tetraradiated skeletal spicules that eventually elongate to form the fully extended skeleton establishing the ophiopluteus shape of the larva (Dylus et al., 2016; Vaughn et al., 2012; Yamashita, 1985).

It is not well known how the skeleton arises in the adult, what the cellular and morphogenetic mechanisms are and whether they resemble in any way embryonic development. In a recent study on sea urchins elegant experiments using transplantation of rhodamine-labelled or GFP-Sm50 transgene expressing SM cells and non-skeletogenic mesoderm cells (NSM, also called secondary mesenchyme cells, which ingress after the SM cells) showed that SM cells from the embryo do not contribute to the formation of juvenile skeletogenic structures, but that NSM cells do contribute at least to the pedicellariae (Yajima and Kiyomoto, 2006). Additional experiments showed that in the absence of SM cells (following removal) NSM cells can transfate to take on this role (Ettensohn and McClay, 1988). These data support the idea of NSM cells having an ancestral function in specification of the skeleton and that the novel role of SM cells in sea urchin embryo skeletogenesis is a relatively recent evolutionary modulation. Although the

embryonic cells are not involved in building the adult skeleton, many of the underlying genes responsible for skeletogenic cell specification and calcite secretion are shared between embryos and adults (Gao and Davidson, 2008).

Most of what is known concerning molecular regulation of skeletogenesis also comes from studies on sea urchin development. The gene regulatory network deployed for the specification of the skeletogenic lineage (Figure 1.5) has been described in much detail including the involvement of signalling pathways, transcription factors (TFs) and differentiation genes, as well as the intricate interactions between them (Livingston et al., 2006; Oliveri et al., 2008; Rafiq et al., 2014; Sharma and Ettensohn, 2011). Approximately 117 genes have been discovered to have a role in this GRN. The initial activation of the network relies on maternal signalling from highly conserved axis specification factors such as *wnt* and *β-catenin* (Logan et al., 1998). The latter is the essential activator of the SM cell-specific transcription factor cascade, which acts via a double-negative gate formed by the two transcriptional repressors *pmar1* and *hesC*. Pmar1 represses the global repressor *hesC* specifically in vegetal cells (Oliveri et al., 2002; Oliveri et al., 2003; Revilla-i-Domingo et al., 2007) allowing the activation of the multi-levelled cascade of downstream skeletogenic transcription factors in the SM lineage, which interact together in complex regulatory interlocking feedback loops. Those genes in turn regulate the expression of terminal differentiation genes involved in biomineralization (Oliveri et al., 2008; Rafiq et al., 2012; Rafiq et al., 2014). FGF and VEGF signalling from the ectoderm surrounding the skeletogenic lineage cells also

plays an important role in activating the biomineralization genes, guiding cell migration and the patterning of the skeleton (Adomako-Ankomah and Ettensohn, 2013; Duloquin et al., 2007; Röttinger et al., 2008). The most highly abundant differentiation genes, which are involved in secreting the biomineralized skeleton, encode integral matrix proteins characterized by containing a c-type lectin domain (*c-lectin*) and a proline-rich repeat domain (all spicule matrix genes, e.g. *sm30* and *sm50*) (Illies et al., 2002; Livingston et al., 2006; Urry et al., 2000). Many other proteins contribute to biomineralization in echinoderms including the MSP130 genes, different collagens, carbonic anhydrases, metalloproteases and cyclophilins (Amore and Davidson, 2006; Illies et al., 2002; Mann et al., 2008a; Mann et al., 2008b; Mann et al., 2010; Suzuki et al., 1997; Urry et al., 2000). A large investigation of potential downstream skeleton-formation genes has been carried out recently showing 180 genes expressed specifically in the SM (Rafiq et al., 2012).

1.4 Evolution of the larval skeleton

The mode of evolution of the extended larval skeleton in brittle stars and sea urchins has been a controversial question. Two scenarios are currently debated given the most recently accepted phylogeny of these animals (Cannon et al., 2014; Telford et al., 2014): the first states that the larval skeleton evolved only once in the ancestor of the Eleutherozoa (Figure 1.3) and was subsequently lost in sea stars and highly reduced in sea cucumbers; the second assumes a convergent evolution of the larval skeleton in brittle stars and sea urchins. It has been suggested that co-option

of the adult skeletogenic molecular program for embryonic development has taken place specifically at the level of the double-negative gate formed by *pmar1* and *hesC* (Gao and Davidson, 2008). Recently, several studies have been published comparing the well-known euechinoid skeletogenic GRN to other echinoderms like cidaroids and ophiuroids, which provided new evidence shedding light on this very interesting evolutionary question. Molecularly, the network circuitry of the cidaroid skeletogenic GRN shows important differences. For example, the lack of the *pmar1* gene and the co-expression of *hesC* with other skeletogenic-specification genes both suggest that the double-negative gate known in euechinoids does not operate in the same way in these species (Erkenbrack and Davidson, 2015; Yamazaki and Minokawa, 2015; Yamazaki et al., 2014). A study from our lab showed that although the ophiuroid and euechinoid embryos share great similarities in the mode of development and the morphology of the larval skeleton, there are numerous differences in the underlying gene regulatory network architecture (Dylus et al., 2016). There is also no ortholog to the *pmar1* gene, and its closest relative *pplx1* does not have the same protein function as its sea urchin counterpart (Dylus et al., 2016). In *A. filiformis hesC* is co-expressed with many of the direct target genes it is repressing in sea urchins, showing differences in network linkages, furthermore several sea urchin downstream key regulatory genes are not expressed in the skeletogenic lineage of the brittle star (*foxb* and *dri*) identifying additional differences in regulatory states (Dylus et al., 2016). Sea cucumbers, which only make small spicules during embryogenesis, have also been recently shown to develop a simple skeletogenic lineage, which like in brittle stars and sea urchins is

characterized by the expression of *alx1* (Dylus et al., 2016; Ettensohn et al., 2003; Koga et al., 2016; McCauley et al., 2012). It has thus been suggested that the acquisition of an embryonic skeletogenic lineage was a result of the re-specification of the ancestral mesoderm into distinct territories with different regulatory states (McCauley et al., 2012). Finally, sea stars make no larval skeleton whatsoever and studies on the expression of sea urchin skeletogenic gene orthologs showed that many of these genes are expressed in the sea star embryonic non-skeletogenic mesoderm, supporting the existence of an ancestral mesoderm territory, which diversified its function in different lineages of echinoderms (McCauley et al., 2010; McCauley et al., 2012). Interestingly, it has been suggested that activation of the VEGF signalling pathway during embryogenesis was one of the key steps in the evolution of the larval skeleton. Brittle stars and sea urchins both express the *vegf* ligand and the *vegfr* receptor during embryogenesis (Duloquin et al., 2007; Morino et al., 2012), whereas sea stars have no VEGF signalling present until juvenile stage (Morino et al., 2012). The comparison of embryonic and adult skeleton development as well as further analysis of brittle star skeletogenic genes would provide essential clues into how the larval skeleton evolved in echinoderms.

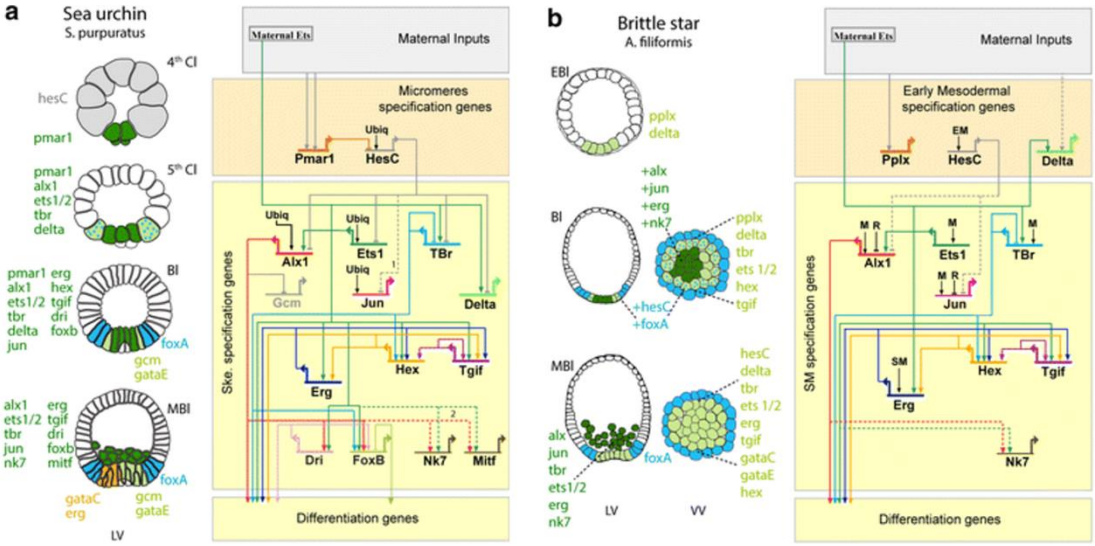

Figure 1.5: Comparison of sea urchin and brittle star skeletogenic gene regulatory networks. A) Skeletogenic GRN of the sea urchin *S. purpuratus* showing the known transcription factors involved activating the differentiation gene cascade and the corresponding dynamics of regulatory state changes in the developing embryo. B) Predicted skeletogenic GRN based on regulatory state analysis in the brittle star *A. filiformis* showing TF genes expressed in the mesodermal territories of the embryo. Adapted from Dylus et al, 2016.

1.5 Model system: the brittle star *Amphiura filiformis*

Amphiura filiformis (O. F. Müller, 1776; *Afi)* is a small, burrowing brittle star found commonly in the North sea and the Mediterranean sea (Figure 1.6) (Rosenberg, 1995). Its disc size can reach approximately 1cm in size and the five thin arms extend to almost 10x the length of the main body. It usually has red-brown pigmentation, the aboral side of its disc is covered with small ossicles, but the oral side is naked with the exception of the ossicles surrounding the mouth and the teeth. The adult can regenerate its entire arms, making it an appealing system for studying regeneration of adult structures. The arms of *A. filiformis,* like other ophiuroids, are complex structures composed of various tissue types organized in repetitive segments, also referred to as metameric units. Each such unit contains five

different skeletal elements – the dermal oral, aboral and lateral shields (or plates), spines, and the internal vertebral ossicles - in addition to a set of two pairs of intervertebral muscles, intervertebral ligaments, and a pair of podia on each side (Figure 1.6). The radial water canal, the different specialized coelomic cavities (i.e., aboral coelomic canal, neural sinuses), a radial nerve cord and peripheral sensory neurons are also present throughout the arm segments (Byrne, 1994). This brittle star is a suspension feeder, meaning it extends its arms vertically out of the mud substrate where it is burrowed, and feeds on the plankton and microparticles in the water column (Loo et al., 1996). This mode of feeding makes its arms vulnerable to predation and *A. filiformis* arms have indeed been found amongst the stomach contents of many crustacean and fish species in its environment (Baden et al., 1990; Duineveld and Van Noort, 1986). This high predation rate may be directly responsible for its rapid arm regeneration ability. *A. filiformis* has been used to understand various aspects of regeneration in brittle stars including morphogenesis, growth rate, and ecological response (Biressi et al., 2010; Burns et al., 2011; Dupont and Thorndyke, 2006; Hu et al., 2014; Purushothaman et al., 2015). Some studies have shown significant variability in regeneration rates of these animals. Many factors could likely influence the regeneration rate, such as animal size, traumatic versus self-amputation, length of the lost arm, or the most pertinent function required at the time (i.e. the differentiation of sensory structures or the growth of arm for locomotion and feeding) (Dupont and Thorndyke, 2006). Due to the availability of transcriptomic information, its rapid arm regeneration process and its small, semi-transparent regenerating arms (which are ideal for microscopy), *A.*

filiformis is highly suitable as a model system for studying regeneration. Additionally, recent work on embryogenesis and skeletogenesis in the embryos of this species of brittle star (Dylus et al., 2016) allow for the comparison of these two developmental contexts on a morphological and molecular level.

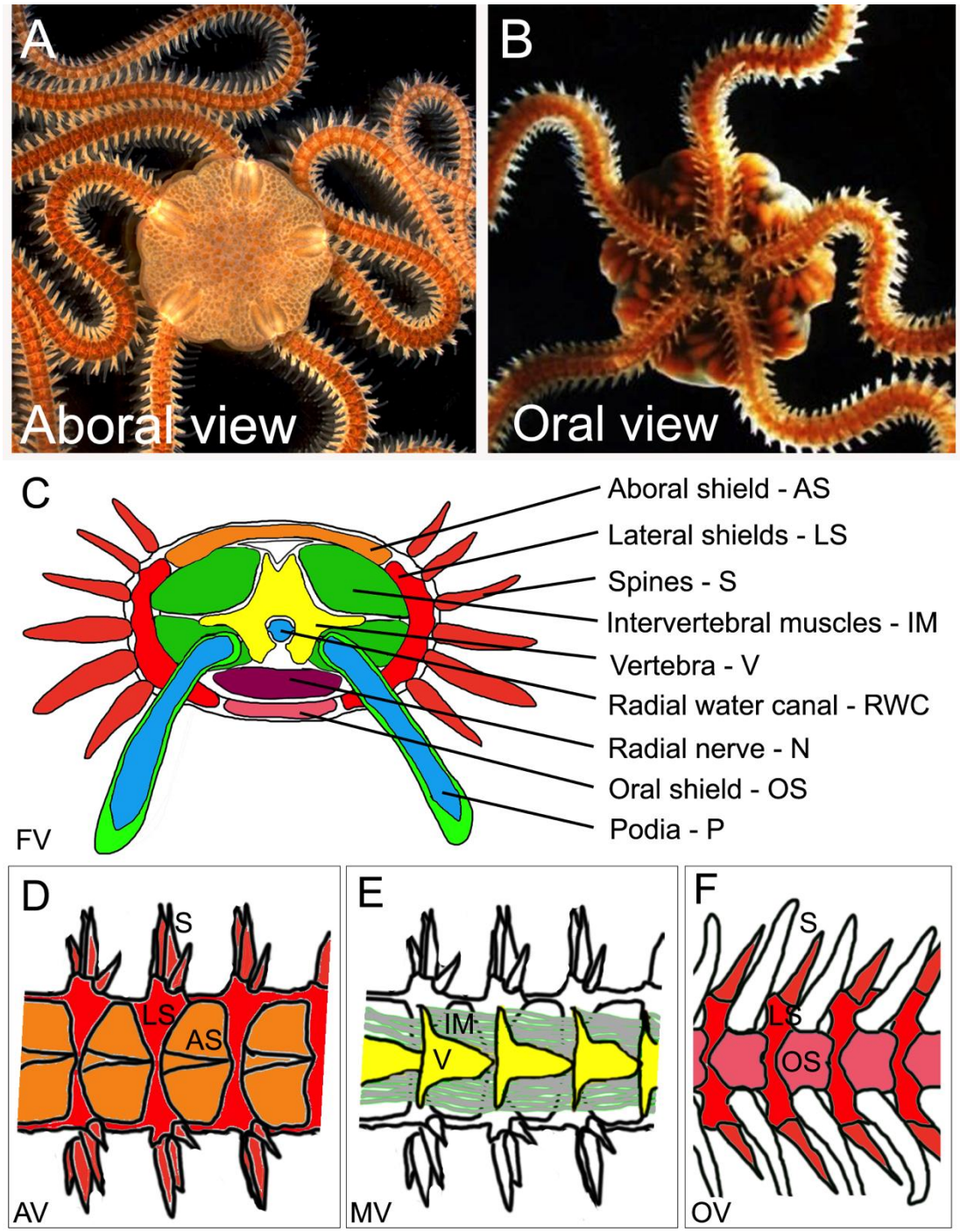

Figure 1.6: The brittle star *Amphiura filiformis*. A) Aboral view of *A. filiformis* showing small ossicles covering the whole animal disc. B) Oral view of *A. filiformis* disc showing mouth and gonads. C) Schematic of frontal view of an adult arm showing internal structures including the skeletal elements, intervertebral muscles, radial water canal, the radial nerve and the aboral coelomic cavity. D) Aboral view of several segments of adult arm showing the position of the aboral and lateral shields and spines. E) Middle inner view of several adult arm segments showing the position of the vertebrae and the intervertebral muscles. F) Oral view of the adult arm showing the oral and lateral shields, spines and podia. *AV – aboral view, FV – frontal view, MV – middle inner view, OV – oral view.*

1.6 Building a gene regulatory network model for regeneration

Development is orchestrated by the precise activation of transcription factors (TF), signalling molecules and their downstream effector genes in a precise spatio-temporal manner, which can be modelled using gene regulatory networks (GRN) (Ben-Tabou de-Leon and Davidson, 2007; Davidson, 2006; Davidson and Peter, 2015). Comparison of gene regulatory networks in different species can yield important insights into the evolution of the development of morphological characters, as was discussed to some extent in terms of the evolution of the larval skeletogenic network in echinoderms (section 1.4). Likewise, it should be considered that establishing the GRNs underlying the development of a specific structure in the embryo and regeneration of that structure in the adult could be a powerful tool for large-scale molecular comparisons between those two processes. Currently lacking in the field of regeneration biology are tools and model systems for such global-view comparisons, and in general a comprehensive understanding of this process at a molecular level. The main experimental requirements for determining gene regulatory networks in regeneration include spatiotemporal reproducibility of the process, accessibility to observation and manipulation and ease of acquiring genetic material (Smith et al., 2011).

GRNs combine many individual subcircuits or modules with specific developmental tasks into a coordinated program driving the development of complex morphological features (Ben-Tabou de-Leon and Davidson, 2006; Oliveri and Davidson, 2007). As shown in the example of the sea urchin skeletogenic GRN (discussed in section 1.3), the structure of this model is

highly hierarchical and dependant on both the timing of expression of individual nodes (genes) in the network as well as their spatial expression in the developing embryo (Materna and Oliveri, 2008; Oliveri et al., 2008). To construct a provisional GRN for the development of a particular structure, during embryogenesis or any other developmental process like regeneration, the first step concerns understanding the cellular and morphological organisation of the developing structure (Figure 1.7). Once the different cellular territories are known, it is crucial to compile the spatial expression patterns of all candidate TFs, signalling molecules and differentiation genes that may be involved in specifying this territory. The set of transcription factors expressed in a cell at any given time define its regulatory state (Davidson et al., 2002a). The dynamic changes of regulatory states of cells (changes in transcription factor spatial expression patterns) drive the formation of discrete structures within the developing body plan, be it cell types, tissues or whole organs, either by activating or repressing a specific cell fate. Changes in the tissue-specific expression of transcription factors, driven by *cis*-regulatory elements, can thus highly impact developmental processes. On the other hand, it is also necessary to understand the expression of signalling ligands and their respective receptors to unravel any potential cell-cell or tissue interactions, which are mediated by signalling pathways, and may input into the GRN. Finally, the effector genes activated downstream of the regulatory machinery define the ultimate differentiation state of a specific cell type and thus their expression pattern both specifies the ultimate output of the gene regulatory network and acts as a marker for that given cell type. The final step of creating a provisional GRN is to use

perturbations and *cis*-regulatory analysis to validate the functional relationships between the regulatory genes in the network. While *cis*-regulatory analysis is impossible without genomic data, which contains the regulatory regions of the genes of interest, functional perturbations can be performed using various established techniques for gene knockdown. Those include specific targeted perturbations of single genes using morpholino antisense oligonucleotides, RNAi or the CRISPR/Cas9 system, small molecule signalling transduction inhibitors targeting signalling pathways, as well as any other molecular techniques available to change the function of a given gene (Materna and Oliveri, 2008). The GRN approach provides a causal explanation of the molecular mechanisms occurring during the development of a specific structure or cell-type.

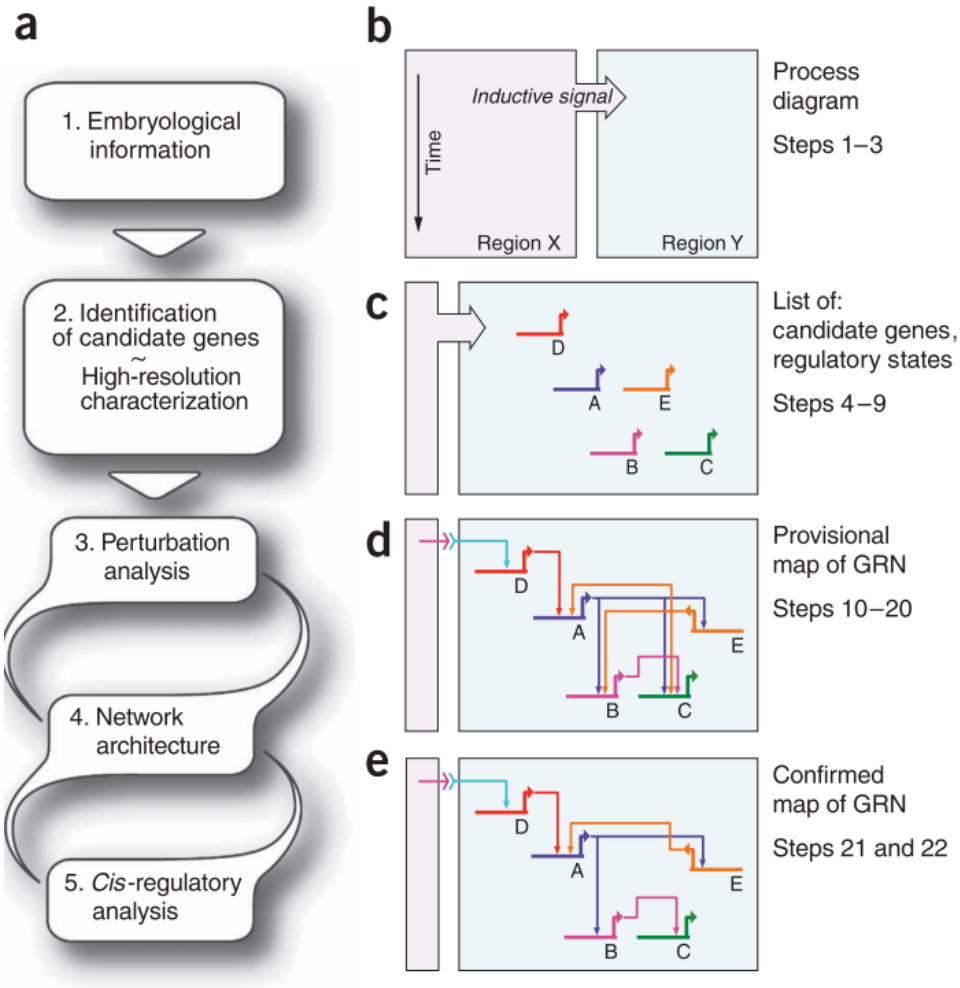

Figure 1.7: Strategy for building a GRN (Materna and Oliveri, 2008).

1.7 Aims and hypothesis

Regeneration is one of the most astounding phenomena in biology. Unravelling the cellular and molecular events underlying this process is not only interesting in terms of basic biological questions, such as the understanding of the mechanisms and evolution of this feature, but can also be of use for developing applications in regenerative medicine. As a developmental process, which takes place in an adult context, it seems natural to compare regeneration of a certain structure, like the limb or an eye, to its counterpart developmental process occurring during embryogenesis. In

this thesis I use the novel model system, the brittle star *Amphiura filiformis*, to compare the development and regeneration of the skeleton as a proxy for understanding if, or to what extent adult regeneration might re-capitulate embryonic development by reactivating the underlying molecular network for the specification and differentiation of the skeletogenic cell lineage.

The aims of this research project are in accordance with the standard steps used to build a GRN model for the development of a specific structure (Materna and Oliveri, 2008; Figure 1.7). The first aim of my thesis is to compile morphological and cellular information to characterize the process of arm regeneration and skeletogenesis and identify the distinct cellular territories, which form during this process (Chapter 3). The second aim is to compile a high-resolution map of gene expression patterns in brittle star arm regeneration to identify the molecular signature of the cells and compile information on the dynamics of regulatory state changes during regeneration. This will allow the first molecular comparison of the skeletogenic lineage in the embryo and the adult arm (Chapter 4). Finally, the third aim of my thesis is to characterize the role of signalling pathways, known to be involved in embryonic skeleton formation, during arm regeneration in *A. filiformis* to identify any functional similarities between the GRN driving skeletogenesis during development and regeneration.

It is likely that the initial inputs necessary to activate the specification and differentiation of skeletogenic cells are likely to be quite different between the adult and the embryo, due to the significant differences in the starting cellular environment in which the network is activated. Wound healing and distal stump cues are likely involved in the adult whereas mostly

maternally expressed genes are at the top of the embryonic network. However, my hypothesis is that the core network of transcription factors and signalling molecules which specify the skeletogenic lineage are likely to be much more conserved between the two processes and that the final differentiation skeletogenic genes are likely to be almost identical in development and regeneration because they form very similar calcitic endoskeletal structures.

The brittle star *Amphiura filiformis* promises to be an excellent model for this type of research due to several reasons (as discussed in section 1.5): 1) the availability of molecular resources for both embryos and regenerating arms, 2) the accessibility of both embryos and regenerating arms for experimental manipulations and microscopic observations, and 3) the vast amount of already existing literature and data on the skeletogenic lineage GRN in other echinoderms, and specifically in the brittle star embryo, serve as a basis for comparison with the adult regeneration program. Thus, in this thesis I aim to use this approach to build a provisional GRN model for the regeneration of the adult skeleton in the brittle star to gain a global overview of the molecular network involved and to compare it with embryonic development.

2 Materials and methods

2.1 Adult animals and embryonic cultures

Adult *Amphiura filiformis* brittle stars were collected in the vicinity of the Sven Lovén Centre for Marine Sciences in Kristineberg, Sweden (58° 15′ N, 11° 25′ E). The animals were sampled from the fjord using a Petterson mud grab at depths of up to 40m. The mud samples were sieved through and the individuals were collected into fresh deep-sea water before transporting them to London. In London the animals were kept in oxygenated tanks with a filtering unit at 12-14°C in artificial seawater (ASW) at a salt concentration of 30ppm. The animals were fed with a few drops of Microvore Microdiet (Brightwell Aquatics) two days per week. Water in the tank was exchanged once a week. For arm amputations the animals were anaesthetized in a 3.5% solution of $MgCl_2 6H_2O$ (35g of dry stock in mixture of 500ml milliQ water and 500ml ASW). The arms were amputated using a scalpel approximately 1cm from the disc to obtain early regenerative stage arms after 4-7 days. For more advanced regenerative stages the animals were cut using previously described guidelines (Dupont and Thorndyke, 2006). The arms were either fixed for further experiments using 4% PFA in 1x PBT (Phosphate buffered saline, 0.1% Tween-20) at room temperature for a minimum of 1h or overnight at 4°C, washed twice with 1x PBT and stored in 100% methanol at -20°C. Embryo cultures, collection and fixation were carried out as described before (Dupont et al., 2009; Dylus et al., 2016).

2.2 Calcein staining

Live animals were incubated with calcein (Sigma) at a dilution of 1:50 of a stock solution (1.25 mg/ml) in artificial seawater to label the newly deposited calcium carbonate and thus visualize the biomineralized structures during the early stages of arm regeneration. Calcein was replenished every day together with adding fresh ASW throughout the duration of the observation period. The animals were washed in filtered seawater several times and anaesthetized in the magnesium chloride solution prior to imaging.

2.3 Paraffin wax embedding and sectioning

For histological sections arms were fixed in Bouin's solution for a few weeks until complete de-calcification was observed. Prior to embedding the samples were washed with distilled water until arms stop releasing fixative and dehydrated in Ethanol. Other samples for sectioning were fixed as usual and de-calcified in 0.5M EDTA for at least 1 day. Arms where then de-hydrated in graded ethanol washes (30%, 50%, 70% 2x 100%). Next, the samples were washed twice in Histoclear (Fischer-Scientific) at room temperature and a third time at 60°C, all washes 15 minutes each. Samples were then washed three times with paraffin wax (Thermo Scientific) at 60°C (30 minutes each) and during the last wash they were placed in the appropriate position and orientation before the wax was allowed to solidify overnight. The next day samples were mounted unto wooden blocks and sectioned (5-10µm thickness) using the Leica RM2155 microtome. Slides containing sections were dried overnight and then sequentially washed twice

in Histoclear, twice in 100% ethanol and then slowly re-hydrated in 95%, 80%, 70%, 50%, 30%, 20% ethanol washes. Finally, the slides were washed twice in deioinized water (or DEPC-treated if meant for further *in situ* hybridization processing) and either processed further or cover-slipped for imaging.

2.4 Milligan's trichrome staining

The Milligan's trichrome technique was used for staining the Bouin's fixed regenerating arm samples for histology. The cut sections were dried on slides overnight as described before and then washed twice in Histoclear (15 minutes and 5 minutes respectively). The slides were then placed twice for 2 minutes in 100% ethanol and once in 95% ethanol. The slides were then incubated in a solution of three parts 3% potassium dichromate to 1 part 10% HCL in 95% ethanol for 5 minutes and washed out with distilled water. Next the slides were stained with 0.1% acid fuchsin for 3 minutes and washed again with distilled water. Slides were then put in 1% phosphomolybdic acid for 3 minutes and stained with orange G for 5 minutes, then washed off with distilled water. For the final staining the slides were incubated in 1% acetic acid for 2 minutes, stained with fast green for 8 minutes and washed again in acetic acid for 3 minutes. The slides were then de-hydrated again in the 95% and 100% ethanol and put in Histoclear before mounting the slides with a coverslip using Histomount (National Diagnostics) for imaging.

2.5 EdU cell proliferation assay

The cell proliferation assay was carried out using the Click-iT® EdU HCS Assay (Invitrogen). Two types of experiments were done using this technique. Pulse experiments revealed a snapshot of the extent of proliferation visible at any given time point. Pulse and chase experiments on the other hand, showed what fate the labelled cells acquire over time and where they migrate. In this latter type the cells are labelled with EdU and left for a specific time period before fixation and visualization. In pulse experiments arms at different regeneration stages (and non-regenerating) were incubated in 5μM EdU in FSW for 2h followed by the standard fixation method. The arms were then washed with 1x PBT a few times and permeabilized for 1h in PBS-T (1x PBS with 0.1% Triton X-100). After two more PBT washes 100μl of the reaction cocktail was added to the samples for 30 min (made according to manufacturer's instructions and using kit reagents). The solution was then removed and the samples were washed for 30 min in Click-IT reaction rinse buffer. The buffer was then also removed followed by two PBT washes and finally DAPI was added. For pulse and chase experiments whole animals were labelled with 5μM EdU in FSW for 2h, washed out and then arms were amputated to yield blastema-staged arms after 4-6 days. The animals were left to regenerate for a required time period after which arms were collected, fixed and the visualization of the stain was carried out as described.

2.6 Immunohistochemistry

Arms fixed in 4% PFA and stored at -20°C in methanol were rehydrated with 5 PBS-T washes (1x PBS with 0.1% Triton X-100). The samples were

then incubated for 30 min at room temperature in blocking solution (1x PBS-T, 4% goat serum) followed by an overnight incubation in blocking solution containing a 1:500 dilution of the primary antibody. The next day the arms were washed again 3 times in PBS-T, before the addition of the secondary antibody at 1:250, and incubated for 2h at room temperature. Lastly, samples were washed with additional 3 PBS-T washes.

2.7 Identification of candidate skeletogenesis genes

Candidate genes for skeletogenesis were chosen based on two approaches. One was finding orthologs to well-known sea urchin skeletogenic GRN transcription factors, signalling molecules and downstream differentiation genes in the *A. filiformis* embryonic (https://brittlestar.shinyapps.io/Amphiura-filiformis, Dylus et al submitted) and regenerating arm (Purushothaman et al., 2015) transcriptomes using the BLAST tool and highest similarity sequence scores. The second was to use the genes identified in a differential screen transcriptome of *A. filiformis* embryos treated with SU5402 and controls, which determined genes upregulated, downregulated and unaffected in the FGF signalling inhibited samples (David Dylus, unpublished). This screen identified a set of novel brittle star genes and genes with unknown function downstream of FGF signalling.

2.8 Total RNA extraction and cDNA synthesis

For RNA extraction ~30 arms from 15 different individuals at required stages were put in RLT buffer (Qiagen) for lysis and stored at -80°C. Figure 2.1 shows a schematic of the collection of tissue at different stages of regeneration. For non-regenerating arms one segment was cut from each arm. Similarly for stage 1 arms at different time points (24hpa, 48hp, 72hpa) only the last segment before the amputated site was collected. For stages 3-5 only the regenerating bud was collected with no additional stump tissues. Finally, for the 50% DI stage arms 5 segments from the proximal side of the regenerate closest to the stump and 5 segments from the distalmost side (excluding the distal cap) were collected corresponding to the most undifferentiated tissues. The RNeasy Micro Kit (Qiagen) was used to extract RNA according to the manufacturer's instructions. Final RNA concentration was checked using the spectrophotometer. RNA was used for the Nanostring nCounter analysis or alternatively the cDNA was synthesized for use in cloning. cDNA was synthesized using the iScript™ cDNA synthesis kit (BIO-RAD) or the RETROscript® Reverse Transcription Kit (Ambion) according to instructions and the PCR was carried out at the following cycling conditions: 1 cycle of 25°C for 5 min, 42°C for 30min and 85°C for 5 min then cooled down to 4°C. The cDNA was diluted to a final concentration of 10ng/µl for cloning or 2.8ng/µl for QPCR.

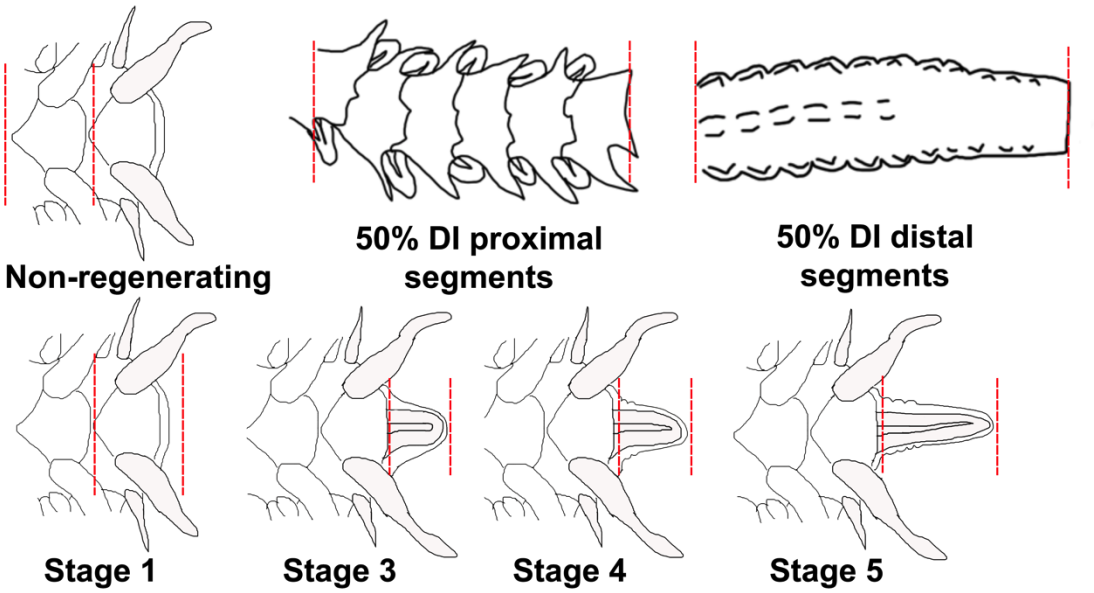

Figure 2.1: Schematics showing method of regenerating arm sampling for RNA extraction at different time points. Red dashed lines show sites of amputation.

2.9 Primer design, PCR and cloning

Primers were designed using the Primer3 software (http://primer3.ut.ee/) default parameters with a few exceptions. The product length was adjusted to fit the template sequence (±200bp) for cloning primers (Appendix **Error! Reference source not found.**), the max poly-x was c hanged to 3.00 and the max 3' stability was changed to 8.00. Designed primers were then ordered from MWG eurofins (http://www.eurofinsgenomics.eu). The genes of interest were amplified using the C1000 Thermal Cycler PCR machine and those specifically designed primers. The High Fidelity PCR system (Roche) was employed according to manufacturer's instructions and the cycling conditions were as follows: 1 cycle 95°C for 5 min, 35 cycles 95°C for 30 sec, 45-65°C for 30 sec and 72°C for 1min/kb fragment, 1 cycle 72°C for 7 min, 4°C till end. The PCR

fragment was then purified using the NucleoSpin® Extract II kit (Macherey-Nagel) and eluted in 20µl. The sample was then tested using gel electrophoresis for the correct molecular weight and spectrophotometer (NanoDrop) for DNA concentration. After PCR the DNA fragment was ligated into the pGEM®-T Easy vector (3kb) (Promega) according to manufacturer's instructions. DNA was added in a 1:6 ligation ratio with the plasmid and left at 15°C overnight before transforming competent *E. coli* cells (Invitrogen™ Subcloning Efficiency™ DH5α™) with the vector. The vector was added, then the cells underwent 42°C heat shock for 20 sec and were incubated in an agitator rocking at 225rpm for 1h at 37°C. Bacteria where then plated on x-gal (0.02%) and ampicillin (0.1%) containing agar plates for antibiotic resistance and blue/white screening. Suitable colonies were grown in 4ml of ampicillin-containing Luria Broth (LB) overnight in an agitating incubator at 225rpm at 37°C. The following day plasmids were purified from the bacteria using the NucleoSpin® Plasmid kit (Macherey-Nagel) and glycerol stocks were created for long-term storage at -80°C. Insertion of the correct fragment was tested using a restriction enzyme digest (*EcoR1*, Promega) and sequencing.

2.10 *In vitro* antisense probe preparation

Template DNA for *in vitro* probe transcription has been prepared using PCR. Taq polymerase and reagents from Invitrogen were employed together with M13 forward and reverse primers according to manufacturer's instructions and miniprep DNA was diluted to 1ng/µl. The cycling conditions were almost identical to the previous PCR program (except 30 cycles instead

of 35) with the hybridization temperature adjusted to 55°C and the extension time adjusted again to fragment length. The template DNA was purified using the NucleoSpin® Extract II kit, detected on an electrophoresis gel and checked for concentration on the NanoDrop. Probes were synthesized from the template using the correct polymerase (Sp6 or T7 from Roche, depending on orientation in vector) to yield the antisense RNA and in the presence of a DIG (digoxigenin) or DNP (dinitrophenyl) labelling hapten molecule. A 10x transcription buffer (Roche) and an RNAse inhibitor (Roche) were also added to the reaction and the DNA was transcribed from 2-5h at 37°C. After this time 1µl of RNAse free DNAse 1 and 2µl of 10x buffer (Roche) were added for another 15 min. Next 30µl of DEPC-treated water and 25µl of $LiCl_2$ were added to precipitate the sample overnight at -20°C. The following day the sample was centrifuged for 10 min at maximum speed, washed with 80% ethanol, vortexed and centrifuged again to obtain the RNA pellet. The supernatant was removed and the pellet was re-suspended in 50µl of DEPC-treated water and diluted to a working concentration of 50ng/µl.

2.11 Whole mount *in situ* hybridization

Two protocols were developed for chromogenic and fluorescent ISH. For both techniques the animals were first re-hydrated with graded ethanol washes (70%, 50% and 30%). The arms were then washed three times in 1x MA Buffer with Tween (MABT; 0.1M Maleic Acid pH 7.5, 0.15M NaCl, 0.1% Tween-20) and pre-hybridized in hybridization buffer (50% deionized formamide, 10% PEG, 0.05M NaCl, 0.1% Tween-20, 0.005M EDTA, 0.02M

Tris ph 7.5, 0.1mg/ml yeast tRNA, 1x Denhart's solution, DEPC-treated water) for 1h at 50°C. Next the arms were put in HB containing 0.2ng/µl antisense probe for 3-7 days at 50°C. Following this period of time the arms were post-hybridized in fresh HB without probe for three hours at 50°C, then washed once in MABT at 50°C and once at room temperature. The samples were then washed three times in 0.1x MABT and then once more with 1x MABT before placing them in blocking solution (MABT, 5% goat serum) for 30 min. The arms were then incubated in 1:1000 anti-DIG AP or anti-DIG-POD antibody solution overnight at 4°C (AP for alkaline phosphatase chromogenic detection and POD for horseradish peroxidase fluorescent detection). Next, the sample was washed 5 times in MABT and 2 times in alkaline phosphatase buffer (Tris pH 9.5, $MgCl_2$, NaCl, Tween-20, levamisole, milliQ water) before adding the staining solution (AP buffer, 10% DMF, 2% NBT/BCIP) for the chromogenic detection. The staining was stopped with MABT washes. Fluorescent staining was performed using the TSA kit by placing arms in amplification reagent for 15 minutes and staining in 1:400 Cy3/Cy5 fluophore for 15 minutes. After washing out the staining solution with 4 MABT washes, DAPI was added for nuclei labelling at 1:5000 (stock concentration 5mg/ml).

2.12 Nanostring nCounter

Nanostring nCounter analysis system (Nanostring Technologies, Seattle, WA, USA) (Geiss et al., 2008) was used for a large-scale quantitative gene expression study. A 123-probe code set was designed based on *A. filiformis* sequences, including six different internal standard

genes (for full list see Appendix Table A.0.2). Genes from different potential functional categories were used for a broad analysis including transcription factors, signalling molecules and genes implicated in cell cycle, neuronal specification and skeletogenesis. Additionally, several genes with unknown functions were selected for analysis based on transcriptomic data obtained in a screen of FGF treated embryos (David Dylus, unpublished). For each embryonic and adult regenerating arm experimental sample, 100ng of total RNA was used, which was extracted from 300 embryos and 10 regenerating arms respectively using the RNeasy Micro Kit (Qiagen). The experiments and analysis were carried out according to manufacturer's instructions. Additionally, the results of the quantification were normalized using the chosen internal standard genes (normalization factor obtained from geometric mean analysis of each lane). For quantifying differential gene expression in perturbed samples a Log2 fold change between controls and treated samples was calculated. The Log2 of ±1 (reflecting a 2-fold difference in change of level of expression) was determined to be biologically significant in correspondence with previously published work (Cui et al., 2014).

2.13 Inhibitor treatments

Signalling pathway perturbations were done using commercially available chemical inhibitors. Arm explants were used for testing the effects of inhibitors on regeneration and skeletogenesis. Adult *Amphiura filiformis* arms were cut at a distance of 1cm from the disc and left to regenerate for 4 days. Arms were then cut again 5mm proximally to the initial amputation site to obtain explants, which were then transferred into 5ml petri dishes and left

for up to 24h to allow proximal wound healing before further manipulation. At stage 2 the inhibitor was added at an appropriate concentration and left for 24h. Samples in artificial filtered seawater (FSW) and 0.1-0.2% DMSO were used as controls. For determining phenotypic effects on spiculogenesis, live calcein (Sigma) staining was employed together with the inhibitor to label any newly forming spicules (see section 3.2.1 calcein staining). After the treatment the arm explants were imaged for any morphological phenotype and fixed for molecular analysis using Nanostring or ISH. A similar procedure was carried out for embryonic analyses. Embryos of *A. filiformis* were cultured as described before (Dupont et al., 2009; Dylus et al., 2016), the inhibitors were added at 18hpf (prior to skeletogenic mesoderm cell ingression) and the embryos were collected at 27hpf. The phenotype was checked between 27hpf until 4 days post-fertilization. The signalling pathway inhibitors used in this thesis were SU5402 (Sigma) for FGF signalling, and Axtinib (Sigma) for VEGF signalling. SU5402 were dissolved in DMSO for a stock concentration of 10mM and Axitinib was dissolved at 5mM. The final working concentration used for experiments was 10μM for SU5402 in regenerating arms, and 20μM for embryos. 200nM Axitinib was used in arms and 75nM in embryos.

2.14 EdU-labelled cell counting using Fiji

Regenerates treated with the SU5402 inhibitor were tested for changes in cell proliferation. The regenerates were labelled and stained following the procedure described above (section 2.5) then imaged using confocal microscopy. For each regenerate between ~100 ±10 slices were taken per Z-

stack (1µm thickness). DAPI-labelled nuclei and EdU-Labelled nuclei per stack were counted automatically using the Fiji plugin TrackMate (Tinevez et al., 2016). Number of EdU labelled nuclei ranged from 672/3375 to 1385/5205 total number of nuclei. The proportion of nuclei labelled with EdU compared to all nuclei labelled with DAPI was calculated as a percentage. Student's T-test was used and showed no significant difference between control (DMSO) and SU5402-treated samples (T-value = 0.261; $p>0.25$).

2.15 Microscopy techniques

The samples for microscopy, kept in 50% glycerol, were mounted onto microscope slides with cover slips over the top and sealed using nail varnish. For differential interference contrast (DIC) images as well as epi-fluorescent images the Zeiss AxioImager M1 microscope was used together with a Zeiss AxioCam HRc camera. For confocal images of fluorescently labelled samples the Leica SPE2 confocal laser scanning microscope was used and the LAS-AF software implemented to capture the image stacks. Images were processed using Adobe Photoshop CS4 and Fiji.

3 Characterization of the morphological stages, internal anatomy, skeletogenesis and proliferation in the regenerating arm of *Amphiura filiformis*

The aim of this chapter is to understand in more detail the process of regeneration of the *Amphiura filiformis* arm with an emphasis on skeleton formation and cell proliferation. First, I devised a staging system, which will be used throughout the thesis, for a more consistent analysis of the regeneration process; second, I characterized how the different components of the arm form during regeneration and the extent of cell proliferation during these stages.

3.1 Staging of early phases of regeneration based on morphological features

The development of a regenerating structure is a dynamic process that proceeds in a step-wise fashion to reconstitute a fully functional structure. To facilitate experimental investigation of arm regeneration in *A. filiformis* I identified five stages, which rely on observable morphological changes. Based on observations of ~100 individuals (three of which are shown in Figure 3.1) I refined the staging system (Figure 3.2), to make it relevant to the phases of regeneration when cell specification, differentiation and initial arm patterning begin to occur.

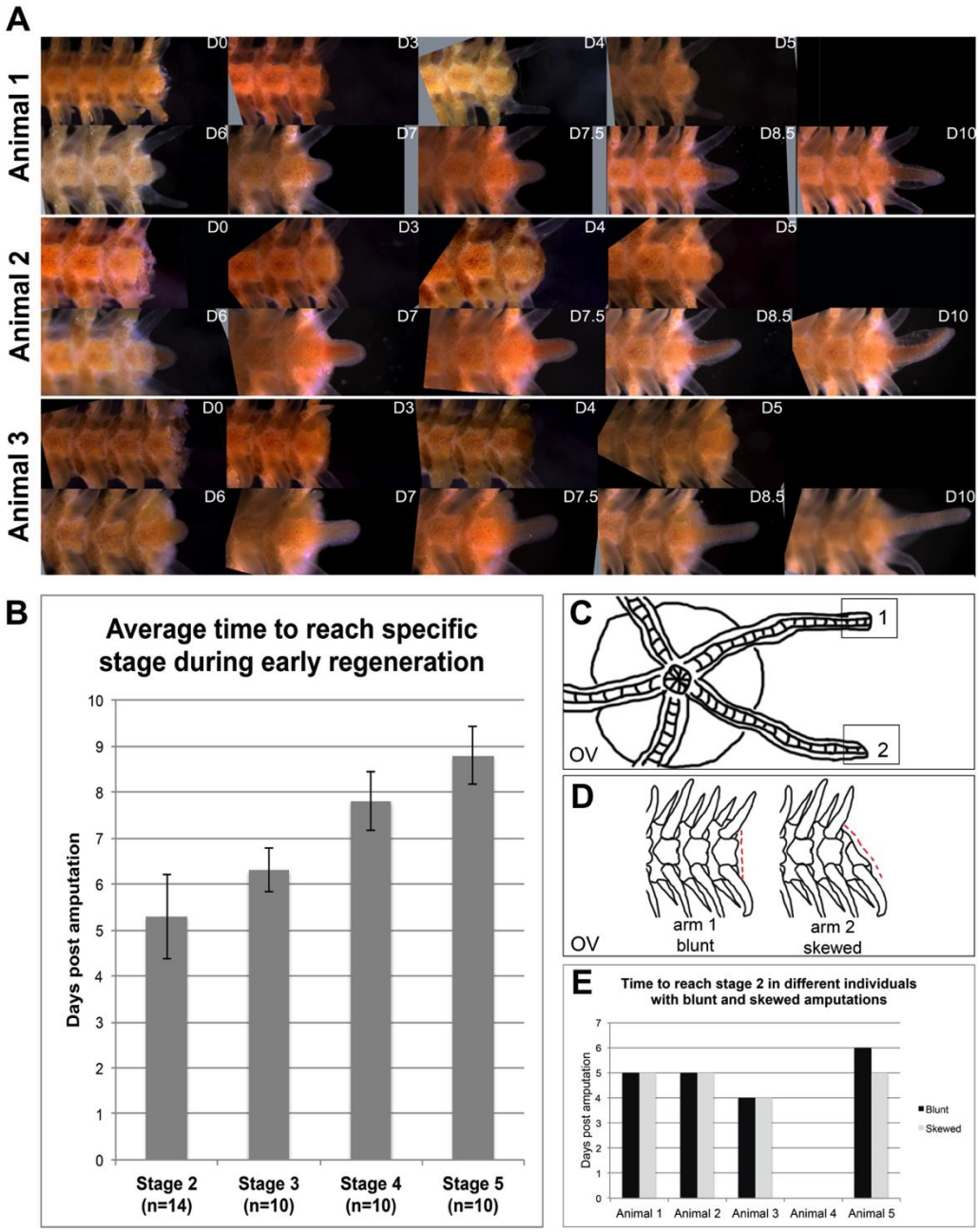

Figure 3.1: Staging of *A. filiformis* early arm regeneration based on morphological landmarks. A) Brittle star arms showing individual variability in the regeneration rate. B) Graph showing averaged temporal variability for arms to reach various stages (2, 3, 4, and 5) of regeneration. Error bars show standard deviation. C-E) Experiment conducted to address the effects of amputation on regeneration rate. C) Schematic diagram of the oral side of an adult *A. filiformis*. Top arm has a blunt and bottom arm has a skewed amputation plane. D) Schematic diagrams of blunt and skewed amputation planes of arms in C. E) Five individual animals of the same size were amputated 1cm from the main body disc and left to regenerate to stage 2. The graph shows individual animal variability in time to reach stage 2 but almost no difference between blunt and skewed amputated arms. Animal 4 did not regenerate at all during this time and died shortly after the experiment. *D – days post amputation*, *OV – oral view*.

The presence of clear morphological landmarks is supported by histological analysis carried out on paraffin sections stained with Milligan's trichrome technique (Milligan, 1946), which detects collagen (cyan) and individual cells (pink/magenta) (see schematic in Figure 3.3; Figure 3.4 and Figure 3.5). The average duration and standard deviation (S.D.) of time it takes for an arm to regenerate up to a given morphological stage is reported in Figure 3.1. The timing of regeneration shows a certain degree of variation in agreement to what has previously been reported (Dupont and Thorndyke, 2006). All of the stages and corresponding average timings have been compiled based on arms amputated 1cm from the central disc. I categorize stage 1 of regeneration as wound healing and re-epithelialization. This phase occurs between 1 and 4 days post-amputation (dpa) (Figure 3.1 and Figure 3.2) and involves changes which mediate the closure of the wound and re-epithelialization and remodeling of the existing tissue; however, from whole mount DIC (differential-interference contrast) observations little or no changes are evident at the amputation plane. On the contrary, at this stage histological sections show (Figure 3.4) the aboral coelomic cavity (ACC), the ectoneural sinus (ES) and the radial water canal (RWC) are sealed off and the wound is completely re-epithelialized by epidermal cells, already covered by a thin and faint cuticle indicated by the asterisk in Figure 3.4 A'. The intervertebral muscles adjacent to the amputation site acquire a disorganized pattern and show morphological signs of histolysis: myocytes lose their elongated shape (Figure 3.4 A'' and B).

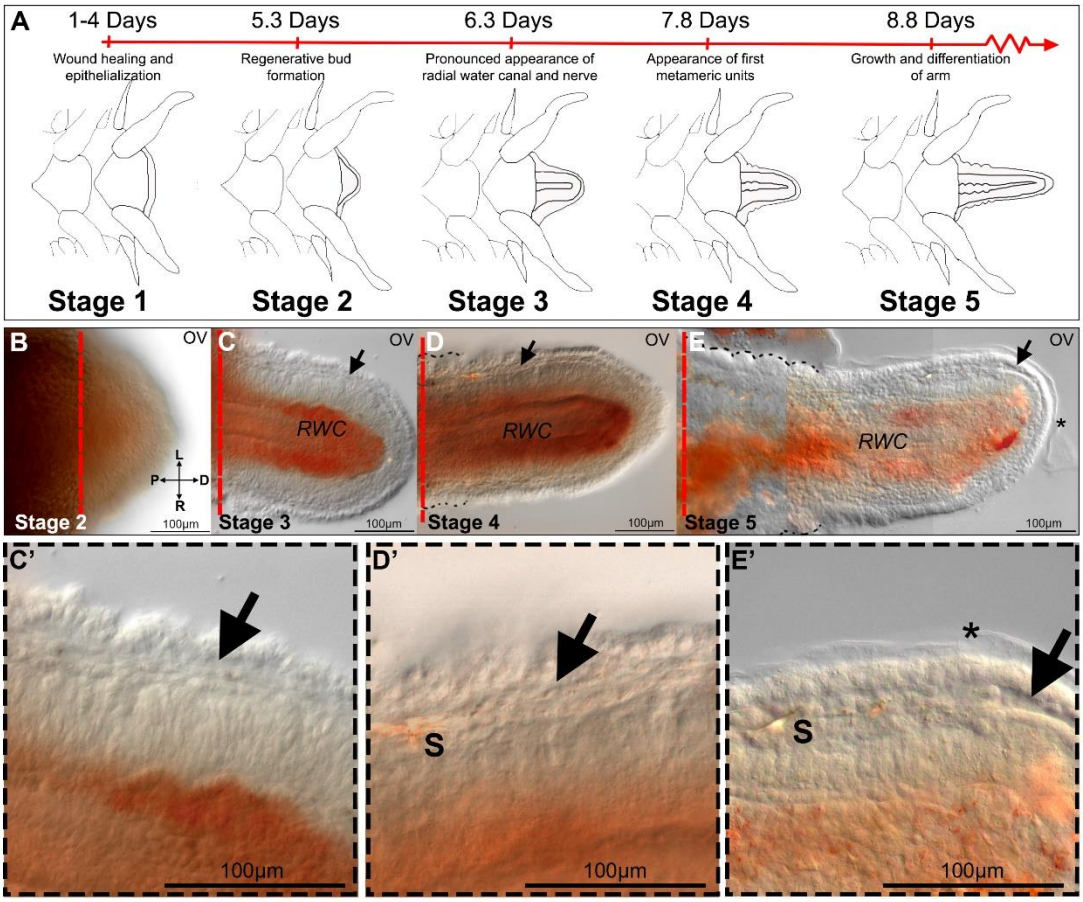

Figure 3.2: Early stages of arm regeneration in the brittle star *Amphiura filiformis*. A) Schematic diagram of early arm regeneration stages and average timing to those stages, based on morphological landmarks. Stage 1 - wound healing and re-epithelialization. Stage 2 - regenerative bud formation. Stage 3 - appearance of the radial water canal, coelomic cavities (aboral coelomic canal, ectoneural and hyponeural sinuses) and radial nerve in the regenerative bud. Stage 4 - appearance of first metameric units (arm segments). Stage 5 - advanced extension of arm, formation of several metameric units at proximal end. B–E) Oral view of fixed arms at stages 2 (B), 3 (C), 4 (D) and 5 (E) shown using DIC microscopy. C') Detail of C focusing on dermal layer. D') Detail of D. E') Detail of E. *Arrows - the dermal layer, asterisk - cuticle, D - distal, L - left, OV - oral view, P - proximal, R - right, RWC - radial water canal, S – spicule.*

The duration of time between amputation and stage 2 shows the highest variability (Figure 3.1). To assess whether the type of traumatic amputation might have an effect on the rate of the wound healing stage and the appearance of a regenerative bud, I amputated two arms from the same animal: one clean, blunt amputation similar to natural autotomy, and the other skewed (amputation at an angle; Figure 3.1 C-D). I used 5 animals of the same size to minimize the individual variability and we documented the process of regeneration of each arm for 10 days. The data reported in Figure 3.1 E reveals a general inter-individual variability in time to reach stage 2, which is not related to the type of amputation.

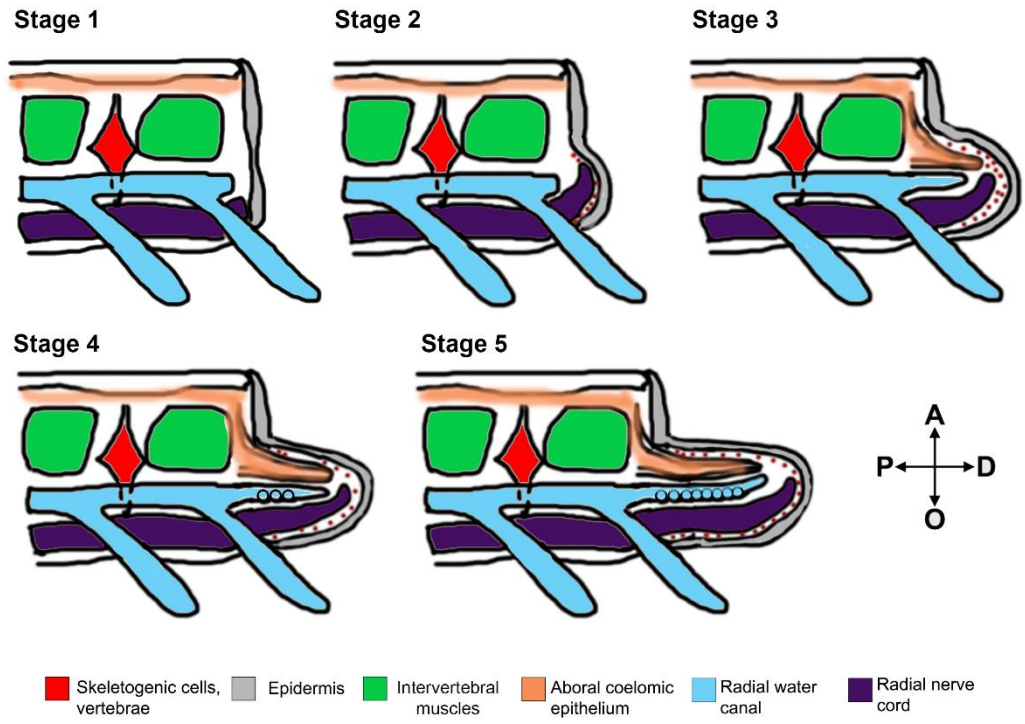

Figure 3.3: Schematic representation of early arm regeneration stages showing two segments of the non-regenerating stump and the regenerating bud at its distal end as observed in sagittal sections. *A – aboral, O – oral, P – proximal, D – distal.*

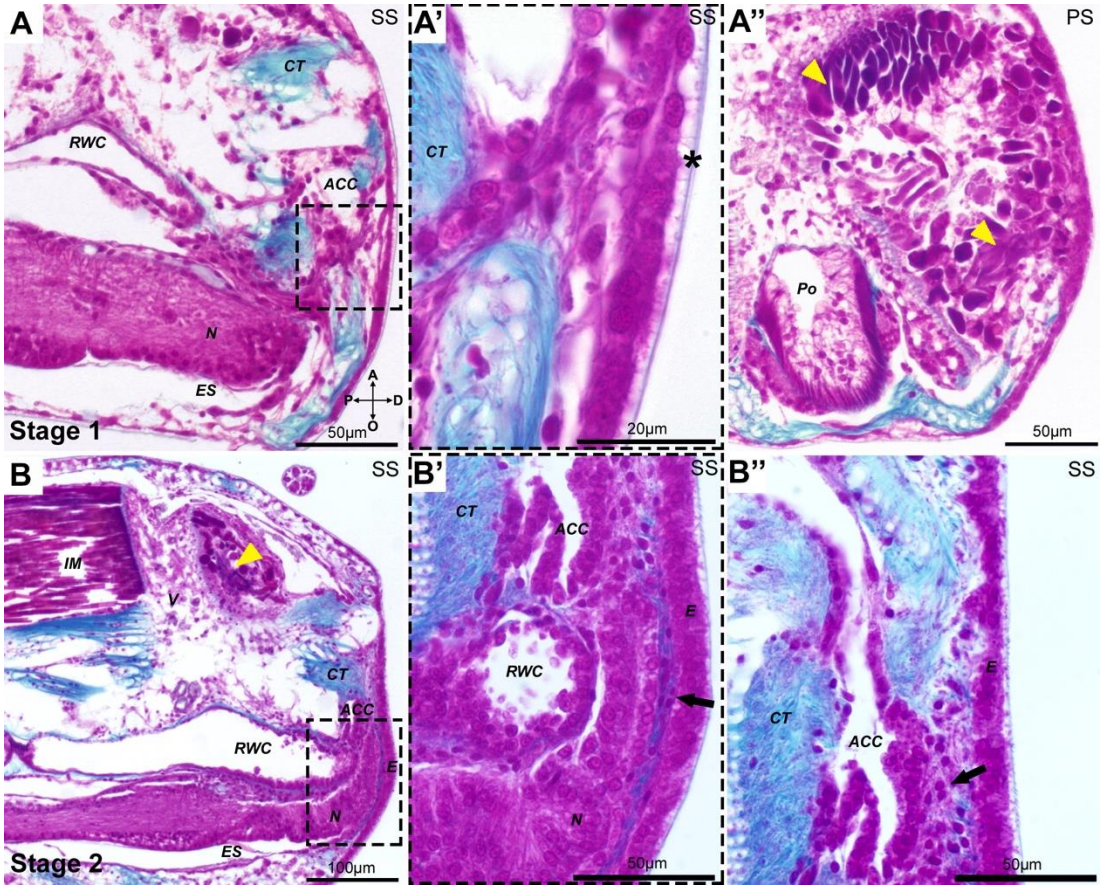

Figure 3.4: Histological sections of the earliest stages of arm regeneration in the brittle star *Amphiura filiformis*. Sagittal (A and A') and parasagittal (A") paraffin sections at stage 1 and sagittal paraffin sections at stage 2 (B) stained with Milligan's trichrome technique. Collagen stained cyan, all cells labelled pink/magenta. A) The wound is completely healed and re-epithelialization occurs. A') Detail on the new thin epithelium with a recognizable cuticle (asterisk). A") Histolysis (arrowheads) of intervertebral muscle bundles proximal to the amputation plane. B) The radial nerve, the radial water canal and the coelomic cavities start regenerating beneath the new epidermis. B') Detail of the mesenchymal cells (arrow). B") Detail of the mesenchymal cells at the level of the aboral dermal layer (arrow). *A - aboral, ACC - aboral coelomic cavity, CT - connective tissue, D - distal, E - epidermis, ES - ectoneural sinus, intervertebral muscles - IM, N - radial nerve, O - oral, P - proximal, Po - podia, PS - parasagittal section, RWC - radial water canal, SS - sagittal section, V – vertebra.*

Once re-epithelialization is accomplished, a small regenerative bud protrudes from the distal end of the stump, in the oral region (Figure 3.1 and Figure 3.2). I defined this as stage 2, which occurs on average after 5.3 dpa ±0.91 S.D. (Figure 3.1). From whole-mount differential interference contrast (DIC) observations the regenerate appears optically homogeneous (Figure 3.2), however histological sections indicate already a certain degree of organization, in which the first outgrowths of the regenerating radial nerve, radial water canal and the aboral coelomic canal are visible (Figure 3.4). A thin layer of connective tissue is present below the wound epidermis where mesenchymal cells are embedded (Figure 3.4 B' and B'').

Stage 3, which occurs on average 6.3 dpa ±0.48 S.D. (Figure 3.1 and Figure 3.2), differs from stage 2 in that the regenerate acquires a more organized and complex inner architecture with loss of the external optical homogeneity; at this stage the radial water canal and the sub-epidermal mesenchymal cells become clearly visible in whole mount DIC images (Figure 3.2 C and C'). Histological sections show the regenerate mainly contains projections of the re-growing radial nerve, radial water canal and aboral coelom, which protrude from the amputation plane (Figure 3.5 A and A''). Mesenchymal cells embedded in collagenous tissues can be detected throughout the dermal layer (Figure 3.5 A' and A'').

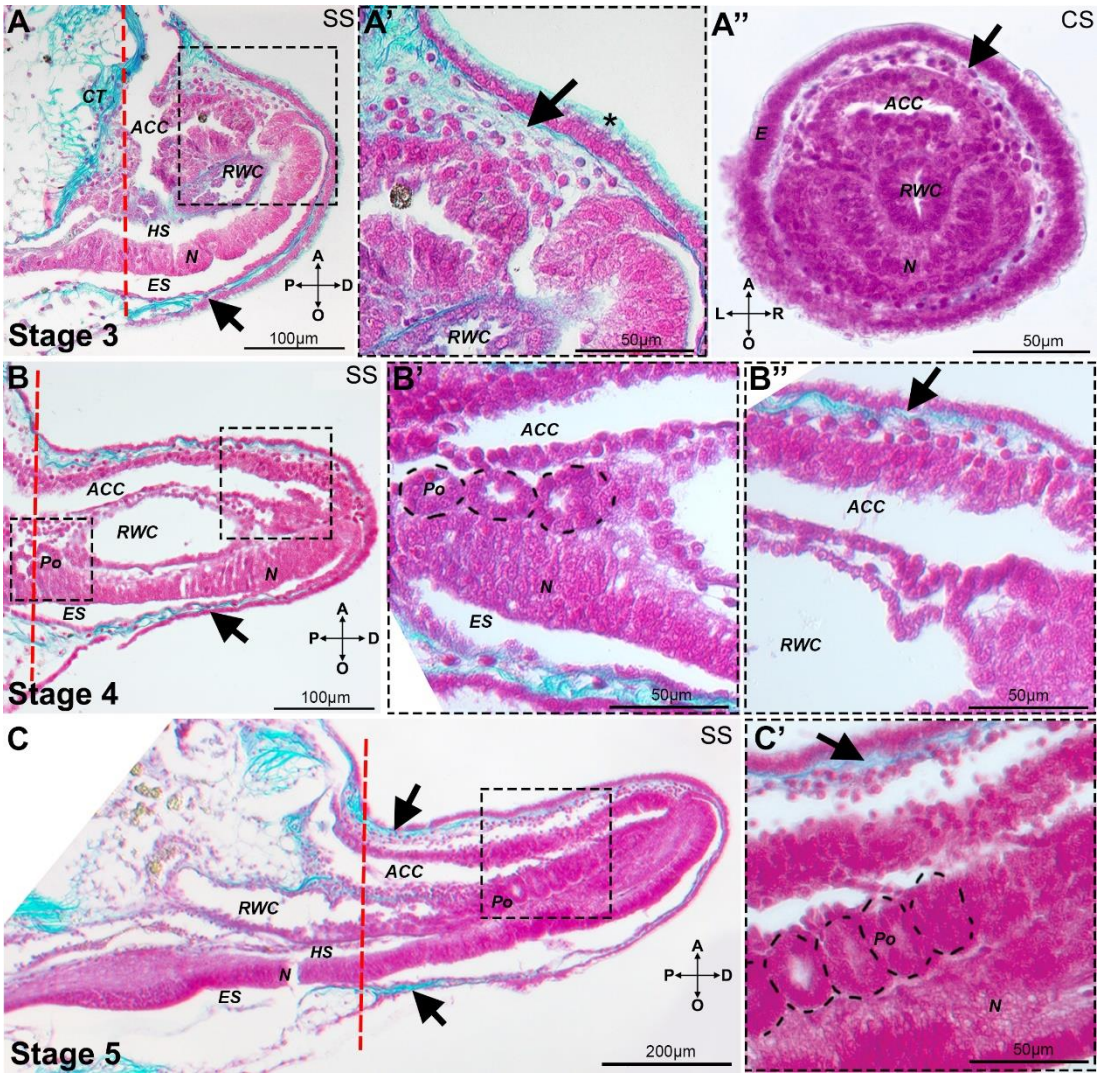

Figure 3.5: Histological sections of regenerating arms at stages 3, 4 and 5. Sagittal and transverse paraffin sections at stage 3 (A and A"), and sagittal sections of stages 4 (B), and 5 (C) stained with Milligan's trichrome technique. Collagen stained cyan, all cells labelled pink/magenta. Red dashed line indicates amputation plane. A) The three regenerating axial structures are enveloped by the dermal layer (arrow) and the new epidermis. A') Detail of A showing mesenchymal cells at the level of the aboral dermal layer (arrow) covered by the new epidermis with its cuticle (asterisk). A") Transverse section of a stage 3 regenerate showing the dermal layer (arrow), developing radial nerve, radial water canal and aboral coelomic cavity. B) The stage 4 regenerate is longer and the radial water canal shows the first signs of podia regeneration. B') Detail of B showing the developing podia (dotted line). B") Detail of B showing the scattered mesenchymal cells in the aboral dermal layer (arrow). C) Further development and differentiation of the three axial structures at stage 5. C') Detail of developing podia (dotted line). *A - aboral, ACC - aboral coelomic cavity, CT - connective tissue, D - distal, E - epidermis, ES - ectoneural sinus, HS - hyponeural sinus, L - left, N - radial nerve, O - oral, P - proximal, Po - developing podia, RWC - radial water canal, R - right, SS - sagittal section, CS - cross section.*

I define stage 4 (on average 7.8 dpa ±0.63 S.D., Figure 3.1 and Figure 3.2) by the appearance of the first metameric unit, which is formed at the most proximal region of the developing regenerate. A small bulging of the epidermis reveals the early segregation of the regenerating segments (dotted lines, Figure 3.2 D). Outpocketing of the radial water canal system, which will eventually form the podia, can start to be distinguished in histological sections (Figure 3.5 B and B').

Finally, stage 5 occurs on average after 8.8 dpa ±0.63 S.D. (Fig. Figure 3.1 and Figure 3.2). This stage is characterized by several small repetitive units, which can be observed bulging at the proximal side (dotted line, Figure 3.2 E) with several podia precursors beginning to form along the new regenerate (Figure 3.5 C and C').

As the regeneration process progresses metameric units form sequentially at the proximal end. The late regeneration stages that I refer to in this thesis corresponds to the 50% (2-3 weeks post-amputation) or 95% (4-5 weeks post-amputation) regeneration stages described before (Dupont and Thorndyke, 2006). These arms have a 50% or 95% differentiation index (DI), which is the ratio between the length of the arm that contains differentiated structures (like spines and podia) and the total regenerate length (Figure 3.6). The duration of regeneration time is highly variable between stage 5 and the 50% stage depending on many aspects including length of arm lost, functional requirements, animal size or environmental factors (Dupont and Thorndyke, 2006). When the arm reaches the 50% differentiation stage (Figure 3.6 A) a number of metameric units are added at the proximal end, which differentiate in a gradient-like manner. Therefore, at

this stage the metameric units are all at a slightly different developmental stage along the proximal–distal axis. The 95% stage is defined by the appearance of pronounced muscle and skeletal structures along the full length of the new arm with the exception of a few distal segments (Figure 3.6 B). The final regenerated structure contains all of the constituents of the adult non-regenerating arm. Interestingly, the distalmost end of the regenerate differentiates relatively early on into a pronounced cap-like structure (after stage 5) containing a terminal ossicle and a terminal podium (Figure 3.6 C and D), referred to here as the distal structure. Therefore, the growth zone, adding new metameric units, is likely positioned directly underneath this distal structure. This type of regeneration is consistent with the distalization-intercalation model discussed in the introduction.

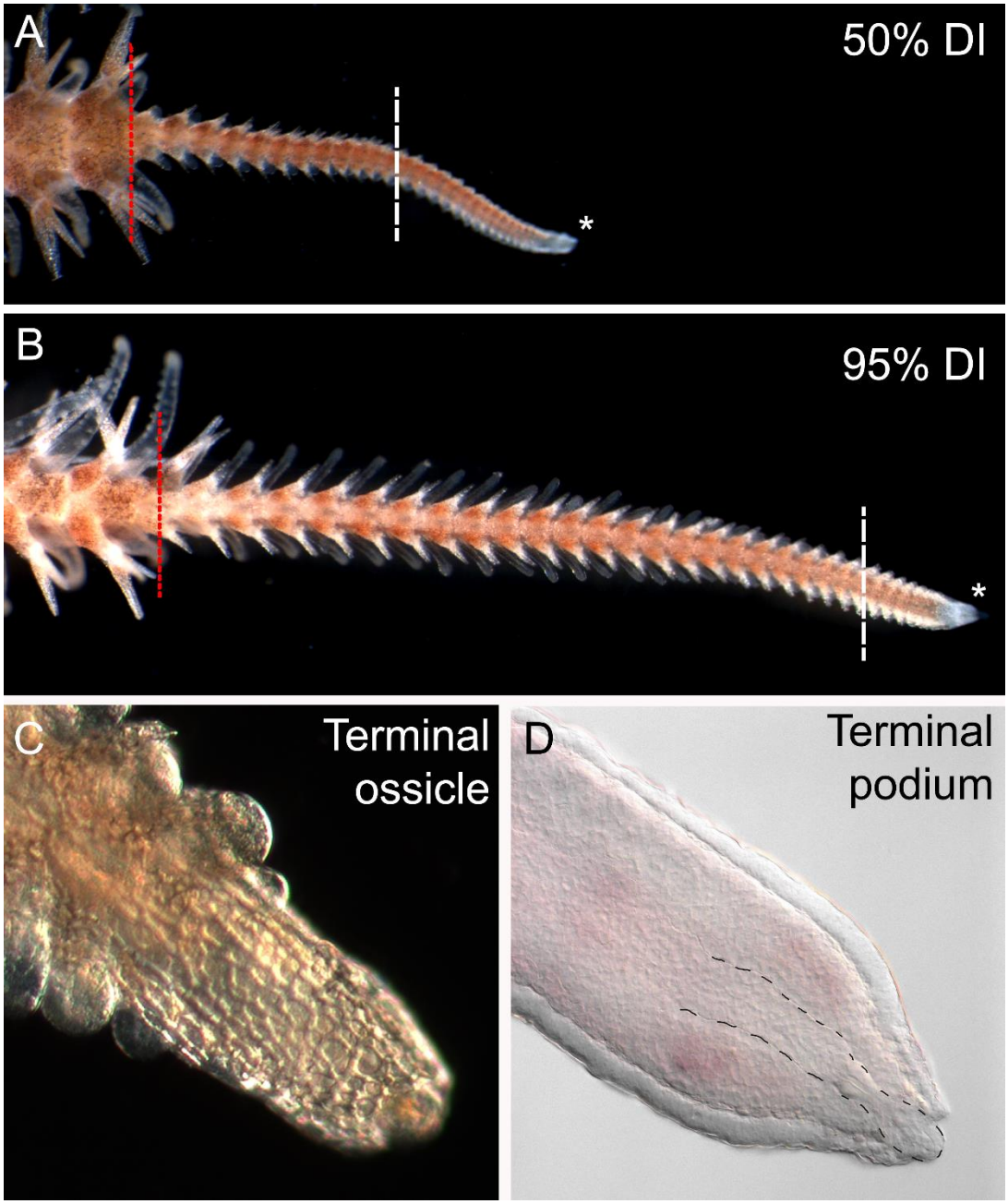

Figure 3.6: Late stages of arm regeneration in *A. filiformis*. A) 50% DI stage of arm regeneration showing a gradient of developing of the metameric units. B) The 95% DI arm has 95% segments with differentiated structures such as podia and spines. C) Magnification of the terminal ossicle located on the distal cap (asterisk) in 50% and 95% DI arms. D) Magnification of the terminal podium located in the distal structure (asterisk) of 50% and 95% DI arms. *Red dashed line – amputation plane. White dashed line – DI percentage cut-off.*

3.2 Skeletogenesis during early and late regeneration stages

To define when and where skeletogenesis occurs during early stages of regeneration in the brittle star arm I combined light transmission microscopy observations of whole regenerates with calcein staining to detect the newly forming mineralized skeleton. High magnification of the regenerates at different stages reveals that the single spicules form just below the well-developed epidermis in the dermal layer (Figure 3.7 A), corresponding to the position of the mesenchymal cells embedded in the collagenous matrix observed in histological sections (Figure 3.4 and Figure 3.5). Calcein is commonly used to visualize calcium carbonate deposition, which is shown as green fluorescence (Guss and Ettensohn, 1997). No fluorescence can be detected at stages 1 and 2 (Figure 3.7 B). Single spots of green fluorescence, corresponding to the forming skeletal primordia, are consistently first observed at stage 3 indicating the earliest stage at which differentiated skeletogenic cells are present (Figure 3.7 C, n=10). At stage 4 more elaborate tri-radiated or tetra-radiated skeletal elements (spicules) can be observed in the regenerate (Figure 3.7 C, n=10). At stage 5, the spicules present in the distal end of the regenerate have no obvious pattern of distribution. In contrast, skeletal elements in the newly forming metameric units, at the proximal end of the regenerate, are formed with a typical bilateral distribution (when observed in a frontal view) that corresponds to where the future lateral shields will be (Figure 3.7 C, n=10).

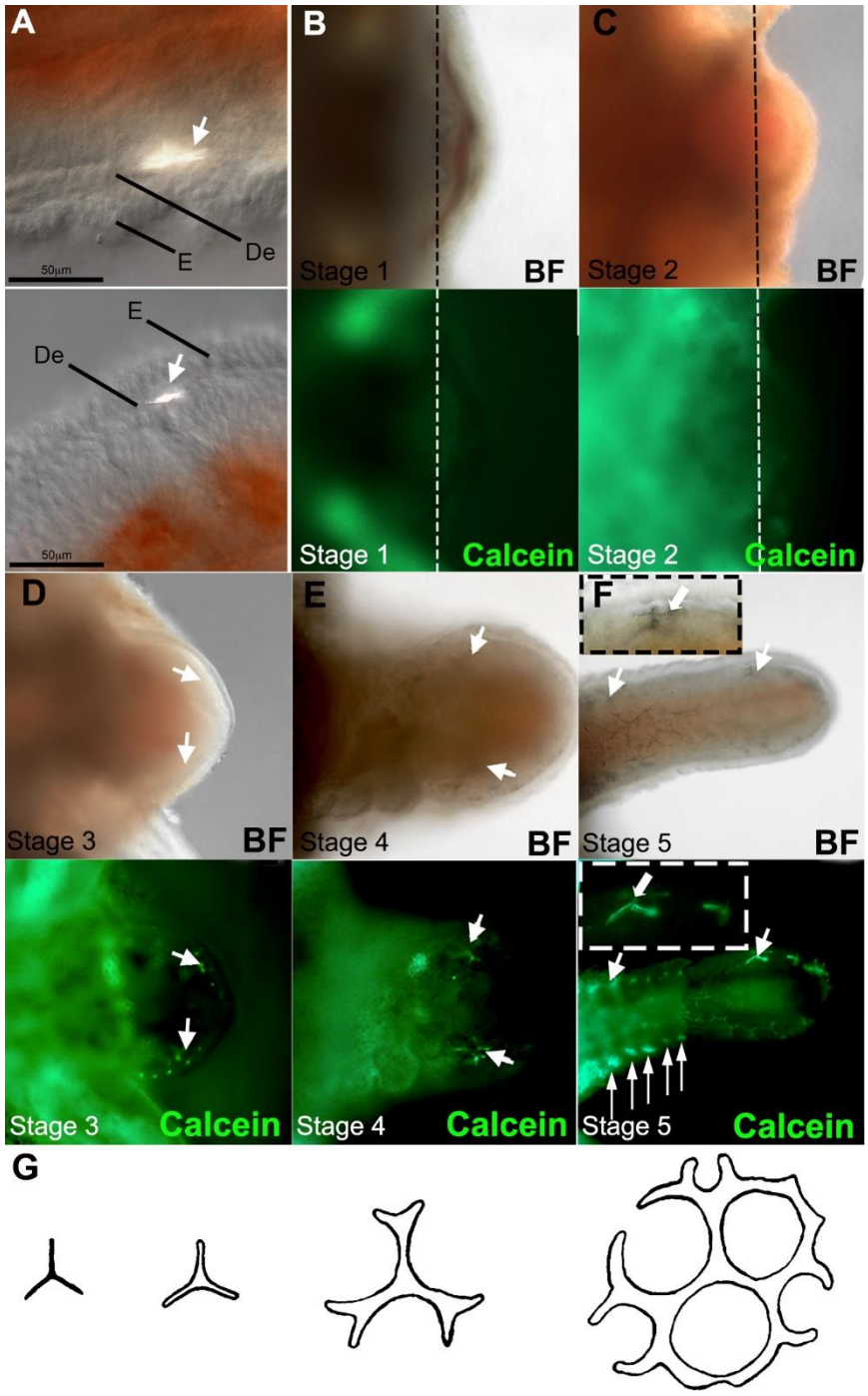

Figure 3.7: Skeletogenesis during early regeneration stages. A) High magnification DIC images showing single spicules localized in the dermal layer (arrow). B) DIC (top panels) and fluorescent images (bottom panels) of calcein-labelled spicules at stages 1, C) and 2 showing no skeletal elements labelled with calcein. Stages D) 3, E) 4 and F) 5. Insets show detail of single spicules. G) Schematic of single tri-radiate spicule to stereom formation in echinoderm skeletogenesis (adapted from Kokorin et al, 2015). *BF – bright field. Arrows - spicules*, *Dashed line - amputation plane*, *E - epidermis, De - dermis.*

Later during regeneration, when the arm reaches the 50% stage (50% DI), the whole maturation of the developing skeleton can be observed (Figure 3.8) simply by analysis of subsequent metameric units from proximal (most mature skeleton) to distal (new elements) using light microscopy. This is due to the birefringent properties of calcified structures. At the distalmost end, the distal structure becomes highly calcified and constitutes the terminal ossicle. The first observable distal metameric unit already contains a tiny tri-radiated lateral spicule (Figure 3.8, first lateral spicule inset). Several metameric units (eight in Figure 3.8) separate the appearance of the first lateral spicules from the appearance of the first vertebral spicules, forming more proximally in the inner layers of the regenerating arm. Contrary to skeletal elements developing during early regeneration and at lateral positions during late regeneration, which always form multi-branched spicules, the vertebrae first appear as two long, non-radiated skeletal rods (Figure 3.8, first vertebral spicule inset). Later, as the skeletal elements mature, they also begin to branch out and the two parallel vertebral elements fuse together at the midline between distal and proximal ends of the metameric unit (Figure 3.8, advanced vertebrae inset). Oral and aboral shields begin to form approximately at the same level as the developing vertebrae (Figure 3.8, first aboral shield inset). In a distal to proximal gradient the segments contain increasingly complex spicule structures that will eventually form the stereom of skeletal ossicles, as is typical for echinoderms (Figure 3.8, advanced shield formation inset). The fully formed structures found in an adult non-regenerating arm are shown in Figure 3.8 (kindly provided by Laura Pioviani).

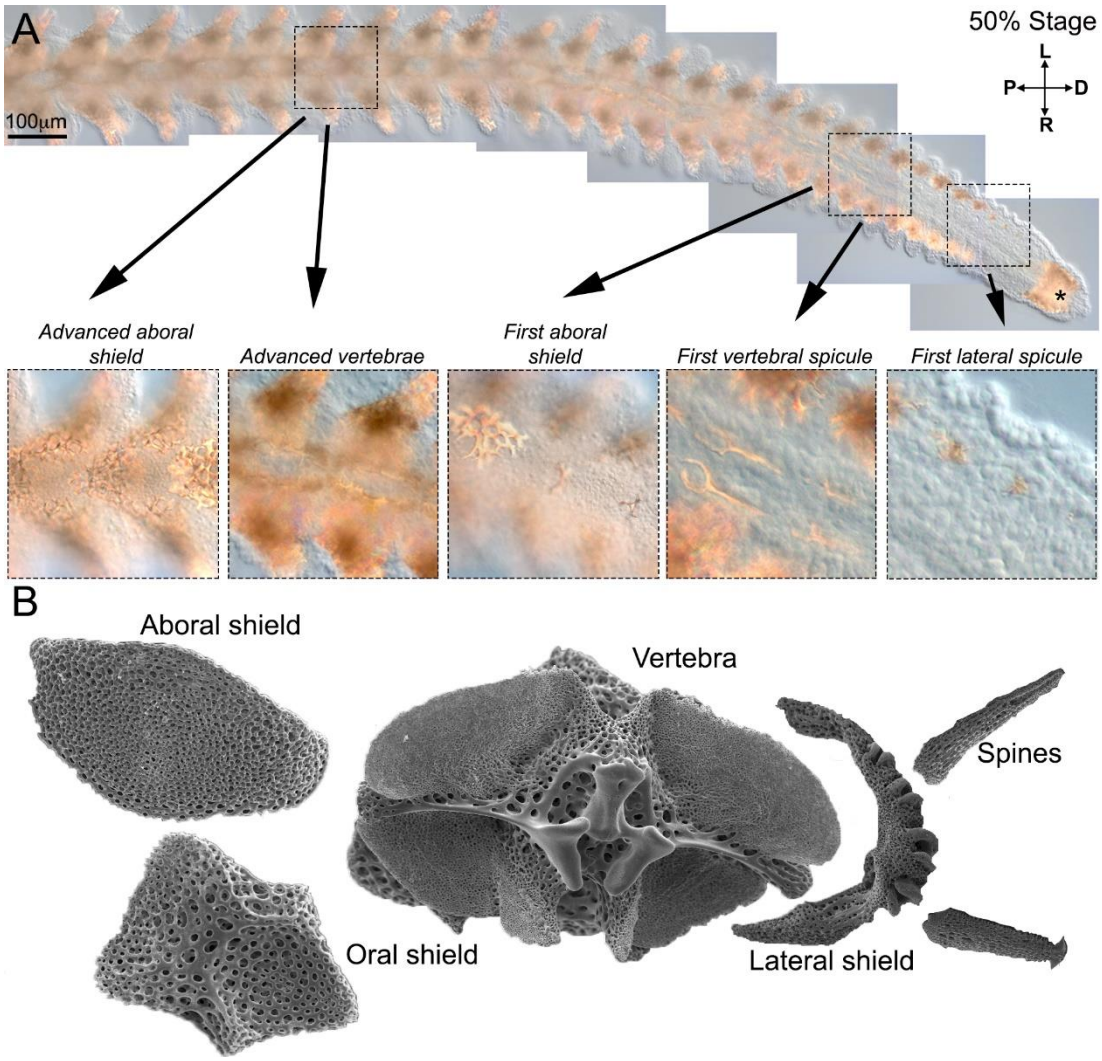

Figure 3.8: Skeletogenesis during late regeneration stages. A) 50 % differentiated arm showing the formation of the skeletal elements (reflective structures). The highly calcified distal cap (terminal ossicle) forms at the distalmost end of the regenerating arm. The spicules, which will form the lateral shields and spines, appear in the first metameric unit (see inset for detail). Proximally, eight metameric units later, first vertebral spicules can be observed (see inset for detail). At the proximal end of the regenerate skeletogenesis is already very advanced and forms the individual stereomic skeletal elements including the oral, aboral and lateral shields, spines and vertebrae (see insets for detail). B) SEM images of differentiated skeletal elements in an adult non-regenerating arm, namely the aboral shield, oral shield, vertebra, spines and lateral shield (kindly contributed by Laura Pioviani). *Asterisk - terminal ossicle, L - left, R - right, P - proximal, D – distal.*

3.3 *Afi-c-lectin* expression confirms molecular signature of skeletogenic cells in the dermal layer

To better characterize the cells involved in skeleton formation during regeneration in the brittle star I assessed the spatial expression pattern of the skeletogenic cell differentiation gene *Afi-c-lectin*. Expression patterns of other genes will be described in more detail in chapter 4. This gene, identified in an *A. filiformis* embryonic transcriptome, is an ortholog of the sea urchin C-lectin. This spicule matrix protein containing a C-type lectin domain is expressed specifically in the skeletogenic mesodermal cells (Illies et al., 2002). Proteomic studies identified the C-lectin protein as an integral part of biomineralized structures both in sea urchin larval spicules and adult test plates and spines (Mann et al., 2008a; Mann et al., 2010), and in ophiuroid adult arm skeletal elements of the species *Ophiocoma wendtii* (Seaver and Livingston, 2015). The expression of the *A. filiformis c-lectin* gene in the larval skeletogenic mesenchyme cells has been reported (Czarkwiani et al., 2016). I have therefore used it as a marker for skeletogenic cells in adult regenerating arms (Figure 3.9). It is first detected by *in situ* hybridization (ISH) at stage 2 of early regeneration in a broad sub-epidermal domain (Figure 3.9 A). It then becomes much more restricted to the dermal layer only by stage 4 (Figure 3.9 C). This is consistent with the developmental changes that occur between these two stages, when the regenerate acquires a more heterogeneous structure containing morphologically differentiated tissue types. Strong colorimetric staining has the tendency to diffuse in the tissue, rendering the precise boundary of expression not clearly distinguishable. To discriminate whether the expression of *Afi-c-lectin* is restricted specifically to

the sub-epidermal mesenchymal cell layer, where spicules form, or extends to other domains of the regenerate, I additionally performed a fluorescent ISH on regenerating arm sections. The expression of this gene is indeed specifically localized to a single cell layer just underneath the epidermis (Figure 3.9 B).

Next, I examined the expression of *Afi-c-lectin* in the 50% DI stage of the regenerating arm (Figure 3.9 D). In the distalmost-undifferentiated segments of the regenerate, *Afi-c-lectin* is expressed in the dermal layer similar to the early stages of regeneration. Towards the proximal side of the regenerating arm, its expression becomes more complex, corresponding to the formation and patterning of the different skeletal elements (Figure 3.9 D'). The scattered mesenchymal cells expressing the marker gene are arranged in regular and repetitive patterns, which mirror the pattern of the stereom structure of the oral, aboral, lateral shields with spines and vertebrae in each of the differentiating segments of the arm. The expression pattern of *Afi-c-lectin* thus coincides specifically with the location and time of appearance of the different skeletal elements; therefore confirming it as a reliable marker of skeletogenesis during regeneration as well as embryonic development. This is further supported by the expression pattern of *Afi-c-lectin* in the most advanced proximal segments of the 95% DI regenerating arms, where expression can be seen outlining the shape of the differentiated skeletal elements such as the vertebrae and spines (Figure 3.9 E-G). Unfortunately, the ISH technique dissolves the calcitic skeletal elements of the arm hindering the detection of spicules adjacent to the cells expressing this gene.

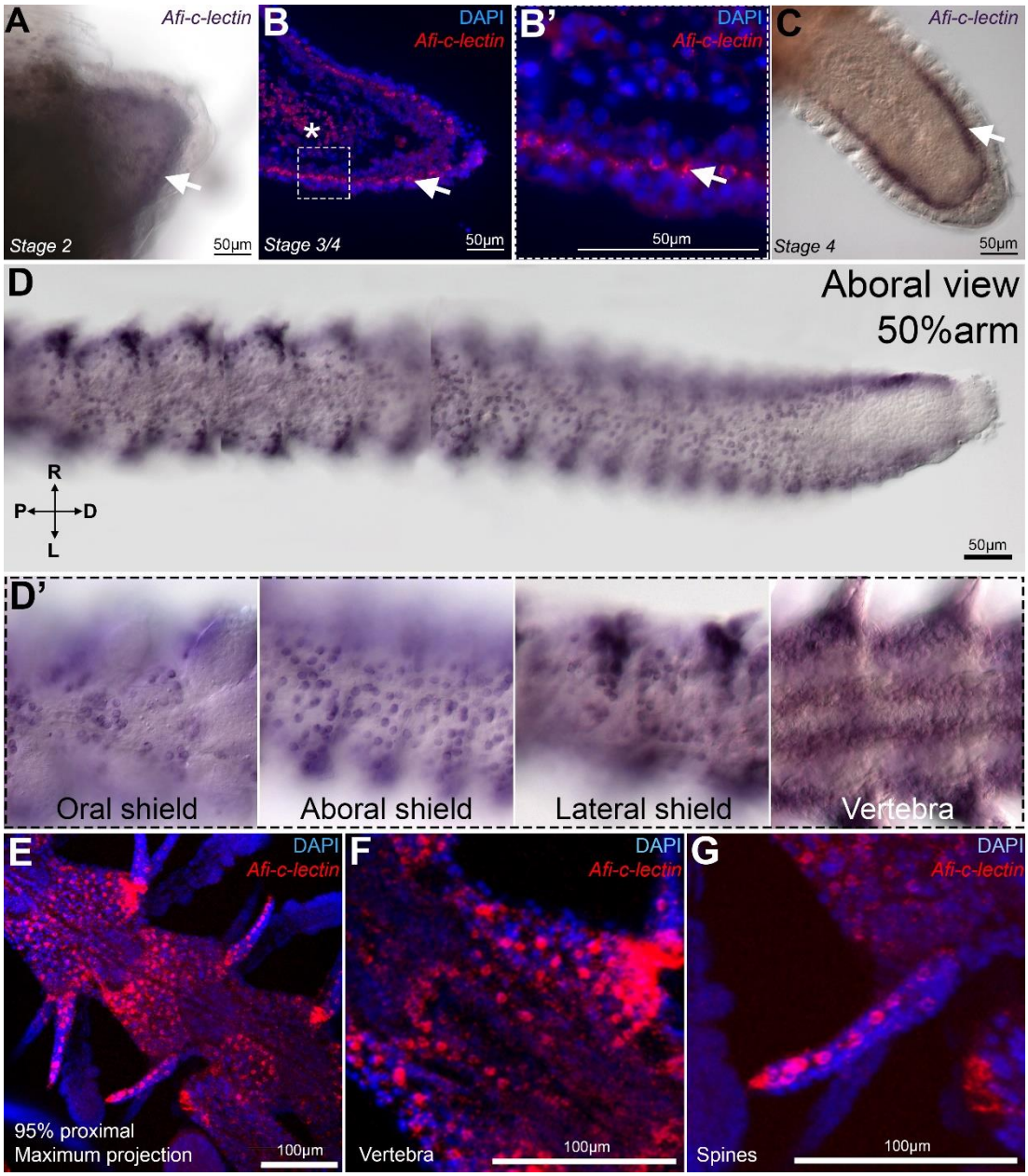

Figure 3.9: *Afi-c-lectin* expression during early and late arm regeneration stages. A) *Afi-c-lectin* expression at stage 2. B) Frontal paraffin section showing fluorescent ISH of *Afi-c-lectin* counterstained with DAPI at stage 3/4. *Afi-c-lectin* is clearly localized to single cells just beneath the epidermis. Asterisk marks cells in dermal layer seen from oral view, due to the slanted plane of sectioning along the oral-aboral axis. B') Higher magnification of arm in B. C) At stage 4 the expression of *Afi-c-lectin* becomes much more restricted to the sub-epidermal domain. D) 50% DI arm showing expression of *Afi-c-lectin*. D') Magnification of different focal planes showing expression in different skeletal domains. E) Fluorescent ISH showing expression at 95% DI stage. F) Magnification of *Afi-c-lectin* expressing cells in vertebra. G) Magnification of *Afi-c-lectin* expressing cells in a spine. *Arrows – dermal layer*.

3.4 Cell proliferation during arm regeneration in *A. filiformis*

To test when active cell proliferation is initiated post amputation and if the skeletogenic cells have the ability to proliferate during regeneration, we used the EdU assay to label cells in, or having gone through S-phase, during the early stages of regeneration. In normal non-regenerating arms some proliferating cells, labelled by EdU, are identifiable in different tissue types including the epidermis, podia, radial water canal and in cells surrounding the vertebrae (Figure 3.10; n=3). On the contrary, no cells are labelled during the first hours (8-24) post-amputation (Figure 3.11; n=3) in the plane of injury. Only at the end of stage 1 (between two and three dpa) is a marked increase in EdU labelling visible at the wound site prior to bulging of the regenerative bud, mainly in correspondence with the position of the radial nerve cord and the radial water canal (Figure 3.11; n=3) in the oral half of the metameric unit. Whether these proliferating cells have migrated there, or cells present started to divide in this location is unknown. Stage 2, which marks the appearance of the regenerative bud, shows extensive cell proliferation in both the epidermis and the inner tissues, containing the outgrowths of the above-mentioned structures (Figure 3.11; n=3).

Five individual arms were used for EdU labelling of stage 3 regenerates. Confocal maximum projections of whole z-stacks also show a large amount of proliferating cells at this stage (Figure 3.12). Notably, closer inspection of individual z-planes reveals that the dermal layer contains cells that are not labelled with EdU, implying that they did not proliferate during the time course of labelling (Figure 3.12 B). This trend is consistently observed also at stages 4 and 5 of regeneration (Figure 3.12 C and D).

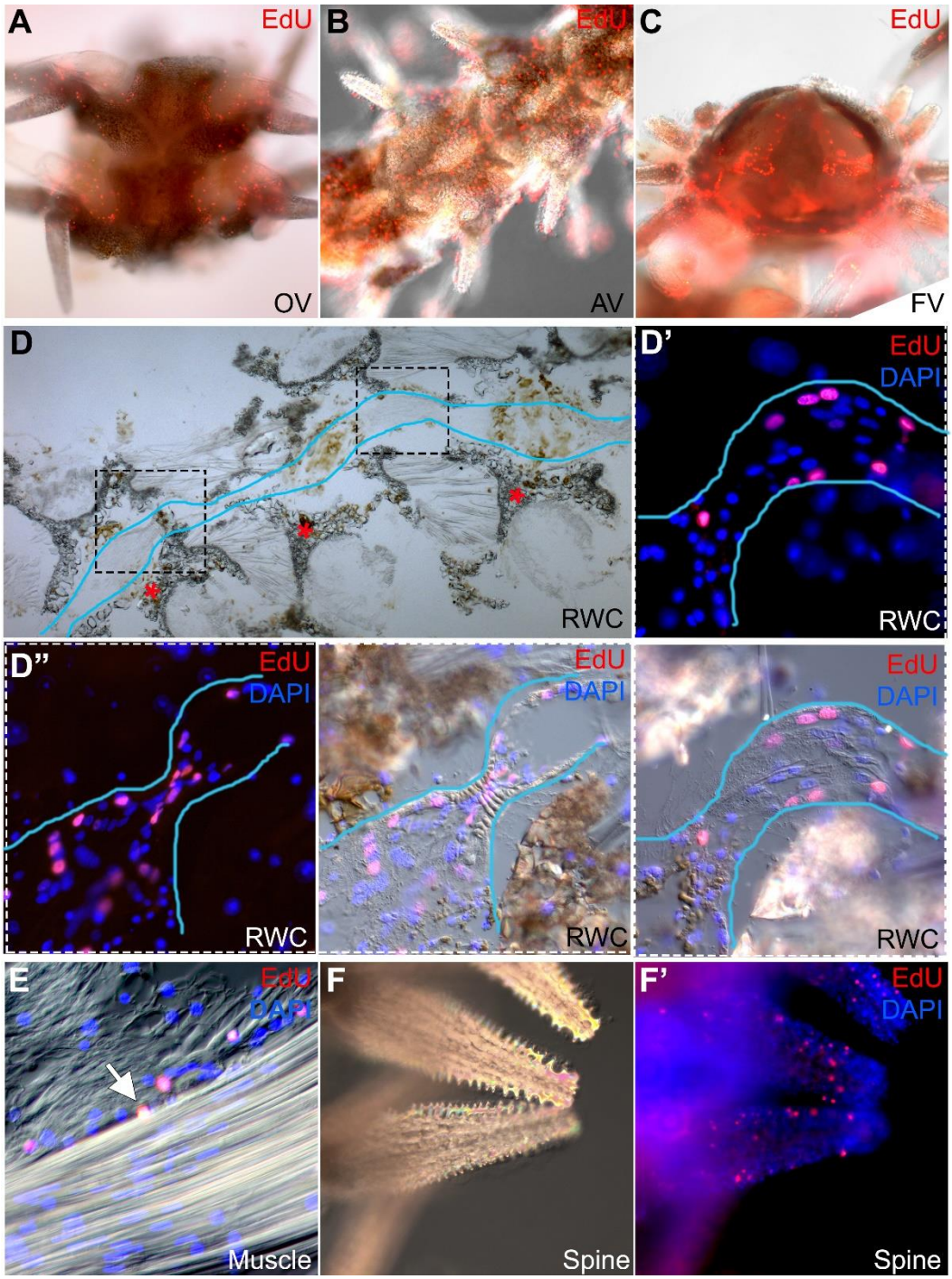

Figure 3.10: EdU labelling in non-regenerating arms. A) Proliferating cells present in the spines and podia. B) Proliferating cells in the aboral shield epidermis. C) Proliferating cells are localized predominantly in the epidermis of the podium. D) A frontal paraffin section showing the position of the radial water canal (blue) and vertebral remains (asterisk). D' and D") Insets show EdU labelling of cells both inside the radial water canal and in its' epithelium. E) A frontal paraffin section of intervertebral muscles showing no red nuclei within the muscle cells but some labelled cells can be observed in close proximity (arrow). F and F') Magnification of calcified spines showing EdU-labelled cells. *AV – aboral view, OV – oral view, RWC – radial water canal.*

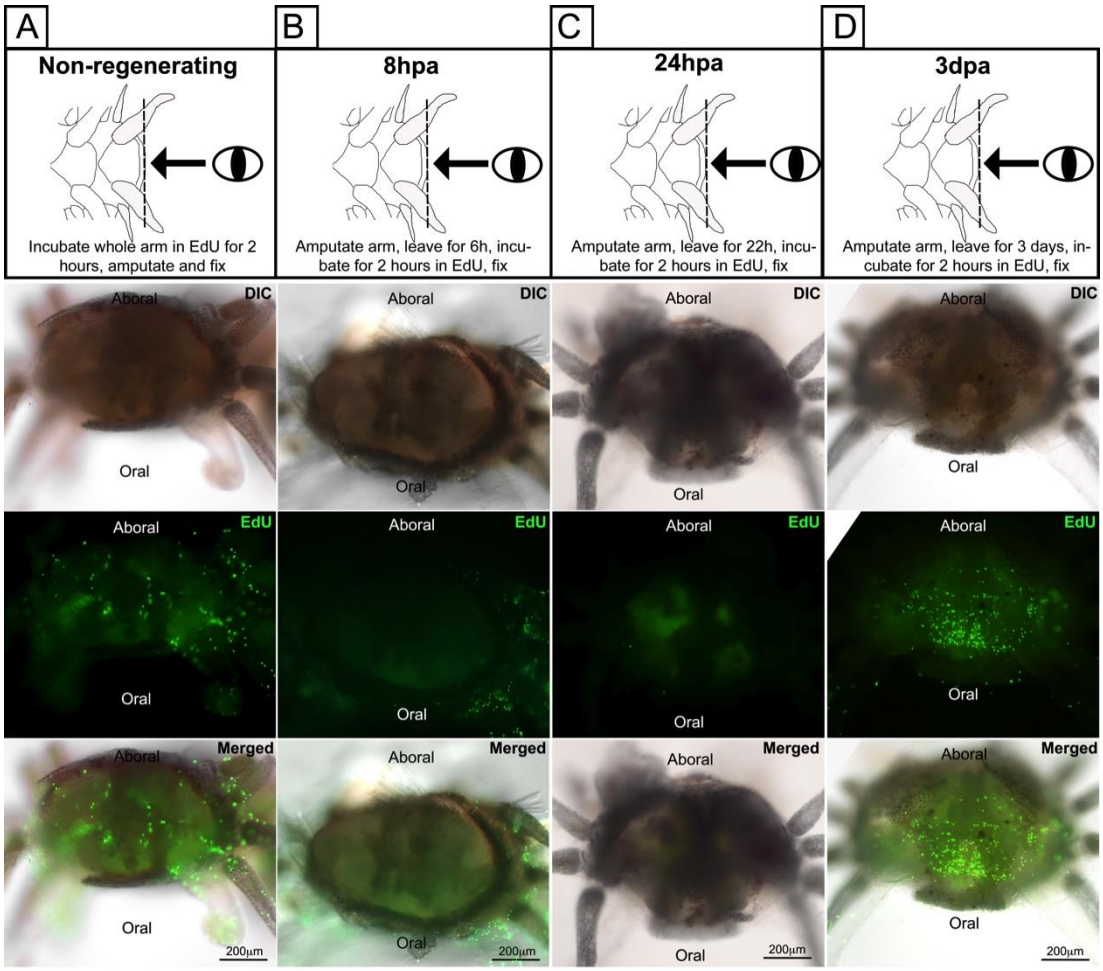

Figure 3.11: EdU labelling showing proliferation in non-regenerating arms (n=5) and at stage 1 of regeneration (n=3) at different time points post amputation. Top panels A-D) Schematic diagrams showing the labelling method and imaging view. Middle panels A-D) Bight field, fluorescent, and merged images of EdU-labelled arms showing the frontal view of the amputation and wound healing site. A) EdU labelling pulse (green) in non-regenerating. Cell proliferation is observed in the epidermis, spines, and podia and in cells surrounding the vertebra. B) EdU pulse in stage 1 arms at 8 hpa shows and almost complete shutdown of cell proliferation during wound healing. Some proliferating cells are still observed in the stump in the epidermis and spines. C) In stage 1 arm at 24 hpa cell proliferation is still absent during the epithelialization phase. D) At end of stage 1, at 3 days pa, EdU labelled cells can be detected at the amputation site and an accumulation of proliferating cells can be observed in the central-oral position corresponding to the site of the future appearance of the regenerative bud.

As the number of cells that express *Afi-c-lectin* clearly increases during the regeneration process, I investigated whether the cells can divide at these late stages. To answer this question, I performed a fluorescent ISH using *Afi-c-lectin* on arms previously labelled with EdU (n=2). If skeletogenic cells marked by the expression of *Afi-c-lectin* were proliferating, cells with a red nucleus (EdU DNA incorporation) and surrounding green cytoplasm (*Afi-c-lectin* RNA expression) would be observed.

Table 3.1: Manual scoring of confocal images of EdU and *Afi-c-lectin* double-labelled arms.

Arms scored	**Stage**	**Segments**	**Separate z-planes scored**	**Green signal** (*C-lectin* in cytoplasm)	**Red signal** (EdU in nucleus)	**Potential overlap***
Arm 1	95% proximal	2	60	214	287	2
Arm 2	50% proximal	2	60	71	381	1

* Potential overlap refers to yellow signal due to overlap between green cytoplasmic staining of *Afi-c-lectin* in one cell and red nuclear EdU labeling of another cell. No cells with red nucleus and green cytoplasm were observed.

Extensive cell proliferation can be observed throughout the regenerating arm at this stage (Figure 3.13). However, closer inspection of individual confocal z-planes shows that none of the green-labelled *Afi-c-lectin* cells overlap with the red EdU^+ cells in a manner indicating that skeletogenic cells have nuclei in the S-phase of mitosis (Figure 3.13; Table 3.1). Specifically, none of the EdU labelled red nuclei are surrounded by green *Afi-c-lectin* labelled cytoplasm (Figure 3.13). This trend is apparent in the whole 50% stage arm as shown in the proximal segments (Figure 3.13) and the distalmost tip (Figure 3.13). Therefore, the *Afi-c-lectin* expressing cells do not proliferate

throughout the whole arm regeneration process, in agreement with the role of *c-lectin* as a final differentiation gene in skeletogenesis. Notably, the distalmost part (terminal ossicle and podium) (Figure 3.13) of the regenerate contains very few proliferating cells. However, the area just proximal to it is a domain of major accumulation of EdU^+ cells, consistent with its role as a growth zone located just underneath (proximally) to the terminal ossicle, which adds new metameric units in a distal to proximal direction.

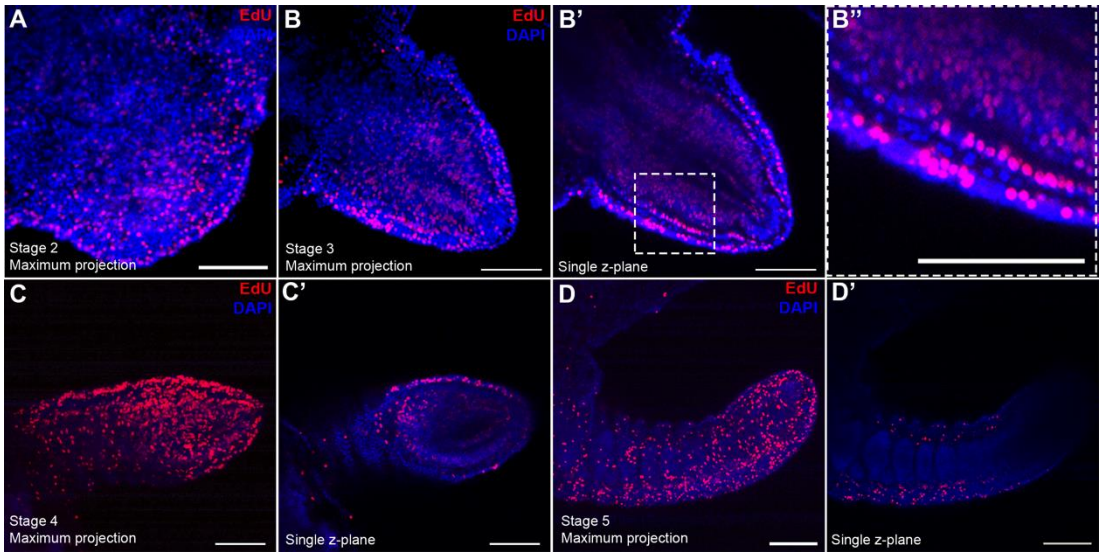

Figure 3.12: Confocal images showing EdU labelling (red) of early stage regenerating arms counterstained with nuclear stain DAPI (blue). A) Stage 2 maximum projection of confocal z-stack showing widespread cell proliferation in regenerative bud. B) Maximum projection of confocal z-stack of stage 3 arm showing continuing cell proliferation in early regenerate. B') Single z-plane of B. B") Detail of B' showing lack of EdU-labelled cells in dermal layer. C) Stage 4 maximum projection of confocal z-stack showing widespread cell proliferation. C') Single z-plane of C. D) Stage 5 maximum projection of confocal z-stack showing widespread cell proliferation. D') Single z-plane of C. *Scale bars - 100μm.*

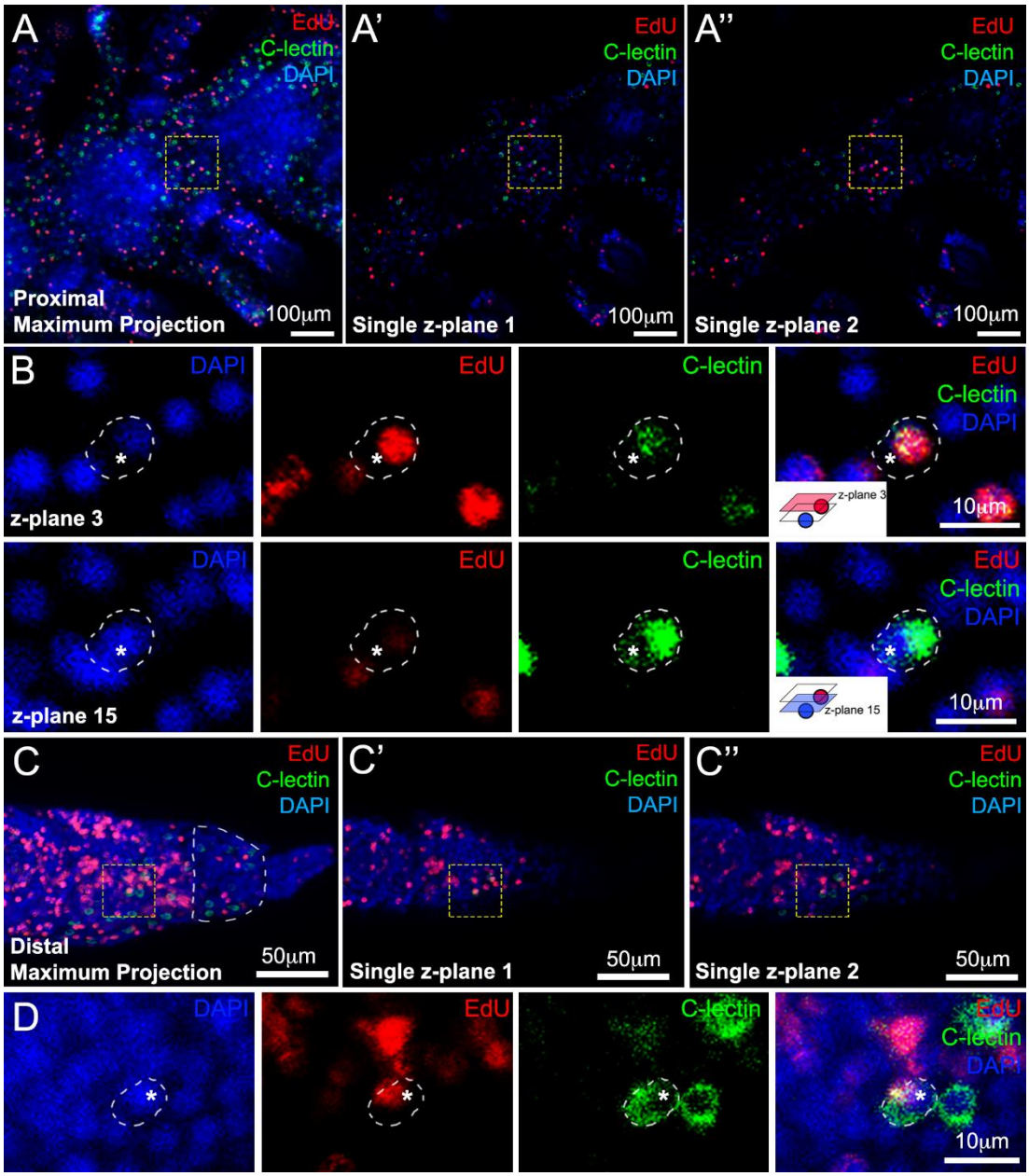

Figure 3.13: *Afi-c-lectin* expression (green) combined with EdU labelling (red) and counterstained with nuclear stain DAPI (blue) showing that skeletogenic cells do not proliferate. A) Maximum projection of proximal segments of 50% arm. A' and A") Single z-planes of A showing *Afi-c-lectin* expressing cells do not overlap with EdU-labelled cells. Yellow dashed box shows one case of yellow signal. B) Magnified image showing cells in confocal stack z-plane 3 and z-plane 15. The EdU labelled red nucleus is seen clearly in z-plane 3 where *Afi-c-lectin* expression is faint, whereas on z-plane 15 where the cytoplasm of the *Afi-c-lectin* cell is clearly visible, the nucleus is labelled with DAPI but not EdU (asterisk). C) Maximum projection of distal-most end. White dashed half-circle indicates position of terminal ossicle. C' and C") Single z-planes of C showing *Afi-c-lectin* expressing cells do not overlap with EdU-labelled cells. D) Magnified image in yellow dashed box from C showing cells in single z-plane. Again, the nucleus of the *Afi-c-lectin* expressing cell is labelled with DAPI (asterisk).

These observations are consistent with the expression of proliferation-associated genes throughout arm regeneration in *A. filiformis* (Figure 3.14; see methods for detailed description of collection method used for temporal expression quantification experiments). Using the Nanostring nCounter I analyzed the expression of cyclin genes *Afi-cycA, Afi-cycB* and *Afi-cycE*, as well as a cell cycle regulating transcription factor *Afi-myc* and a DNA replication factor *Afi-pcna.* Those genes should show increased expression when levels of cell proliferation are high. In fact, very low levels of expression are detected in non-regenerating control arm segments (Figure 3.14 showing abundance relative to highest peak of expression; see Appendix Table A.0.3 for counts). During the first 24 hpa most of these genes remain at very low levels and even show a decrease in expression consistently with the lack of observed EdU-labelled nuclei at this stage. Between 48 and 72hpa the genes begin to be upregulated, especially *Afi-myc*, again coinciding with the re-appearance of EdU-labelled nuclei at this stage. All of these proliferation-associated genes become significantly upregulated during stages 3-5 when the regenerating bud has fully formed and extensive EdU-labelling can be observed. Finally, at the 50% stage of regeneration these genes are still highly expressed in the growth zone region of the regenerate but have a dip in expression in the proximal differentiating segments, again resembling the pattern of observed EdU-labelled cells at this late stage of regeneration.

EdU labelling also allows tracking the migration of proliferating cells as well as their potential contribution to the forming tissues during regeneration. To find out how the proliferating cells in non-regenerating arms contribute to the regeneration process I carried out pulse and chase experiments as

outlined in Figure 3.15, comparing regenerating arms labelled with EdU on the day of sampling with arms labelled before amputation and left to regenerate until the same stages. Interestingly, I find that there is a large amount of labelled cells contributing to the internal layers, such as the radial water canal, nerve cord and aboral coelomic cavity, but almost none contribute to the formation of the epidermis. This experiment shows that although there are many proliferating cells found in the epidermis of the regenerating arm at stages 3 and 5, very few of them arise from a pre-existing pool of proliferating cells in the non-regenerating stump (Figure 3.15). Additionally, this experiment suggests a role for cell migration in regeneration of the brittle star arm, as pre-existing cells from the stump clearly end up in the regenerate. However, the extent of the contribution of this process is not clear and further work would elucidate where these cells have originally migrated from.

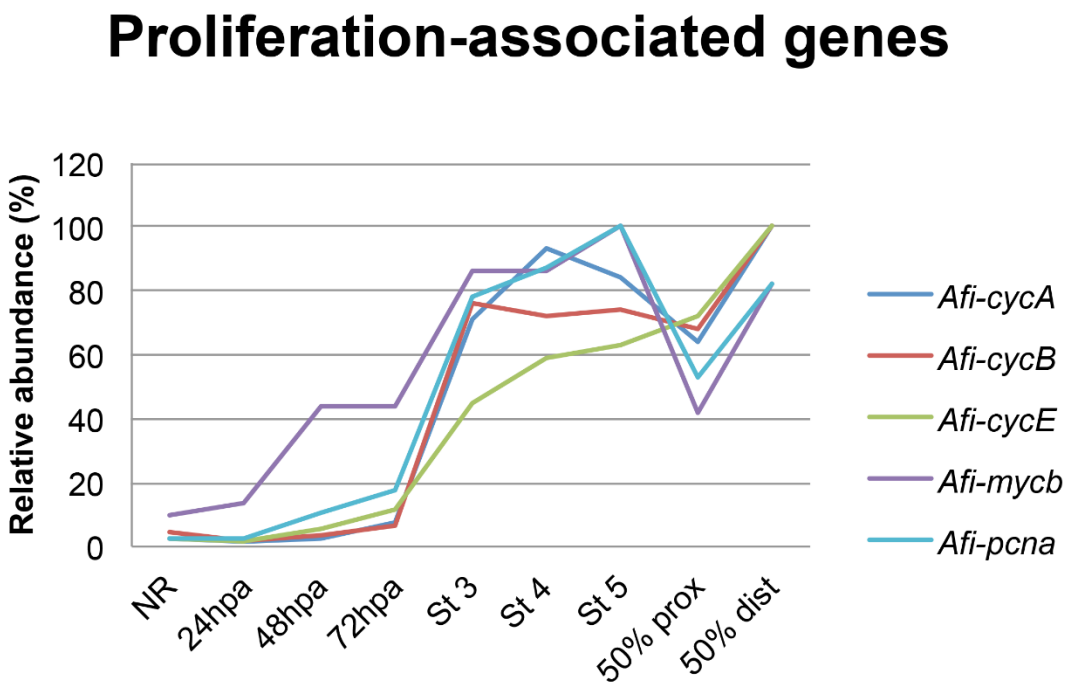

Figure 3.14: Cell proliferation-associated gene expression during arm regeneration in *A. filiformis*. Nanostring nCounter data for the expression of cyclin genes *Afi-cycA, Afi-cycB* and *Afi-cycE*, cell cycle regulating transcription factor *Afi-myc* and the DNA replication gene *Afi-pcna* during different stages of regeneration. Abundance represented as percentage relative to the highest expression value. *NR – non-regenerating control arms, hpa – hours post amputation, st – stage, prox – proximal segments, dist – distal segments excluding the distal cap*. See methods for diagram on arm collections for quantification experiments.

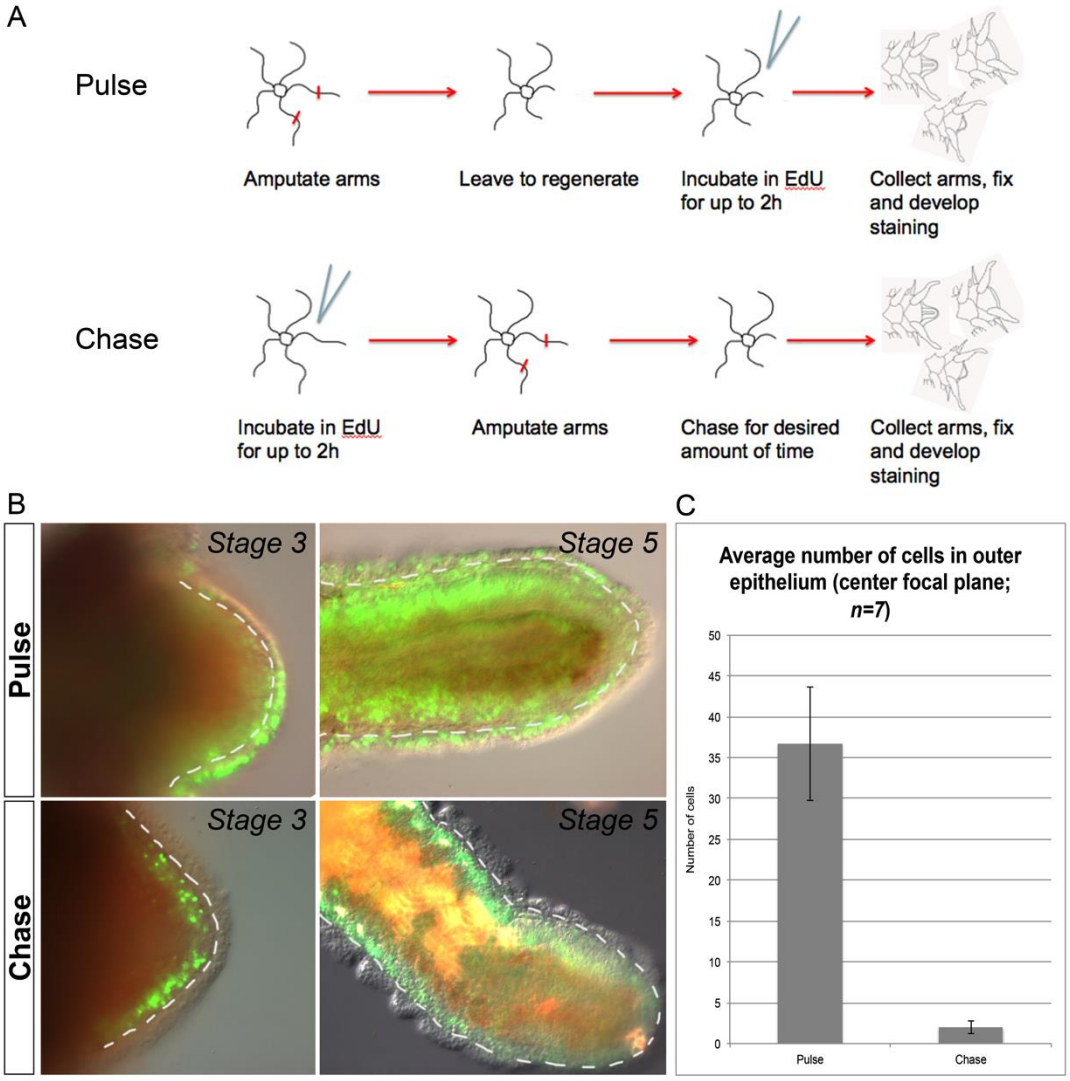

Figure 3.15: Pulse and chase EdU experiments showing the contribution of proliferating cells in the adult to the regenerating arm. A) Scheme of pulse and chase experiments for EdU labelling of proliferating cells. Top: in pulse experiments I first amputated the arms, left them to regenerate and incubated with EdU at the desired stage prior to collecting the arms for fixation and staining. Bottom: in chase experiments I labelled the animals with EdU before arm amputation, next collected the arms for fixation and staining once they have regenerated to the desired stage. B) Merged images of EdU labelled cells (green) over a DIC image of the regenerating arms at stages 3 and 5 for pulse and chase experiments. Pulsed animals show the normal extensive amount of proliferating cells in the regenerating arm. Chased animals show that although many cells in the regenerate arise from previously proliferating cells in normal non-regenerating adult arms, none of the cells in the epidermis come from the same pool of cells. C) Quantification of amount of labelled cells in the epidermis in pulse and chase experiments.

4 Large-scale analysis of gene expression patterns in the regenerating arm of *A. filiformis*

Understanding the spatiality and timing of the expression of genes is crucial for finding their role in developmental processes. Here, I examine the expression patterns of ~40 genes during early and late stages of regeneration to begin to characterise the dynamics of changes in expression occurring during brittle star arm regeneration. Specifically, I aimed to determine the molecular signature and regulatory states of the mesodermal cells in the regenerating arm during development of the skeleton to compile an expression profile map necessary for building a GRN model. Using whole mount *in situ* hybridization (WMISH) I determine the domains of expression of transcription factors and differentiation genes during arm regeneration. Figure 4.1 shows schematic representations and orientation of the presented WMISH experiments on the early regenerating arms, which I imaged primarily from the aboral view, and the late regenerates. These schematics should aid in interpretation of the spatial expression patterns presented here. Additionally, to control for the effectiveness of detecting specific mRNA localization and to further characterize the different territories within the developing arm, I examined several neuronal genes expressed in very different territories from my primary genes of interest. Finally, I present the temporal expression data obtained using the Nanostring nCounter transcript quantification method.

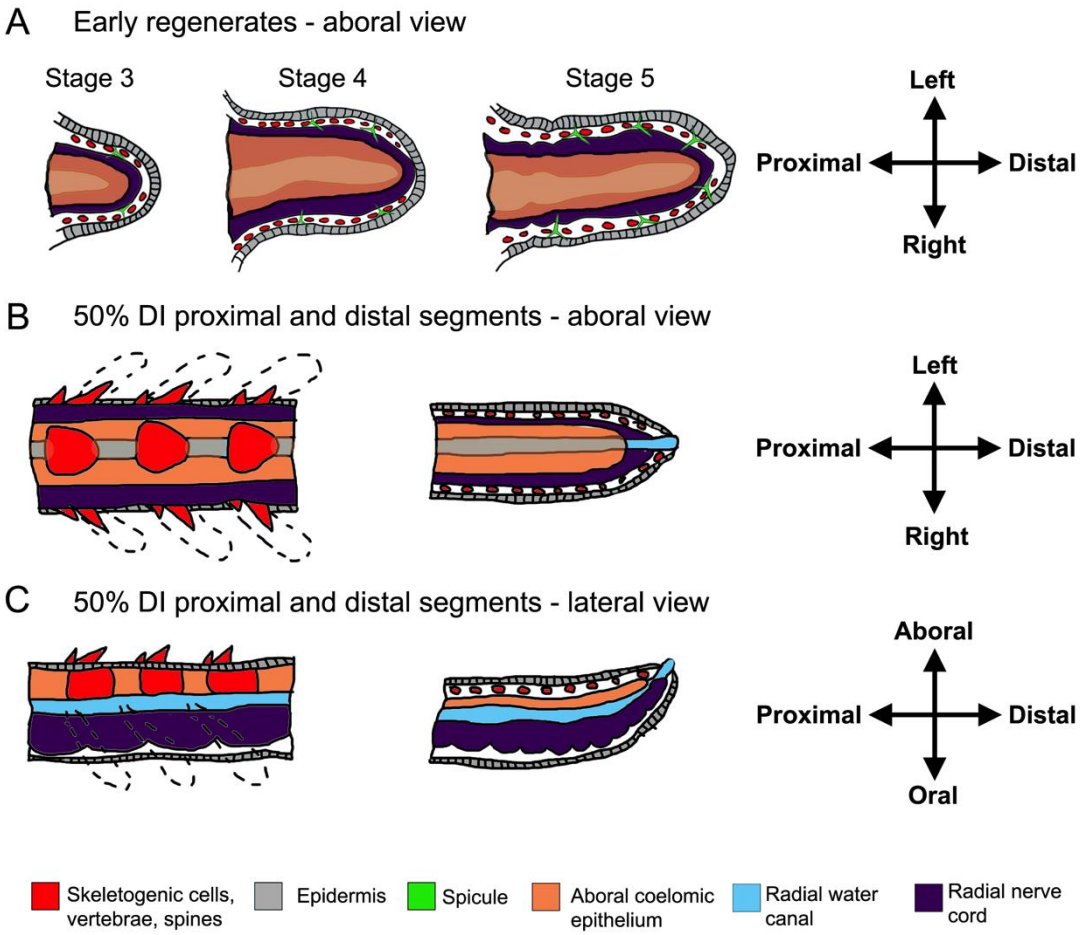

Figure 4.1: Schematics of regenerating arms as orientated in WMISH experiments showing the main cellular territories. A) Schematics of stage 3, 4, and 5 regenerates showing the position of skeletogenic cells in the dermal layer, the site of spicule formation, the epidermis and the aboral coelomic epithelium as seen from the aboral view. B) Schematics showing the tissue organization in proximal and distal segments of 50% regenerates as viewed from the aboral side. C) Schematics showing the tissue organization in proximal and distal segments of 50% regenerates as viewed from the lateral side.

4.1 Spatial expression of skeletogenic differentiation genes in regenerating arms

Biomineralization in echinoderms has been a subject of study for many years in the sea urchin and has been characterized thoroughly from the perspective of cell biology, proteomics, gene expression analysis and biochemistry. To understand the molecular underpinnings of skeleton

regeneration in the brittle star I first assessed the spatial expression patterns of evolutionary conserved skeletogenic differentiation genes expressed in the skeletogenic mesenchyme cells of developing brittle star and sea urchin embryos (Dylus et al., 2016; Oliveri et al., 2008; Rafiq et al., 2014; see Appendix Figure A.0.1) or found in proteomic screens of adult skeletal components (Mann et al., 2008b; Mann et al., 2010; Seaver and Livingston, 2015), to serve as potential markers of skeletogenic cells in the adult. During the early stages of regeneration seven genes (in addition to *Afi-c-lectin* described in chapter 3) were found expressed specifically in the dermal layer where spicules form, namely*, Afi-caraX, Afi-p19, Afi-msp130L, Afi-slc4a10, Afi-p58a, Afi-p58b,* and *Afi-l1* (Figure 4.2 A-O)*. Afi-col2a1, Afi-kirrelL* and *Afi-tetraspanin* are not detectable by *in situ* hybridization very early (stage 2-3) but show expression in stage 4-5 regenerates. *Afi-col2a1* is expressed in the aboral dermal layer and coelomic epithelium (Figure 4.2 P)*. Afi-tetraspanin* and *Afi-kirrelL* are localized to the dermal layer only in stage 5 regenerates (Figure 4.2 Q-R). The expression of several biomineralization genes specifically in the domain where skeletal spicules form is in agreement with the hypothesis that the cells in the dermal layer are indeed producing the skeleton, extends the molecular signature of these cells and confirms that a multitude of biomineralization genes likely act together during their specification and differentiation.

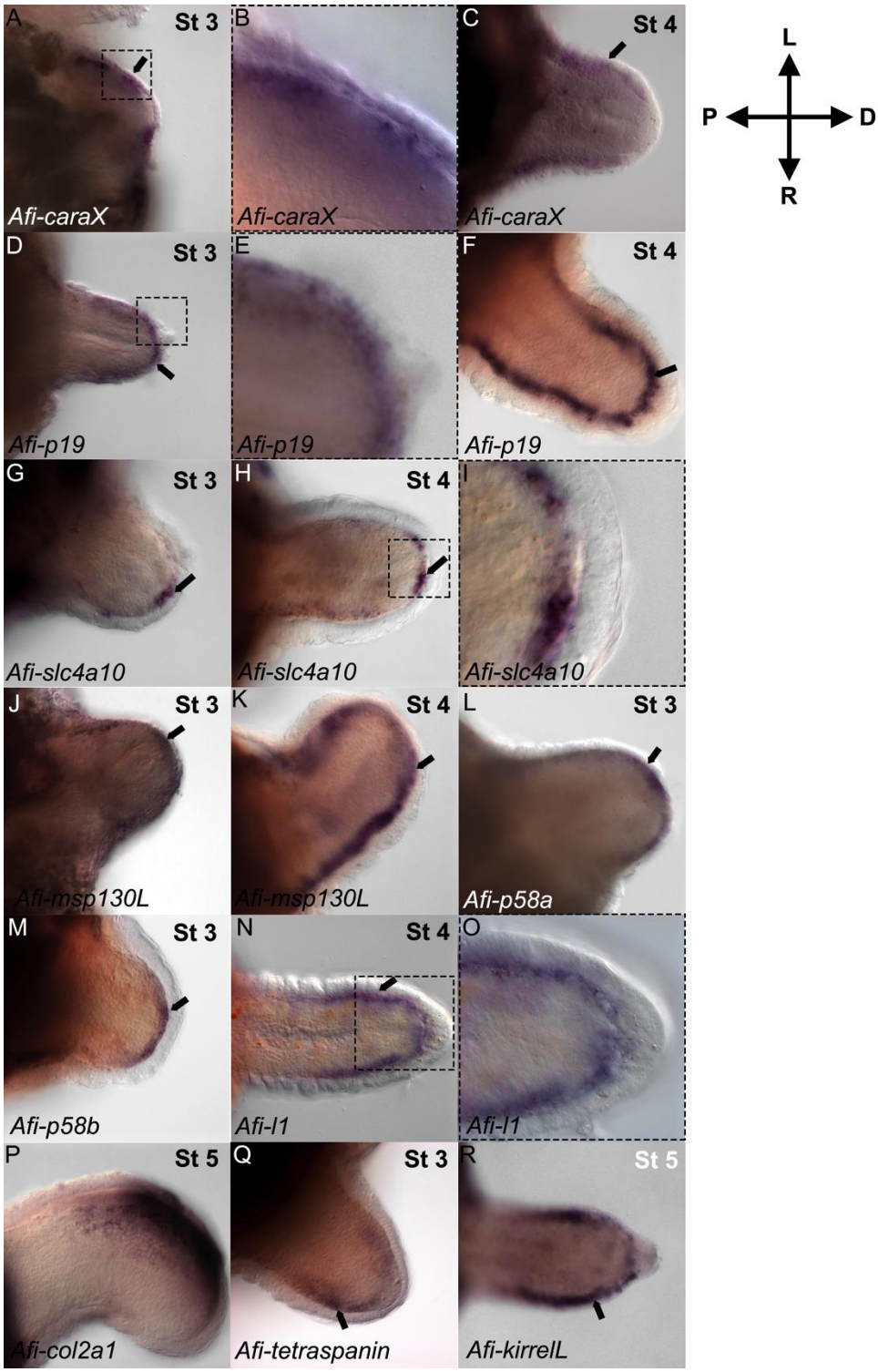

Figure 4.2: WMISH of differentiation genes in the early stages of arm regeneration. Panel shows expression from the aboral view of A-C) *Afi-caraX*, D-F) *Afi-p19*, G-H) *Afi-slc4a10*, J-K) *Afi-msp130L*, L) *Afi-p58a*, M) *Afi-p58b*, N-O) *Afi-l1* Q) *Afi-tetraspanin* and R) *Afi-kirrelL* in the dermal layer of the regenerating arm of *A. filiformis* at stages 3-5. P) *Afi-col2a1* (arm slightly twisted laterally) is expressed in the aboral dermal layer and coelomic epithelium at stage 5. *Black arrows – dermal layer. L – left, R – right, D – distal, P – proximal. Images in dashed lines are enlargements of previous images.*

Unlike *Afi-c-lectin,* most of the other identified genes are not expressed in all skeletogenic cells throughout regeneration, but rather in distinct domains at different regenerative stages. During late stages of regeneration, when differentiation of the five skeletal elements begins, the genes obtain varying expression patterns suggesting their diverging roles compared to the initial phases of regeneration (Figure 4.3). Similarly to *Afi-c-lectin*, *Afi-col2a1* seems to be expressed in all skeletal domains in the proximal regions of the 50% and 95% regenerating arms. *Afi-msp130L* is expressed in all external skeletal domains (shields and spines) but not in the vertebrae. *Afi-caraX, Afi-p58a, Afi-p58b, Afi-tetraspanin* and *Afi-kirrelL* are all restricted to vertebrae and spines forming in the differentiating segments. *Afi-p19* is preferentially expressed in vertebrae, spines and oral shields while *Afi-slc4a10* is expressed in vertebrae, spines and aboral shields. *Afi-fn3-egff* and *Afi-lrr-igr* are only expressed in vertebrae. *Afi-l1* stops being confined to the skeletal domain at late stages of regeneration and begins to be localized to the terminal podium in the distal end and to the podia and radial nerve cord in the proximal segments. In the distal region of late stage arms most of these genes are expressed in the dermal layer (or not at all) similarly to their expression in the early stages of regeneration. Taken together, it can be concluded that although initial differentiation of skeletogenic cells during the earliest stages of regeneration likely involves the co-expression of most of the biomineralization genes, the final patterning and formation of the complex skeletal elements in the advanced stages of regeneration uses unique combinations of those same genes.

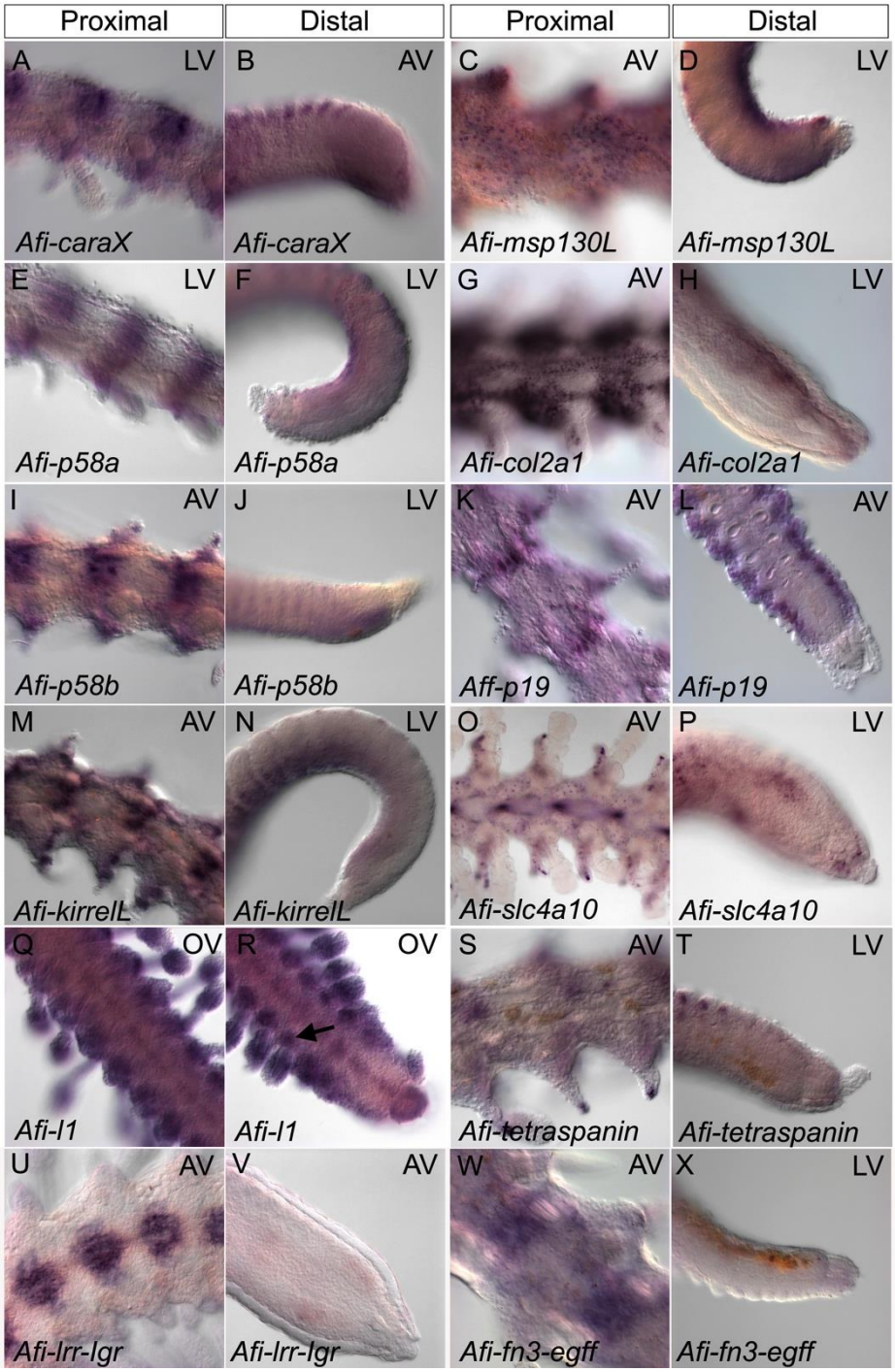

Figure 4.3: WMISH showing expression of differentiation genes in the late stages of arm regeneration (50-95% DI). Panel shows the expression of A-B) *Afi-caraX*, C-D*) Afi-msp130L,* E-F) *Afi-p58a*, G-H) *Afi-col2a1,* I-J) *Afi-p58b,* K-L) *Afi-p19,* M-N) *Afi-kirrelL,* O-P) *Afi-slc4a10,* Q-R) *Afi-l1,* S-T) *Afi-tetraspanin,* U-V) *Afi-lrr-igr* and *W-X*) *Afi-fn3-egff* in proximal (differentiated) and distal (undifferentiated and distal cap) segments of the late stage regenerating arms of *A. filiformis*. Different genes are expressed in varying skeletal domains. Q-R) *Afi-l1* is no longer confined to the skeletal domain but is also expressed in the radial nerve cord, the podia nerve plexuses (arrow) and the terminal podium. *AV – aboral view, LV – lateral view, OV – oral view*.

4.2 Expression of transcription factors previously implicated in embryonic skeletogenic gene regulatory networks

Once I confirmed the molecular signature of skeletogenic cells within the regenerating arm of *A. filiformis*, I wanted to determine the expression patterns of a set of key transcription factors, for which a literature search revealed potential roles in mesoderm specification and skeletogenesis, to understand whether they also might play a role in adult regeneration. The primary set of genes that I investigated has been previously described to have a role in the sea urchin and/or brittle star skeletogenesis GRNs (see chapter 1: *hesC, pplx, tbr, alx1, ets1/2, erg, tgif, hex, foxB, dri*). Furthermore I cloned genes only recently identified as putative components of this GRN (*nk7;* Dylus et al., 2016; Rafiq et al., 2014), as well as an additional transcription factor known to be involved in cartilage formation in vertebrates (*soxE;* Tarazona et al., 2016) and a novel TF identified in brittle stars (*rreb1,* David Dylus, unpublished data).

The first set of investigated TFs, *Afi-alx1, Afi-ets1/2* and *Afi-gataC*, and *Afi-nk7,* show expression in a broad sub-epidermal layer spanning both the dermal layer of skeletogenic cells and the aboral coelomic epithelium in the early stages of regeneration (Figure 4.4 A-L). *Afi-nk7* is additionally expressed in the epidermis. It should be noted that at stages 4 and 5, *Afi-ets1/2, Afi-gataC* and *Afi-nk7* are localized primarily to the distal end of the regenerate suggesting a potentially more transient role in early specification compared to *Afi-alx1* which is consistently expressed throughout the length of the regenerate during early regeneration.

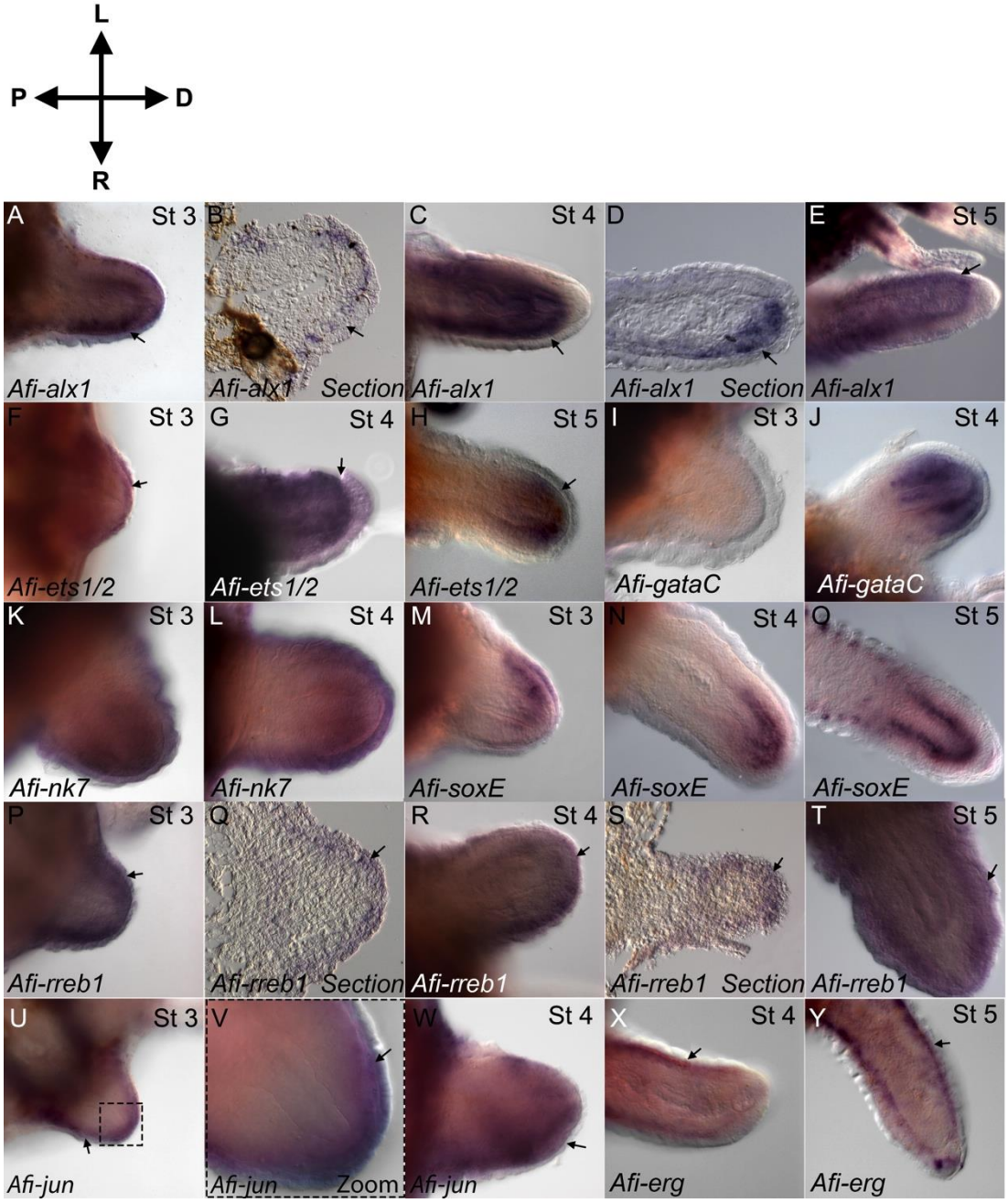

Figure 4.4: WMISH showing expression of mesodermal transcription factors in the early stages of arm regeneration. Panel shows aboral views of expression patterns of A-E) *Afi-alx1*, F-H) *Afi-ets1/2*, I-J) *Afi-gataC*, K-L) *Afi-nk7*, M-O) *Afi-soxE*, P-T) *Afi-rreb1*, U-W) *Afi-jun* and X-Y) *Afi-erg* in the early stages of regenerating arms. Panels A-L show genes expressed in a broad sub-epidermal pattern corresponding to dermal layer and aboral coelomic epithelium. M-O) *Afi-soxE* is expressed only in the aboral coelomic epithelium at the distal end of the regenerate and O) in forming lateral spicules at the distal end of stage 5 arms. Panels P-Y show genes localized to the dermal layer of the regenerate only, namely *Afi-rreb1, Afi-jun* and *Afi-erg*. *L – left, R – right, D – distal, P – proximal, st – stage.*

Interestingly, the transcription factor *Afi-soxE* (Figure 4.4 M-O), is expressed only in the distal aboral coelomic epithelium and in the developing spines in the proximal regions of stage 5 regenerates, which may indicate alternative roles in early mesodermal territory specification and then the early differentiation of spines. On the other hand, *Afi-rreb1, Afi-jun* and *Afi-erg* are localized specifically to the dermal layer similarly to skeletogenic differentiation genes (Figure 4.4 P-Y). The expression of several TFs implicated in embryonic skeletogenic lineage specification in the aboral coelomic epithelium suggests that this tissue could be a potential source of skeletogenic cells in the regenerating arm, which then migrate into the dermal layer where they differentiate (express biomineralization genes) and secrete skeletal spicules. However, it is highly likely that this tissue also gives rise to other putative mesodermal cell types (e.g. connective tissue, muscle etc.).

We then observed that a few of the transcription factors present in the sea urchin embryonic skeletogenic mesoderm are not expressed in the skeletogenic territory of the regenerating arm (Figure 4.5). *Afi-tbr* expression is completely undetectable at all stages of adult regeneration (Figure 4.5 A) (see quantitative analysis section 4.4). *Afi-hex* is not expressed in the early regenerate until stage 5 and then shows a weak expression in the epidermis and a strongly localized spot of expressing cells at the distal end of the regenerate (Figure 4.5 B). *Afi-foxB* (Figure 4.5 C)*, Afi-tgif* (Figure 4.5 E)*, Afi-pplx* (Figure 4.5 G) and *Afi-dri* (Figure 4.5 K) are all expressed in the epidermis only, as shown in the whole-mounts, in the cryosection of *Afi-foxB* (also weakly in the radial water canal; Figure 4.5 D), and in magnified images

of the top-most focal plane showing specific expression in the outer-most layers of the early regenerate for *Afi-dri* (Figure 4.5 L) and *Afi-tgif* (Figure 4.5 F). However, *Afi-pplx* shows a very weak staining compared to the other genes and may be considered as background, due to the lengthy process of staining relative to other samples (see quantitative analysis section 4.4). The expression (or lack of) of this set of genes, in contrast to their presence in the skeletogenic mesoderm of sea urchin embryos, suggests they do not play a role in adult *A. filiformis* skeletogenesis. *Afi-hesC* shows a complex expression pattern (Figure 4.5 I-J) in various tissue types - patched expression in the epidermis, in the regenerating radial nerve cord, the radial water canal and in a segmental pattern at the site of the future metameric units, which suggests various roles in adult regeneration.

At late stages of regeneration the expression patterns of the different transcription factors acquire more complex, often non-overlapping patterns. In the distal, undifferentiated end of the regenerates *Afi-alx1* (Figure 4.6 B) and *Afi-hex* (Figure 4.6 N) both show a localized expression in the dermal layer. *Afi-ets1/2, Afi-jun, Afi-rreb1* and *Afi-gataC* (Figure 4.6 D, F, J and P) are all expressed in a broad sub-epidermal domain. *Afi-soxE* (Figure 4.6 L) is localized to the aboral coelomic epithelium only while *Afi-erg* (Figure 4.6 H) is not expressed in this region. The two non-skeletogenic TFs *Afi-dri* and *Afi-tgif* (Figure 4.6 R and T) are expressed consistently with their expression during early stages, namely they remain confined to the epidermis. In proximal segments the differentiating skeletal elements express various combinations of transcription factors.

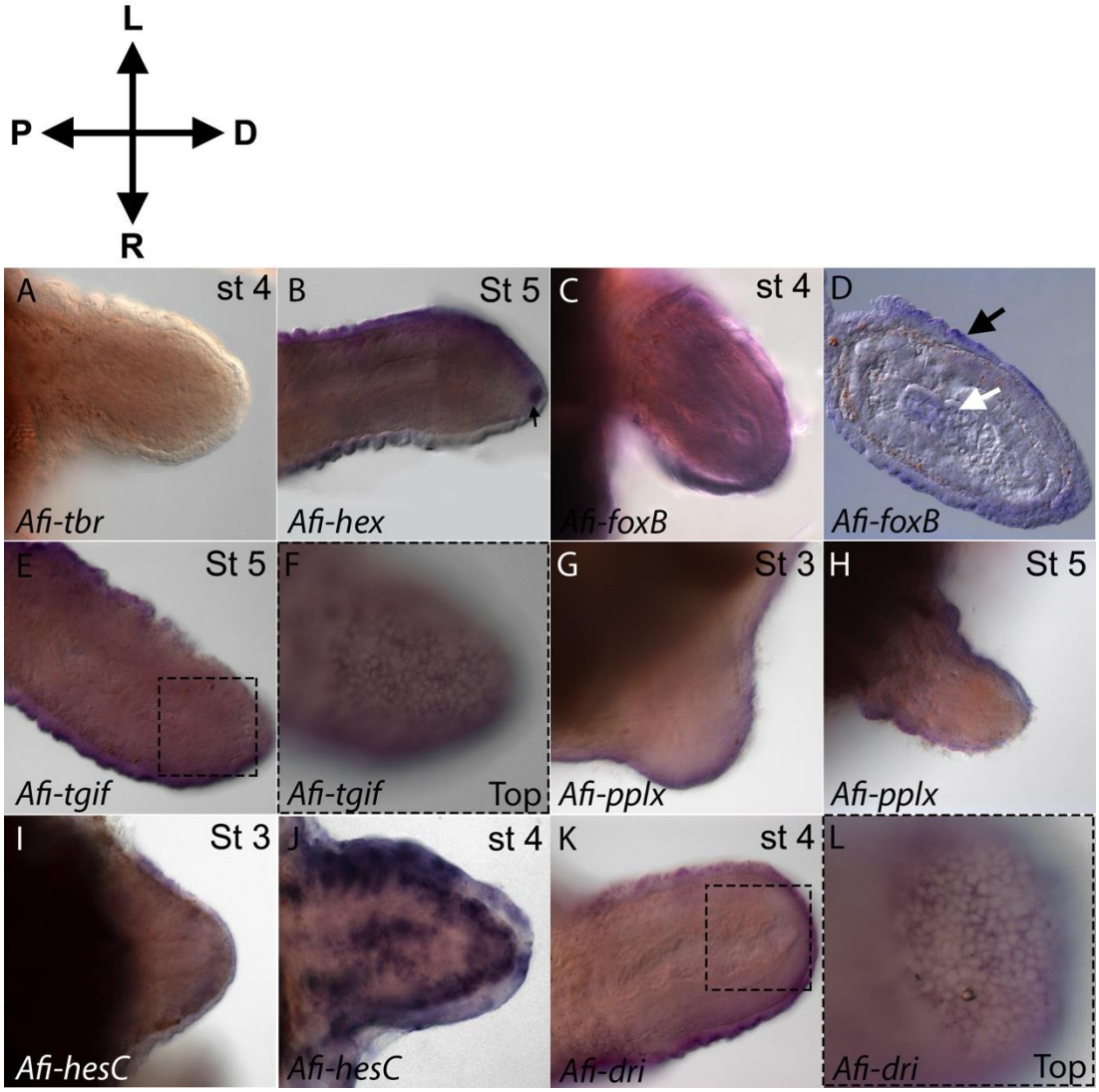

Figure 4.5: WMISH showing expression of transcription factors present in sea urchin skeletogenic GRN, which are not expressed in the mesodermal territory in the regenerating arm. A) *Afi-tbr* is completely absent in the early regenerating arm. B) *Afi-hex* is only expressed in the epidermis and at the distal end of the regenerate (small arrow). C) *Afi-foxB* is localized primarily to the epidermis. D) Cryosection of *Afi-foxB* showing expression in epidermis (black arrow) and weakly in the radial water canal (white arrow). E-F) *Afi-tgif* is localized to the epidermis only. G-H) *Afi-pplx* shows faint expression. I) At stage 3 *Afi-hesC* is expressed weakly in the epidermis, but J) at stage 4 *Afi-hesC* is expressed in a patchy pattern in the epidermis, in the radial nerve, radial water canal and at lateral positions corresponding to newly forming metameric units. K-L) *Afi-dri* is expressed only in the epidermis. *L – left, R – right, D – distal, P – proximal. Images in dashed lines are enlargements of previous images.*

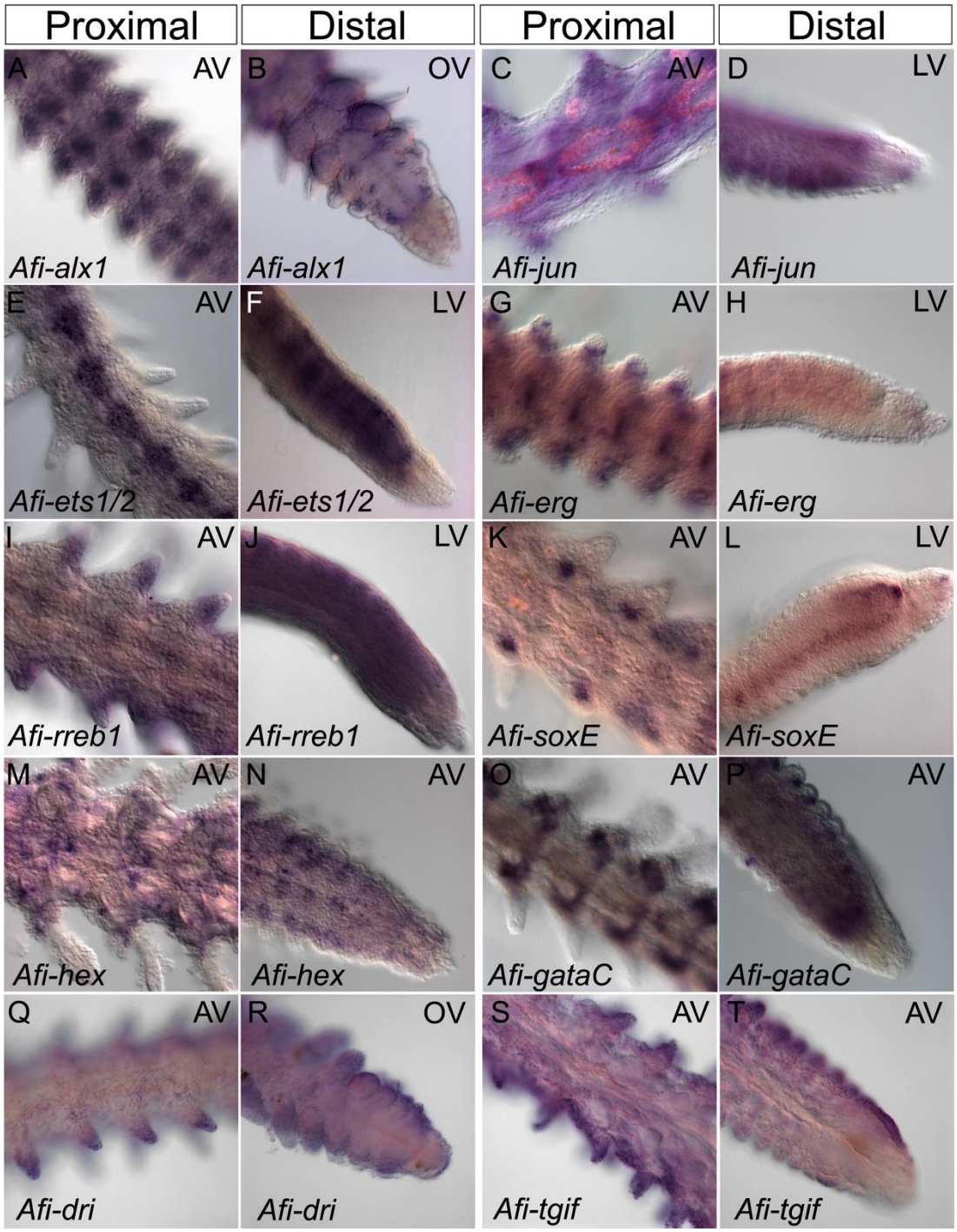

Figure 4.6: WMISH showing expression of transcription factors in late stages of arm regeneration. Panel shows expression of A-B) *Afi-alx1*, C-D) *Afi-jun,* E-F) *Afi-ets1/2*, G-H) *Afi-erg,* I-J) *Afi-rreb1,* K-L) *Afi-soxE,* M-N) *Afi-hex*, O-P) *Afi-gataC*, Q-R) *Afi-dri* and S-T) *Afi-tgif* in the proximal (differentiated) and distal (undifferentiated and distal cap) segments of late stage regenerating arms (50-95% DI). Many TFs are expressed in individual skeletal domains such as spines and vertebrae (A-N) or lateral shields (O-P). The two non-skeletogenic TFs, *Afi-dri* (Q-R) and *Afi-tgif* (S-T)*,* continue to be localized to the epidermis at late stages.

For example, *Afi-rreb1, Afi-jun, Afi-hex,* and *Afi-erg* (Figure 4.6 C, G and N) are all expressed in vertebrae and spines, while *Afi-ets1/2* is only expressed in the vertebra (Figure 4.65 E) and *Afi-soxE* is only expressed at the base of spines (Figure 4.6 K), whereas *Afi-gataC* is expressed only in the lateral shields (Figure 4.6 O). These spatial expression patterns are in line with what we observed for downstream skeletogenic genes, namely, that the development of skeletal elements at late stages of regeneration is associated with the expression of different combinatorial sets of genes. Taken together, an interesting pattern emerges (Figure 4.7 A), revealing that the vertebrae, spines and lateral shields all express many more genes (both regulatory and differentiation genes) compared to the aboral and oral shield territories. This is concomitant with the morphological appearance of the different skeletal elements (Figure 4.7 B and C). The vertebrae have the most complex three-dimensional calcitic structures with variable stereom densities; specialized grooves for the passage of the radial nerve cord, coelomic cavity and radial water canal; and articulations, which join two vertebrae together. The lateral shields are composed of the half-moon shape plate and highly dense protrusions, which form the point of attachment of spines. The spines themselves have a conical calcite structure and different spines have different shapes (long and thin, slightly thicker and with hammer-shape tip). By contrast, the oral and aboral shields have a much more simplified, essentially flat structure with not much variability in pore size or density across the plate and no specialized features. In conclusion, the complexity of morphologies of the different skeletal structure may reflect the underlying differences in molecular patterning.

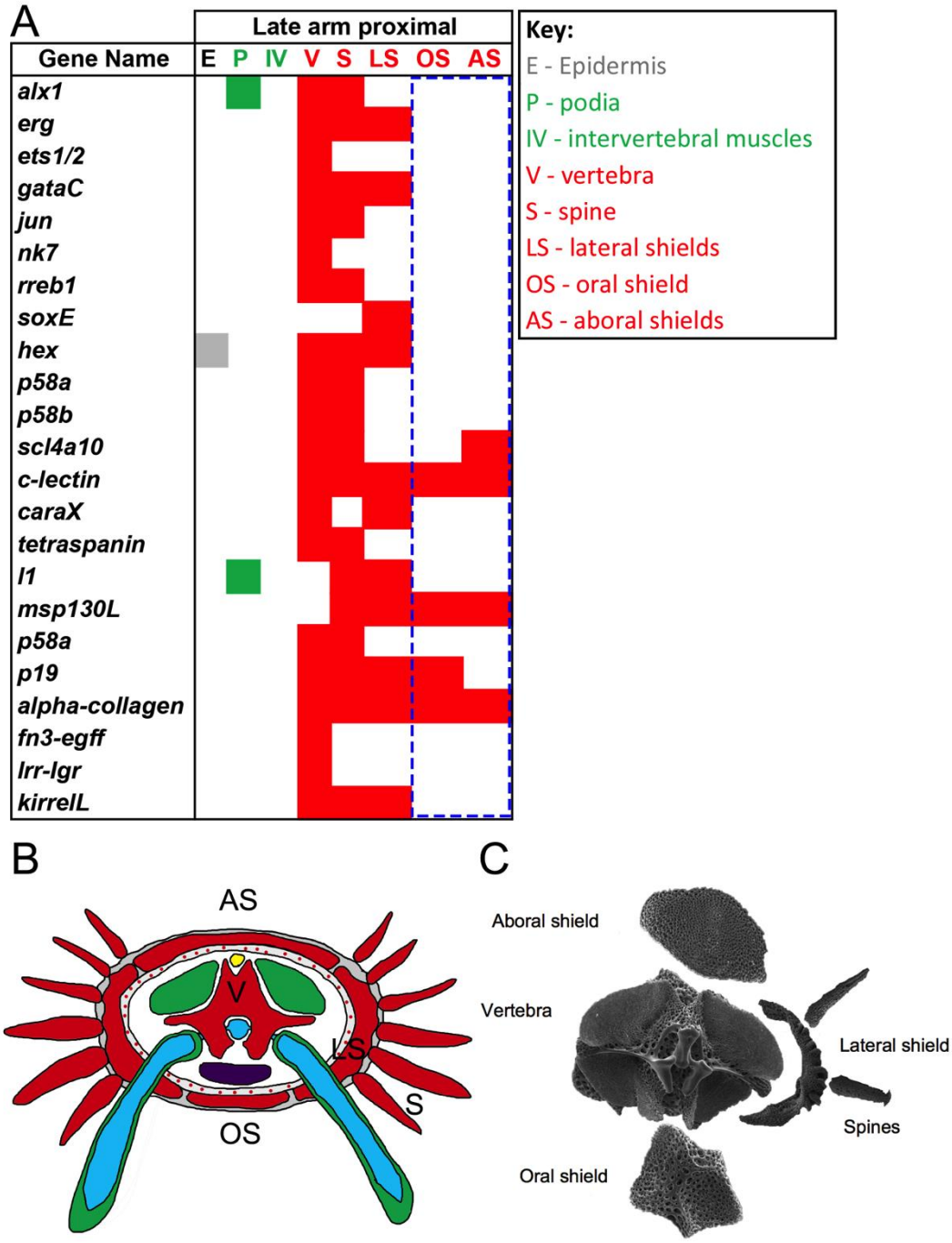

Figure 4.7: Summary of expression patterns of skeletogenic genes in differentiating skeletal elements of late stage regenerating arms. A) Table summarizing expression of the different transcription factors and biomineralization genes in vertebra, spines, lateral shields, oral shields and/or aboral shields. Expression of genes in skeletal elements is shown in red. Blue dashed box shows that oral and aboral shields share expression of the least amount of genes out of all the skeletal elements B) Schematic diagram of the *A. filiformis* arm from a frontal view showing the organization of the different skeletal elements. C) SEM images of the individual skeletal elements corresponding to the schematic in B. The SEM images show differences in complexity of the vertebrae, spines and lateral shields compared to aboral and oral shields (provided by Laura Pioviani).

4.3 Expression of a set of neuronal genes during arm regeneration

To further characterize, on a molecular level, the different tissue domains in the regenerating arm I selected a subset of neuronal genes and determined their expression. I used WMISH to examine the expression of *Afi-elav, Afi-soxB1, Afi-soxB2, Afi-soxC, Afi-pax6* and *Afi-six3* during early and late regeneration of the *A. filiformis* arm (Figure 4.8). *six3* has been shown to be required for the development of all neurons in the sea urchin embryo (Burke et al., 2006; Wei et al., 2009). Recently, it has been shown that *soxC* and *soxB2* are expressed in neural progenitors in sea urchin embryos while elav is involved in the final differentiation stages of neurogenesis (Burke et al., 2006; Garner et al., 2015). *soxb1* and *soxb2* are both involved in neuronal differentiation and patterning. Finally, *pax6* expression has not been extensively studied in the sea urchin embryo but it is expressed in adult sea urchin tube feet where it is presumed to have a role in photoreception (Burke et al., 2006; Lesser et al., 2011). During early stages of regeneration (2-3) of *A. filiformis, Afi-elav*, *Afi-soxC, Afi-soxb1, Afi-six3* and *Afi-pax6* have a strong expression in the distal region of the arm (Figure 4.8; early stages panel). *Afi-elav* and *Afi-soxB1* then become localized to only a few cells at the tip (stage 4-5), while *Afi-pax6* and *Afi-soxC* are strongly expressed in the developing distal structures. Interestingly, their expression precedes the morphological differentiation of the distal structures including the terminal podium surrounded by the terminal ossicle. In addition to their strong distal expression, *Afi-six3* is also expressed in a line of cells corresponding to the regenerating radial nerve cord and *Afi-pax6* is also expressed in the podia primordia. *Afi-soxB2* is only localized to the epidermis

at first, once when the arms reach stage 4 it begins to be expressed in a highly specific striped pattern in the regenerating nerve cord surrounding the radial water canal. It appears that this pattern precedes the morphological differentiation of the newly forming metameric units (Figure 4.8; early stages panel). At late stages of regeneration *Afi-elav* and *Afi-pax6* are both expressed in the distalmost structure, although the latter is only localized to the terminal podium (Figure 4.8; 50% distal panel). The remaining genes are not expressed in this structure but rather mark distinct territories in the newly forming and differentiating neuronal domains. *Afi-elav, Afi-soxB1*, *Afi-soxC* and *Afi-six3* share a highly localized segmental pattern of expression in the oral side of the regenerating arm corresponding to a discrete number of cell bodies of the radial nerve cord (Figure 4.8; 50% proximal panel). *Afi-soxB2* is expressed in the epidermis of the distal region and then together with *Afi-pax6* are expressed in the regenerating podia although in very different patterns – the former is expressed in scattered single cells in the podia and the latter is expressed all along the length of the podia, corresponding to the nerve plexus. With the exception of *Afi-six3* and *Afi-soxB2*, the genes are also expressed in the podia of adult non-regenerating brittle star arms though in distinct patterns (Figure 4.8; podium panel). *Afi-elav*, *Afi-soxC* and *Afi-pax6* are expressed in a ring around the base of the tip of the podium, while *Afi-soxB1* is expressed at the very distal tip of the podium. The expression patterns of these six neuronal genes reveal the positions of different elements of the nervous system such as the epidermis, podia and the terminal podium, which likely give rise to ‘peripheral’ sensory-type neurons, and the cells in the radial nerve cord. These developmental genes not only

serve as excellent markers for these complex domains of the regenerating arms but also confirm the efficiency of the WMISH protocol for *A. filiformis* adult tissues.

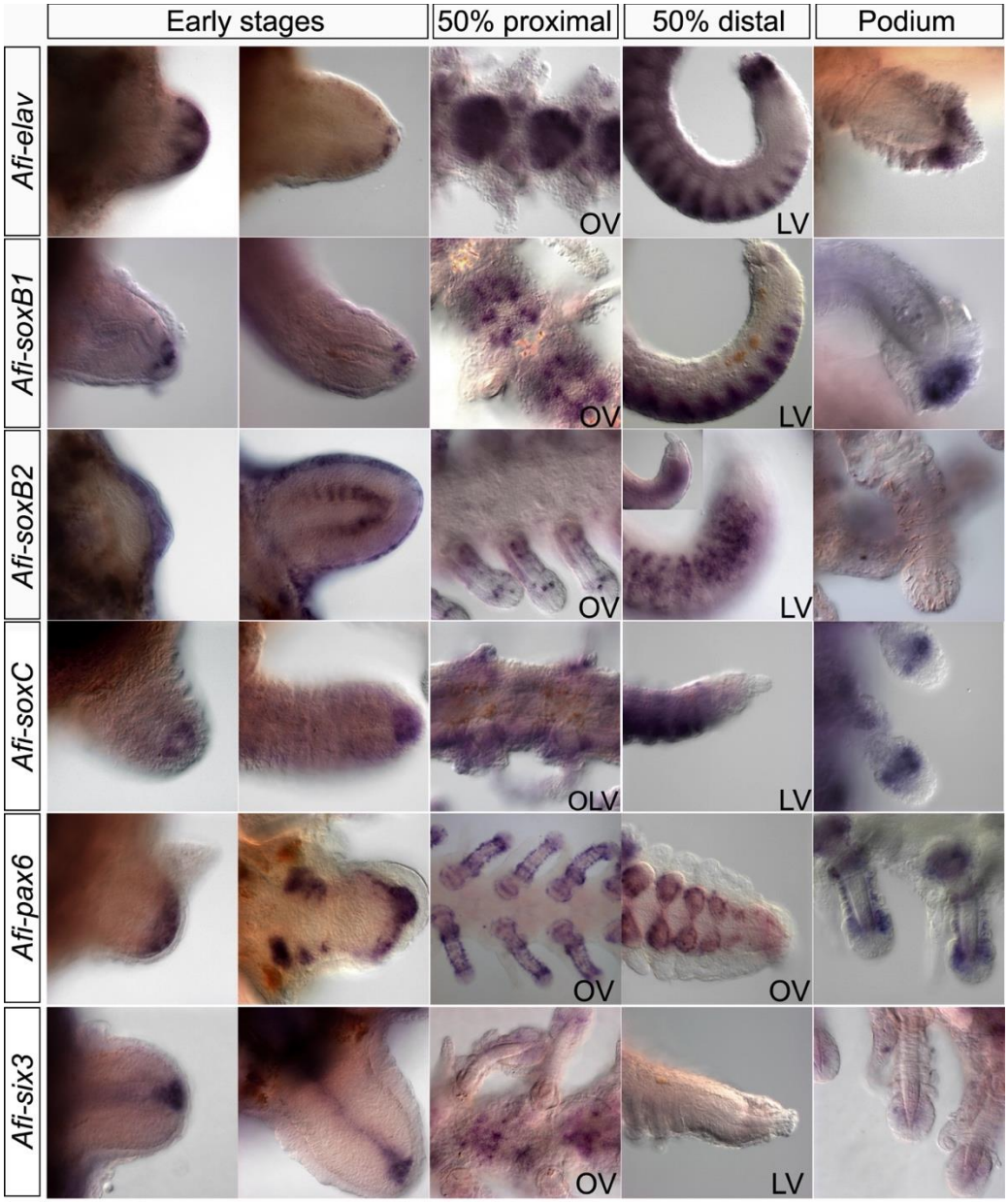

Figure 4.8: WMISH showing expression of neuronal genes in early and late stages of regeneration. Panel shows expression of *Afi-elav, Afi-soxB1, Afi-soxB2, Afi-soxC, Afi-pax6* and *Afi-six3* in early stages of regeneration (oral view; stages 2-3, stages 4-5), in proximal segments of 50% DI arms and in distal ends of the 50% DI arms as well as in adult non-regenerating podia. *OV – oral view, LV – lateral view*, *OLV – oral-lateral view*.

4.4 Quantitative analysis of expressional profiles during regeneration gives insight into putative gene functions

To obtain time-courses and precise levels of gene expression for an expanded gene set during arm regeneration in *A. filiformis* we used the Nanostring nCounter technology and designed a 123-probe code set to analyse our candidate genes. Nanostring is a multiplex hybridization-based technique that allows precise simultaneous quantification of up to 800 transcripts in the same sample (Geiss et al., 2008). There are several advantages to using this method in contrast to other techniques, such as quantitative PCR (QPCR) or RNAseq. Firstly, it is less costly and more feasible for the quantification of a large number of genes if you have many different samples (various regenerative stages, several experimental treatments, embryonic samples etc.) compared with RNAseq, and far less laborious than QPCR. Secondly, the Nanostring nCounter, in contrast with QPCR, does not rely on amplification of nucleic acids but rather on hybridization resulting in a higher sensitivity and precision, and can detect RNA even in very small volumes of the sample. The only disadvantage of this method, compared with RNAseq, is that it is a biased approach dependent on cherry-picking potential genes of interest. Our code set thus included the genes analysed by *in situ* hybridization, as well as additional potential genes of interest including: developmental transcription factors, signalling molecules, putative stem cell genes, cell cycling genes (see chapter 3), neuronal genes, muscle-related and endoderm-related genes, immunity-related genes, putative skeletogenic genes, a set of genes identified in the embryonic transcriptome with unknown functions (see further

analysis in chapter 5) and finally a set of six housekeeping genes to serve as internal standard controls (see Appendix Table A.0.2 for full list of genes). I collected eight samples from *A. filiformis* arms, each compiling 10 different individuals, (see details of technique in methods) corresponding to different developmental time-points: 1) non-regenerating arm segments, 2) stage 1 final arm segments at 24hpa, 3) stage 1 final arm segments at 48hpa, 4) stage 1 final arm segments at 72hpa, 4) stage 3 regenerates, 5) stage 4 regenerates, 6) stage 5 regenerates, 7) 50% DI stage proximal arm segments, and 8) 50% DI stage distal arm segments. Importantly, I did not include the distalmost structures in the distal arm segment collection because, according to our hypothesis for the distalization-intercalation mode of regeneration, it is likely to correspond to a 'later' developmental time-point containing fully differentiated structures.

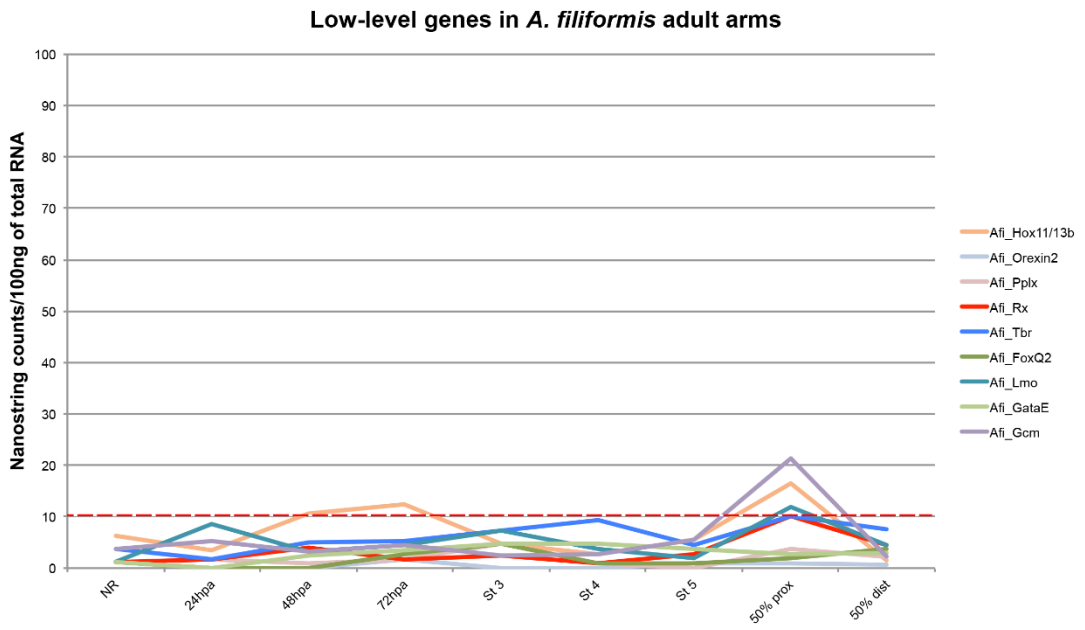

Figure 4.9: Genes expressed at low or undetectable levels in the adult brittle star arm. The graph shows quantitative expression of genes with <20 detected counts/100ng of RNA in the Nanostring analysis: *Afi-hox11/13b, Afi-orexin2, Afi-pplx, Afi-rx, Afi-tbr, Afi-foxQ2, Afi-lmo, Afi-gataE* and *Afi-gcm*. *NR – non-regenerating, hpa – hours post amputation, st – stage, prox – 50% proximal, dist – 50% distal segments. Red dashed line – threshold at 10 indicates average background level counts detected in negative controls.*

I found that several genes show very low, bordering on undetectable, levels of expression throughout regeneration and in non-regenerating arms (Figure 4.9). These genes all have levels ranging from 0 to a maximum of 20 counts/100ng of total RNA in the Nanostring. The average number of counts detected in negative controls is 10 ±2 indicating anything below that level to be background. *Afi-tbr* and *Afi-pplx* show low levels of expression, which explains the inability to detect them via WMISH (*Afi-tbr* expression was also not detected by QPCR as published previously in Czarkwiani et al., 2013). Additionally, known embryonic genes like *Afi-hox11/13b, Afi-gataE* and *Afi-gcm*, and neuronal genes *Afi-rx*, *Afi-foxQ2* or *Afi-orexin2*, are not expressed in the adult arm (Figure 4.9; see Appendix Table A.0.3 for full list of low-level

genes). This result could suggest these genes may not play any role in adult arm regeneration.

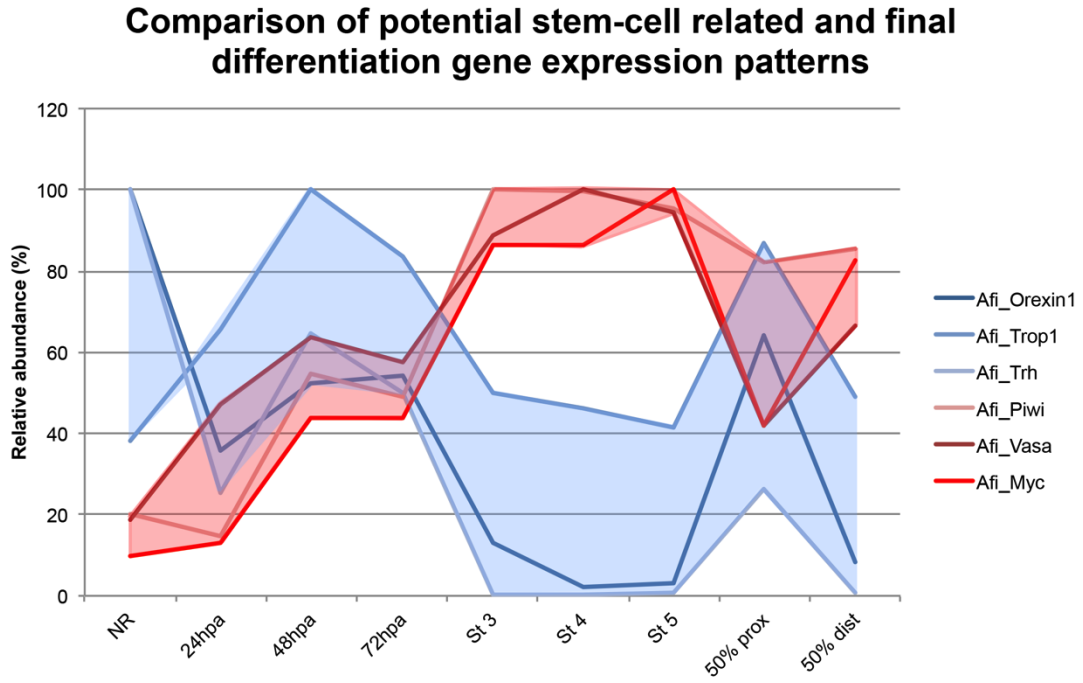

Figure 4.10: Comparison of potential stem cell related and final differentiation temporal gene expression patterns. The graph shows the relative expression of muscle differentiation gene *Afi-trop1*, and neuropeptide genes *Afi-trh* and *Afi-orexin1* clustered together (blue) and putative stem cell markers *Afi-piwi, Afi-vasa* and *Afi-myc* clustered together (red) revealing opposite patterns. The blue genes are most highly expressed in non-regenerating and 50% proximal arm segments suggesting role in differentiation/homeostasis while the red genes are most highly expressed during the regenerative stages (first 72hpa, st3-5 and distal segments of 50% DI arms). Abundance represented as percentage relative to the highest expression value. *NR – non-regenerating, hpa – hours post amputation, st – stage, prox – 50% DI proximal segments, dist – 50% DI distal segments.*

The quantitative gene expression patterns of the selected genes can yield interesting implications for understanding their potential function during adult arm regeneration. Several genes showed highest levels of expression in non-regenerating and 50% DI proximal arm segments (Figure 4.10). These genes often related to final differentiation processes for example the muscle marker *Afi-trop1* or the neuropeptides *Afi-trh* and *Afi-orexin1*. These

expression patterns confirm the differentiation status of proximal segments in a 50% DI arm and shows that these segments have a developmental stage similar to a fully formed adult non-regenerating arm (compare NR with 50% prox in Figure 4.10). By contrast, other genes show the opposite pattern of expression resembling the trend observed for the proliferation-related genes (see chapter 3, Figure 3.14). These include putative stem cell markers like *Afi-piwi*, *Afi-vasa* and *Afi-myc*. These genes show a two-step upregulation, first during the first three days post amputation and then an even higher upregulation during stages 3-5. The lowest expression of these genes is detected in non-regenerating and proximal 50% DI arm segments (Figure 4.10). This trend of expression is consistent with a potential important role of these genes specifically in regeneration rather than simply a homeostatic role in the adult arm.

I then analysed the temporal expression patterns of our candidate skeletogenic genes (transcription factors and differentiation genes) to further characterize the dynamicity of gene expression during arm regeneration in *A. filiformis*. The biomineralization genes appear to have the highest level of expression at the 50% DI stage in the proximal arm segments undergoing differentiation (Figure 4.11 A-C). This is consistent with the WMISH results as well as morphological observations. However, the expression patterns of regulatory genes have a less clear pattern of relative abundance during regeneration. While genes like *Afi-alx1, Afi-ets1/2* and *Afi-rreb1* appear to consistently increase in expression levels during regeneration and have the lowest abundance in uncut, non-regenerating arms (Figure 4.11 D), *Afi-jun* shows an opposite trend whereby the highest expression levels are detected

in NR arms and in proximal segments of the 50% DI stage arms (Figure 4.11 E). The non-skeletogenic transcription factor *Afi-foxB* shows yet another, very different pattern of expression where it becomes upregulated only at stage 5 and late stages of regeneration. Finally, transcription factors *Afi-erg, Afi-nk7* and *Afi-gataC* have highly dynamic patterns of temporal expression, which do not easily fall into discernable categories (Figure 4.11 F). *Afi-erg*, for example, has a bimodal expression pattern with the first spike of expression between 24 and 72hpa, which then falls during early regenerative stages and is again highly upregulated in proximal segments of 50% DI arms.

In conclusion, the large-scale analysis of temporal and spatial expression patterns revealed the high degree of dynamic changes of regulatory states of cells during both early and late stages of arm regeneration in *A. filiformis*. It also confirmed that the cells in the dermal layer identified by histological analysis (see chapter 3) indeed express several molecular markers for biomineralization, and likewise the regenerating nerve and neuronal-related structures (podia) express molecular markers for neurogenesis. Finally, the quantitative analysis of gene expression supports potential biological functions of several selected genes. It also underline the complexity and irregularity of the regenerative process of an adult arm when compared with a developing embryo, for which temporal expression patterns are often more linear (Appendix Table A.0.4). Although not all of the 123 gene time-courses have been analysed in this work both adult regenerating arms and embryonic time-courses can be found in Appendix Table A.0.3 and Table A.0.4, which can aid future investigations into brittle star development

and regeneration. Additional WMISH experiments performed but not discussed in detail can be found in Appendix Figure A.0.2.

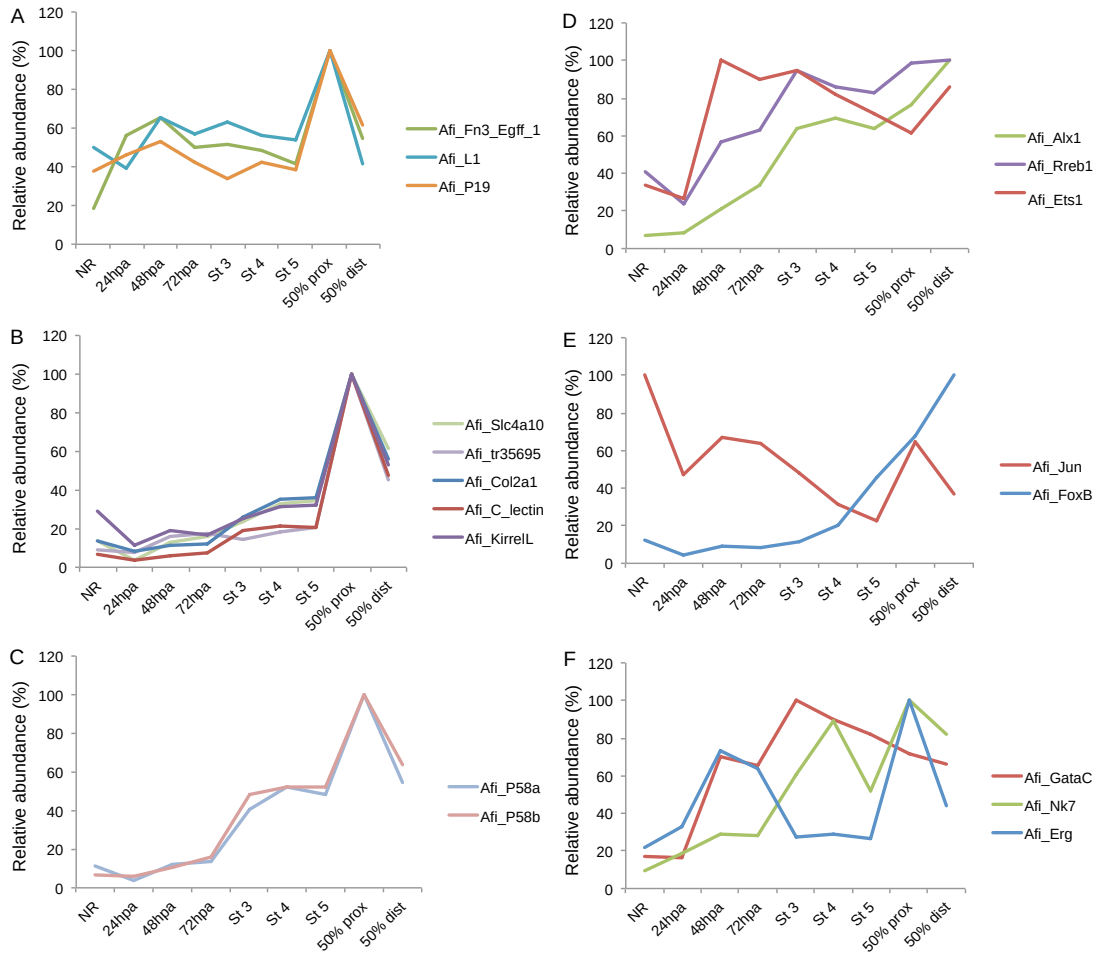

Figure 4.11: Dynamics of temporal gene expression patterns of differentiation genes and transcription factors detected using the Nanostring nCounter. A) Expression of *Afi-fn3-egff, Afi-l1 and Afi-p19*, B) *Afi-slc4a10, Afi-tr35695, Afi-col2a1, Afi-clectin, Afi-kirrelL* and C) *Afi-p58a* and *Afi-58b* group in similar expression patterns in uncut adult arms and during regeneration. Their peak of expression levels is in 50% proximal segments. Expression of D) *Afi-alx1, Afi-rreb1* and *Afi-ets1/2*, E) *Afi-foxB, Afi-jun* and F) *Afi-gataC, Afi-nk7* and *Afi-erg* in uncut adult arms and during regeneration show a higher degree of variability in expression patterns.

5 Role of FGF and VEGF signalling pathways in skeleton regeneration of *A. filiformis*

The role of FGF and VEGF signalling pathways in skeletogenesis have been studied extensively in sea urchin embryonic development (Adomako-Ankomah and Ettensohn, 2013; Duloquin et al., 2007; Lapraz et al., 2006; Röttinger et al., 2008). It has been shown that FGF signalling is necessary for guiding skeletogenic mesenchymal cell migration and formation of the embryonic skeleton in the sea urchin *Paracentrotus lividus* (Röttinger et al., 2008). Interestingly, in a different species, *Lytechinus variegatus*, FGF inhibition using an *fgfa* morpholino produces a much milder phenotype, whereby the mesenchymal cells migrate normally and the embryos even form shortened skeletal rods (Adomako-Ankomah and Ettensohn, 2013). In both species the VEGF signalling pathway seems to play a more pertinent role in skeletogenesis than the FGF pathway (Adomako-Ankomah and Ettensohn, 2013; Duloquin et al., 2007). Perturbation of the *vegf3* ligand in the sea urchin interferes with both correct skeletogenic cell migration and skeletal rod formation. Although it seems clear that both these pathways have essential and non-redundant roles in skeletogenesis in the sea urchin embryo, it is not well understood whether these pathways regulate different downstream effector genes and whether their role is conserved during adult skeletogenesis in echinoderms.

5.1 Expression of FGF and VEGF signalling genes during arm regeneration

The embryonic (http://www.echinonet.eu/shiny/Amphiura_filiformis/) and adult regenerating arm (Purushothaman et al., 2015) transcriptomes of the brittle star were surveyed for candidate genes of the FGF and VEGF signalling pathways. Three FGF ligands could be identified in the brittle star transcriptome – an ortholog of the sea urchin *fgf8/17/18, fgfA* (also referred to as *fgf9/16/20*) and a ligand not identified in any other species here named *Afi-fgf6* (not expressed during embryogenesis). *A. filiformis* has two FGF receptors orthologous to the sea urchin *fgfr1* and *fgfr2*. On the other hand, two ligands of the VEGF pathway could be found in the transcriptome - *vegf2* and *vegf3*, and only one receptor orthologous to the sea urchin *vegfr10*. I characterised the expression of FGF and VEGF ligands and receptors orthologous to the genes previously implicated in sea urchin development (*Afi-fgf9/16/20, Afi-fgfr1, Afi-fgfr2, Afi-vegf3, Afi-vegfr*) during the early stages of arm regeneration in *A. filiformis* using WMISH. *Afi-fgf9/16/20* and *Afi-vegf3* are both expressed in the epidermis throughout early stages of regeneration (stage 3-5; Figure 5.1 A-C and J-K), similarly to their expression in the ectoderm during embryogenesis (Appendix Figure A.0.1). At stage 5, both ligands have an additional domain of expression adjacent to the radial water canal in patches of cells that foresee the newly forming metameric units of the regenerating arm (Figure 5.1 C and K). *Afi-fgfr2* and *Afi-vegfr* receptors are expressed weakly at stage 3 (Figure 5.1 G and J) but then have clear localization in the dermal layer containing skeletogenic cells at stages 4 and 5 (Figure 5.1 H-I and N-O), again corresponding to what was observed in

embryos (Appendix Figure A.0.1). The other FGF receptor *Afi-fgfr1,* which is not expressed in skeletogenic cells in the embryo (Appendix Figure A.0.1), has a highly dynamic expression in several territories (not related to skeletogenic cells) including the epidermis, coelomic epithelium and radial water canal (Figure 5.1 D-F). During late stages of regeneration the two ligands (*Afi-fgf9/16/20* and *Afi-vegf3*) continue to be expressed throughout the epidermis of the regenerating arm (Figure 5.2 A, C, E, G I, K). Conversely, the two receptors previously expressed in the skeletogenic cells of the dermal layer are still expressed in the dermal layer of the distal end (Figure 5.2 J, L) of the regenerates and in the developing skeletal elements in the proximal segments. *Afi-fgfr2* is expressed in a pattern corresponding to all the skeletal elements, while *Afi-vegfr* is present in all the shields and spines but not the vertebrae (Figure 5.2 B, D, F, H). The presence of expression of these receptors in the dermal layer and differentiating skeletal elements suggests the FGF and VEGF signalling pathways are involved in the formation of the skeleton during adult arm regeneration in *A. filiformis*.

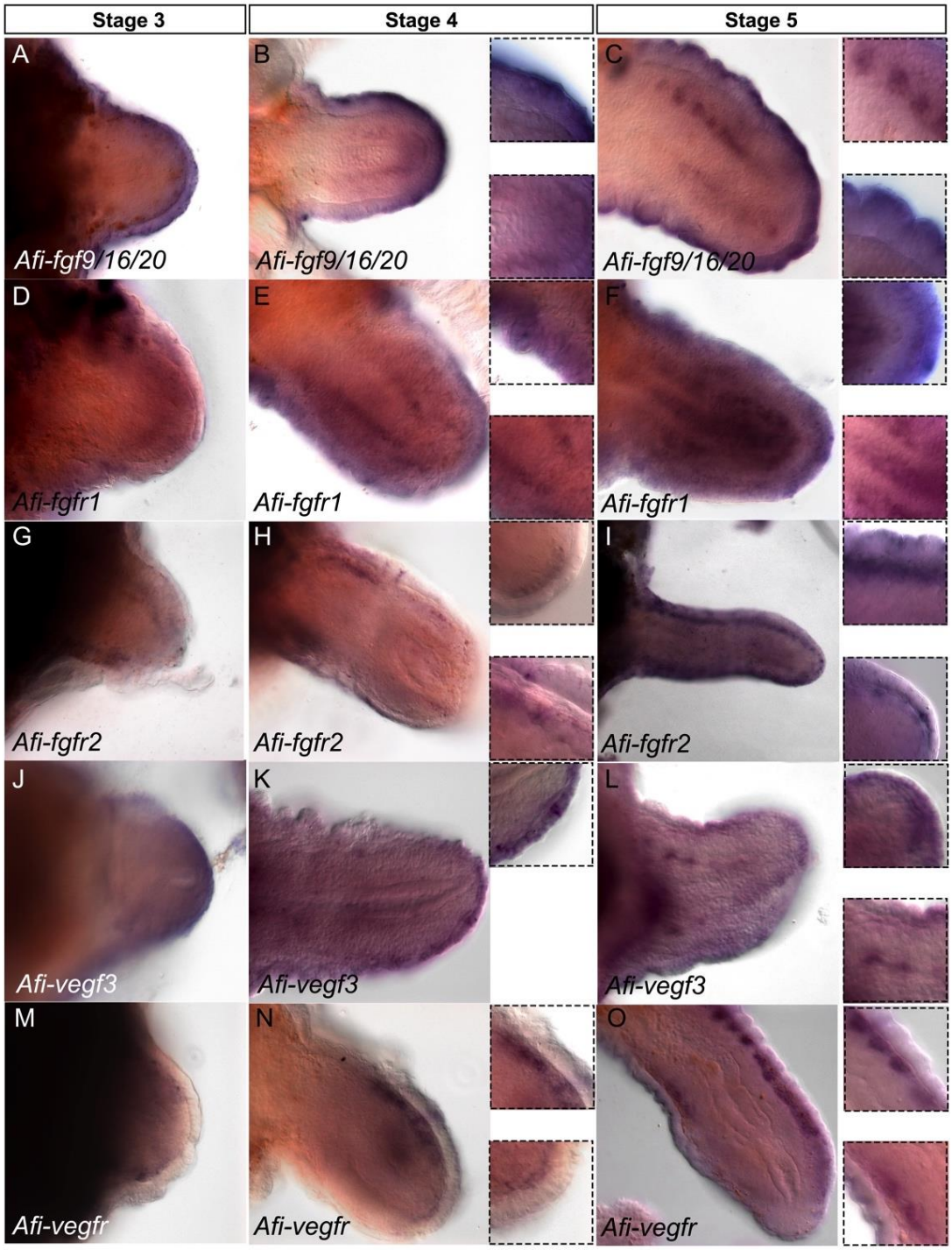

Figure 5.1: WMISH of FGF and VEGF signalling components during early stages of regeneration. Expression of A-C) *Afi-fgf9/16/20,* D-F*) Afi-fgfr1*, G-I) *Afi-fgfr2*, J-L) *Afi-vegf3,* and M-O) *Afi-vegfr* in early stage regenerates. The ligands *Afi-fgf9/16/20* and *Afi-vegf3* are first confined to the epidermis at stage 3 (A and J) and then are additionally expressed in a pattern corresponding to newly forming segments (C and L). The receptors likely involved in skeletogenesis - *Afi-fgfr2* and *Afi-vegfr*, are localized to the dermal layer (H-I, N-O). *Afi-fgfr1* is not expressed in the skeletogenic domain but is observed in the epidermis, radial water canal and coelomic epithelium (D-F). Insets show magnified regions of interest.

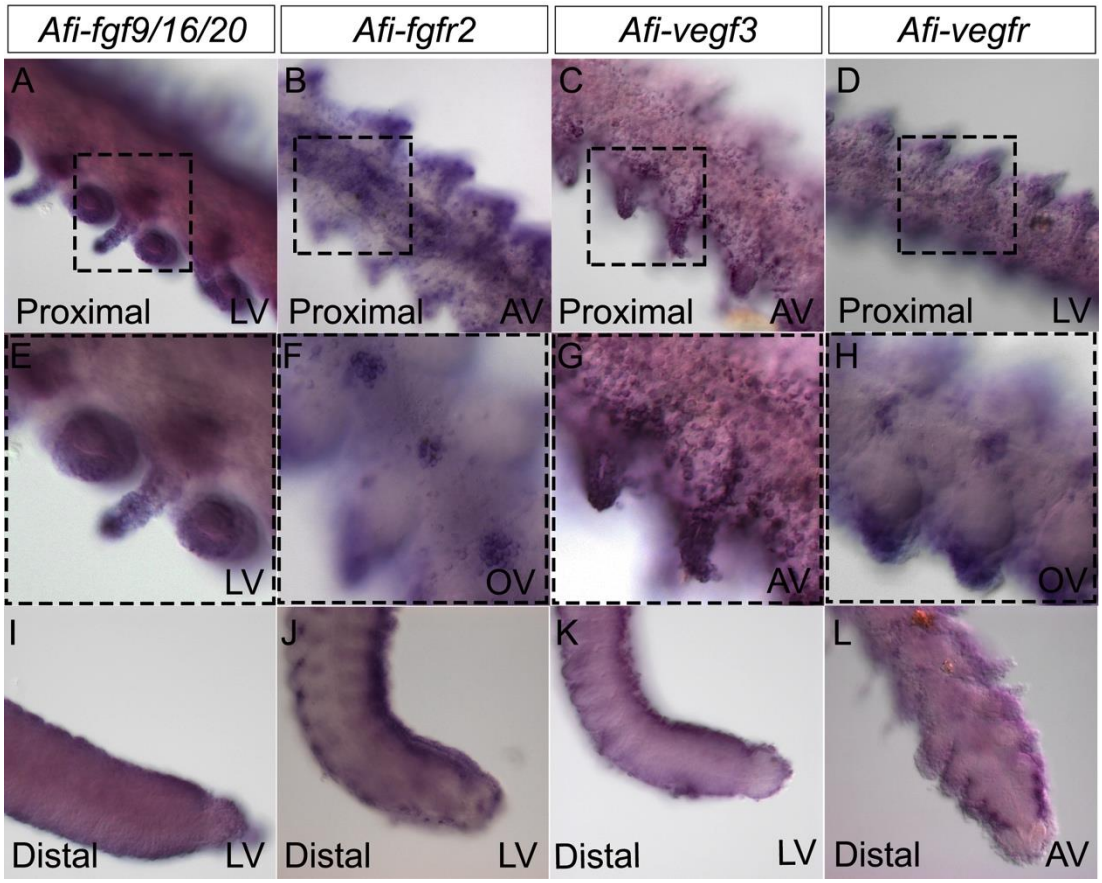

Figure 5.2: WMISH showing expression of FGF and VEGF signalling components during late stages of regeneration. A-D) expression of *Afi-fgf9/16/20, Afi-fgfr2, Afi-vegf3* and *Afi-vegfr* in proximal segments of late stage (50-95% DI) regenerates. E-H) Higher magnification images of region outlined in previous panels. I-L) Distal expression of *Afi-fgf9/16/20, Afi-fgfr2, Afi-vegf3* and *Afi-vegfr.* The two ligands *Afi-fgf9/16/20* and *Afi-vegf3* continue to be expressed in the epidermis only, whereas the two receptors are expressed in the dermal layer in the distal portion of the arm and localize to different skeletal domains in the proximal regions. *Afi-fgfr2* is expressed in all the domains (vertebrae, spines and lateral shields expression seen in B, oral shield expression seen in F). *Afi-vegfr* is localized to the aboral shields, lateral shields, spines (seen in D) and oral shields (seen in H) but not to vertebrae. *AV- aboral view, LV- lateral view, OV – oral view.*

5.2 Inhibition of growth factor signalling pathways

To analyse the roles of FGF and VEGF signalling in skeletogenesis during brittle star adult arm regeneration, I used pharmacological treatment with the SU5402 and axitinib inhibitors respectively. SU5402 is a small molecule (indolinone) that inhibits FGFR function by competing with ATP for the binding site of the catalytic domain of the tyrosine kinase (Mohammadi et al., 1997) and has been used in various organisms to inhibit FGF signalling during both embryogenesis and regeneration (Eblaghie et al., 2003; Hu and Marcucio, 2012; Lin and Slack, 2008; Saradamba et al., 2013). Axitinib, on the other hand, selectively inhibits VEGF receptors by blocking their cellular autophosphorylation (Hu-Lowe et al., 2008). I also took advantage of a unique property of some echinoderm species (including *A. filiformis*), namely, amputated arm explants that can survive separated from the main body for several weeks (Burns et al., 2012) and continue regenerating. I first amputated the arms and let them heal and regenerate until stage 2 (prior to formation of skeletal spicules; see Figure 3.7 in chapter 3) then amputated again 0.5cm proximally to create an explant (Figure 5.3 A). This method allowed the perturbation of the two signalling pathways in the arm only, without affecting the main body of the animal, and limited the potential harmful effects to the survivability of the individual. The explants were then incubated in SU5402 or axitinib together with calcein for 24h after which they were scored for phenotype and collected for Nanostring analysis of differentially expressed genes (Figure 5.3 B).

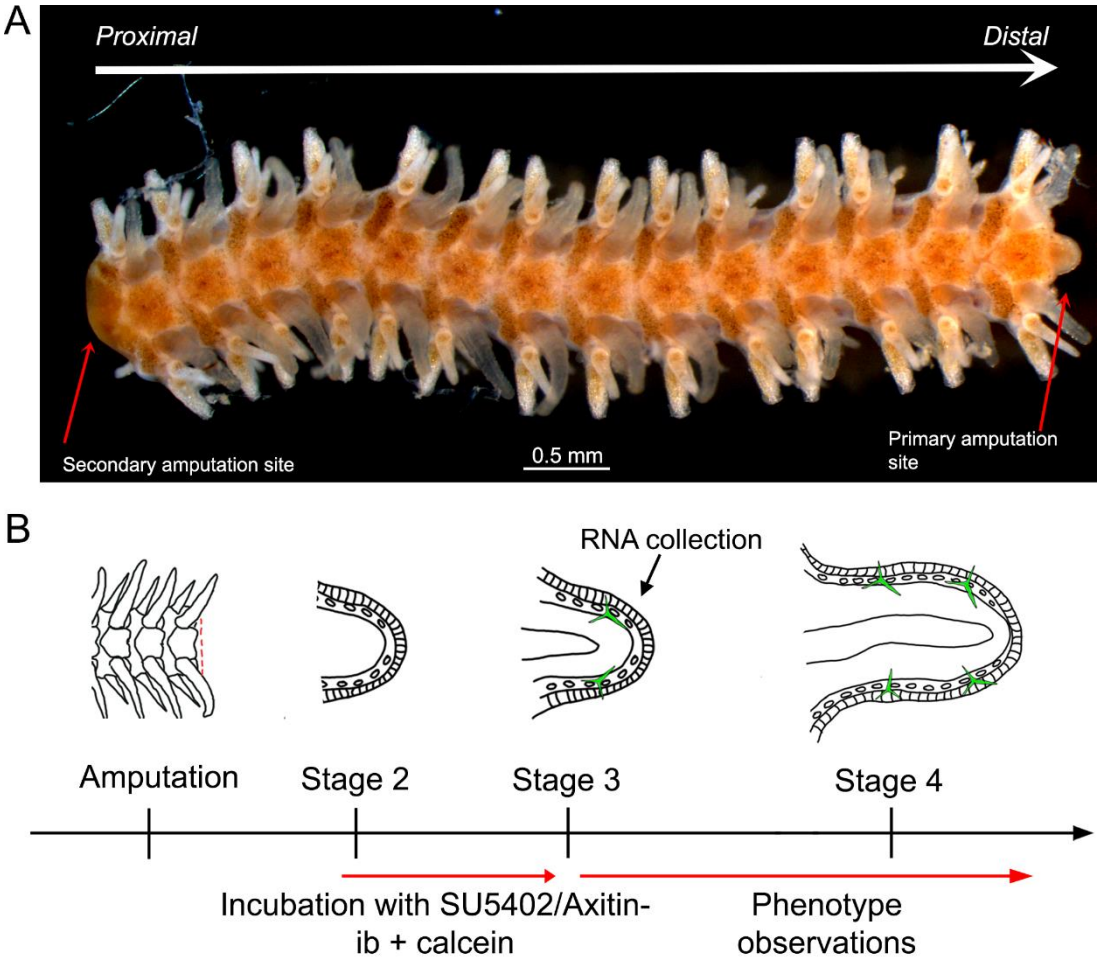

Figure 5.3: Strategy for pharmacological treatments in regenerating arm explants of *A. filiformis*. A) Diagram showing a double amputated arm explant for use in inhibitor studies. B) Strategy for inhibitor studies. The arms are first amputated 1cm from the disc, and the second proximal amputation is carried out at stage 2. The explant is then treated with the inhibitors (SU5402 or Axitinib) and calcein is added to visualize spicule formation for 24h until it reaches stage 3. At stage 3 RNA is collected from the regenerate for Nanostring quantification and remaining explants are left in the inhibitor longer for further phenotypic assessment. Skeletal spicules are shown in green (representing calcein).

FGF signalling perturbation using this method caused inhibition of skeletal spicule formation (Figure 5.4) in 78.1% of arms (n=41) compared with 0.1% DMSO control where only 7.7% of arms failed to form spicules (n=39) and 8.1% in non-treated filtered seawater (FSW) controls (n=37). All arm explants were alive and mobile after treatment, however only the DMSO and FSW controls continued to regenerate 48h after treatment (Figure 5.5).

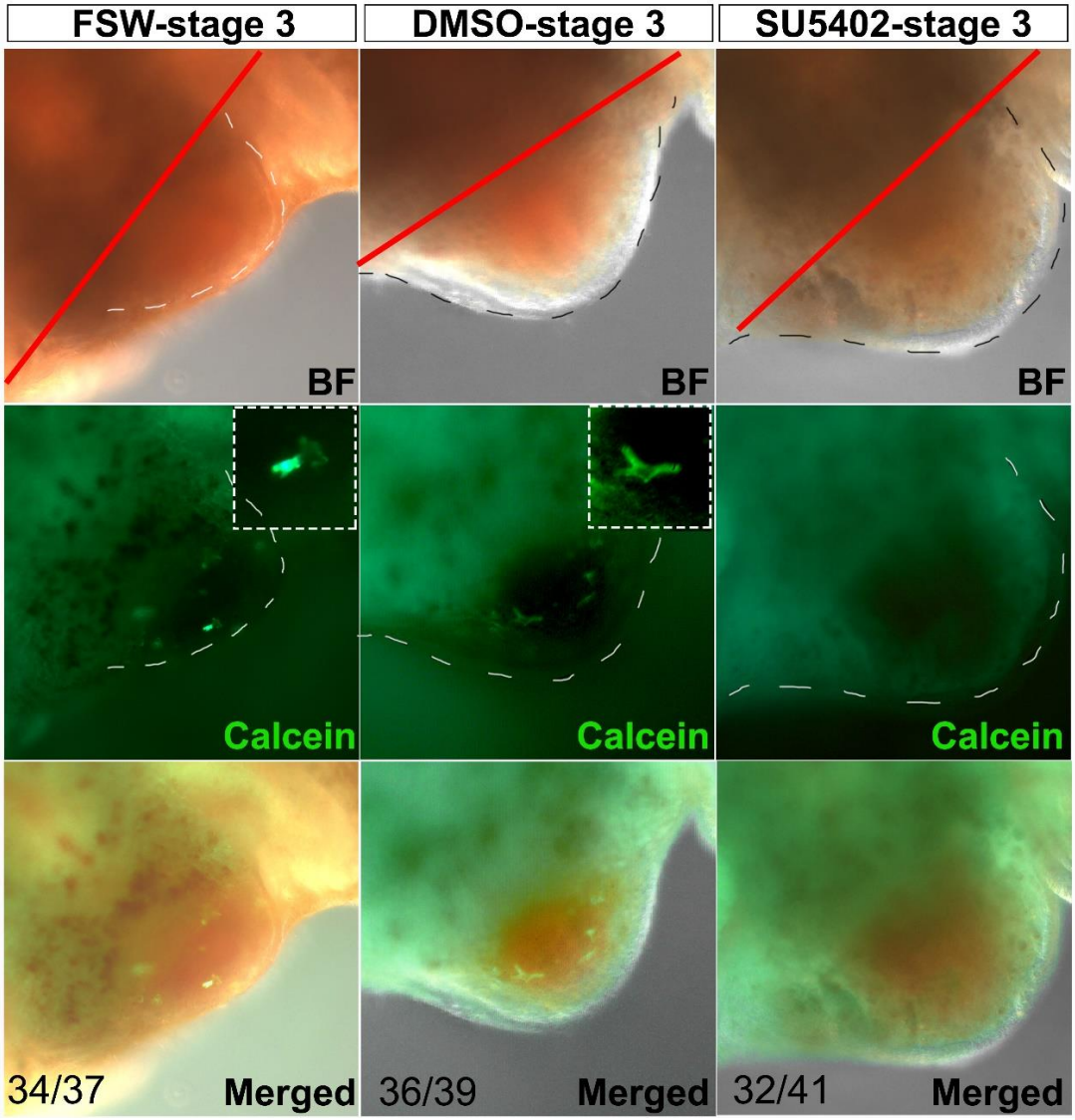

Figure 5.4: SU5402 treatment in regenerating arm explants inhibits skeletal spicule formation. Calcein was used to visualize spicule formation in the regenerating arm explants. FSW and DMSO controls show normal spicules at stage 3, whereas SU5402-treated arms fail to form any spicules. Numbers indicate the number of arms with represented phenotype. *Red line – amputation plane.*

Interestingly, despite the fact that SU5402-treated explants failed to regenerate further (n=8; Figure 5.5 A) we found that cell proliferation was not affected by the inhibition of FGF signalling (n=4; see methods section 2.14 for details on quantification; Figure 5.5 B and C). On the contrary Axitinib, the VEGF signalling inhibitor, had a significantly milder effect on skeleton regeneration with only 36.6% of treated arms (n=41) having reduced or

absent spicules compared to 13.6% in DMSO controls (n=44) and 10% in FSW controls (n=40) (Figure 5.6).

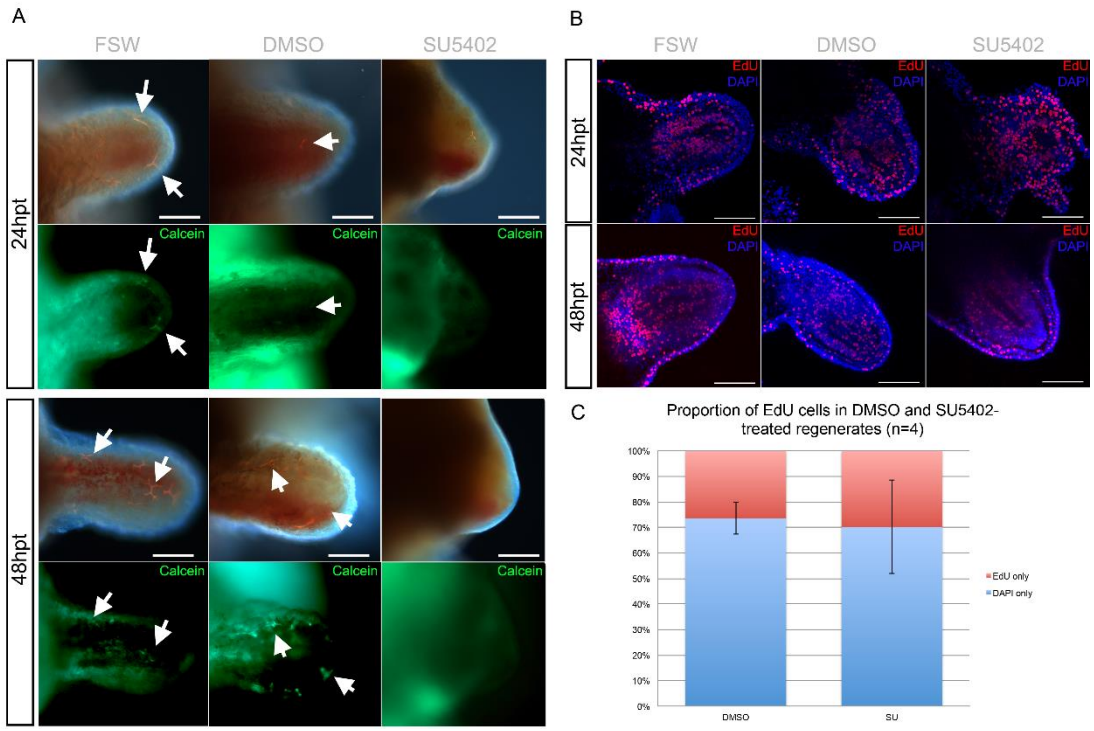

Figure 5.5: SU5402 treatment phenotypes after prolonged incubation. A) Explants treated with SU5402 fail to regenerate compared to the controls. B) Cell proliferation, measured by EdU cell labelling, is not affected in SU5402-treated explants. C) Quantification of EdU cells in DMSO and SU5402-treated arms shows no significant difference in proportion of EdU-labelled nuclei in the regenerates. *Hpt – hours post treatment, arrows- spicules*.

To compare the effect of these inhibitors during embryonic development, I treated brittle star embryos as described in Figure 5.7 A. SU5402-treated embryos completely fail to develop a larval skeleton (100%, n=114; Figure 5.7 B) and Axitinib treated embryos usually make one spicule during early development (75.4%, n=118) and this spicule elongates but fails to be patterned correctly (Figure 5.7 C). Altogether these results suggest already the first similarity between the function of FGF and VEGF signalling pathways in development and regeneration of the skeleton.

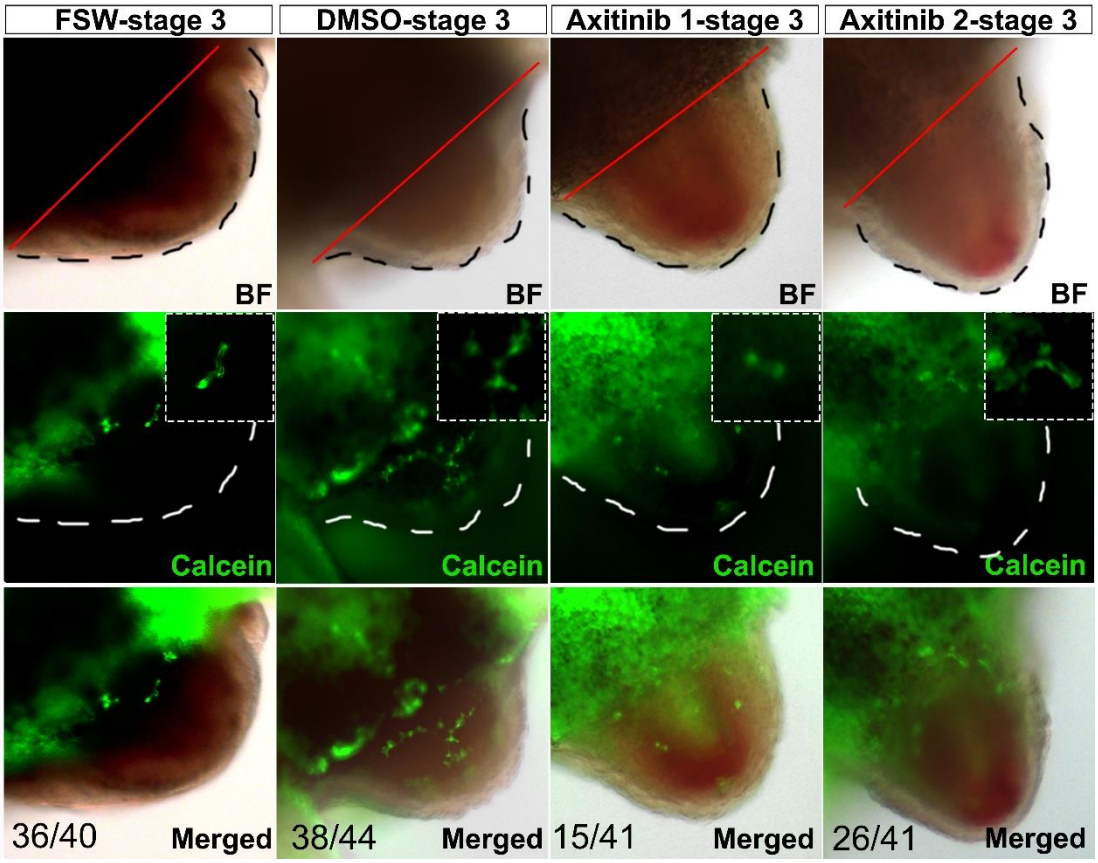

Figure 5.6: Axitinib treatment in regenerating arm explants does not significantly inhibit skeletal spicule formation. Calcein was used to visualize spicule formation in the regenerating arm explants. FSW and DMSO controls show normal spicules at stage 3. Axitinib treatment did not significantly affect spicule formation with most of the arms showing either slightly reduced (Axitinib 1) or normal spicules (Axitinib 2). Numbers indicate the amount of arms with the shown phenotype. *BF – brightfield*, *red line – amputation plane.*

Figure 5.7 (following page): Embryo treatments with SU5402 and Axitinib. A) Experimental strategy for pharmacological treatments of A. filiformis embryos. Skeletal spicules are shown in green (representing calcein). B) Phenotypic analysis of SU5402-treated and control embryos shows that FGF signalling inhibition does not interfere with skeletogenic mesoderm ingression (asterisk) but the embryos completely fail to make spicules. C) Phenotypic analysis of Axitinib-treated and control embryos shows that VEGF signalling inhibition mildly interferes with skeletogenesis as observed at 51 hpf (only one spicule forms, arrow) and the embryo often partially recovers to form a poorly patterned skeletal element at pluteus larva stage (arrow). Note, calcein staining beyond spicules in embryos is un-specific background.

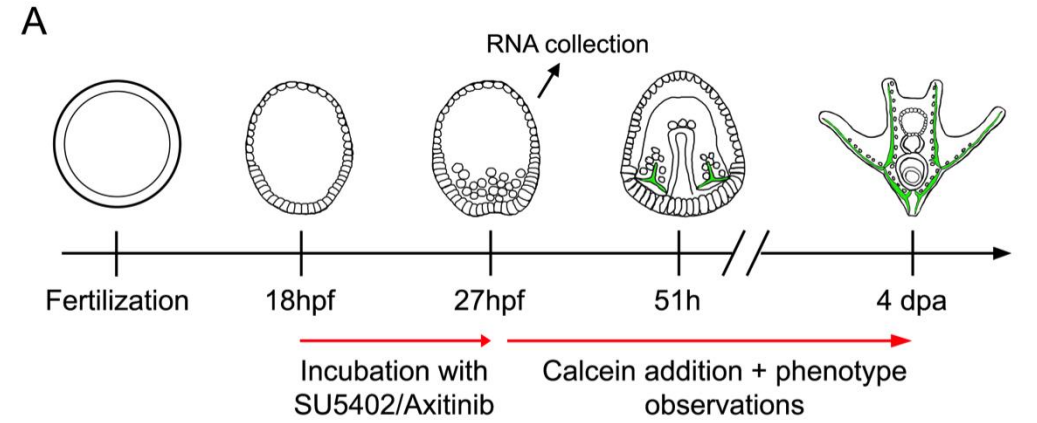
A
RNA collection
Fertilization
18hpf
27hpf
51h
4 dpa
Incubation with SU5402/Axitinib
Calcein addition + phenotype observations

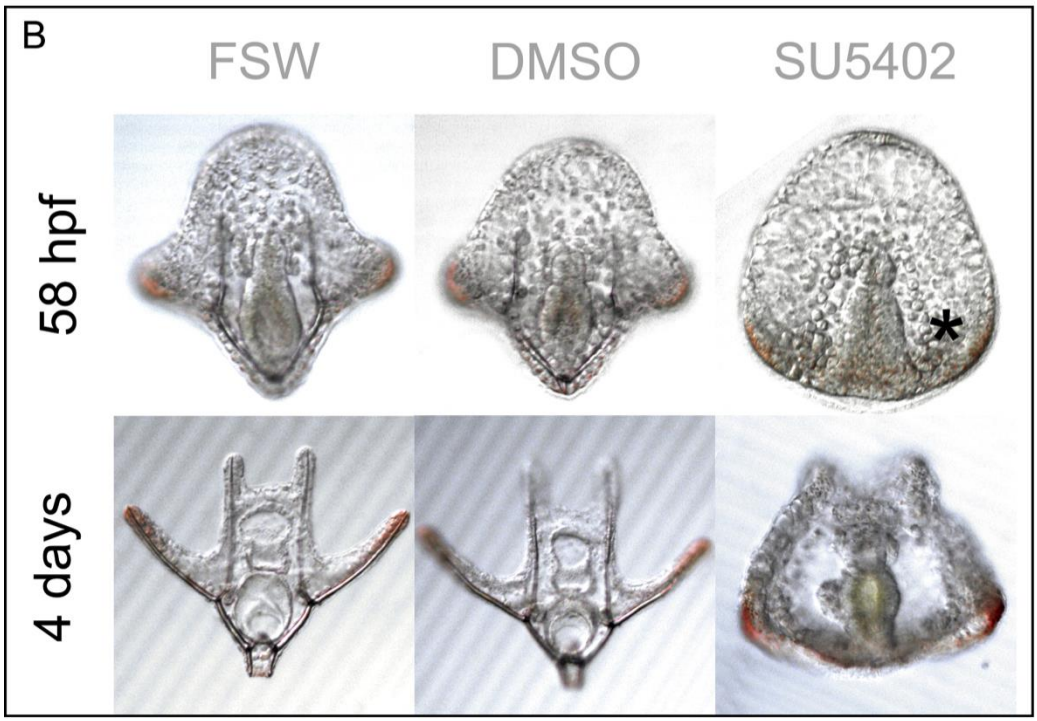
B
FSW
DMSO
SU5402
58 hpf
4 days

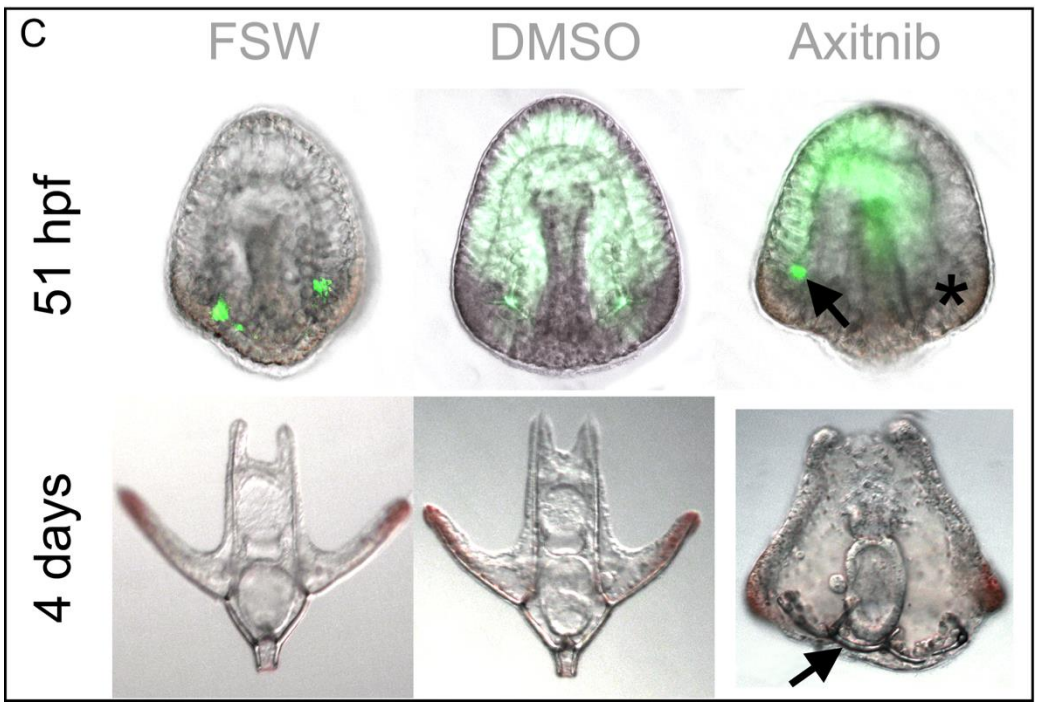
C
FSW
DMSO
Axitnib
51 hpf
4 days

5.3 Analysis of differentially expressed genes in regenerating arms treated with FGF and VEGF signalling inhibitors

To investigate the genes transcriptionally regulated by FGF and VEGF signalling during adult regeneration I performed a large-scale analysis of the effects of SU5402 and Axitinib perturbations in the explants using the Nanostring nCounter (see appendix for probe set and methods for information concerning sample collection and RNA extraction procedures). Three independent experiments were analysed for SU5402-treated samples and one for Axitinib-treated samples (due to time constraints). A comparison of FGF and VEGF treatments revealed that the two inhibitors similarly affect only a handful of genes (five genes including *Afi-egr, Afi-pea, Afi-slc4a10*). 16 genes were differentially expressed in SU5402-treated arms only (7 upregulated and 9 downregulated) and four genes were downregulated in Axitinib-treated arms only (see Appendix Table A.0.5; over the threshold of ± 1 on a log2 scale, see methods). Out of the known skeletogenic genes only the biomineralization genes *Afi-p58a* and *Afi-slc4a10* and the transcription factors *Afi-nk7* appear to be under the influence of VEGF signalling, which might account for its milder phenotypic effect on skeletal spicule formation compared to FGF signalling which affects over twice as many genes and has a clear no-skeleton phenotype. However, the experiment using Axitinib-treated arms was only carried out once in a single batch of arms and so it would have to be repeated for statistical significance to yield a more definitive conclusion.

5.4 Comparison of genes affected by SU5402 treatment in embryos and regenerating arms of the brittle star

As SU5402 treatment had a stronger effect on skeletogenesis than Axitinib in both embryos and adults, I wanted to compare the molecular effects of FGF inhibition between adult regenerating arms and embryos of *A. filiformis*. We found that ~83% of the quantified genes (not including internal standard genes and low level expression genes) showed a similar trend of expression (meaning they were downregulated, upregulated or unaffected) in both embryos and adults (see Appendix Table A.0.5 for full list of Nanostring experimental results). The embryonic results from the Nanostring nCounter are highly consistent with transcriptome and QPCR quantifications carried out previously in the lab (see transcriptome batch in Appendix Table A.0.5; David Dylus, unpublished). Most of the putative skeletogenic genes (Figure 5.8 A), are downregulated in both cases (for example *Afi-msp130L, Afi-slc4a10;* over threshold of -1 log2; ≤1 standard error of the mean). Three genes, namely an uncharacterized tyrosine kinase *Afi-tk8/Cad96a, Afi-vegf2* and *Afi-alx/arx* are upregulated (over threshold of +1 log2; ≤1 standard error of the mean). Interestingly, many genes, which were differentially regulated by FGF signalling in the adult regenerating arms compared with the embryos (Figure 5.8 B), were proliferation-related genes (TFs *Afi-runt1* and *Afi-fos*) and signalling genes belonging to other pathways (*Afi-serrate*). Several differentiation genes (*Afi-col2a1* and *Afi-c-lectin*) and potential upstream transcription factors (*Afi-alx1*, *Afi-ets1/2* and *Afi-jun*) are not affected by FGF signalling inhibition neither in embryos nor adults (Figure 5.8 C).

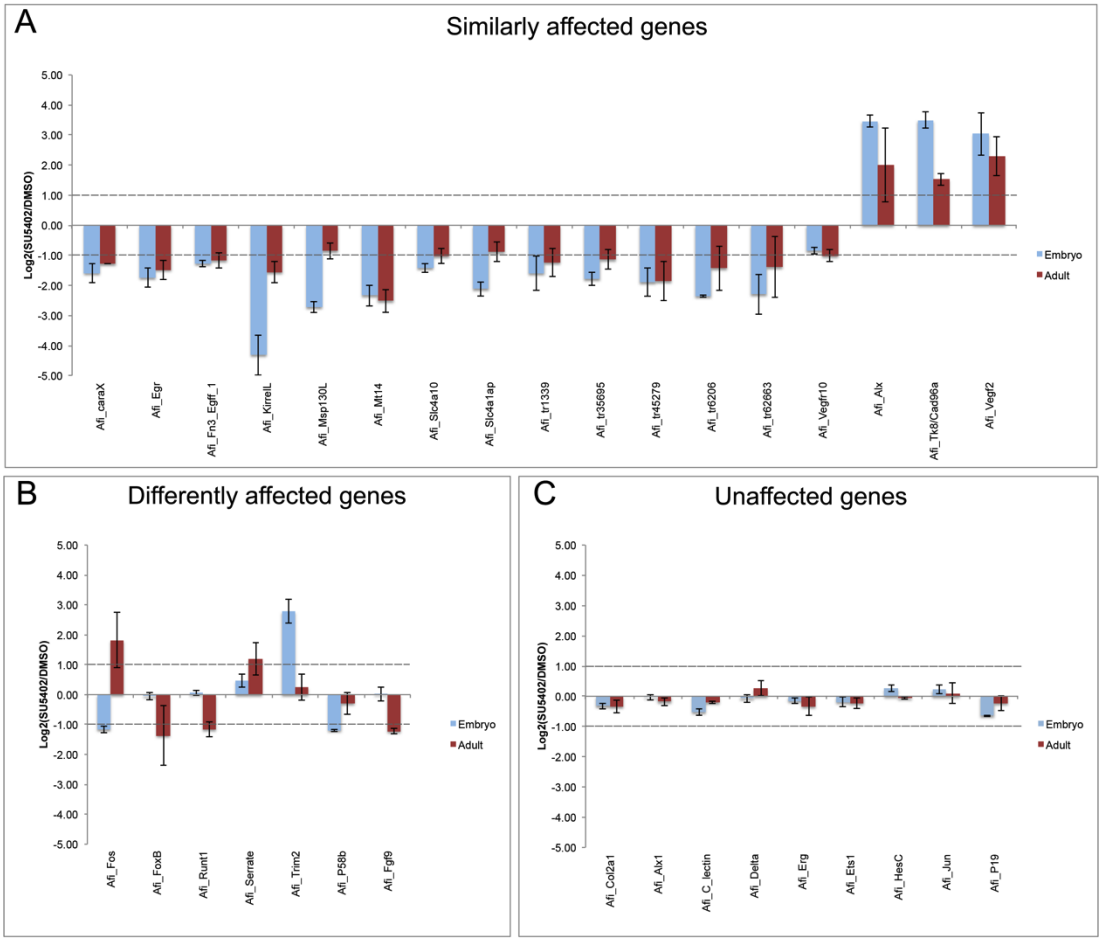

Figure 5.8: Comparison of differentially expressed genes in adult regenerating arms and embryos of *A. filiformis* treated with SU5402. A) Cohort of genes similarly downregulated (e.g. *Afi-egr, Afi-kirrelL* or *Afi-slc4a10*) or upregulated (e.g. *Afi-vegf2* and *Afi-alx/arx*) in both embryos and adults. B) Genes affected differently by SU5402 treatment in embryos and adults. C) Genes unaffected by treatment in either embryos or adults (e.g. *Afi-alx1, Afi-jun* or *Afi-erg*). Error bars show standard error of the mean from different biological replicas. Threshold of significance is ±1 log2(SU5402/DMSO) equivalent to 2-folds of difference.

Additionally, several novel genes with unknown functions, here identified by their assembly transcript number (e.g. *tr35695*), were identified already in a previous transcriptome-wide differential analysis of SU5402-treated embryos (also confirmed by QPCR; David Dylus, unpublished). I analysed five of those genes, also significantly downregulated by SU5402 treatment in regenerating arms (threshold of -1 log2; ≤1 standard error of the mean). These genes do not show immediate orthology to known

skeletogenic genes and their consistent response to the inhibitor of FGF signalling suggests they are novel genes involved in skeletogenesis of *A. filiformis*. Using tools for conserved domain identification (e.g. CDART and PFAM) and cellular localization (SignalP;), as well as quantitative and spatial expression analysis, I examined if they might play a role in skeletogenesis (Table 5.1; Figure 5.9). Although two of the genes had no significant BLAST hit to any other species present in the NCBI non-redundant database, all of the genes found similar sequences in other ophiuroids (*O. brevispinum*, *A. muricatum, O. spiculata*) and some also in asteroids (*L. clathrata, L. annulatus*) and crinoids (*A. mediterannea*) confirming their presence in echinoderms (EchinoDB, http://echinodb.uncc.edu/blast/). *Afi_tr31926, Afi_tr35695* and *Afi_tr6202* are all only found in ophiuroids suggesting they may be taxon-restricted genes. Since some of those genes are suspected secreted proteins, they could be potentially involved in biomineralization, considering the skeleton of echinoderms is secreted as extracellular matrix. Spatial expression (supported by quantitative expression; Figure 5.9 B) revealed that those genes are expressed in differentiating skeletal elements in the 50% DI arm proximal segments. No expression could be detected in early stages by ISH (Figure 5.9 A) though quantitative data revealed low levels of expression (Appendix Table A.0.3). However, *Afi_tr35696* is also specifically expressed in skeletogenic cells in early regenerating stages (Figure 5.9). Altogether, this approach allowed me to identify novel, potentially skeletogenic genes downstream of FGF signalling, which may be unique to the echinoderm phylum.

Table 5.1: Five novel genes downregulated by FGF perturbation with unknown function. BLAST results reveal that two of the genes have no immediate similarity to any other species found in the NCBI non-redundant (NR) database, while the other three find hits though with relatively poor similarity. All of the genes could be identified in another brittle star species (*O. brevispinum* or *O. spiculata*) with high confidence and often at least partial hits were found in other echinoderms (e.g. asteroid *L. annulatus*) or crinoids (*A. mediterannea*). Four of the five genes are likely to encode for secreted proteins due to the signal peptide prediction using SignalP. The CDART tool only found conserved domains in two out of the five genes.

Gene name	NCBI BLAST (NR)[1]	E-value	*EchinoDB BLAST**	*E-value*	*S. purpuratus genome**	*P. miniata genome**	*Secreted (SignalP)*[2]	Predicted GO terms (Predict Protein[3])	Conserved domains (CDART/PFAM[4])
Afi_tr31926	No hit	N/A	*O. brevispinum*[#]	5E-05	no	no	yes	Binding, catalytic activity	N/A
Afi_tr35695	No hit	N/A	*O. brevispinum*	2E-09	no	no	yes	Cation binding, calcium ion binding	N/A
Afi_tr45279	PREDICTED: uncharacterized protein [S. purpuratus]	2E-06	*L. annulatus*	10E-19	no	yes	yes	Protein binding, antigen binding	Ig superfamily
			O. brevispinum	5E-10					
			A. mediterannea	6E-07					
Afi_tr6206	PREDICTED: titin-like [S. kowalevskii]	2E-02	*A. muricatum*	2E-37	no	no	yes	Protein binding, IgG binding	N/A
			O. brevispinum	7E-34					
Afi_tr9107	PREDICTED: exoenzymes regulatory protein AepA-like [Acropora digitifera]	1E-41	*A. muricatum*	2E-68	no	yes	no	Hydrolase activity, catalytic activity	Amidohydrolase domain
			L. clathrata	3E-62					
			O. spiculata	2E-22					

* based on reciprocal blast
[#] colour scheme for echinoderm species: ophiuroid, asteroid, crinoid
[1] NCBI non-redundant database - blast.ncbi.nlm.nih.gov/Blast.cgi
[2] SignalP - cbs.dtu.dk/services/SignalP
[3] Predict protein - predictprotein.org
[4] CDART - ncbi.nlm.nih.gov/Structure/lexington/lexington.cgi; PFAM - pfam.xfam.org

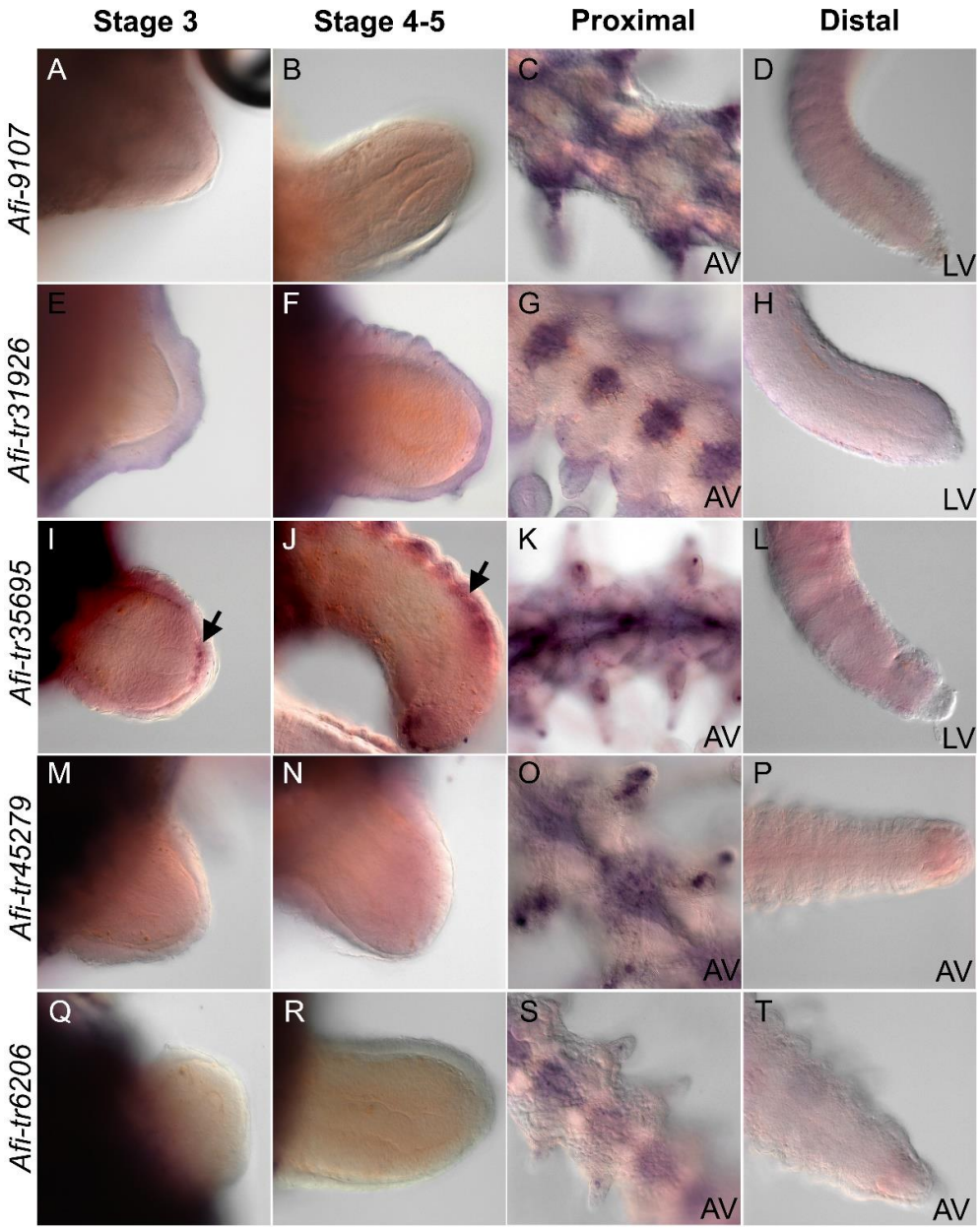
Stage 3
Stage 4-5
Proximal
Distal
Afi-9107
Afi-tr31926
Afi-tr35695
Afi-tr45279
Afi-tr6206
A
B
C
D
E
F
G
H
I
J
K
L
M
N
O
P
Q
R
S
T
AV
LV

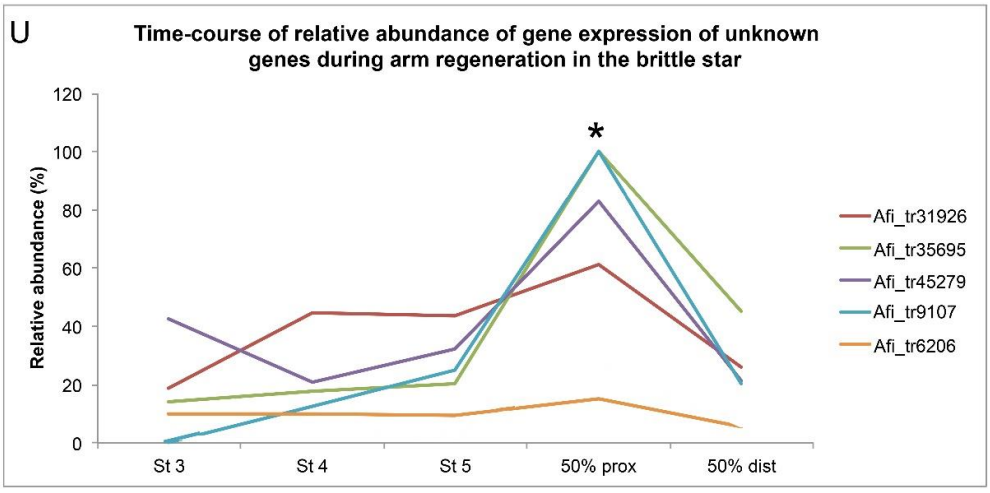
U
Time-course of relative abundance of gene expression of unknown genes during arm regeneration in the brittle star
Relative abundance (%)
120
100
80
60
40
20
0
*
St 3
St 4
St 5
50% prox
50% dist
Afi_tr31926
Afi_tr35695
Afi_tr45279
Afi_tr9107
Afi_tr6206

Figure 5.9 (previous page): Spatio-temporal expression of novel FGF target genes during arm regeneration of the brittle star. A-T) WMISH showing expression of *Afi_tr9107, Afi_tr31926, Afi_tr35695, Afi_tr45279* and *Afi_tr6206* during early (aboral view, stages 3-5) and late (50% DI proximal and distal segments) regeneration. Except for *Afi_tr35695*, no expression of these genes could be detected using ISH in the early stages of the distal segments of regenerating arms. *Afi_tr35695* showed specific expression in the dermal layer. In the 50% DI arm proximal segments *Afi_tr31926* showed expression in the vertebrae, *Afi_tr9107, Afi_tr45279* and *Afi_6202* were expressed in both vertebrae and spines and *Afi_tr35695* was expressed in spines, vertebrae and in the aboral shields. U) Consistent with the WMISH data, the Nanostring quantification for all the five genes showed the highest peak of relative abundance of transcripts in the 50% proximal segments (asterisk). Abundance represented as percentage relative to the highest expression value (note, non-regenerating and stage 1 samples are not shown). *st – stage, prox – 50% DI proximal segments, dist – 50% DI distal segments. AV – aboral view, LV – lateral view.*

To validate the results of the quantification of expression using the Nanostring and confirm that putative skeletogenic genes expressed in the dermal layer are inhibited by FGF perturbation, we additionally performed WMISH on treated and control explants and embryos (Figure 5.10). The transcription factor *Afi-egr*, which is normally expressed in the epidermis of the regenerate and the ectodermal layer of the embryo (resembling the expression of the signalling ligands *Afi-fgf9/16/20* and *Afi-vegf3*), shows a downregulation consistent with the quantification analyses (Figure 5.10 A-F). Similarly, a clear and specific downregulation of dermal/skeletogenic mesoderm expression of the differentiation genes *Afi-msp130L* (Figure 5.10 G-L) and *Afi-slc4a10* (Figure 5.10 M-R) can be observed. As a control the unaffected gene *Afi-p58b* was tested using ISH in regenerating arms, showing no effect on its specific expression (Figure 5.10 S-U), and analogously *Afi-col2a1* showed no change in expression in SU5402-treated embryos (Figure 5.10 V-X). Altogether, the evidence provided in this chapter strongly suggests that the molecular network driving skeletogenesis

downstream of FGF signalling is functionally conserved between embryogenesis and regeneration.

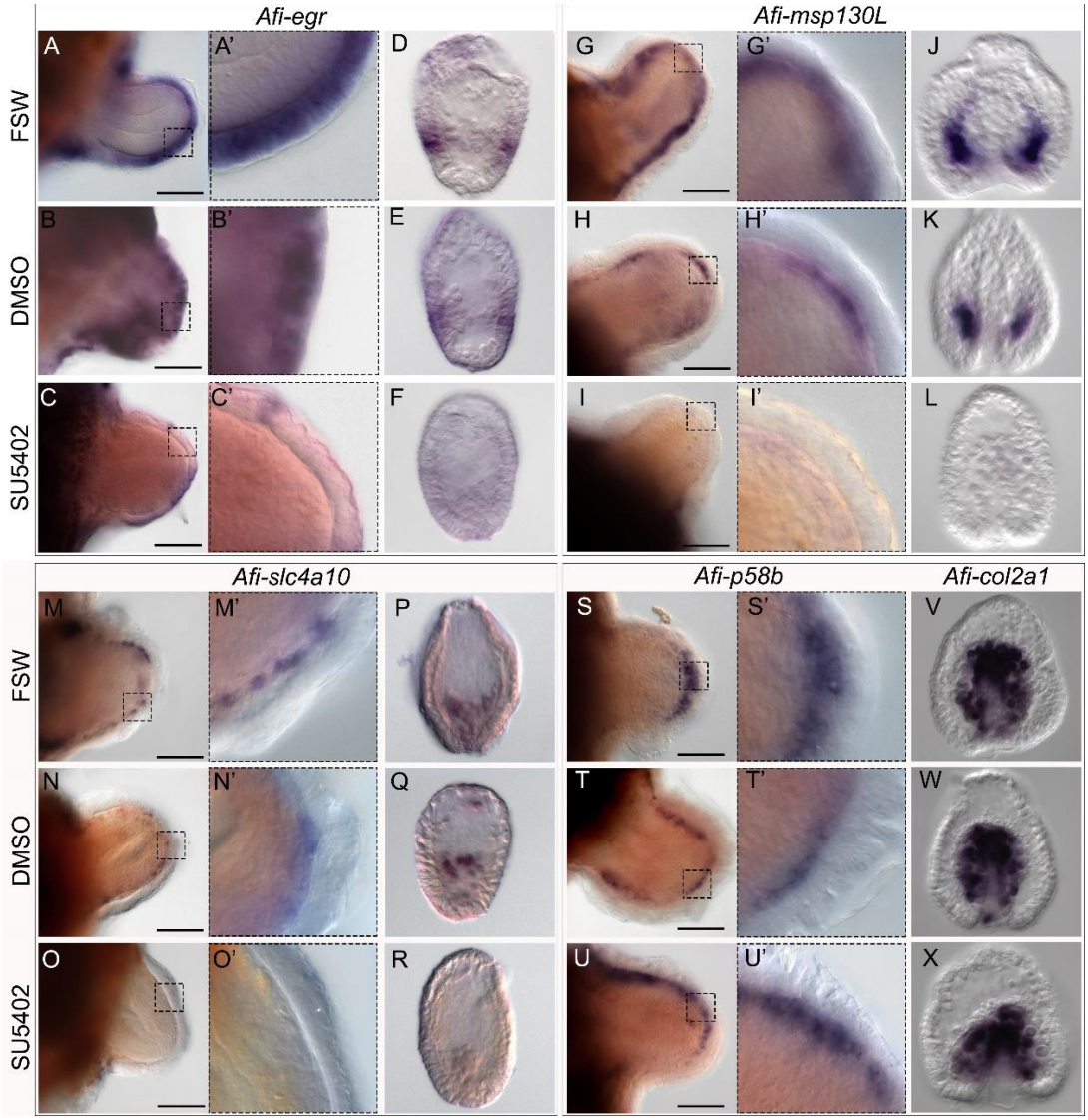

Figure 5.10: WMISH showing expression of genes in regenerating arms and embryos treated with SU5402 compared with controls. A-C') expression of *Afi-egr* in FSW, DMSO and SU5402-treated regenerating arms and E-F) embryos. G-I') expression of *Afi-msp130L* in FSW, DMSO and SU5402-treated regenerating arms and J-L) embryos. M-O') expression of *Afi-slc4a10* in FSW, DMSO and SU5402-treated regenerating arms and P-R) embryos. S-U') expression of *Afi-p58b* in FSW, DMSO and SU5402-treated regenerating arms. T-X) expression of *Afi-col2a1* in FSW, DMSO and SU5402-treated embryos. *Scale bars – 100µm.*

6 Discussion

6.1 Redefining ophiuroid regeneration

The high capacity and speed of *A. filiformis* arm regeneration, likely evolved to escape predation (Dupont and Thorndyke, 2006), is ideal for the investigation of the developmental process underlying the regrowth of a completely functional arm constituted by many different cell types and tissues. In this study, I describe the major developmental events occurring during early and late phases of arm regeneration in this brittle star. The use of histological, molecular and cell-proliferation assays allowed me to re-examine historical preconceptions about ophiuroid regeneration and redefine it accordingly.

6.1.1 Staging

The regeneration process, like embryonic development, is characterized by transient stages. At the base of any molecular and cellular investigation of dynamic developmental processes lays the clear understanding of the sequence of events taking place during these stages. Thus, in this study, I first identify five major early regenerative stages (Figure 3.2) easily recognizable by external morphology in living animals. These stages subdivide the regenerate starting at the wound healing and repair phase (stage 1), to initial growth (stage 2; also described as blastema in other studies; Biressi et al., 2010; Dupont and Thorndyke, 2006), into more and more complex cellular layers and structures (during stages 3 to 5) that

foresee the organization of the future rebuilt arm. There are two previously published staging systems for arm regeneration in *Amphiura filiformis.* The division described by Dupont and Thorndyke (2006) only distinguishes an early, uncharacterized phase (called blastema), from two rather advanced stages of regeneration (50% and 95% DI), in which several metameric units of the regenerate are already present and contain differentiated structures. This staging system, although useful for studying late stages of regeneration and quantifying growth rate, completely bypasses early developmental and morphological events. According to this classification, all my early stages would be classified generally as 0% DI; therefore, this system is not relevant for the aim of understanding cell specification and morphogenesis. On the other hand, the staging system devised by Biressi et al (2010) is focused largely on the very early phases post amputation. This system first subdivides early regeneration into a repair phase (immediately after amputation, 1 dpa) and an early regenerative phase (1-3 dpa), both of which correspond to my stage 1. My EdU labelling experiments (Figure 3.11) show that the events taking place during this stage do not involve cell proliferation. The two remaining phases described, namely an intermediate regenerative phase (3-12 dpa) and an advanced regenerative phase (11-24 dpa), do not discriminate at high enough resolution the events taking place within this time frame. This is essential to understanding how morphology is generated, and how specification and differentiation of skeletogenic cells occur. For instance, I show that the stage 3 regenerate (average 6.3 dpa) is already characterized by a clear organization of different tissues (Figure 3.5), but is still quite different from stage 4 (average 7.8 dpa) when the metameric units that will

form the arm begin to appear. This revised staging system is more relevant for the precise study of the developmental processes taking place during *A. filiformis* regeneration. It also allows more homogeneous sampling by identifying regenerating arms at specific stages, which are directly comparable, despite coming from animals with different regeneration rates.

6.1.2 Blastema

Historically, ophiuroid and crinoid arm regeneration were thought to follow a typical epimorphic mode characterized by the formation of a blastema (Bannister et al., 2005; Cardia and Daniela, 2006; Thorndyke et al., 2001). Old definitions of the blastema characterize it as a mass of undifferentiated, pluripotent cells, which give rise to the regenerating structure (Morgan, 1901). However, research in recent years showed that in many cases these proliferative cells are not truly undifferentiated, but rather retain a memory of tissue origin and often have a limited progenitor potentiality (Kragl et al., 2009; Tanaka et al., 2016). More recently, Biressi and co-authors described that the ophiuroid blastema is composed of presumptive undifferentiated coelomocytes and it is retained at the distal portion of the arm throughout regeneration (Biressi et al., 2010). In my morphological and molecular investigation of *A. filiformis* regeneration, I have failed to observe a true undifferentiated blastema forming at any point during regeneration. In contrast, high magnification microscopic and histological analyses show that it is the nerve that regenerates first and forms the regenerative bud at stage 2 (Figure 3.4), covered by a collagenous dermal layer and an epidermis. Already at stage 3 I observed a high degree of

organization of the internal structures into the aboral coelomic cavity, the radial water canal in addition to the nerve at the oral side (Figure 3.5). Additionally, what was previously described as the ‘distal blastema’ in fact differentiates very early into the distal structure containing a terminal ossicle and podium (Figure 3.6 and Figure 3.8), and it is the region directly underneath it, which retains proliferative capacity and intercalates new metameric units (Figure 3.13 and Figure 3.14). However, even this ‘growth zone’ is composed of organized heterogeneous tissues (aboral coelomic epithelium, epidermis, dermal layer, radial water canal and nerve cord). This is confirmed by the expression patterns of molecular markers of the nervous system. *Afi-elav, Afi-soxB1*, *Afi-soxC* and *Afi-pax6*, well-known neuronal genes, are expressed very early in the distal tip of the regenerate, which will eventually form the distal podium (Figure 4.8). Additionally, *Afi-six3* is expressed in both this distal tip and throughout the length of the regenerating radial nerve cord (Figure 4.8). Although the regenerative bud of *A. filiformis* cannot thus be called a typical blastema, it is highly proliferative (as shown by EdU labelling; Figure 3.12). It is important to note however, that EdU labelling experiments were limited to 2-hour pulses (based on experimental procedures described for other echinoderms and planarians) and further investigations of cell cycling kinetics in this animal would be necessary to draw definitive conclusions concerning proliferation during regeneration in *A. filiformis.* Nonetheless, in addition to the previously described coelomocytes, the cells of the aboral coelomic epithelium and radial nerve cord might also re-enter the cell cycle and contribute to different regenerating structures. It remains to be investigated whether any stem-like progenitor cells or mostly

dedifferentiated cells are involved in arm regeneration in the brittle star. For example, I show that *Afi-c-lectin* expressing cells are not labelled with EdU at any time during regeneration (Figure 3.12 and Figure 3.13); however, their number increases during regeneration, as does the number of skeletal structures. This suggests that there must be a constant supply of skeletogenic cells since they themselves appear to have no proliferative capacity. Due to the lack of knowledge on cell cycle kinetics in *Amphiura*, additional experiments testing longer and shorter EdU incubation periods would have to be used in future experiments to determine that those cells definitely do not proliferate throughout regeneration. However based on my preliminary results I can speculate that, for example, a small pool of local progenitor cells that proliferate and give rise to daughter cells, which then molecularly and morphologically differentiate, could maintain the cell population. Alternatively, the newly formed cells could also be supplied from the adjacent tissues such as the aboral coelomic epithelium, which shows high levels of cell proliferation and also putative skeletogenic regulatory genes like *Afi-alx1, Afi-ets1/2, Afi-nk7* and *Afi-soxE* are expressed in this tissue (Figure 4.4). Furthermore, our histological analysis of early stage regenerates reveals mesenchymal cells, which appear to be ‘sprouting’ from the aboral coelomic epithelium (Figure 3.5). Alternatively, the radial water canal has also been implicated as a major source of cells in the regenerative bud (Biressi et al., 2010) and, as they are mesenchymal, skeletogenic cells could migrate from there into their final dermal location. However, preliminary cell-tracking data obtained using DiI labelling show no migration of cells out of the radial water canal (Appendix Figure A.0.3). Nevertheless, the

preliminary EdU pulse and chase labelling experiments suggest that cell migration is likely to contribute to regeneration overall (Figure 3.15). Therefore, although no stereotypical blastema containing undifferentiated progenitor cells can be found in arm regeneration of this brittle star, the precise identity and origin of the cells in the regenerative bud still remains to be elucidated. The possibility to track small numbers of cells during the development of the complex arm should be further explored to address this question.

6.1.3 Distalization-intercalation mode of regeneration

An important observation arising from this study concerns the mode of brittle star arm regeneration. By looking at the development of skeletal elements in the 50% DI arms I can observe the whole gradient of regenerative developmental stages from the oldest differentiated proximal metameric units to the newest un-differentiated distal metameric unit with skeletal primordia (Figure 3.8). However, the distalmost tip containing the terminal ossicle and podium is differentiated and the growth zone adding new metameric units is located just proximally to it. This suggests that after a transient stage of formation of the regenerative bud, the brittle star could regenerate its arm following a distalization-intercalation model similar to what has been described in sea star (Ben Khadra et al., 2015b), insect (Anderson and French, 1985; Hopkins, 2001), planarian or salamander regeneration (Agata et al., 2003; Agata et al., 2007; Nye et al., 2003). According to this model regenerating organisms first form the distalmost part of the regenerate, which acts as a re-organization centre, and then add new

structures by sequential intercalation of newly generated tissues between the distal part and the stump following a distal-proximal gradient. The following observations are consistent with this model of regeneration in the brittle star: 1) the small amount of EdU^+ cells in the distalmost tip of late regenerates compared with the underlying growth zone (Figure 3.13) supports the differentiation status of this terminal element; 2) the early appearance of skeletal elements in the distalmost tip, which suggests early differentiation of the terminal ossicle (stage 5, Figure 3.7); 3) the appearance of forming segments in an intermediate position between the terminal tip and stump, 4) expression of some signalling molecules in the distal structure (*Afi-delta*, data from Prudence Lui). This is consistent with gene expression studies of transcription factors known to be involved in early specification of mesodermal and neuronal cells (e.g., *alx1, ets1/2, gataC, soxC*) localized in the growth zone, but not in the distalmost tip (Figure 4.6 and Figure 4.8). On the other hand, the distal structure cells express skeletogenic genes like *Afi-c-lectin*, and sensory nervous system genes like *Afi-pax6* and *Afi-elav* (Figure 4.6 and Figure 4.7). A similar mode of regeneration has been recently reported for sea stars, in which the distalmost element is represented by the terminal tube foot and associated terminal ossicle and the growth zone is located just at the base of this structure (Ben Khadra et al., 2015b; Hotchkiss, 2009). Whether the terminal structures of both brittle stars and sea stars have only protective and sensory functions, or also act as true signalling centres to the patterning of regenerating tissues, remains to be elucidated. Like in embryonic development, various signalling pathways (including Wnt, hedgehog, BMP and FGF) have been implicated in

establishing positional information during regeneration of various organisms. In Hydra, multiple Wnt signalling pathway components are expressed in the anterior part of the animal after amputation and are implicated in head organizer activity (Broun et al., 2005; Hobmayer et al., 2000; Lengfeld et al., 2009). In planarians, both Wnt and FGF signalling have been shown to be involved in the specification of anterior structures (like the brain) (Adell et al., 2010; Schmid et al., 2009). In insects, the EGF and Wnt signalling pathways have been shown to be important for establishing proximo-distal identity during leg regeneration (Nakamura et al., 2007; Nakamura et al., 2008). Alternatively, different mechanisms could be employed for the patterning and segment formation during arm regeneration in the brittle star. For example, a mechanism similar to vertebrate somitogenesis. Segmentation of the somites relies on an intrinsic molecular clock, which drives the periodic activation of various signalling pathways including Notch, FGF and Wnt and a wavefront of travelling signal gradients resulting in gradual maturation and separation of the somites (reviewed in Hubaud and Pourquié, 2014). During cockroach development, segmentation is achieved by a sequential addition of new metameric units through the proliferation of a posterior growth zone. This highly resembles segmentation in the vertebrate posterior paraxial mesoderm and also relies on the activity of Notch signalling (Pueyo et al., 2008). Exploring the expression and role of components of these highly conserved developmental signalling transduction pathways in brittle star arm regeneration might reveal whether the distal structure acts as an intercalary signalling centre to pattern the regenerate along the proximal-distal axis, or whether segmentation relies on an intrinsic molecular clock. Transplantation

and dissection experiments could also aid in understanding if regeneration and metamerization is dependent on the formation of this distal structure.

6.2 Similarities and differences in skeleton regeneration and development

Regeneration has been hypothesized to evolve multiple times in all the different animal phyla by re-using pre-existent developmental regulatory modules (Brockes and Kumar, 2008; Smith et al., 2011). Here, I present the comparison of skeletogenesis during embryogenesis and adult regeneration in the same species revealing vast similarities between the two developmental processes.

6.2.1 Morphological similarities of skeletogenic cells and spicules between the embryo and regenerating arm

Skeletogenesis of echinoderm embryos has been studied extensively in sea urchins and, more recently, in brittle stars providing an excellent basis for comparing the development of the skeleton with adult regeneration. In sea urchin and brittle star embryos skeletogenic cells become specified at late cleavage stage (Davidson et al., 1998; Dylus et al., 2016; Okazaki, 1975; Wilt and Ettensohn, 2008), which is exemplified by expression of the key activator of the skeletogenic GRN - *alx1* (Dylus et al., 2016; Ettensohn et al., 2003; Koga et al., 2016). These cells then undergo an epithelial-to-mesenchymal transition and remain mesenchymal throughout skeletal development. In chapter 3 I show that the cells, which express skeletogenic TFs including *Afi-alx1* and *Afi-jun,* and downstream genes like *Afi-c-lectin,*

are also mesenchymal cells located in the dermal, collagenous layer of connective tissue in the early regenerate (Figure 3.5). My observations of the formation of the skeleton during early regenerating stages suggest that cells undergo specification and differentiation events very early during the regeneration process (Figure 3.7). The spicule primordia observed at stage 3 resemble the granule-like skeletal rudiment of *A. filiformis* embryos (Dylus et al., 2016), and both sea urchin embryos (Okazaki, 1975; Wilt and Ettensohn, 2008) and juveniles (Yajima and Kiyomoto, 2006) at the earliest step in the development of the skeleton, which then branch into tri-radiated and tetra-radiated spicules.

6.2.2 Late differentiation and patterning of the skeleton

The 50% differentiated arm shows the developmental progress of the skeleton from single spicules up to the formation of complex mesh-like structures of the dermal plates (lateral, oral and aboral shields), spines and vertebrae (Figure 3.8). The program used to form these intricate patterns of skeletal elements in the adult might be similar to the mechanism of patterning of the pluteus shape skeletal rods in the larva. Several studies have shown that the interaction of the skeletogenic mesoderm with its adjacent ectoderm is crucial for the correct patterning of the larval skeleton in sea urchins and brittle stars (Mcintyre et al., 2014). FGF and VEGF ligands are expressed in the ectoderm and their interaction with their respective receptors, expressed by skeletogenic cells, mediate correct migration of SM cells, as well as localization and elongation of the skeletal rods (Adomako-Ankomah and Ettensohn, 2013; Duloquin et al., 2007; Morino et al., 2012; Röttinger et al.,

2008). pax2/5/8 and wnt5 expressed in the ectoderm overlying the SM both in sea urchin and brittle star larvae have also been implicated in the development of the pluteus skeleton (McIntyre et al., 2013; Morino et al., 2016). I found that FGF and VEGF signalling genes are expressed in a topologically conserved relationship during adult arm regeneration in A. filiformis at late stages (Figure 5.2), and thus could play a role in patterning of the different skeletal elements differentiating in proximal segments. This will need to be confirmed by future analysis of the effects of FGF/VEGF perturbation at late stages of regeneration.

Interestingly, the vertebral spicules, which are internal skeletal elements, appear much later than those involved in the formation of the lateral shields and spines (Figure 3.8). As seen in SEM images, the complete vertebrae in adult non-regenerating arms of ophiuroids are composed of two conjoined ambulacral plates (Gage, 1990; Irimura and Fujita, 2003; Stöhr et al., 2012), which could explain why during regeneration the vertebrae appear to form by a fusion of skeletal elements from bilateral halves of each segment (Figure 3.8). The same SEM studies also show that they are clearly the most complex and dense skeletal elements in the ophiuroid arms (Gage, 1990; Irimura and Fujita, 2003; Stöhr et al., 2012). Taken together, these data suggest molecular differences and possibly that a separate developmental program might be involved in the formation of those internal-most skeletal structures compared to the sparser stereom constituting the lateral shields and spines. This is supported by differences in expression of genes present in all skeletal territories compared to those localized preferentially in only some skeletal elements (Figure 4.7). Interestingly, a

combination of different sets of differentiation genes has also been observed in skeletogenic cells of the late pluteus larva in sea urchins (Sun and Ettensohn, 2014). Certainly different positional cues must be required to shape different skeletal elements. While it is conceivable that the epidermis acts as a signalling centre for the underlying dermal layer of skeletogenic cells, as the ectoderm provides essential positional cues in the sea urchin embryos (Duloquin et al., 2007), this is unlikely to be the case for the skeletogenic cells forming the vertebrae. Nevertheless, the presence of FGF and VEGF ligand expression in patches of expression deeper in the tissue (Figure 5.1) might suggest these signalling pathways are also involved in vertebrae formation, though either through a different set of receptors or the receptor expression in the vertebral skeletogenic cells is undetectable. It would be interesting to test what potential signalling pathways might be involved in the formation of individual skeletal ossicles during brittle star arm regeneration.

6.3 Molecular comparison of skeleton regeneration and development

6.3.1 Molecular signature and regulatory state conservation

Interesting similarities and differences arise from comparing the expression patterns of putative skeletogenic GRN components between the adult regenerating arm and the developing embryo of *A. filiformis* (Figure 6.1). When comparing the expression pattern of putative skeletogenic genes during stages 2-5 (this work) in the regenerating arm with the blastula and mesenchyme blastula stages of embryogenesis (Dylus et al., 2016;

appendix) several similarities are apparent. During stages 2-3 of regeneration several of the downstream differentiation genes are not yet expressed (e.g. *Afi-lrr-igr, Afi-fn3-egff, Afi-p19*), resembling the blastula stage of embryogenesis. However, many other genes including *Afi-p58a, Afi-p58b, Afi-slc4a10* and *Afi-c-lectin* are already expressed as early as stage 2-3, suggesting a slightly more differentiated state of the skeletogenic mesenchymal cells in the regenerating arm compared to the blastula stage pre-mesenchymal SM cells of the embryo. Most embryonic biomineralization genes start to be expressed when the cells ingress into the blastocoel. At mesenchyme blastula stage all the investigated skeletogenic genes are already activated, and those genes, which are also expressed during regeneration, have similar expression restricted specifically to the skeletogenic cells. The expression of TFs *Afi-alx1, Afi-erg, Afi-jun, Afi-nk7,* and *Afi-rreb1* in the skeletogenic territory is conserved between the two processes. Additionally, the broad sub-epidermal expression of *Afi-ets1/2* in the regenerate is reminiscent of its expression in both the skeletogenic and non-skeletogenic mesoderm in the embryo. *Afi-foxB* and *Afi-dri*, which are transiently expressed in the skeletogenic cells during ingression in the sea urchin (Amore et al., 2003; Minokawa et al., 2004), are never expressed in skeletogenic cells in either embryos (Dylus et al., 2016) or regenerating arms of the brittle star. Finally, the distinct expression patterns of *fgf* and *vegf* ligands in the ectoderm/epidermis and receptors in the skeletogenic cells during development and regeneration are conserved.

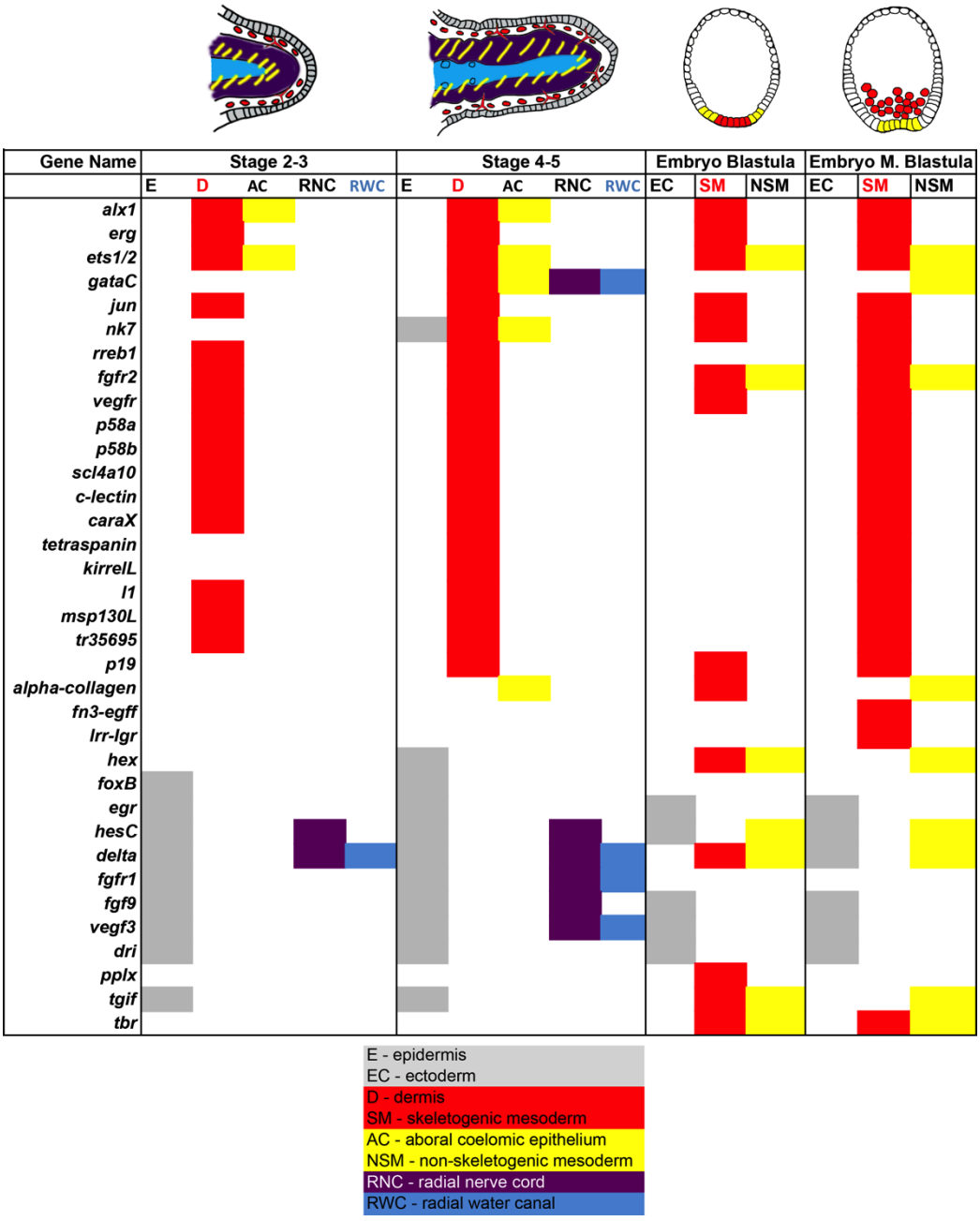

Figure 6.1: Comparison of gene expression between early regenerating arm stages and early embryonic stages of the brittle star *A. filiformis*. Top) Schematics of different territories in the early regenerating arm. Schematics of the blastula and mesenchyme blastula stages of development of the brittle star. Bottom) Table showing summary of expression patterns of genes discussed in this thesis. A large degree of conservation can be observed when comparing the expression domains of differentiation genes (e.g. *Afi-p19*) and mesodermal transcription factors (e.g. *Afi-ets1/2, Afi-erg*). Several genes also show similarity in expression in the epidermis/ectoderm (e.g. *Afi-egr, Afi-dri*). Some differences can also be observed for example the absence of *Afi-tbr* and *Afi-pplx* in adult arms.

This comparison reveals a high degree of conservation of both the molecular signature of these cells (defined by expression of differentiation genes) in regeneration and development as well as their regulatory states (defined by expression of transcription factors and signalling molecules). However, a few differences can also be observed. *Afi-tbr, Afi-pplx* and *Afi-tgif* are either not present at all during regeneration or are not expressed in the skeletogenic domains, whereas those genes show (although mostly transient) expression in skeletogenic cells of the embryo. This suggests that those genes are unique to the embryonic mesoderm formation in the brittle star.

6.3.2 Functionality of skeletogenic GRN downstream of FGF signalling is highly conserved between regeneration and embryonic development

In this thesis I show that *A. filiformis* adult skeleton regeneration relies heavily on the presence of FGF and to a lesser extent VEGF signalling, similarly to embryonic development (Figure 5.4 - Figure 5.7). The lines of evidence for this are as follows: 1) the expression pattern of *fgf* and *vegf* ligands and receptors during development and regeneration allows for the ectodermal-mesodermal tissue interaction shown previously to be crucial for skeletogenesis in sea urchin embryos (Adomako-Ankomah and Ettensohn, 2013; Duloquin et al., 2007; Röttinger et al., 2008); 2) perturbation of the FGF pathway using the universal pharmacological agent SU5402, but not the VEGF pathway using Axitinib, resulted in complete inhibition of skeletal spicule formation in both adult arms and embryos; and 3) FGF signalling inhibition specifically downregulated a larger set of differentiation genes compared to VEGF inhibition. The underlying molecular network downstream

of FGF signalling driving skeletogenic cell differentiation is highly conserved between regeneration and development with 15 genes being specifically downregulated in both cases e.g. the transcription factor *Afi-egr* or the differentiation genes *Afi-kirrelL, Afi-mt14/mmpl7* and *Afi-slc4a10*. Additionally, a previously uncharacterized tyrosine kinase receptor (*Afi-tK8/Cad96a*), *Afi-vegf2* and *Afi-alx/arx* are all upregulated in both embryos and adult arms. Similarly to what was suggested for sea urchins (Röttinger et al., 2008), we show the role of FGF signalling during skeletogenesis in the brittle star appears to be confined primarily to downstream differentiation of skeletogenic cells (via genes like *Afi-msp130L*, *Afi-slc4a10*), as upstream specification transcription factors (including *Afi-alx1*, *Afi-ets1/2* and *Afi-jun*) are unaffected (Figure 5.8). For example *Afi-caraX*, which is downregulated, is a member of the carbonic anhydrase gene family, which have been implicated in calcium carbonate deposition in various organisms including sea urchins (Livingston et al., 2006; Mann et al., 2008b) and molluscs (Mann et al., 2012). Proteomic studies revealed hundreds of proteins associated with both the sea urchin and brittle star skeletal matrix (Mann et al., 2010; Seaver and Livingston, 2015). Consistently with those results, it is clear that biomineralization in the brittle star requires a multitude of skeletogenic genes to be activated. FGF signalling perturbation specifically downregulated many skeletogenic differentiation genes while having no effect on others (e.g. *Afi-p19, Afi-c-lectin, Afi-col2a1*), and so it appears to only regulate a subset of the skeletogenic differentiation gene cassette likely to be necessary for the last step of skeleton formation.

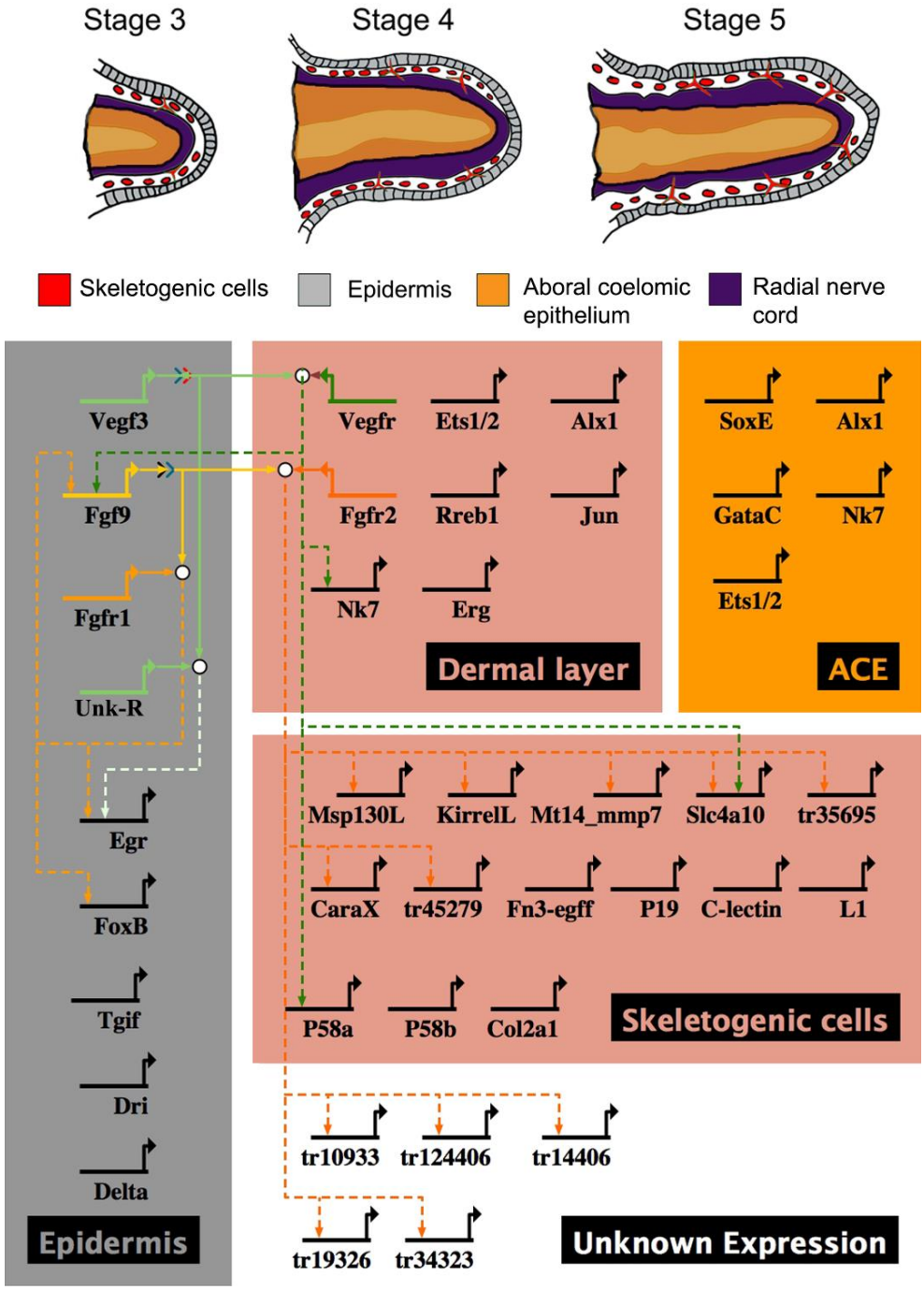

Figure 6.2: Provisional gene regulatory network for the specification and differentiation of skeletogenic cells during arm regeneration in the brittle star. Top) Schematics of regenerates showing cellular domains. Bottom) Provisional GRN drawn using BioTapestry (biotapestry.org) showing the presence of specific transcription factors, signalling genes and differentiation genes in the early regenerate. Each gene is represented as horizontal line with arrow. Dashed lines show functional relationships between FGF and VEGF signalling and their targets (probably acting indirectly via unknown regulatory genes). White dots symbolize signalling interaction. *Unk-R – potential unknown VEGF receptor*.

Due to the lack of skeletal elements in perturbed embryonic and adult regenerating arm samples (Figure 5.4 and Figure 5.7) I can conclude that a specific combinatorial expression of those genes is required for biomineralization to occur. This analysis, together with the gene expression investigation of candidate skeletogenic genes allowed me to model a provisional gene regulatory network for skeletogenesis in the adult regenerating arm of *A. filiformis* (Figure 6.2). Taken together, this data provides the first large-scale comparison of the molecular networks driving development and regeneration of the same species, and shows support for the theory of regeneration re-capitulating development, at least at the level of cell specification/differentiation (compare adult network with embryonic network in Dylus et al., 2016). It remains to be found whether the initiating inputs upstream of this signalling pathway are conserved between embryonic development and adult regeneration.

6.4 New genes with unknown functions identified in the differential screen

It remains unclear, which genes specifically downstream of FGF signalling truly play a role in skeletogenesis. Although one can easily speculate on the role of genes like *Afi-caraX, Afislc4a10, or Afi-msp130L*, which have consistently been identified as biomineralization-related proteins in echinoderms and other animals (Harkey et al., 1992; Illies et al., 2002; Le Roy et al., 2014; Rafiq et al., 2014; Tambutt?? et al., 2007; Zito et al., 2015), it is more difficult to understand how the novel or unknown genes (differentially affected by SU5402) are involved in this process.

6.4.1 Transcription factors *Afi-egr* and *Afi-rreb1*

Afi-egr, expressed in the epidermis of the arms (Figure 5.10) and the ectoderm of the embryos (Figure A.0.1) similarly to the sea urchin (Materna et al., 2006), was one of the genes significantly downregulated by FGF inhibition. It is an ortholog of Early growth response-1 (Egr-1), a Cys2-His2-type zinc finger transcription factor, which has been implicated in various cellular processes such as cell proliferation, differentiation or apoptosis and many human diseases including cancer (Pagel and Deindl, 2011). Also in vertebrates, FGF signalling is a potent activator of Egr-1 (Damon et al., 1997; Santiago et al., 1999). This gene has been implicated in regeneration of the liver by regulating hepatocyte proliferation (Liao et al., 2004) and is strongly upregulated at early stages of regeneration in the salamander blastema (Stewart et al., 2013; Voss et al., 2015). Since SU5402 treatment in the adult inhibits arm regeneration, *Afi-egr* might play an important role in regeneration overall rather than specifically in skeletogenesis. Nevertheless, the specific expression of *Afi-egr* in the adjacent ectoderm/epidermis (Fig. 5.10) may be an indication of its role in skeletogenesis via the mesoderm-ectoderm tissue interaction mediated by FGF signalling. For example, it could play a role in modulating the strength of the signalling. It would be interesting to determine the expression of FGF and VEGF signalling components in SU5402 treated samples using WMISH to identify potential subtle changes in expression.

Another C2H2 zinc finger transcription factor identified in our lab, though not as being consistently downstream of FGF signalling, is *Afi-rreb1*, expressed specifically in skeletogenic cells both in embryos and regenerates (appendix, Fig. 4.3). Not much is known about the function of the Ras-

responsive transcriptional element binding protein 1 (Rreb1) in other systems. In the sea urchin it is transiently expressed in the non-skeletogenic mesoderm (Materna et al., 2006). During *Drosophila* embryogenesis the *Rreb1* homolog *hindsight* (*hnt*) is expressed in the midgut and the tracheal system and was shown to be involved in cell differentiation, cell adhesion and collective cell migration (Melani et al., 2008; Wilk et al., 2000). Although its expression in vertebrate development is unknown it has been implicated in tumour suppression in cancer as part of the Ras signalling transduction pathway (Thiagalingam et al., 1996). Interestingly, in axolotl regeneration there is an increase in *rreb* expression around 20 days post amputation, concomitant with the upregulation of chondrogenic and osteoclast genes including *col2a1* and *mmp13* (Voss et al., 2015). As *Afi-rreb1* is not affected by FGF nor VEGF signalling it might play a role upstream in the hierarchy of the skeletogenic GRN of the brittle star, perhaps in the migration of the skeletogenic mesenchymal cells.

6.4.2 Potential taxonomically restricted genes *Afi-tr31926, Afi-tr35695, Afi-tr45279, Afi-6202* and *Afi-tr9107*

Taxonomically restricted genes, or lineage-specific genes, are genes found in only one species or particular taxonomic group, without detectable sequence similarity in organisms outside of that group. They have been identified in most sequenced genomes to date and usually constitute approximately 10-20% of all genes (Khalturin et al., 2009; Wilson, 2005). It has been proposed that those genes play important roles in driving morphological evolution, additionally to cis-regulatory changes and gene

duplications, for example by allowing the organism to specialize and adapt to different conditions. Some examples include: taxon-restricted genes expressed in honey bee workers, which have been linked to the evolution of sociality (Johnson and Tsutsui, 2011); cnidarian-specific genes involved in specialized structures called nematocytes (Milde et al., 2009); and specialized venoms taxonomically restricted to some lizards (Fry et al., 2010). In this work, I identified putative echinoderm and ophiuroid-specific genes that may be involved in biomineralization. Especially the gene found only in ophiuroids, *Afi-tr35695*, could be important for understanding both the evolution of skeleton in this class of echinoderms, as also in studying the evolution of the larval skeleton in brittle stars and sea urchins. It's putative role in biomineralization is probable due to the presence of a signal peptide, and it's expression specifically in the skeletogenic cells during regeneration (Figure 5.9) and embryonic development (data not shown). Further analysis of the expression and role of these taxonomically-restricted genes in the brittle star could yield important insight into the evolution of skeletogenesis in the brittle star, echinoderms, and deuterostomes in general.

6.5 Evolutionary implications for skeletogenesis in deuterostomes

The conservation of the gene regulatory network driving skeletogenesis between adult regeneration and embryonic development in the brittle star invites further questions about the potential evolutionary conservation of this network. This includes both the evolution of the skeleton in echinoderms as well as deuterostomes as a whole.

6.5.1 Implications for evolution of larval skeleton in echinoderms

Recent work showed that despite a striking similarity in the morphology and development of the larval skeleton in sea urchins and brittle stars, the dynamics of their regulatory states are very different, suggesting alternative re-wiring of the network in the two classes (Dylus et al., 2016). Additional differences have been identified in the skeletogenic GRN of euechinoids, like *S. purpuratus,* and pencil sea urchin species, like *P. baculosa*, which further complicates a clear understanding of the evolution of the larval skeleton (Yamazaki et al., 2014). It has been suggested that the larval skeleton in euechinoids evolved by re-activating the ancient pleisiomorphic regulatory apparatus for driving the skeletogenic differentiation gene batteries in the adult (Gao and Davidson, 2008). Comparing the larval skeleton GRN to the adult one in different echinoderm species has the potential of establishing the common network for skeletogenesis for all adult echinoderms as well as identifying individual genes involved in larval co-option.

Several regulatory genes have been identified in the juvenile skeletogenic centres of sea urchins and sea stars including *alx1, ets1/2, hex, tgif, jun, dri* and *vegfr* (Gao and Davidson, 2008; Morino et al., 2012). *foxB* and *tbr*, on the other hand, were not expressed in the juvenile skeletogenic cells suggesting that these genes might be unique to embryogenesis. In *A. filiformis* several genes of this ‘core’ regulatory apparatus are present both in the embryos and adults including *Afi-alx1, Afi-ets1/2, Afi-erg, Afi-jun* and *Afi-vegfr,* possibly confirming them as part of the ancient, conserved adult skeletogenic network. However, there are also several differences: 1) neither

Afi-foxB nor *Afi-dri* are expressed in the skeleton of brittle star embryos or adults; 2) *Afi-hex* is expressed in the skeletal domain only during late differentiation of skeletal elements during regeneration and is likely not part of the initial specification of skeletogenic cells; 3) *Afi-tgif* is not expressed in the adult skeletogenic cells of *A. filiformis*, 4); and finally 4) *Afi-rreb1* is expressed in embryos and adult regenerating arms of the brittle star but not in the skeletogenic cells of the sea urchin embryos, as far as we know (Materna et al., 2006). In order to resolve the evolutionary question of independent or homologous co-option of the adult skeletogenic network it would be important to identify whether there are more similarities between the embryonic and adult skeletogenic networks within individual echinoderm species as opposed to similarities between adult networks of different echinoderms. This work provides a basis for comparison of these networks and their differences.

In sea urchin embryos, FGF signalling components are expressed in a complimentary pattern, whereby the *fgfr2* receptor is specifically expressed by the skeletogenic mesoderm cells and the *fgfa* ligand is expressed in overlying ectoderm flanking those cells (Adomako-Ankomah and Ettensohn, 2013; Röttinger et al., 2008). Recent work showed that this pattern of expression is also observed for the VEGF signalling genes in both sea urchin (Adomako-Ankomah and Ettensohn, 2013; Duloquin et al., 2007) and brittle stars embryos, as well as in sea star juveniles (Morino et al., 2012). It has been suggested that the heterochronic activation of this pathway in sea urchin and brittle star embryos lead to the co-option of the adult skeleton into the larva (Gao and Davidson, 2008; Morino et al., 2012), as sea star

embryos do not have those genes expressed in the embryonic stage and have no larval skeleton. I show here that both VEGF and FGF genes are expressed in a strikingly similar pattern in embryos and adult regenerating arms of *A. filiformis* (Figure 5.1 and Appendix Figure A.0.1*),* suggesting that the interaction of the skeletogenic cells with the ectoderm, mediated by those signalling pathways, may be a conserved feature for adult echinoderms, and has in fact been co-opted in the embryos of sea urchins and brittle stars to form a larval skeleton. However, the transcriptional regulation downstream of FGF signalling appears to be significantly different in brittle stars and sea urchins. Several lines of evidence are presented here: 1) Several taxonomically-restricted genes with no sea urchins homologs have been identified (e.g. *tr35695* and *tr31926*); 2) some genes with homologs are not specifically expressed in the skeletogenic lineage in the sea urchin (e.g. *rreb1;* Materna et al., 2006). Furthermore, VEGF signalling appears to play a more prominent role in sea urchin skeletogenesis than in brittle star skeletogenesis (a more drastic phenotypic effect and more genes affected by perturbation; Adomako-Ankomah and Ettensohn, 2013; Duloquin et al., 2007). The high degree of conservation of the brittle star embryonic and adult network downstream of FGF signalling, together with the conservation of the regulatory state of skeletogenic cells, and coupled with the differences in signalling contribution and regulatory state of sea urchin and brittle star embryonic skeletogenic mesoderm, suggests that the embryonic program for skeletogenesis could have been independently co-opted in brittle stars and sea urchins. Further work on comparing adult and embryonic echinoderm skeletogenesis could help resolve this interesting question in the future.

6.5.2 Evolutionary similarities and differences in skeletogenesis among deuterostomes

Skeletal regeneration is observed in other deuterostome groups: for example in cirri regeneration of amphioxus (Kaneto and Wada, 2011), and in appendage regeneration of different vertebrates (reviewed in Ferretti and Health, 2013). It has even been suggested that adult bone repair and regeneration may recapitulate embryonic bone development at a molecular level (Ferguson et al., 1999), therefore comparing the skeleton developmental program between embryogenesis and regeneration can be vital to looking at the evolution of the skeleton in deuterostomes. Although the skeleton of echinoderms is composed of calcium carbonate, instead of calcium phosphate, similarities of its ontogeny can be observed when compared to vertebrates. For example, in both groups of animals the trunk skeletal precursor cells are mesoderm-derived, motile mesenchymal cells (Dylus et al., 2016; Guss and Ettensohn, 1997; Okazaki, 1975; Yang, 2013; this study) already suggesting some conserved features of skeletogenesis in deuterostomes. Gene expression can also aid in understanding the extent of potential similarities. The key regulators of the sea urchin (and likely brittle star) skeletogenic GRN include transcription factors *alx1*, *ets1/2* and *erg* (Ettensohn et al., 2003; Koga et al., 2010; Koga et al., 2016; Rizzo et al., 2006). Members of the Cart/Alx3/Alx4 group of transcription factors are also involved in skeletal development in vertebrates. They are expressed in embryonic lateral plate mesoderm, limb buds, cartilage and ectomesenchyme, and deletions of these genes result in cranial and vertebral malformations (Brouwer et al., 2003; ten Berge et al., 1998; Zhao et

al., 1996). ETS family transcription factors (including homologs of *ets1/2* and *erg*) have also been implicated in vertebrate skeletogenesis (Iwamoto et al., 2007; Kola et al., 1993; Li et al., 2004; Raouf and Seth, 2000; Raouf and Seth, 2002; Vlaeminck-Guillem et al., 2000). FGF signalling has a highly conserved role in skeletogenesis in deuterostomes, as demonstrated in sea urchins (Röttinger et al., 2008) and lampreys (Jandzik et al., 2014), as well as chickens (Mina and Havens, 2007) and mice (Sarkar et al., 2001; Yu and Ornitz, 2008). It has been shown to regulate mesenchymal skeletogenic cell differentiation by affecting the expression of specific chondrogenic genes in many animals. This is very similar to what I observed in the brittle star, whereby FGF signalling downregulates skeletogenic differentiation genes rather than transcription factors. However, it has been recently found that FGF inhibition results in a strong reduction of the of the chondrogenic marker *SoxE1*, which likely drives the expression of cartilage effector genes like *Col2a1* from lampreys (Jandzik et al., 2014) to mice (Schmid et al., 2009; Yu and Ornitz, 2008). Although *Afi-col2a1*, a homolog of the vertebrate *COL2A1* (Metsaranta et al., 1991; Ng et al., 1997), is specifically expressed in differentiating skeletal elements during late stages of *A. filiformis* regeneration, I did not observe any downregulation of *Afi-col2a1* in SU5402 treated stage 3 arms suggesting this specific link might not be conserved in brittle stars, although perhaps this occurs later during regeneration.

Overall, in terms of the downstream biomineralization genes, it seems that the network has diverged significantly between echinoderms and vertebrates. Most of the biomineralization genes identified in sea urchins and brittle stars do not have apparent homologues in vertebrates or other non-

vertebrate deuterostomes (Dylus et al., 2016; Livingston et al., 2006; Seaver and Livingston, 2015). Interestingly, the recent genome of the brachiopod *Lingula anatine*, which like distantly related vertebrates forms its shell using calcium phosphate, also reveals a unique set of genes involved in biomineralization (Luo et al., 2015). Those differences in the set of biomineralization genes used by brachiopods, echinoderms and vertebrates have prompted researchers to suggest that these animals independently evolved a core differentiation gene cassette for building their calcium-based skeletons.

Interestingly, a recently published article suggested a cell type should be defined by the regulatory mechanism that drove the evolution of this new identity from a sister cell type, rather than by the lineage-specific phenotypic differences (Arendt et al., 2016). In fact, despite the differentiation gene cohort and the final biochemical composition of the skeleton varies, the initiation cascade, including the ancient signalling pathways and transcription factors involved in skeletogenesis, appears to be conserved among many different animals (Jackson et al., 2006; Jackson et al., 2010; Livingston et al., 2006; Luo et al., 2015; Murdock and Donoghue, 2011). In light of this theory of the evolution of different cell types and the data here presented, it is tempting to suggest that the core skeleton-forming mesodermal cell type has been present already in the common ancestor of deuterostomes.

6.6 Conclusive remarks

Regeneration of adult tissues has been a hot topic in biology for centuries. A vast array of wonderful studies have demonstrated the

complexity of this process in terms of cellular contributions, the involvement of wound healing and repair mechanisms and the evolutionary adaptations of different regenerating animals. The least amount of progress has been made in comprehensive analyses of the molecular mechanisms underlying this ability. GRN analysis is quickly gaining interest in the field of regeneration as the most systematic approach to understand the molecular mechanisms of adult developmental processes at a level similar to what has been carried out for embryogenesis, with studies being carried out for nervous system regeneration (Smith et al., 2011; van Kesteren et al., 2011) and *in silico* for planarian regeneration (Lobo and Levin, 2015). The gene regulatory network approach has been employed successfully for various embryonic developmental processes, such as the specification of the sea urchin endoderm and skeletogenic mesoderm (Davidson et al., 2002b; Oliveri et al., 2008; Peter and Davidson, 2010), specification of the central nervous system in ciona (Atou et al., 2015; Imai et al., 2009) and insects (Suryamohan et al., 2016) or the vertebrate forebrain (Beccari et al., 2013). Unravelling GRNs driving regeneration of adult structures will not only allow us to determine to what extent the pre-existing developmental program is re-used in this new context but also aid our understanding of how regeneration is differentially regulated across evolutionary distant animals (Smith et al., 2011). The limitation of the comparative GRN approach in embryogenesis and adult regeneration is that it is biased towards the similarity in observed gene expression. These studies should be complimented by alternative strategies that focus on studying the differences, for example in the initiation of the gene regulatory networks driving cell fate specification and differentiation. An

unbiased comparative transcriptomic approach could yield the genes that are alternatively regulated during embryonic development and adult regeneration in the brittle star. Also studying the biological processes unique to regeneration, such as nerve dependence and the immune response, in *A. filiformis* could give important insights into the initiation signals upstream of the developmental GRNs acting during regeneration.

The brittle star *Amphiura filiformis* provides a unique system to directly compare the molecular make-up of developmental processes in embryogenesis and regeneration in the same animal. In this thesis I have laid down the groundwork for future extensive work on the cellular mechanisms of regeneration and the underlying GRN by following the preliminary steps to building a GRN as outlined by Materna and Oliveri, 2008. As the general layout of the GRN requires firstly the information on the layout and developmental mode of the cell type/structure in question and the tissue domains involved in its specification, I carried out extensive histological and morphological observations to determine the cellular domains of the regenerating arm especially with focus on skeletogenic cells (Chapter 3). The second step towards building GRNs involves the identification and characterization at high resolution of the candidate regulatory genes and downstream genes, which may play a role in the specification and differentiation of the structure of interest. In this thesis, I have analysed over 30 different candidate genes both in terms of the dynamics of spatio-temporal expression during regeneration and their levels using quantitative methods (Chapter 4). Finally, I began perturbation analysis of regulatory genes (in this case signalling molecules of the FGF and VEGF

pathways) as a way to functionally assess the potential linkages between the genes in the provisional network (Chapter 5). Much work remains to be done to understand the function and relationships between putative network nodes. Individual gene knockdown experiments will be required to complete the GRN for the regeneration of the adult skeleton in the brittle star. Additionally, a lot remains to be elucidated concerning the regenerative process in the brittle star, including the contribution and origin of different cell types during regeneration. A list of experiments performed but not discussed in this thesis provides insight into what types of manipulations might be viable for further studies of *Amphiura filiformis* (Table A.0.6). This work provides a solid basis for this exciting future work. Furthermore, this work acts as the first demonstration of the re-deployment of (at least) a section of an embryonic regulatory network during adult regeneration.

References

Adell, T., Cebrià, F. and Saló, E. (2010). Gradients in planarian regeneration and homeostasis. *Cold Spring Harb. Perspect. Biol.* **2**, 1–14.

Adomako-Ankomah, A. and Ettensohn, C. a (2013). Growth factor-mediated mesodermal cell guidance and skeletogenesis during sea urchin gastrulation. *Development* **140**, 4214–25.

Agata, K., Tanaka, T., Kobayashi, C., Kato, K. and Saitoh, Y. (2003). Intercalary regeneration in planarians. *Dev. Dyn.* **226**, 308–316.

Agata, K., Saito, Y. and Nakajima, E. (2007). Unifying principles of regeneration I: Epimorphosis versus morphallaxis. *Dev. Growth Differ.* **49**, 73–78.

Amore, G. and Davidson, E. H. (2006). cis-Regulatory control of cyclophilin, a member of the ETS-DRI skeletogenic gene battery in the sea urchin embryo. *Dev. Biol.* **293**, 555–564.

Amore, G., Yavrouian, R. G., Peterson, K. J., Ransick, A., McClay, D. R. and Davidson, E. H. (2003). Spdeadringer, a sea urchin embryo gene required separately in skeletogenic and oral ectoderm gene regulatory networks. *Dev. Biol.* **261**, 55–81.

Anderson, H. and French, V. (1985). Cell division during intercalary regeneration in the cockroach leg. *J. Embryol. Exp. Morphol.* **90**, 57–78.

Arendt, D., Musser, J. M., Baker, C. V. H., Bergman, A., Cepko, C., Erwin, D. H., Pavlicev, M., Schlosser, G., Widder, S., Laubichler, M. D., et al. (2016). The origin and evolution of cell types. *Nat. Rev. Genet.* **17**,

744–757.

Atou, B. Y. S., Mai, K. S. I., Satou, Y. and Imai, K. S. (2015). Gene regulatory systems that control gene expression in the Ciona embryo. *Proc. Jpn. Acad. Ser. B. Phys. Biol. Sci.* **91**, 33–51.

Baden, S. P., Loo, L.-O., Pihl, L. and Rosenberg, R. (1990). Effects eutrophication on benthic communities including fish : Swedish west coast. *AMBIO A J. Hum. Environ.* **19**, 113–122.

Balser, E. J. (1998). Cloning by ophiuroid echinoderm larvae. *Biol. Bull.* **194**, 187–193.

Bannister, R., McGonnell, I. M., Graham, a., Thorndyke, M. C. and Beesley, P. W. (2005). Afuni, a novel transforming growth factor-β gene is involved in arm regeneration by the brittle star Amphiura filiformis. *Dev. Genes Evol.* **215**, 393–401.

Bannister, R., McGonnell, I. M., Graham, A., Thorndyke, M. C. and Beesley, P. W. (2008). Coelomic expression of a novel bone morphogenetic protein in regenerating arms of the brittle star Amphiura filiformis. *Dev. Genes Evol.* **218**, 33–38.

Beccari, L., Marco-Ferreres, R. and Bovolenta, P. (2013). The logic of gene regulatory networks in early vertebrate forebrain patterning. *Mech. Dev.* **130**, 95–111.

Ben-Tabou de-Leon, S. and Davidson, E. H. (2006). Deciphering the underlying mechanism of specification and differentiation: the sea urchin gene regulatory network. *Sci. Signal.* **2006**, 47.

Ben-Tabou de-Leon, S. and Davidson, E. H. (2007). Gene regulation: gene control network in development. *Annu Rev Biophys Biomol Struct* **36**,

191.

Ben Khadra, Y., Ferrario, C., Di Benedetto, C., Said, K., Bonasoro, F., Candia Carnevali, M. D. and Sugni, M. (2015a). Wound repair during arm regeneration in the red starfish Echinaster sepositus. *Wound Repair Regen.* **23**, 611–622.

Ben Khadra, Y., Ferrario, C., Benedetto, C. Di, Said, K., Bonasoro, F., Candia Carnevali, M. D. and Sugni, M. (2015b). Re-growth, morphogenesis, and differentiation during starfish arm regeneration. *Wound Repair Regen.* **23**, 623–634.

Biressi, A. C. M., Zou, T., Dupont, S., Dahlberg, C., Di Benedetto, C., Bonasoro, F., Thorndyke, M. and Carnevali, M. D. C. (2010). Wound healing and arm regeneration in Ophioderma longicaudum and Amphiura filiformis (Ophiuroidea, Echinodermata): Comparative morphogenesis and histogenesis. *Zoomorphology* **129**, 1–19.

Bonasoro, F., Ferro, P., Di Benedetto, C., Sugni, M., Mozzi, D. and Candia Carnevali, M. D. (2004). Regenerative potential of echinoid test. In *Echinoderms: Munchen* (ed. Heinzeller, T.) and Nebelsick, J.), pp. 97–103.

Bosch, T. C. G. (2007). Why polyps regenerate and we don't: Towards a cellular and molecular framework for Hydra regeneration. *Dev. Biol.* **303**, 421–433.

Brockes, J. P. (2005). Appendage Regeneration in Adult Vertebrates and Implications for Regenerative Medicine. *Science (80).* **310**, 1919–1923.

Brockes, J. P. and Kumar, A. (2008). Comparative aspects of animal regeneration. *Annu. Rev. Cell Dev. Biol.* **24**, 525–49.

Broun, M., Gee, L., Reinhardt, B. and Bode, H. R. (2005). Formation of the head organizer in hydra involves the canonical Wnt pathway. *Development* **132**, 2907–2916.

Brouwer, A., ten Berge, D., Wiegerinck, R. and Meijlink, F. (2003). The OAR/aristaless domain of the homeodomain protein Cart1 has an attentuating role in vivo. *Mech. Dev.* **120**, 241–252.

Brusca, R. C., Moore, W. and Shuster, S. M. (2016). *Invertebrates*. 3rd ed. Sinauer Associates Inc.

Burke, R. D., Angerer, L. M., Elphick, M. R., Humphrey, G. W., Yaguchi, S., Kiyama, T., Liang, S., Mu, X., Agca, C., Klein, W. H., et al. (2006). A genomic view of the sea urchin nervous system. *Dev. Biol.* **300**, 434–460.

Burns, G., Ortega-Martinez, O., Thorndyke, M. C., Peck, L. S., Dupont, S. and Clark, M. S. (2011). Dynamic gene expression profiles during arm regeneration in the brittle star Amphiura filiformis. *J. Exp. Mar. Bio. Ecol.* **407**, 315–322.

Burns, G., Ortega-Martinez, O., Dupont, S., Thorndyke, M. C., Peck, L. S. and Clark, M. S. (2012). Intrinsic gene expression during regeneration in arm explants of Amphiura filiformis. *J. Exp. Mar. Bio. Ecol.* **413**, 106–112.

Burns, G., Thorndyke, M. C., Peck, L. S. and Clark, M. S. (2013). Transcriptome pyrosequencing of the Antarctic brittle star Ophionotus victoriae. *Mar. Genomics* **9**, 9–15.

Byrne, M. (1994). Ophiuroidea. In *Microscopic anatomy of invertebrates*, pp. 247–343.

Candia Carnevali, M. D., Bonasoro, F. and Biale, A. (1997). Pattern of bromodeoxyuridine incorporation in the advanced stages of arm regeneration in the feather star Antedon mediterranea. *Cell Tissue Res.* **289**, 363–374.

Cannon, J. T., Kocot, K. M., Waits, D. S., Weese, D. A., Swalla, B. J., Santos, S. R. and Halanych, K. M. (2014). Phylogenomic resolution of the hemichordate and echinoderm clade. *Curr. Biol.* **24**, 2827–2832.

Cardia, C. and Daniela, M. (2006). Regeneration in Echinoderms: repair, regrowth, cloning. *Invertebr. Surviv. J.* **3**, 64–76.

Carlson, B. M. (2007). *Principles of Regenerative Biology*. Elsevier Inc.

Carnevali, M. D. C., Lucca, E. and Bonasoro, F. (1993). Mechanisms of arm regeneration in the feather star Antedon mediterranea: Healing of wound and early stages of development. *J. Exp. Zool.* **267**, 299–317.

Carnevali, C., Bonasoro, F., Patruno, M. and Thorndyke, M. C. (1998). Cellular and molecular mechanisms of arm regeneration in crinoid echinoderms: The potential of arm explants. *Dev. Genes Evol.* **208**, 421–430.

Chadwick, H. C. (1929). Regeneration of spines in Echinus esculentus. **124**, 760–761.

Charlina, N. a. and Dolmatov, I. Y. (2009). Regeneration of a complex of structures of the ophiuroid Amphipholis kochii Lütken, 1872 (Ophiurae) after disk autotomy. *Russ. J. Mar. Biol.* **34**, 369–373.

Che-Yi Lin, Y.-H. S. (2015). Genome editing in sea urchin embryos by using a CRISPR/Cas9 system. *Dev. Biol.* **409**, 1–9.

Cheatle Jarvela, A. M. and Hinman, V. (2014). A method for microinjection

of Patiria miniata zygotes. *J. Vis. Exp.* e51913.

Chera, S., Ghila, L., Dobretz, K., Wenger, Y., Bauer, C., Buzgariu, W., Martinou, J. C. and Galliot, B. (2009). Apoptotic Cells Provide an Unexpected Source of Wnt3 Signaling to Drive Hydra Head Regeneration. *Dev. Cell* **17**, 279–289.

Clark, M. S. and Souster, T. (2012). Slow arm regeneration in the Antarctic brittle star Ophiura crassa (Echinodermata, Ophiuroidea). *Aquat. Biol.* **16**, 105–113.

Coffman, J. A., Dickey-Sims, C., Haug, J. S., McCarthy, J. J. and Robertson, A. J. (2004). Evaluation of developmental phenotypes produced by morpholino antisense targeting of a sea urchin Runx gene. *BMC Biol.* **2**, 6.

Cui, M., Siriwon, N., Li, E., Davidson, E. H. and Peter, I. S. (2014). Specific functions of the Wnt signaling system in gene regulatory networks throughout the early sea urchin embryo. *Proc. Natl. Acad. Sci. U. S. A.* **111**, E5029-38.

Cummings, S. G. and Bode, H. R. (1984). Head regeneration and polarity reversal in Hydra attenuata can occur in the absence of DNA synthesis. *Wilhelm Roux's Arch. Dev. Biol.* **194**, 79–86.

Cunningham, M., Seto, M., Ratisoontorn, C., Heike, C. and Hing, A. (2007). Syndromic craniosynostosis : from history to hydrogen bonds. *Orthod Craniofacial Res* **10**, 67–81.

Czarkwiani, A., Dylus, D. V. and Oliveri, P. (2013). Expression of skeletogenic genes during arm regeneration in the brittle star Amphiura filiformis. *Gene Expr. Patterns* **13**, 464–472.

Czarkwiani, A., Ferrario, C., Dylus, D. V., Sugni, M. and Oliveri, P. (2016). Skeletal regeneration in the brittle star Amphiura filiformis. *Front. Zool.* **13**, 18.

Damon, D. H., Lange, D. L. and Hattler, B. G. (1997). In vitro and in vivo vascular actions of basic fibroblast growth factor (bFGF) in normotensive and spontaneously hypertensive rats. *J. Cardiovasc. Pharmacol.* **30**, 278–284.

David, C. N. and Murphy, S. (1977). Characterization of interstitial stem cells in hydra by cloning. *Dev. Biol.* **58**, 372–383.

Davidson, E. H. (2006). The regulatory genome: gene regulatory networks in development and evolution. *Dev. Biol.* **310**, 304.

Davidson, E. H. and Peter, I. S. (2015). *Genomic Control Process*.

Davidson, E. H., Cameron, R. a and Ransick, a (1998). Specification of cell fate in the sea urchin embryo: summary and some proposed mechanisms. *Development* **125**, 3269–3290.

Davidson, E. H., Rast, J. P., Oliveri, P., Ransick, A., Calestani, C., Yuh, C.-H., Minokawa, T., Amore, G., Hinman, V., Arenas-Mena, C., et al. (2002a). A Genomic Regulatory Network for Development. *Science (80-.).* **295**, 1669–1679.

Davidson, E. H., Rast, J. P., Oliveri, P., Ransick, A., Calestani, C., Yuh, C.-H., Minokawa, T., Amore, G., Hinman, V., Arenas-Mena, C., et al. (2002b). A provisional regulatory gene network for specification of endomesoderm in the sea urchin embryo. *Dev. Biol.* **246**, 162–90.

Delroisse, J., Ortega-Martinez, O., Dupont, S., Mallefet, J. and Flammang, P. (2015). De novo transcriptome of the European brittle

star Amphiura filiformis pluteus larvae. *Mar. Genomics* **23**, 109–121.

Delroisse, J., Mallefet, J. and Flammang, P. (2016). De Novo Adult Transcriptomes of Two European Brittle Stars: Spotlight on Opsin-Based Photoreception. *PLoS One* **11**,.

Dubois, P. and Ameye, L. (2001). Regeneration of Spines and Pedicellariae in Echinoderms: A Review. *Microsc. Res. Tech.* **55**, 427–437.

Ducati, C., Barker, M. and Candia Carnevali, M. (2004). Regenerative potential and fissiparity in the forcipulate starfish Coscinasterias muricata. In *Echinoderms: München* (ed. Heinzeller, T.) and Nebelsick, J. .), pp. 113–118.

Duineveld, G. C. A. and Van Noort, G. J. (1986). Observations on the population dynamics of amphiura filiformis (ophiuroidea: echinodermata) in the southern north sea and its exploitation by the dab, Limanda limanda. *Netherlands J. Sea Res.* **20**, 85–94.

Duloquin, L., Lhomond, G. and Gache, C. (2007). Localized VEGF signaling from ectoderm to mesenchyme cells controls morphogenesis of the sea urchin embryo skeleton. *Development* **134**, 2293–2302.

Dupont, S. and Thorndyke, M. C. (2006). Growth or differentiation? Adaptive regeneration in the brittlestar Amphiura filiformis. *J. Exp. Biol.* **209**, 3873–3881.

Dupont, S. and Thorndyke, M. (2007). Bridging the regeneration gap: insights from echinoderm models. *Nat. Rev. Genet.* **8**, 8–10.

Dupont, S., Thorndyke, W., Thorndyke, M. C. and Burke, R. D. (2009). Neural development of the brittlestar Amphiura filiformis. *Dev. Genes Evol.* **219**, 159–166.

Dylus, D. V., Czarkwiani, A., Stångberg, J., Ortega-Martinez, O., Dupont, S. and Oliveri, P. (2016). Large-scale gene expression study in the ophiuroid Amphiura filiformis provides insights into evolution of gene regulatory networks. *Evodevo* **7**, 2.

Eaves, A. A. and Palmer, A. R. (2003). Reproduction: Widespread cloning in echinoderm larvae. *Nature* **425**, 146–146.

Eblaghie, M., Simon, L., Dickinson, R., Munsterberg, A., Sanz-Ezquerro, J., Farrell, E., Mathers, J., Keyse, S., Storey, K. and Tickle, C. (2003). Negative Feedback Regulation of FGF Signaling Levels by Pyst1/MKP3 in Chick Embryos. *Curr. Biol.* **13**, 1009–1018.

Endo, T., Bryant, S. V. and Gardiner, D. M. (2004). A stepwise model system for limb regeneration. *Dev. Biol.* **270**, 135–145.

Erkenbrack, E. M. and Davidson, E. H. (2015). Evolutionary rewiring of gene regulatory network linkages at divergence of the echinoid subclasses. *Proc. Natl. Acad. Sci. U. S. A.* **112**, E4075-4084.

Ettensohn, C. A. and McClay, D. R. (1988). Cell lineage conversion in the sea urchin embryo. *Dev Biol* **125**, 396–409.

Ettensohn, C. A., Illies, M. R., Oliveri, P. and De Jong, D. L. (2003). Alx1, a member of the Cart1/Alx3/Alx4 subfamily of Paired-class homeodomain proteins, is an essential component of the gene network controlling skeletogenic fate specification in the sea urchin embryo. *Development* **130**, 2917–2928.

Ferguson, C., Alpern, E., Miclau, T. and Helms, J. A. (1999). Does adult fracture repair recapitulate embryonic skeletal formation? *Mech. Dev.* **87**, 57–66.

Ferretti, P. and Health, C. (2006). Regeneration of vertebrate appendages. *eLS* 1–7.

Fry, B. G., Roelants, K., Winter, K., Hodgson, W. C., Griesman, L., Kwok, H. F., Scanlon, D., Karas, J., Shaw, C., Wong, L., et al. (2010). Novel venom proteins produced by differential domain-expression strategies in beaded lizards and gila monsters (genus Heloderma). *Mol. Biol. Evol.* **27**, 395–407.

Gage, J. D. (1990). Skeletal growth bands in brittle stars: microstructure and significance as age markers. *J. mar. biol. Ass. U.K.* **70**, 209–224.

Gao, F. and Davidson, E. H. (2008). Transfer of a large gene regulatory apparatus to a new developmental address in echinoid evolution. *Proc. Natl. Acad. Sci. U. S. A.* **105**, 6091–6.

Gao, F., Thompson, J. R., Petsios, E., Erkenbrack, E., Moats, R. A., Bottjer, D. J. and Davidson, E. H. (2015). Juvenile skeletogenesis in anciently diverged sea urchin clades. *Dev. Biol.* **400**, 148–158.

García-arrarás, J. E. and Greenberg, M. J. (2001). Visceral Regeneration in Holothurians. *Microsc. Res. Tech.* **55**, 438–451.

García-ArraráS, J. E., Estrada-Rodgers, L., Santiago, R., Torres, I. I., Díaz-Miranda, L. and Torres-Avillán, I. (1998). Cellular mechanisms of intestine regeneration in the sea cucumber, Holothuria glaberrima selenka (Holothuroidea:Echinodermata). *J. Exp. Zool.* **281**, 288–304.

Garner, S., Zysk, I., Byrne, G., Kramer, M., Moller, D., Taylor, V. and Burke, R. D. (2015). Neurogenesis in sea urchin embryos and the diversity of deuterostome neurogenic mechanisms. *Development* 286–297.

Geiss, G. K., Bumgarner, R. E., Birditt, B., Dahl, T., Dowidar, N., Dunaway, D. L., Fell, H. P., Ferree, S., George, R. D., Grogan, T., et al. (2008). Direct multiplexed measurement of gene expression with color-coded probe pairs. *Nat. Biotechnol.* **26**, 317–25.

Gorzelak, P., Stolarski, J., Dubois, P., Kopp, C. and Meibom, A. (2011). 26Mg labeling of the sea urchin regenerating spine: Insights into echinoderm biomineralization process. *J. Struct. Biol.* **176**, 119–126.

Grillo, M., Konstantinides, N. and Averof, M. (2016). Old questions, new models: unraveling complex organ regeneration with new exoperimental approaches. *Curr. Opin. Genet. Dev.* **40**, 23–31.

Guss, K. A. and Ettensohn, C. A. (1997). Skeletal morphogenesis in the sea urchin embryo: regulation of primary mesenchyme gene expression and skeletal rod growth by ectoderm-derived cues. *Development* **124**, 1899–1908.

Harkey, M. A., Whiteley, H. R. and Whiteley, A. H. (1992). Differential expression of the msp130 gene among skeletal lineage cells in the sea urchin embryo: a three dimensional in situ hybridization analysis. *Mech. Dev.* **37**, 173–184.

Heatfield, B. M. and Travis, D. F. (1975). Ultrastructural studies of regenerating spines of the sea urchin Strongylocentrotus purpuratus. II. Cell types with spherules. *J. Morphol.* **145**, 51–71.

Heyland, A., Hodin, J. and Bishop, C. (2014). Manipulation of developing juvenile structures in purple sea urchins (Strongylocentrotus purpuratus) by morpholino injection into late stage larvae. *PLoS One* **9**, 1–22.

Hobmayer, B., Rentzsch, F., Kuhn, K., Happel, C. M., von Laue, C. C.,

Snyder, P., Rothbächer, U. and Holstein, T. W. (2000). WNT signalling molecules act in axis formation in the diploblastic metazoan Hydra. *Nature* **407**, 186–189.

Hopkins, P. M. (2001). Regeneration in Crustaceans and Insects. *Encycl. Life Sci.* 1–7.

Hosoi, S., Sakuma, T., Sakamoto, N. and Yamamoto, T. (2014). Targeted mutagenesis in sea urchin embryos using TALENs. *Dev. Growth Differ.* **56**, 92–97.

Hotchkiss, F. H. C. (2009). Arm stumps and regeneration models in Asteroidea (Echinodermata). *Proc. Biol. Soc. Washingt.* **122**, 342–354.

Hu, D. and Marcucio, R. S. (2012). Neural crest cells pattern the surface cephalic ectoderm during FEZ formation. *Dev. Dyn.* **241**, 732–740.

Hu, M. Y., Casties, I., Stumpp, M., Ortega-Martinez, O. and Dupont, S. (2014). Energy metabolism and regeneration are impaired by seawater acidification in the infaunal brittlestar Amphiura filiformis. *J. Exp. Biol.* **217**, 2411–21.

Hu-Lowe, D. D., Zou, H. Y., Grazzini, M. L., Hallin, M. E., Wickman, G. R., Amundson, K., Chen, J. H., Rewolinski, D. A., Yamazaki, S., Wu, E. Y., et al. (2008). Nonclinical antiangiogenesis and antitumor activities of axitinib (AG-013736), an oral, potent, and selective inhibitor of vascular endothelial growth factor receptor tyrosine kinases 1, 2, 3. *Clin. Cancer Res.* **14**, 7272–7283.

Hubaud, A. and Pourquié, O. (2014). Signalling dynamics in vertebrate segmentation. *Nat. Rev. Mol. Cell Biol.* **15**, 709–721.

Huet, P. M. (1975). Le rôle du système nerveux an cours de la régénération

du bras chez une Etoile de mer: Asterina gibbosa Penn.(Echinoderme, Astéride). *J. Embryol. Exp. Morphol.* **33**, 535–552.

Illies, M. R., Peeler, M. T., Dechtiaruk, A. M. and Ettensohn, C. A. (2002). Identification and developmental expression of new biomineralization proteins in the sea urchin Strongylocentrotus purpuratus. *Dev. Genes Evol.* **212**, 419–431.

Imai, K. S., Stolfi, A., Levine, M. and Satou, Y. (2009). Gene regulatory networks underlying the compartmentalization of the Ciona central nervous system. *Development* **136**, 285–293.

Imokawa, Y. and Yoshizato, K. (1997). Expression of Sonic hedgehog gene in regenerating newt limb blastemas recapitulates that in developing limb buds. *Proc. Natl. Acad. Sci. U. S. A.* **94**, 9159–9164.

Irimura, S. and Fujita, T. (2003). Interspecific variation of vertebral ossicle morphology in the Ophiuroidea. In *Echinoderm Research 2001: proceedings of the 6th European Conference on Echinoderm Research, Banyuls-sur-mer, 3-7 September 2001*, pp. 161–167.

Iwamoto, M., Tamamura, Y., Koyama, E., Komori, T., Takeshita, N., Williams, J. A., Nakamura, T., Enomoto-Iwamoto, M. and Pacifici, M. (2007). Transcription factor ERG and joint and articular cartilage formation during mouse limb and spine skeletogenesis. *Dev. Biol.* **305**, 40–51.

Jackson, D. J., McDougall, C., Green, K., Simpson, F., Wörheide, G. and Degnan, B. M. (2006). A rapidly evolving secretome builds and patterns a sea shell. *BMC Biol.* **4**, 40.

Jackson, D. J., McDougall, C., Woodcroft, B., Moase, P., Rose, R. A.,

Kube, M., Reinhardt, R., Rokhsar, D. S., Montagnani, C., Joubert, C., et al. (2010). Parallel Evolution of Nacre Building Gene Sets in Molluscs. *Mol. Biol. Evol.* **27**, 591–608.

Jandzik, D., Hawkins, M. B., Cattell, M. V, Cerny, R., Square, T. a and Medeiros, D. M. (2014). Roles for FGF in lamprey pharyngeal pouch formation and skeletogenesis highlight ancestral functions in the vertebrate head. *Development* **141**, 629–38.

Johnson, B. R. and Tsutsui, N. D. (2011). Taxonomically restricted genes are associated with the evolution of sociality in the honey bee. *BMC Genomics* **12**, 164.

Kaneto, S. and Wada, H. (2011). Regeneration of amphioxus oral cirri and its skeletal rods: Implications for the origin of the vertebrate skeleton. *J. Exp. Zool. Part B Mol. Dev. Evol.* **316 B**, 409–417.

Khalturin, K., Hemmrich, G., Fraune, S. and Bosch, T. C. G. (2009). More than just orphans : are taxonomically-restricted genes important in evolution ? *Trends Genet.*

Killian, C. E. and Wilt, F. H. (2008). Molecular aspects of biomineralization of the Echinoderm endoskeleton. *Chem. Rev.* **108**, 4463–4474.

King, R. S. and Newmark, P. A. (2012). The cell biology of regeneration. *J. Cell Biol.* **196**, 553–562.

Koga, H., Matsubara, M., Fujitani, H., Miyamoto, N., Komatsu, M., Kiyomoto, M., Akasaka, K. and Wada, H. (2010). Functional evolution of Ets in echinoderms with focus on the evolution of echinoderm larval skeletons. *Dev. Genes Evol.* **220**, 107–115.

Koga, H., Fujitani, H., Morino, Y., Miyamoto, N., Tsuchimoto, J., Shibata,

T. F., Nozawa, M., Shigenobu, S., Ogura, A., Tachibana, K., et al. (2016). Experimental approach reveals the role of alx1 in the evolution of the echinoderm larval skeleton. *PLoS One* **11**, 1–19.

Kola, I., Brookes, S., Green, a R., Garber, R., Tymms, M., Papas, T. S. and Seth, a (1993). The Ets1 transcription factor is widely expressed during murine embryo development and is associated with mesodermal cells involved in morphogenetic processes such as organ formation. *Proc. Natl. Acad. Sci. U. S. A.* **90**, 7588–7592.

Kondo, M. and Akasaka, K. (2010). Regeneration in crinoids. *Dev. Growth Differ.* **52**, 57–68.

Konstantinides, N. and Averof, M. (2014). A common cellular basis for muscle regeneration in arthropods and vertebrates. *Science* **343**, 788–91.

Kragl, M., Knapp, D., Nacu, E., Khattak, S., Maden, M., Epperlein, H. H. and Tanaka, E. M. (2009). Cells keep a memory of their tissue origin during axolotl limb regeneration. *Nature* **460**, 60–65.

Kumar, A. and Brockes, J. P. (2012). Nerve dependence in tissue, organ, and appendage regeneration. *Trends Neurosci.* **35**, 691–699.

Lapraz, F., Röttinger, E., Duboc, V., Range, R., Duloquin, L., Walton, K., Wu, S.-Y., Bradham, C., Loza, M. A., Hibino, T., et al. (2006). RTK and TGF-β signaling pathways genes in the sea urchin genome. *Dev. Biol.* **300**, 132–152.

Laube, F., Heister, M., Scholz, C., Borchardt, T. and Braun, T. (2006). Re-programming of newt cardiomyocytes is induced by tissue regeneration. *J. Cell Sci.* **119**, 4719–4729.

Le Roy, N., Jackson, D. J., Marie, B., Ramos-Silva, P. and Marin, F. (2014). The evolution of metazoan α-carbonic anhydrases and their roles in calcium carbonate biomineralization. *Front. Zool.* **11**, 75.

Lee, Y., Grill, S., Sanchez, A., Murphy-Ryan, M. and Poss, K. D. (2005). Fgf signaling instructs position-dependent growth rate during zebrafish fin regeneration. *Development* **132**, 5173–83.

Lengfeld, T., Watanabe, H., Simakov, O., Lindgens, D., Gee, L., Law, L., Schmidt, H. A., Özbek, S., Bode, H. and Holstein, T. W. (2009). Multiple Wnts are involved in Hydra organizer formation and regeneration. *Dev. Biol.* **330**, 186–199.

Lepilina, A., Coon, A. N., Kikuchi, K., Holdway, J. E., Roberts, R. W., Burns, C. G. and Poss, K. D. (2006). A Dynamic Epicardial Injury Response Supports Progenitor Cell Activity during Zebrafish Heart Regeneration. *Cell* **127**, 607–619.

Lesser, M. P., Carleton, K. L., Bottger, S. A., Barry, T. M. and Walker, C. W. (2011). Sea urchin tube feet are photosensory organs that express a rhabdomeric-like opsin and PAX6. *Proc. R. Soc. B Biol. Sci.* **278**, 3371–3379.

Levin, M. (2009). Bioelectric mechanisms in regeneration: unique aspects and future perspectives. *Semin. Cell Dev. Biol.* **20**, 543–556.

Li, V., Raouf, A., Kitching, R. and Seth, A. (2004). Ets2 transcription factor inhibits mineralization and affects target gene expression during osteoblast maturation. *In Vivo (Brooklyn).* **18**, 517–524.

Liao, Y., Shikapwashya, O. N., Shteyer, E., Dieckgraefe, B. K., Hruz, P. W. and Rudnick, D. A. (2004). Delayed hepatocellular mitotic

progression and impaired liver regeneration in early growth response-1-deficient mice. *J. Biol. Chem.* **279**, 43107–43116.

Lin, G. and Slack, J. M. W. (2008). Requirement for Wnt and FGF signaling in Xenopus tadpole tail regeneration. *Dev. Biol.* **316**, 323–335.

Livingston, B. T., Killian, C. E., Wilt, F., Cameron, A., Landrum, M. J., Ermolaeva, O., Sapojnikov, V., Maglott, D. R., Buchanan, A. M. and Ettensohn, C. A. (2006). A genome-wide analysis of biomineralization-related proteins in the sea urchin Strongylocentrotus purpuratus. *Dev. Biol.* **300**, 335–348.

Lobo, D. and Levin, M. (2015). Inferring Regulatory Networks from Experimental Morphological Phenotypes: A Computational Method Reverse-Engineers Planarian Regeneration. *PLoS Comput. Biol.* **11**, 1–28.

Logan, C. Y., Miller, J. R., Ferkowicz, M. J. and McClay, D. R. (1998). Nuclear beta-catenin is required to specify vegetal cell fates in the sea urchin embryo. *Development* **126**, 345–357.

Loo, L. O., Jonsson, P. R., Sk??ld, M. and Karlsson, ??rjan (1996). Passive suspension feeding in Amphiura filiformis (Echinodermata: Ophiuroidea): Feeding behaviour in flume flow and potential feeding rate of field populations. *Mar. Ecol. Prog. Ser.* **139**, 143–155.

Lucca, E., Bonasoro, F., Carnevali, M. D. C. and Thorndyke, M. C. (1995). Pattern of Cell-Proliferation in the Early Stages of Arm Regeneration in the Feather Star Antedon Mediterranea. *J. Exp. Zool.* **272**, 464–474.

Luo, Y.-J., Takeuchi, T., Koyanagi, R., Yamada, L., Kanda, M., Khalturina, M., Fujie, M., Yamasaki, S.-I., Endo, K. and Satoh, N.

(2015). The Lingula genome provides insights into brachiopod evolution and the origin of phosphate biomineralization. *Nat. Commun.* **6**, 1–10.

Makanae, A., Mitogawa, K. and Satoh, A. (2014). Co-operative Bmp- and Fgf-signaling inputs convert skin wound healing to limb formation in urodele amphibians. *Dev. Biol.* **396**, 57–66.

Mann, K., Poustka, A. J. and Mann, M. (2008a). In-depth, high-accuracy proteomics of sea urchin tooth organic matrix. *Proteome Sci.* **6**, 33.

Mann, K., Poustka, A. J. and Mann, M. (2008b). The sea urchin (Strongylocentrotus purpuratus) test and spine proteomes. *Proteome Sience* **6**, 22–32.

Mann, K., Wilt, F. H. and Poustka, A. J. (2010). Proteomic analysis of sea urchin (Strongylocentrotus purpuratus) spicule matrix. *Proteome Sci.* **8**, 33.

Mann, K., Edsinger-Gonzales, E. and Mann, M. (2012). In-depth proteomic analysis of a mollusc shell: acid-soluble and acid-insoluble matrix of the limpet Lottia gigantea. *Proteome Sci.* **10**, 28–46.

Marie, P. J., Coffin, J. D. and Hurley, M. M. (2005). FGF and FGFR signaling in chondrodysplasias and craniosynostosis. *J. Cell. Biochem.* **96**, 888–896.

Mashanov, V. S. and García-Arrarás, J. E. (2011). Gut regeneration in holothurians: A snapshot of recent developments. *Biol. Bull.* **221**, 93–109.

Mashanov, V. S., Dolmatov, I. Y. and Heinzeller, T. (2005). Transdifferentiation in holothurian gut regeneration. *Biol. Bull.* **209**, 184–193.

Mashanov, V. S., Zueva, O. R. and Heinzeller, T. (2008). Regeneration of the radial nerve cord in a holothurian: A promising new model system for studying post-traumatic recovery in the adult nervous system. *Tissue Cell* **40**, 351–372.

Mashanov, V. S., Zueva, O. R. and García-arrarás, J. E. (2014). Transcriptomic changes during regeneration of the central nervous system in an echinoderm. 1–21.

Mashanov, V. S., Zueva, O. R. and García-Arrarás, J. E. (2015a). Myc regulates programmed cell death and radial glia dedifferentiation after neural injury in an echinoderm. *BMC Dev. Biol.* **15**, 24.

Mashanov, V. S., Zueva, O. R. and Garcia-Arraras, J. E. (2015b). Expression of pluripotency factors in echinoderm regeneration. *Cell Tissue Res.* **359**, 521–536.

Materna, S. C. and Oliveri, P. (2008). A protocol for unraveling gene regulatory networks. *Nat. Protoc.* **3**, 1876–87.

Materna, S. C., Howard-Ashby, M., Gray, R. F. and Davidson, E. H. (2006). The C2H2 zinc finger genes of Strongylocentrotus purpuratus and their expression in embryonic development. *Dev. Biol.* **300**, 108–120.

McCauley, B. S., Weideman, E. P. and Hinman, V. F. (2010). A conserved gene regulatory network subcircuit drives different developmental fates in the vegetal pole of highly divergent echinoderm embryos. *Dev. Biol.* **340**, 200–208.

McCauley, B. S., Wright, E. P., Exner, C., Kitazawa, C. and Hinman, V. F. (2012). Development of an embryonic skeletogenic mesenchyme

lineage in a sea cucumber reveals the trajectory of change for the evolution of novel structures in echinoderms. *Evodevo* **3**, 17.

Mcintyre, D. C., Lyons, D. C., Martik, M. and Mcclay, D. R. (2014). Branching out: Origins of the sea urchin larval skeleton in development and evolution. *Genesis* **52**, 173–185.

McIntyre, D. C., Seay, N. W., Croce, J. C. and McClay, D. R. (2013). Short-range Wnt5 signaling initiates specification of sea urchin posterior ectoderm. *Development* **140**, 4881–9.

Melani, M., Simpson, K. J., Brugge, J. S. and Montell, D. (2008). Regulation of Cell Adhesion and Collective Cell Migration by Hindsight and Its Human Homolog RREB1. *Curr. Biol.* **18**, 532–537.

Mercader, N., Leonardo, E., Piedra, M. E., Martínez-A, C., Ros, M. a and Torres, M. (2000). Opposing RA and FGF signals control proximodistal vertebrate limb development through regulation of Meis genes. *Development* **127**, 3961–3970.

Mercader, N., Tanaka, E. M. and Torres, M. (2005). Proximodistal identity during vertebrate limb regeneration is regulated by Meis homeodomain proteins. *Development* **132**, 4131–42.

Metsaranta, M., Toman, D., de Crombrugghe, B. and Vuorio, E. (1991). Mouse Type II Collagen Gene. **266**, 16862–16869.

Milde, S., Hemmrich, G., Anton-Erxleben, F., Khalturin, K., Wittlieb, J. and Bosch, T. C. G. (2009). Characterization of taxonomically restricted genes in a phylum-restricted cell type. *Genome Biol.* **10**, R8.

Milligan, M. (1946). Trichrome stain for formalin-fixed tissue. *Am. J. Clin. Pathol.* **10**, 184.

Mina, M. and Havens, B. (2007). FGF signaling in mandibular skeletogenesis. *Orthod Craniofacial Res* **10**, 59=66.

Minokawa, T., Rast, J. P., Arenas-Mena, C., Franco, C. B. and Davidson, E. H. (2004). Expression patterns of four different regulatory genes that function during sea urchin development. *Gene Expr. Patterns* **4**, 449–456.

Mohammadi, M., McMahon, G., Sun, L., Tang, C., Hirth, P., Yeh, B. K., Hubbard, S. R. and Schlessinger, J. (1997). Structures of the tyrosine kinase domain of fibroblast growth factor receptor in complex with inhibitors. *Science* **276**, 955–960.

Montgomery, J. R. and Coward, S. J. (1974). On the minimal size of a planarian capable of regeneration. *Trans. Am. Microsc. Soc.* **93**, 386–391.

Morgan, T. H. (1901). Regeneration. *Columbia Univ. Biol. Ser. VII.* 342.

Morino, Y., Koga, H., Tachibana, K., Shoguchi, E., Kiyomoto, M. and Wada, H. (2012). Heterochronic activation of VEGF signaling and the evolution of the skeleton in echinoderm pluteus larvae. *Evol. Dev.* **14**, 428–436.

Morino, Y., Koga, H. and Wada, H. (2016). The conserved genetic background for pluteus arm development in brittle stars and sea urchin. *Evol. Dev.* **18**, 89–95.

Moss, C., Hunter, A. J. and Thorndyke, M. C. (1998). Patterns of bromodeoxyuridine incorporation and neuropeptide immunoreactivity during arm regeneration in the star fish Asterias rubens. *Phil. Trans. R. Soc. Lond.* **354**, 421–436.

Mozzi, D., Dolmatov, I. Y., Bonasoro, F. and Candia Carnevali, M. D. (2006). Visceral regeneration in the crinoid Antedon mediterranea: basic mechanisms, tissues and cells involved in gut regrowth. *Cent. Eur. J. Biol.* **1**, 609–635.

Müller, O. F. (1776). Zoologiae Danicae Prodromus seu Animalium Daniae et Norvegiae indigenarum characteres, nomina, et synonyma imprimis popularium. *Havniae, Typis Hallageriis* 224–226.

Murdock, D. J. E. and Donoghue, P. C. J. (2011). Evolutionary origins of animal skeletal biomineralization. *Cells Tissues Organs* **194**, 98–102.

Nakamura, T., Mito, T., Tanaka, Y., Bando, T., Ohuchi, H. and Noji, S. (2007). Involvement of canonical Wnt/Wingless signaling in the determination of the positional values within the leg segment of the cricket Gryllus bimaculatus. *Dev. Growth Differ.* **49**, 79–88.

Nakamura, T., Mito, T., Miyawaki, K., Ohuchi, H. and Noji, S. (2008). EGFR signaling is required for re-establishing the proximodistal axis during distal leg regeneration in the cricket Gryllus bimaculatus nymph. *Dev. Biol.* **319**, 46–55.

Newmark, P. a and Sánchez Alvarado, a (2000). Bromodeoxyuridine specifically labels the regenerative stem cells of planarians. *Dev. Biol.* **220**, 142–53.

Ng, L. J., Wheatley, S., Muscat, G. E., Conway-Campbell, J., Bowles, J., Wright, E., Bell, D. M., Tam, P. P., Cheah, K. S. and Koopman, P. (1997). Sox9 binds DNA, activates transcription, and coexpresses with type II collagen during chondrogenesis in the mouse. *Dev. Biol.* **183**, 108–121.

Nilsson, H. C. and Sköld, M. (1996). Arm regeneration and spawning in the brittle star Amphiura filiformis (O.F. Muller) during hypoxia. *J. Exp. Mar. Bio. Ecol.* **199**, 193–206.

Nye, H. L. D., Cameron, J. A., Chernoff, E. A. G. and Stocum, D. L. (2003). Regeneration of the urodele limb: A review. *Dev. Dyn.* **226**, 280–294.

Oji, T. (2001). Fossil Record of Echinoderm Regeneration with Special Regard to Crinoids. *Microsc. Res. Tech.* **55**, 397–402.

Okazaki, K. (1975). Spicule formation by isolated micromeres of the sea urchin embryo. *Integr. Comp. Biol.* **15**, 567–581.

Oliveri, P. and Davidson, E. H. (2007). Development. Built to run, not fail. *Science* **315**, 1510–1511.

Oliveri, P., Carrick, D. M. and Davidson, E. H. (2002). A regulatory gene network that directs micromere specification in the sea urchin embryo. *Dev. Biol.* **246**, 209–228.

Oliveri, P., Davidson, E. H. and McClay, D. R. (2003). Activation of pmar1 controls specification of micromeres in the sea urchin embryo. *Dev. Biol.* **258**, 32–43.

Oliveri, P., Tu, Q. and Davidson, E. H. (2008). Global regulatory logic for specification of an embryonic cell lineage. *Proc. Natl. Acad. Sci. U. S. A.* **105**, 5955–5962.

Oulhen, N. and Wessel, G. M. (2016). Albinism as a visual, in vivo guide for CRISPR/Cas9 functionality in the sea urchin embryo. *Mol. Reprod. Dev.*

Oulhen, N., Heyland, A., Carrier, T. J., Zazueta-Novoa, V., Fresques, T., Laird, J., Onorato, T. M., Janies, D. and Wessel, G. (2016).

Regeneration in bipinnaria larvae of the bat star Patiria miniata induces rapid and broad new gene expression. *Mech. Dev.* **142**, 10–21.

Özpolat, B. D., Zapata, M., Daniel Frugé, J., Coote, J., Lee, J., Muneoka, K. and Anderson, R. (2012). Regeneration of the elbow joint in the developing chick embryo recapitulates development. *Dev. Biol.* **372**, 229–238.

Pagel, J.-I. and Deindl, E. (2011). Early growth response 1--a transcription factor in the crossfire of signal transduction cascades. *Indian J. Biochem. Biophys.* **48**, 226–35.

Patruno, M., Smertenko, A., Candia Carnevali, M. D., Bonasoro, F., Beesley, P. W. and Thorndyke, M. C. (2002). Expression of transforming growth factor beta-like molecules in normal and regenerating arms of the crinoid Antedon mediterranea: immunocytochemical and biochemical evidence. *Proc. Biol. Sci.* **269**, 1741–7.

Peter, I. S. and Davidson, E. H. (2010). The endoderm gene regulatory network in sea urchin embryos up to mid-blastula stage. *Dev. Biol.* **340**, 188–199.

Pineda, D., Rossi, L., Batistoni, R., Salvetti, A., Marsal, M., Gremigni, V., Falleni, A., Gonzalez-Linares, J., Deri, P. and Saló, E. (2002). The genetic network of prototypic planarian eye regeneration is Pax6 independent. *Development* **129**, 1423–1434.

Poss, K. D., Shen, J., Nechiporuk, a, McMahon, G., Thisse, B., Thisse, C. and Keating, M. T. (2000). Roles for Fgf signaling during zebrafish fin regeneration. *Dev. Biol.* **222**, 347–358.

Poss, K. D., Keating, M. T. and Nechiporuk, A. (2003). Tales of regeneration in zebrafish. *Dev. Dyn.* **226**, 202–210.

Pueyo, J. I., Lanfear, R. and Couso, J. P. (2008). Ancestral Notch-mediated segmentation revealed in the cockroach Periplaneta americana. *Proc. Natl. Acad. Sci. U. S. A.* **105**, 16614–16619.

Purushothaman, S., Saxena, S., Meghah, V., Swamy, C. V. B., Ortega-Martinez, O., Dupont, S. and Idris, M. (2015). Transcriptomic and proteomic analyses of Amphiura filiformis arm tissue-undergoing regeneration. *J. Proteomics* **112**, 113–124.

Rafiq, K., Cheers, M. S. and Ettensohn, C. a (2012). The genomic regulatory control of skeletal morphogenesis in the sea urchin. *Development* **139**, 579–90.

Rafiq, K., Shashikant, T., McManus, C. J. and Ettensohn, C. a (2014). Genome-wide analysis of the skeletogenic gene regulatory network of sea urchins. *Development* **141**, 950–61.

Raouf, a and Seth, a (2000). Ets transcription factors and targets in osteogenesis. *Oncogene* **19**, 6455–6463.

Raouf, A. and Seth, A. (2002). Discovery of osteoblast-associated genes using cDNA microarrays. *Bone* **30**, 463–471.

Reddien, P. W. and Alvarado, A. S. (2004). Fundamentals of Planarian Regeneration. *Annu. Rev. Cell Dev. Biol.* **20**, 725–757.

Reich, A., Dunn, C., Akasaka, K. and Wessel, G. (2015). Phylogenomic analyses of echinodermata support the sister groups of Asterozoa and Echinozoa. *PLoS One* **10**, 1–11.

Reinardy, H. C., Emerson, C. E., Manley, J. M. and Bodnar, A. G. (2015).

Tissue regeneration and biomineralization in sea urchins: Role of Notch signaling and presence of stem cell markers. *PLoS One* **10**, 1–15.

Revilla-i-Domingo, R., Oliveri, P. and Davidson, E. H. (2007). A missing link in the sea urchin embryo gene regulatory network: hesC and the double-negative specification of micromeres. *Proc. Natl. Acad. Sci. U. S. A.* **104**, 12383–12388.

Rizzo, F., Fernandez-Serra, M., Squarzoni, P., Archimandritis, A. and Arnone, M. I. (2006). Identification and developmental expression of the ets gene family in the sea urchin (Strongylocentrotus purpuratus). *Dev. Biol.* **300**, 35–48.

Roensch, K., Tazaki, A., Chara, O. and Tanaka, E. M. (2013). Progressive specification rather than intercalation of segments during limb regeneration. *Science (80-.).* **342**, 1375–9.

Roscioli, T., Flanagan, S., Kumar, P., Masel, J., Gattas, M., Hyland, V. J. and Glass, I. A. (2000). Clinical findings in a patient with FGFR1 P252R mutation and comparison with the literature. *Am. J. Med. Genet.* **93**, 22–25.

Rosenberg, R. (1995). Benthic marine fauna structured by hydrodynamic processes and food availability. *Netherlands J. Sea Res.* **34**, 303–317.

Röttinger, E., Saudemont, A., Duboc, V., Besnardeau, L., McClay, D. and Lepage, T. (2008). FGF signals guide migration of mesenchymal cells, control skeletal morphogenesis and regulate gastrulation during sea urchin development. *Development* **135**, 353–365.

Rubilar, T., Pastor, C. and Díaz de Vivar, E. (2005). Timing of fission in the starfish Allostichaster capensis (Echinodermata: Asteroidea) in

laboratory. *Rev. Biol. Trop.* **53 Suppl 3**, 299–303.

Saló, E., Pineda, D., Marsal, M., Gonzalez, J., Gremigni, V. and Batistoni, R. (2002). Genetic network of the eye in Platyhelminthes: Expression and functional analysis of some players during planarian regeneration. *Gene* **287**, 67–74.

Sanchez Alvarado, A. and Tsonis, P. A. (2006). Bridging the regeneration gap: genetic insights from diverse animal models. *Nat Rev Genet* **7**, 873–884.

Sandoval-Guzmán, T., Wang, H., Khattak, S., Schuez, M., Roensch, K., Nacu, E., Tazaki, A., Joven, A., Tanaka, E. M. and Simon, A. (2014). Fundamental differences in dedifferentiation and stem cell recruitment during skeletal muscle regeneration in two salamander species. *Cell Stem Cell* **14**, 174–187.

Santiago, F. S., Lowe, H. C., Day, F. L., Chesterman, C. N. and Khachigian, L. M. (1999). Early growth response factor-1 induction by injury is triggered by release and paracrine activation by fibroblast growth factor-2. *Am. J. Pathol.* **154**, 937–44.

Saradamba, A., Buch, P. R., Murawala, H. A. and Balakrishnan, S. (2013). SU5402, a pharmacological inhibitor of fibroblast growth factor receptor (FGFR), effectively hampers the initiation and progression of fin regeneration in teleost fish. *Eur. J. Zool. Res.* **2**, 1–9.

Sarkar, S., Petiot, a, Copp, a, Ferretti, P. and Thorogood, P. (2001). FGF2 promotes skeletogenic differentiation of cranial neural crest cells. *Development* **128**, 2143–2152.

Schmid, G., Kobayashi, C., Sandell, L. and Ornitz, D. M. (2009).

Fibroblast Growth Factor expression during skeletal fracture healing in mice. *Dev. Dyn.* **238**, 766–774.

Seaver, R. W. and Livingston, B. T. (2015). Examination of the skeletal proteome of the brittle star Ophiocoma wendtii reveals overall conservation of proteins but variation in spicule matrix proteins. *Proteome Sci.* **13**, 7.

Sharma, T. and Ettensohn, C. a (2011). Regulative deployment of the skeletogenic gene regulatory network during sea urchin development. *Development* **138**, 2581–2590.

Shibata, E., Yokota, Y., Horita, N., Kudo, A., Abe, G., Kawakami, K. and Kawakami, A. (2016). Fgf signalling controls diverse aspects of fin regeneration. *Development* **143**, 2920–2929.

Smith, J., Morgan, J. R., Zottoli, S. J., Smith, P. J., Buxbaum, J. D. and Bloom, O. E. (2011). Regeneration in the Era of Functional Genomics and Gene Network Analysis. *Biol. Bull.* **221**, 18–24.

Sodergren, E., Weinstock, G. M., Davidson, E. H., Cameron, R. A., Gibbs, R. a, Angerer, R. C., Angerer, L. M., Arnone, M. I., Burgess, D. R., Burke, R. D., et al. (2006). The genome of the sea urchin Strongylocentrotus purpuratus. *Science* **314**, 941–952.

Stewart, R., Rascón, C. A., Tian, S., Nie, J., Barry, C., Chu, L. F., Ardalani, H., Wagner, R. J., Probasco, M. D., Bolin, J. M., et al. (2013). Comparative RNA-seq Analysis in the Unsequenced Axolotl: The Oncogene Burst Highlights Early Gene Expression in the Blastema. *PLoS Comput. Biol.* **9**, e1002936.

Stöhr, S., O'Hara, T. D. and Thuy, B. (2012). Global diversity of brittle stars

(Echinodermata: Ophiuroidea). *PLoS One* **7**, e31940.

Sun, Z. and Ettensohn, C. A. (2014). Signal-dependent regulation of the sea urchin skeletogenic gene regulatory network. *Gene Expr. Patterns* **16**, 93–103.

Sun, L., Yang, H., Chen, M., Ma, D. and Lin, C. (2013). RNA-Seq Reveals Dynamic Changes of Gene Expression in Key Stages of Intestine Regeneration in the Sea Cucumber Apostichopus japonicas. *PLoS One* **8**,.

Suryamohan, K., Hanson, C., Andrews, E., Sinha, S., Scheel, M. D. and Halfon, M. S. (2016). Redeployment of a conserved gene regulatory network during Aedes aegypti development. *Dev. Biol.* **416**, 402–413.

Suzuki, H., Reiter, R., D'Alessio, M., Di Liberto, M., Ramirez, F., Exposito, J., Gambino, R. and Solursh, M. (1997). Comparative analysis of fibrillar and basement membrane collagen expression in embryos of the sea urchin, Strongylocentrtus purpuratus. *Zoolog. Sci.* **14**, 449–454.

Suzuki, M., Yakushiji, N., Nakada, Y., Satoh, A., Ide, H. and Tamura, K. (2006). Limb Regeneration in *Xenopus laevis* Froglet. *Sci. World J.* **6**, 26–37.

Tambutt??, S., Tambutt??, E., Zoccola, D., Caminiti, N., Lotto, S., Moya, A., Allemand, D. and Adkins, J. (2007). Characterization and role of carbonic anhydrase in the calcification process of the azooxanthellate coral Tubastrea aurea. *Mar. Biol.* **151**, 71–83.

Tanaka, E. M., Drechsel, D. N. and Brockes, J. P. (1999). Thrombin regulates S-phase re-entry by cultured newt myotubes. *Curr. Biol.* **9**,

792–799.

Tanaka, H. V., Ng, N. C. Y., Yang Yu, Z., Casco-Robles, M. M., Maruo, F., Tsonis, P. A. and Chiba, C. (2016). A developmentally regulated switch from stem cells to dedifferentiation for limb muscle regeneration in newts. *Nat. Commun.* **7**, 11069.

Tarazona, O. A., Slota, L. A., Lopez, D. H., Zhang, G. and Cohn, M. J. (2016). The genetic program for cartilage development has deep homology within Bilateria. *Nature* **533**, 1–15.

Telford, M. J., Lowe, C. J., Cameron, C. B., Ortega-Martinez, O., Aronowicz, J., Oliveri, P. and Copley, R. R. (2014). Phylogenomic analysis of echinoderm class relationships supports Asterozoa. *Proc. R. Soc. B Biol. Sci.* **281**, 20140479–20140479.

ten Berge, D., Brouwer, a, el Bahi, S., Guénet, J. L., Robert, B. and Meijlink, F. (1998). Mouse Alx3: an aristaless-like homeobox gene expressed during embryogenesis in ectomesenchyme and lateral plate mesoderm. *Dev. Biol.* **199**, 11–25.

Teven, C. M., Farina, E. M., Rivas, J. and Reid, R. R. (2014). Fibroblast growth factor (FGF) signaling in development and skeletal diseases. *Genes Dis.* **1**, 199–213.

Thiagalingam, a, De Bustros, a, Borges, M., Jasti, R., Compton, D., Diamond, L., Mabry, M., Ball, D. W., Baylin, S. B. and Nelkin, B. D. (1996). RREB-1, a novel zinc finger protein, is involved in the differentiation response to Ras in human medullary thyroid carcinomas. *Mol. Cell. Biol.* **16**, 5335–45.

Thorndyke, M. C., Patruno, M., Dewael, Y., Dupont, S. and Mallefet, J.

(2001). Regeneration in the ophiuroid Amphiura filiformis: Cell biology, physiology and luminescence. In *Echinoderm Research 2001: proceedings of the 6th European Conference on Echinoderm Research, Banyuls-sur-mer, 3-7 September 2001*, pp. 193–199.

Tinevez, J.-Y., Perry, N., Schindelin, J., Hoopes, G. M., Reynolds, G. D., Laplantine, E., Bednarek, S. Y., Shorte, S. L. and Eliceiri, K. W. (2016). TrackMate: an open and extensible platform for single-particle tracking. *Methods* **115**, 80–90.

Urry, L. A., Hamilton, P. C., Killian, C. E. and Wilt, F. H. (2000). Expression of spicule matrix proteins in the sea urchin embryo during normal and experimentally altered spiculogenesis. *Dev. Biol.* **225**, 201–213.

van Kesteren, R. E., Mason, M. R. J., MacGillavry, H. D., Smit, A. B. and Verhaagen, J. (2011). A Gene Network Perspective on Axonal Regeneration. *Front. Mol. Neurosci.* **4**, 1–6.

Vaughn, R., Garnhardt, N., Garey, J. R., Thomas, W. K. and Livingston, B. T. (2012). Sequencing and analysis of the gastrula transcriptome of the brittle star Ophiocoma wendtii. *Evodevo* **3**, 19.

Vlaeminck-Guillem, V., Carrere, S., Dewitte, F., Stehelin, D., Desbiens, X. and Duterque-Coquillaud, M. (2000). The Ets family member Erg gene is expressed in mesodermal tissues and neural crests at fundamental steps during mouse embryogenesis. *Mech. Dev.* **91**, 331–335.

Voss, S. R., Palumbo, A., Nagarajan, R., Gardiner, D. M., Muneoka, K., Stromberg, A. J. and Athippozhy, A. T. (2015). Gene expression during the first 28 days of axolotl limb regeneration I: Experimental

design and global analysis of gene expression. *Regen. (Oxford, England)* **2**, 120–136.

Wagner, D. E., Wang, I. E. and Reddien, P. W. (2011). Clonogenic Neoblasts Are Pluripotent Adult Stem Cells That Underlie Planarian Regeneration. *Science (80-.).* **332**, 811–816.

Wei, Z., Yaguchi, J., Yaguchi, S., Angerer, R. C. and Angerer, L. M. (2009). The sea urchin animal pole domain is a Six3-dependent neurogenic patterning center. *Development* **136**, 1179–1189.

Wenger, Y., Buzgariu, W., Reiter, S. and Galliot, B. (2014). Injury-induced immune responses in Hydra. *Semin. Immunol.* **26**, 277–294.

Wilk, R., Reed, B. H., Tepass, U. and Lipshitz, H. D. (2000). The hindsight gene is required for epithelial maintenance and differentiation of the tracheal system in Drosophila. *Dev. Biol.* **219**, 183–196.

Wilson, G. A. (2005). Orphans as taxonomically restricted and ecologically important genes. *Microbiology* **151**, 2499–2501.

Wilt, F. H. and Ettensohn, C. A. (2008). The Morphogenesis and Biomineralization of the Sea Urchin Larval Skeleton. *Handb. Biominer. Biol. Asp. Struct. Form.* **1**, 182–210.

Wilt, F. H., Killian, C. E. and Livingston, B. T. (2003). Development of calcareous skeletal elements in invertebrates. *Differentiation* **71**, 237–250.

Wittlieb, J., Khalturin, K., Lohmann, J. U., Anton-Erxleben, F. and Bosch, T. C. G. (2006). Transgenic Hydra allow in vivo tracking of individual stem cells during morphogenesis. *Proc. Natl. Acad. Sci. U. S. A.* **103**, 6208–6211.

Yajima, M. and Kiyomoto, M. (2006). Study of larval and adult skeletogenic cells in developing sea urchin larvae. *Biol. Bull.* **211**, 183–192.

Yamashita, M. (1985). Embryonic development of the brittle-star Amphipholis kochii in laboratory culture. *Biol. Bull.* **169**, 131–142.

Yamazaki, A. and Minokawa, T. (2015). Expession patterns of mesenchyme specification genes in two distantly related echinoids, Glyptocidaris crenularis and Echinocardium cordatum. *Gene Expr. Patterns* **17**, 87–97.

Yamazaki, A., Kidachi, Y., Yamaguchi, M. and Minokawa, T. (2014). Larval mesenchyme cell specification in the primitive echinoid occurs independently of the double-negative gate. *Development* **141**, 2669–79.

Yang, Y. (2013). Skeletal morphogenesis and embryonic development. In *Primer on the Metabolic Bone Diseases and Disorders of Mineral Metabolism*, pp. 1–14.

Yankura, K. A., Koechlein, C. S., Cryan, A. F., Cheatle, A. and Hinman, V. F. (2013). Gene regulatory network for neurogenesis in a sea star embryo connects broad neural specification and localized patterning. *Proc. Natl. Acad. Sci. U. S. A.* **110**, 8591–6.

Yokoyama, L. Q. and Amaral, A. C. Z. (2010). Arm regeneration in two populations of Ophionereis reticulata (Echinodermata, Ophiuroidea). *Iheringia Ser. Zool.* **100**, 123–127.

Young, H. E., Bailey, C. F. and Dalley, B. K. (1983). Gross morphological analysis of limb regeneration in postmetamorphic adult Ambystoma. *Anat. Rec.* **206**, 295–306.

Yu, K. and Ornitz, D. M. (2008). FGF signaling regulates mesenchymal

differentiation and skeletal patterning along the limb bud proximodistal axis. *Development* **135**, 483–91.

Zito, F., Koop, D., Byrne, M. and Matranga, V. (2015). Carbonic anhydrase inhibition blocks skeletogenesis and echinochrome production in Paracentrotus lividus and Heliocidaris tuberculata embryos and larvae. *Dev. Growth Differ.* **57**, 507–514.

Appendix

Table A.0.1: List of cloning primers for genes used in the thesis. For all undeposited sequences transcriptome AfiCDS IDs are given (http://echinonet.eu/shiny/Amphiura_filiformis). F – forward, R – reverse, O – outer, I – inner, Bp – product length in base pairs.

Gene	F/R	Sequence	Bp	Accession/AfiCDS	Publication/Database
Afi-alx1	5O	CTTGCGCCATTTAGCTCTG	634	KC788414	Czarkwiani et al, 2013
Afi-alx1	5I	GCCATTTAGCTCTGCGATTT	634	KC788414	Czarkwiani et al, 2013
Afi-c-lectin	F	AGCAGCAATGAAGGTCTGGT	1317	KT936152	Czarkwiani et al, 2016
Afi-c-lectin	R	AAGACTGGAAGAAAACAAGA	1317	KT936152	Czarkwiani et al, 2016
Afi-caraX	F	ACTTCTCTTTGGTCCGTCGA	1207		Echinonet.eu
Afi-caraX	R	TATAGCGGTACCTGCGTTGT	1207		Echinonet.eu
Afi-col2a1	F	Library clone P2A8	3000	JG391435	Burns et al, 2011
Afi-col2a1	R	Library clone P2A8	3000	JG391435	Burns et al, 2011
Afi-dri	5O	GTCTTCCCTCACGACGATTG	1482	KM816847	Dylus et al, 2016
Afi-dri	5I	CTCACGACGATTGCCATCTA	1482	KM816847	Dylus et al, 2016
Afi-egr	F	TACCCTCTCTCAAGTCGCAC	1301	id86638.tr27818	Echinonet.eu
Afi-egr	R	TTCTCGCGAATTTCCTTCCG	1301	id86638.tr27818	Echinonet.eu
Afi-erg	F	GCGCATCGTGGTCAAATACC	2149	KM816844	Dylus et al, 2016
Afi-erg	R	GCTTGACGCAACTTGGGAAG	2149	KM816844	Dylus et al, 2016
Afi-ets1/2	5O	ACCATGGACGGATCAAACAT	700	KC788415	Czarkwiani et al, 2013
Afi-ets1/2	5I	CGACGACTCCAGGCTGTAA	700	KC788415	Czarkwiani et al, 2013
Afi-fgf9/16/20	F	TGGTGTCAGTGCTAGCTTGA	1397	id10652.tr44814	Echinonet.eu
Afi-fgf9/16/20	R	TTTGCTTTCGTCCTTGCTCC	1397	id10652.tr44814	Echinonet.eu
Afi-fgfr1	F	ATGGGAATGTAGCCGATGTG	743	id89069.tr36121	Echinonet.eu
Afi-fgfr1	R	TGACAAACTCTCTGACAGTCTGA	743	id89069.tr36121	Echinonet.eu
Afi-fgfr2	3O	CCATTGAGTCTTGGGCTGAT	759	id62424.tr60943	Echinonet.eu
Afi-fgfr2	3I	CACTGGGTGCCAGACCTTAT	759	id62424.tr60943	Echinonet.eu
Afi-foxB	F	AACACCCARMGNTGGCAGAA	424	KC788416	Czarkwiani et al, 2013
Afi-foxB	R	GATGATRTTCTCGATRGTGAA	424	KC788416	Czarkwiani et al, 2013
Afi-gataC	3O	ACCGCGTGGTTATAAGGAG	1019	KC788417	Czarkwiani et al, 2013

Gene	F/R	Sequence	Bp	Accession/AfiCDS	Publication/Database
Afi-gataC	3I	GAGTAGGCCTGTGGACTGA	1019	KC788417	Czarkwiani et al, 2013
Afi-hesC	3O	TGTTTCCTGGAAGCTGTGTG	1414	KM816842	Dylus et al, 2016
Afi-hesC	3I	CATTGTCTTTGCCCTTGTT	1414	KM816842	Dylus et al, 2016
Afi-hex	F	TTGTCAAGTGGGCAGTTCGT	1243	KM816845	Dylus et al, 2016
Afi-hex	R	CTTTGGCACAACAGCACTGG	1243	KM816845	Dylus et al, 2016
Afi-jun	5O	ACCATGGACGGATCAAACAT	429	KM816839	Dylus et al, 2016
Afi-jun	5I	GCCATTTAGCTCTGCGATTT	429	KM816839	Dylus et al, 2016
Afi-kirrelL	F	GGTGAAACCGCAACTCTGAA	1647	id74191.tr58590	Echinonet.eu
Afi-kirrelL	R	TGTTGAGTTCGTATCTGCGC	1647	id74191.tr58590	Echinonet.eu
Afi-l1	F	AGCAGTCAGCTGCTTCATACC	584	id37274.tr11372	Echinonet.eu
Afi-l1	R	TGGCAAGCTGTCCTCAGAC	584	id37274.tr11372	Echinonet.eu
Afi-lrr-igr	F	TACGGCTTGGAGATCTGGAC	1316	id2489.tr22088	Echinonet.eu
Afi-lrr-igr	R	CGCAGATTCGGTAGTGCAAA	1316	id2489.tr22088	Echinonet.eu
Afi-msp130L	F	CGTCTTACTCGTACCAGCCT	878	id75849.tr3754	Echinonet.eu
Afi-msp130L	R	CTACTCCTGCTGCTGTTCCT	878	id75849.tr3754	Echinonet.eu
Afi-nk7	F	TTCAGCCCGACAATGTTTCC	1183	id63655.tr58557	Echinonet.eu
Afi-nk7	R	CTTCGTCCCGCTTCCTCTT	1183	id63655.tr58557	Echinonet.eu
Afi-p19	3O	TCGCATAGGTCTTGGGAAAC	697	KM816840	Dylus et al, 2016
Afi-p19	3I	CCCTCCAACAGACCAAGAAA	697	KM816840	Dylus et al, 2016
Afi-p58a	F	CCGTTCGAAACTAAGCATCGT	600	id59203.tr30563	Echinonet.eu
Afi-p58a	R	AGGTACCAGCTTTACTCTTGTT	600	id59203.tr30563	Echinonet.eu
Afi-p58b	F	TGCTAAAGGAGGTGCTAAGGA	702	id28024.tr11245	Echinonet.eu
Afi-p58b	R	AATTCCTCCTCCAGCTCGTC	702	id28024.tr11245	Echinonet.eu
Afi-pplx	F	GCTTCGTGAGAAAGCGATGC	799	KM816841	Dylus et al, 2016
Afi-pplx	R	TAGCTTGGCAAGTTCACGGG	799	KM816841	Dylus et al, 2016
Afi-rreb1	F	TCAACTGCCAACGTCACATG	893	id64870.tr47807	Echinonet.eu
Afi-rreb1	R	CTTAGCTGCCGTCTGAGAGT	893	id64870.tr47807	Echinonet.eu
Afi-slc4a10	F	CGATCCCTACTCGGTTCCTC	988	id61902.tr45342	Echinonet.eu
Afi-slc4a10	R	TCGCAGTCTTCCATAGCGAT	988	id61902.tr45342	Echinonet.eu
Afi-soxE	F	TCACGACGACATGGAAAGAC	1232	id90635.tr47043	Echinonet.eu
Afi-soxE	R	GGACTGAATCTGCAACGTCC	1232	id90635.tr47043	Echinonet.eu
Afi-tbr	5O	TGTTTCCTGGAAGCTGTGTG	1127	KC788418	Czarkwiani et al, 2013
Afi-tbr	5I	CATTGTCTTTGCCCTTGTT	1127	KC788418	Czarkwiani et al, 2013
Afi-trspn	F	GGCGCTCGATGGCTGTTC	716	id30755.tr5407	Echinonet.eu

Gene	F/R	Sequence	Bp	Accession/AfiCDS	Publication/Database
Afi-trspn	R	GAGGCTGTTTCCGTAAATCTTGA	716	id30755.tr5407	Echinonet.eu
Afi-tgif	F	TCGCCAAAGCTAGCTGTCAA	1305	KM816846	Dylus et al, 2016
Afi-tgif	R	CCGAGTCTGACTTCAGCTTCAT	1305	KM816846	Dylus et al, 2016
Afi-tr31926	F	ATCTCTAGCTTTCCCAGGCC	582	id88683.tr31926	Echinonet.eu
Afi-tr31926	R	CACCAATAGCTGTGCCCAAA	582	id88683.tr31926	Echinonet.eu
Afi-tr9107	F	ATCTTGCTGCACCAACCTTG	862	id70646.tr9107	Echinonet.eu
Afi-tr9107	R	ACCACTAGATCGGCTTGCTT	862	id70646.tr9107	Echinonet.eu
Afi-tr1339	F	TGTTGGATGTTTGACTGCGG	901	id43930.tr1339	Echinonet.eu
Afi-tr1339	R	TCACACTGACTTCACCCTCC	901	id43930.tr1339	Echinonet.eu
Afi-tr35695	F	GTTCCCAATTGGCGATCCC	534	id66499.tr35695	Echinonet.eu
Afi-tr35695	R	TGTCTCCAATAACGGCGGAT	534	id66499.tr35695	Echinonet.eu
Afi-tr45279	F	TGACCCAGGCTCTCAAACTT	1847	id53027.tr45279	Echinonet.eu
Afi-tr45279	R	AAGGCGAATCTGGTGGAAGA	1847	id53027.tr45279	Echinonet.eu
Afi-tr6206	F	ACGCTTTCATGCATTGCTCT	935	id7469.tr6206	Echinonet.eu
Afi-tr6206	R	TGGTCCGTTTCAAATCGGTG	935	id7469.tr6206	Echinonet.eu
Afi-62663	F	TCAACTTGCACCATGTCACC	916	id4513.tr62663	Echinonet.eu
Afi-62663	R	GTTGATGTTGATGGCGTACTGA	916	id4513.tr62663	Echinonet.eu
Afi-vegf2	F	TAGTGGTGATGGCAGGAGTG	1197	id11730.tr8523	Echinonet.eu
Afi-vegf2	R	TCATGTGCATCCGTTAGTGC	1197	id11730.tr8523	Echinonet.eu
Afi-vegf3	F	CCAATAGTCATGGCACGGTG	1152	id52846.tr38849	Echinonet.eu
Afi-vegf3	R	GTTTAGGCATGGTGGTGTGG	1152	id52846.tr38849	Echinonet.eu
Afi-vegfr	F	TTGTTGCGTTCCAGACTGTG	1834	id89175.tr20202	Echinonet.eu
Afi-vegfr	R	GGACATTACGAGCTGCCAAG	1834	id89175.tr20202	Echinonet.eu

Table A.0.2: Nanostring nCounter probe sequences.

Gene	Accession number (Echinonet.eu)	Probe sequence
Afi-AcSc	AfiCDS.id80603.tr35946	CACAAGCAGTTGCCAGAAGAAATGAAAGGGAGA GAAATCGTGTGAAATTGGTGAACTCTGGCTTTTC AAGCCTTCGACAACAGCTTCCAAATGGTGTGAA
Afi-Col2a1	JG391435.1	GCATCACGTGCAGCACAGGGCAAAGAAGGCAAT GTTGACTTGACCGACAGGGAAATCATGGCCGCT TTGGCATCATTGAACGAACAGATTGAGAGCATGA
Afi-Alx/arx	AfiCDS.id68561.tr6658	CGGGTGCAGGTTTGGTTCCAAAACAGACGAGCA AAATGGCGCAAACGTGACAAATCTGGTTTACCAC ACTGTCTCCCACCTCCTCCACATCATCATCATC
Afi-Alx1	AfiCDS.id52740.tr55899	GTAGAGGGCGCTATGCTACGAATTTGCCGAAATC TTCAAAATCTGCGACGGGAATTTGACTCGCGGAA ATTGTCCACAACTGCACCAGCGGTCTCGGAAG
Afi-Brn1/2/4	AfiCDS.id14584.tr47003	ACATCATCTTGGCATCCATAATGGACACCATCAT GACCCTATCGAAGAAGGAGATGTCGTTGTGACG GAAGAATGCGACACTCCGAGCTCCGATGATTTG
Afi-CaraNo	AfiCDS.id11259.tr29884	CACCACCACTTTTCCACTGAACACACTTATGCCA AATGATCTCTCAAGGTTCTATCGTTACGATGGAT CGCTAACAACTCCTGGTTGCTATGAGACTGTA
Afi-CycA	AfiCDS.id13700.tr1836	GATGATTCTCCTATGGTGCTAGACATATCGTGCA ATGAAAGAACGCAACCAGAGGTGATCGACATTGA CGATGTAGACAGGACAGAGTGTGTCATCAGTG
Afi-CycB	AfiCDS.id59130.tr6192	TGAGGACGAATCTGAGTCTCCTGTTTTTGTTGAC ATTGATGAGGAGAACAAAGAAGATCCAAATCAGG CGCCAGTCTATGCTCGGGACATCTTTAAGTAT
Afi-CycE	AfiCDS.id15771.tr3905	AACTCCTGGGTACCAATTTCACATTCATCAGGCT TCGAGCGTAGCACACTAATACCAACACCTCACAG AGAACCAACAACTCCATCAGACGAACTTTTAG
Afi-Cytchrmeb	AfiCDS.id91776.tr67065	TTGTCGAGATGTCAATTATGGCTGGCTTCTTCGT AAAATCCATACAAATGGGGCGTCTCTTTTCTTTGT

Gene	Accession number (Echinonet.eu)	Probe sequence
		GTGCATGTATGTGCATATCGGGCGGGGACTT
Afi-C-lectin	AfiCDS.id44128.tr27068	CAAAAATTGGGCAAGAGGAAGCCCGAACAACGG TGGTAATTCTGATTGCGTCGCCATGCCAGCAGAA CAACCAGGAGCTGTATGGTTTTCTGTGCCTTGT
Afi-Delta	AfiCDS.id13088.tr30325	AGCACTGGTTCAGGGTTCGAGTGTTTGTGTCCAG ATGATTACACTGGCGAGTTTTGCGAGTTCTACGA ACCTCCAGTAAGCACCACCGCAGCACCAAGAT
Afi-Dlx	AfiCDS.id79904.tr21930	TCAACACGAGGTTCCAGAGGACTCAATATTTAGC GTTACCTGAGAGAGCGGATCTGGCAGCGGCTTT GGGGCTTACTCAGACTCAGATTAAAATATGGTT
Afi-Dri	AfiCDS.id16344.tr60844	CCGCCAAGACAAACAAGGAGTCCACTAGATGATT CCTTCAAAATAAATGGAGAACAGGACCCAATCAA GGACAGATCGTTATCTCCACCTATAACTCCTA
Afi-EgifL2	AfiCDS.id85082.tr39719	TTGTTGAACTAACCACTTCTGATTTCACTGCAACT GGAGGAGCGGATTATGTTTCACTGACGAATCGG CAACTCATATTTGAACCTGGGGATACCATTCA
Afi-Egr	AfiCDS.id86638.tr27818	CAAGCTCAATCACAACTCGAACAATCCATCAAAG TCAATGTTGACGGCATCCTAAAGTATACATGGCC TGTAAGTCAAGATATGGGCTCAGCATTCGGAA
Afi-ElavL	AfiCDS.id11028.tr61396	ATCATATGCACGGCCCAGCAGTCAGGCCATCAA AGATGCCAACTTGTACATCAGCGGTATCCCAAAA GACTACACACAGGCCGAATTGGACAGATTGTTT
Afi-Erg	AfiCDS.id86317.tr2242	CAGCTTCTTAGACCAGGACTTCGGTAAACTCTCA ACACAGATTCTCTTGGCCTCAAGAGCATACAAAG GGAGTGGTCAGATCCAACTGTGGCAATTTCTA
Afi-Ese	AfiCDS.id53998.tr2182	CTGGTGGAGAAGAAATAGATAACGACGACAGTT GCAGTGAAGCCAGTTTTGATCTTTCAACCACGAG TAATTCAGGAGATGACAGTTTGGACGCCATCAT
Afi-Ets1/2	AfiCDS.id20811.tr66263	CAGATTATTACAGCCTGGAGTCGTCGCCGAGCT CCAACAACTACTTGGAGGCGGCCACGCCGGAAT TCTACAATAACCCAATGATGTTTGATCCGTCCAT

Gene	Accession number (Echinonet.eu)	Probe sequence
Afi-Fgf6	DD-3Fgf-6-T7	CTATGCCAAACGCAATTATTACCTGGGTCTCAGT AGACGAGGCAGAGTGCGCCCTGCCAGCAAAGTT GTAGCTGGTCAGAATTGTGCCAAATTCTTGCAC
Afi-Fgf8/17/18	AfiCDS.id48495.tr550751	AGGGAGATAGATGCCAAAGGACAGGAAAGAGAC GAATTTGCAAGGTTAATCATCACAAGTAAGAGAT TTGATGGTGTAACGATACAAGGTGAACGGACTG
Afi-Fgf9/16/20	AfiCDS.id10652.tr44814	ACGGGACTATCAATGGCACTAAACGAATAGACAA CCCATATACGTTGATGCAGATATCAGCGAGATCC TGGGGTGTCGTTTCTATCAGAGGGGTGTATAG
Afi-Fgfr1	AfiCDS.id89069.tr36121	TTTGGGATCAAGCTCAATATCATACTGGGAGGAC GACAGCTTTGTTGAACCAGAAGGCGAATACCCTC CTGTATTTATCAAAGTGAACCGATACCTGGAG
Afi-Fgfr2	AfiCDS.id62424.tr60943	ACCGCCATCGTCCGTGGATGGCTCAATATACCA GTCAATATCACGTGTAAATTCTCAGGTTATCCCG TCCCGCGTGTCACATGGTTCCACAACGGTGTTC
Afi-Fn3-Egff-1	AfiCDS.id85261.tr60838	TGATACACAAACCCAGTTTTCACCTCATATTCATC CAGGAGTGACACACTACACAGTCAGGGATTTGG AGCCCGAATCACAGTACACAATTTGCATTAAC
Afi-Fos	AfiCDS.id35018.tr7958	GTCTCCACTAATAAAGGAAGAGTTACGCACAACC ATCAGAAACAGACGATTTGGAAGCGGTATGGAG GAATTGGTTATTGACGACTCTCCAAAAGAACCT
Afi-FoxA	AfiCDS.id85717.tr16742	CGCAAGCACAGGCCGATATCAACCGTGCTCGCG CTGAGAAGACGTACCGTCGATCCTACACACATGC TAAACCACCGTATTCGTACATCTCGCTCATCAC
Afi-FoxB	AfiCDS.id1937.tr11127	GCCAAAGTTTTGCCTCCGTATCCAATGGGTTACG GATGCTCACCTTATGGTGTGCAAGCAATGTCTCC ACCACCACGTATACCAATAAGTCCAGTAGCAA
Afi-FoxJ1	AfiCDS.id76906.tr158	TGGTCAGGACATCTTCAGTGCATCATGTGCAACC GACCTATTCAAGTATAGAACAGGTGGACTATAAG AACAACCAGTATGTGAAGCCACCTTATTCCTA
Afi-FoxN2/3	AfiCDS.id838.tr63418	CGGGATGGAAGAACTCTGTTAGACACAACTTGTC

Gene	Accession number (Echinonet.eu)	Probe sequence
		GCTAAATAAATGCTTCCGAAAAGTGGACAAAATG AAAGGACAGACTTTAGGCAAAGGTTCTCTGTG
Afi-FoxQ2	AfiCDS.id15015.tr19544	ATAATGACAGAAGTTGGCGTAACAGCATCCGTCA CAACTTGTCTCTCAATGAATGTTTCGTCAAGTGC GGAAGAAGCGGCGATGGCAGAGGCAACTTTTG
Afi-GataC	AfiCDS.id14825.tr63157	GCACTCATCCGCAGACAAGTCCTCATTTGTTTAA CTTTCCACCAACACCTCCTAAGGATACCACGCCA GATAGTCTGAATCTTACGCACTCTTCTTCAAA
Afi-GataE	AfiCDS.id38615.tr1992	GCGGTAACAGCTTCGGTGGCTCAACCGACCTAC GAGTCACCATTTATTCACTCCGCCAACAGCCCTG TTTATGTGCCATCCACACGTGCTCCTGTGCTTA
Afi-Gcm	AfiCDS.id38146.tr47389	ATCGATGTCAGCCTGTTACTACCAACCAATACAT CAGCCTTCAGAAATGCGCTCATCCGCATTGCCTC TCTACGACACGTATTCTTCTTACAGCGCTAAT
Afi-HesC	AfiCDS.id79437.tr59210	AAGCAATCAGGCAGCGGCTCAAACAGCCCAACC AACGTTAGCCAATTCCATGCTGGCTTCAGCGAAT GCCTCAGTGAAGTCTCTCGATTCCTCAGCAACT
Afi-Hex	AfiCDS.id81692.tr22161	TGGAAAAGTTCCTGGTAAATTTCTATGGAATCCC TTCATACAGAGGCCACTACACAAGCGAAAAGGTG GTCAGGTCCGGTTCTCAAACGACCAAACCTTA
Afi-Hox11/13	AfiCDS.id72747.tr52756	CGGCTGCGGCGGCAAGACAGTACAATCCATTTG GAAATGTTTCGCCAAGTTTTCTGGCTGCAACGGC ACAATCGTCACATCCTTCCCACCATCACCATCA
Afi-Jun	AfiCDS.id55428.tr60572	ACATGGAAACCCAAGAAAGAATCAAGGCAGAAC GCAAGAAGTTGAGGAACCGTGTAGCAGCCAGCA AGTGCCGCAAGCGCAAGTTGGAACGCATCGCCC G
Afi-Khdrbh2	AfiCDS.id64042.tr13527	AGACAAGCAGAAGGAGGAGGACCATAGAAAAGA AGGTATGGCAAAACATGCTCATCTTCACGAGGAT TTGCATGTGAACATCGAAGTGTATGCGCAAGCG
Afi-KirrelL	AfiCDS.id74191.tr58590	AAGACAATGGAATAACATTCACCTGTAAGGCTGA

Gene	Accession number (Echinonet.eu)	Probe sequence
		AAGTCCCGCACTTCTCACGCCACGCAAATGTTCT GTTACACCGATGAAGATCGCACCCGTCGTACA
Afi-Klf4	AfiCDS.id5641.tr52835	GATTATCCGCATTGTCAGCAGCAGCAACATCAGC AGTTTACACAACCTCAAATGATGCCTACAGATTT GACGGGTCTGGAGATGGACCATATCTTAAGTA
Afi-L1	AfiCDS.id37274.tr11372	GCTTATTAATGGTAAACCAGAGAGTGAAGTAGAA GCAAACCCACGACGTACTATAACTTCTGGACAAG GTAGCGGTCAGATTATCGTAACTAATGCCGAG
Afi-Lmo	afiReg.id150643.tr412948	CTCACATTGAGAGCATTTGAAGCATTCTAGATGG TAGACACGGTCCTGTGTGACGGTCATCACTTGCT CATATGCAGGTATAGGACGTTTACATGAAGCA
Afi-MhC	AfiCDS.id71941.tr36216	GAACAGGAAGAGTATCAACGAGAGGGTATCGAG TGGAAGTTCATTGACTTTGGCCTGGATCTTCAGC CTTGTATTGACTTGATTGAGAAGCCAATGGGTG
Afi-Msp130L	AfiCDS.id75849.tr3754	CATTACCCGGAGGTTCATCACGAGGACTTAATGG TTGGGATACTGCTCCAGTCGTCAACCAGCAACCA ATAAGTGGCCGTACTAACCACCAGAATGTCGG
Afi-Msp130r6	AfiCDS.id75232.tr63542	ATTCTTCGAGTTCAATGGTCATGGGTATATCGCT ACTGGCAATGAAGGTGGAACTATTAAATTAGAAG CCGGTGCACGAAGTTGGACTGATGCGAAGAGA
Afi-Mt14/mmpL7	AfiCDS.id74676.tr52643	GGTCGCGAGTACCATGGCGATCCCTATCCTTTTG ATGGTGTCGGTTTTACTTTGGCCCATGCTTATCC ACCAATGAGCGGTTTTGGAGATCTTGACGGAG
Afi-Musashi	lcl|AfiCDS.id55115.tr52827	CCTAAGCCTGTCACAAGGACAAAGAAAATATTCG TTGGAGGTTTAGCAGCGCAAACGACGGTGGATG ATCTAAAGAATTACTTCCAACAATTTGGCAAGG
Afi-Myc	AfiCDS.id53162.tr21813	CTCTGACTCTGAAAAGAAACTGGTACGGTGTTCG TCTCCACCTCCTCTTGTACCCGTGTCTTCGGATT ACAGTGTAACTTCAGATTGTGTGGACCCTGCA
Afi-MyoD2	GKWICZJ01E6B10	GACGGCACCTCACACTATCACCAGCATGTCCTC GCACCAGGACCAGAAAACAGACCCGACAGACAA

Gene	Accession number (Echinonet.eu)	Probe sequence
		TGCTTATTATGGGCGTGTAAAGCTTGTAAGAGAA
Afi-Ncbp1	AfiCDS.id5543.tr45273	TATTTGGGAAACCGAAAGAAAGACCATCTTCCCA TGTTGAGAGTATGGCATAGTGATTCACCTCATCC ACAAGAAGATTATCTAGACAGCTTATGGGCTC
Afi-NeuroD	AfiCDS.id1482.tr19514	ATTACATTTCGGCATTGTCTGATATTCTGCGTACT GGAAGAGTGCCGGACACGATTGCATTTGCGCAG ACGTTGTCTCAAGGGTTATCACAGCCGACGAC
Afi-Neurogenin	AfiCDS.id31185.tr60499	CTATGGCTGTTGATGCAGAAATTGAGAACACACC TGTATGCAGAGATTCCAGAAATAAACTCAAGCAG CAGAAGAAGAAAGACGGCGGTGCTAAGACTAA
Afi-Nk7	AfiCDS.id63655.tr58557	TCAAAGAACCACTCGATGAGCTGGTAACAAATGG AACAGAATCTGAACCAACAGACCATCCGTGCGAT AAAGGCGCCGATTCCGACTCCAAAGATTCCGG
Afi-Nkx2.1	AfiCDS.id21551.tr13724	AATGAATATGAATATGTCCTCTTTAGGCGGTGTT GGAGGTGACCTGATGGGAAAGCCGATGTTACCG ACAGCTCAACGAAGAAAAAGAAGAGTGCTGTTC
Afi-Nkx3.2	AfiCDS.id65058.tr52703	CAAAGCCAGGAAAAAGCGGTCTCGTGCTGCGTT CTCACACGCGCAAGTTTTTGAATTGGAGAGACGA TTTAGCCACCAACGTTACCTTTCTGGACCAGAA
Afi-Notch	AfiCDS.id22437.tr30372	TGTCAGTCATCAGGAACTGGCACGTATACATGTC AATGTCAGCCACAATACACAGGAACCAATTGTGA AATTGCACCAGATCCATGTCAGAATCTACCTT
Afi-Oct1/2	AfiCDS.id47652.tr963	TGCAGGCACACAGGCTGTCGTTACCAAGGATAA CAAGATGTGGGTGCAGCAGCAACAACAGGCTCA ATTGCAACATTACCAGCCGCAGAATCAGATCACA
Afi-Orexin1	Unigene59589-6-Amphiura-filiformis-Orexin1-precursor	TAGCTATCAGGAACAGAAATGAAGTTCTTAGCGT GCCTTTTGGCATCACTGGCTCTGCTGGTCGCTG CATTAGCTGTACCTTCAAGAGGTAACCGGGCTT
Afi-Orexin2	Unigene37411-6- Amphiura-filiformis-Orexin2-precursor	TTACACCCTTTAGTAGATTTGCAGCATGCCCTTT GTGCCAGTGTCCCAGTTAGGTATACCAATATCCC AAGCAGAATCAGTGTTAGAAATTGTCCAGGCC

Gene	Accession number (Echinonet.eu)	Probe sequence
Afi-Otx	AfiCDS.id6059.tr24500	GGTCCAGTGACATCATCGCAGCACCAGGATGTTT TGGCAGCGATGGGTGGAGGTGGTGCGGGTGCA TTTCCTCATCCATTTTACCATCACATACAAGGAT
Afi-P19	AfiCDS.id5444.tr13385	GGTGAGGAAGGCGCAGAAGGTGAAGCAGCCGA AGGCGAAGAAAAAGGAGGGAAGGGAGGAAAGA GGGGTCGCAAATGGCCTTGGTCAAGGAAAGGCG GTG
Afi-P58a	AfiCDS.id59203.tr30563	AAATCACACGATGGATTTTTGGCCGTTCCGGTCT TAGGACTGGGTTTGGAATACTTTGCGGCATCATA CGCAGCAAGTGGTTTGGATAGATCTCAGATGA
Afi-P58b	AfiCDS.id28024.tr11245	GGCGTTGATTTCCCACAAGTATAAAACAGAGCAA AAGCAAGATTGGATGCGATTAATGTCATTTAATG CAGATTATCAGATGCCGCTTGGAAAGGGGGCA
Afi-Pax2/5/8	AfiCDS.id86711.tr30481	GGAGTGTGTGAAAAGGATAATGTGCCCAGTGTTA GCTCCATCAACAGAATCGTAAGGAACAAATTAAG TGACAAAAAGGAGGGAGATACCAGCATGACGT
Afi-Pax6	AfiCDS.id10654.tr45582	CCCAGCACCACTTAACCACCATGAACCATTGAAA AAAGAAGTTTCAGATGGGAGCTATAATTGGTCGT GGTCAGTATTGCAGCTAGGCTCATCCAAAGCA
Afi-Pcna	AfiCDS.id17064.tr965	GAGCCAGTGTCACTGACCTTTGCCAGCCGTTACA TGTGTTTCTTCACCAAGGCTACACCTCTCTCACC AACAGTCCAACTTCAAATGACCAAAGATTCAC
Afi-Pea	AfiCDS.id25833.tr52646	CTGCCAGTCAGAGACCTTTCCAGCGACAGAATTC AGAACCTTCGTTCTTGTTATTCAAGCAGCAAAAC CAGCCAGGGCACCCTTTCAACAAACCGTACAG
Afi-Phb1	AfiCDS.id4652.tr32715	GAATACTACCACAGCTACAACTCTACAGAAACTA CCAGTTCTCGTCACAAGAAGACGTCGCCGTTCTC CATTGAAAGAATCTTGGGAATAGATCAACAAA
Afi-Piwi	AfiCDS.id28519.tr1927	CCTTGCCTTTGACGGCATGGTCCTGTTCTTAGTG CGGAGATTGCCAGAGAGGGTGACTAAAATTCTCT CTCGCAAGAAGGACGGCACCGATGTTGAATTG

Gene	Accession number (Echinonet.eu)	Probe sequence
Afi-Pplx	KM816841.1	TTCTTCAGAAGCTGTCAGCCTTTGTCACCGGAAG CCATCGCCGTTCTCCATTGAAGCAATCTTGGGAC TAAATCAAGCTCCTCCGATGACTTCGTTACCA
Afi-Prox	AfiCDS.id52648.tr11706	AAGCTGTTACAGCCAATGAGATGATGAGACATCC ATTCATGCCTGCGTTTTTGCCCACCTCTGTTGCA ATTCCAAATCCAAGCTTACATCCTTTCTCAGC
Afi-Rreb1	AfiCDS.id64870.tr47807	CAAGCGGGTGCCTTCAAAACGACTGTTAGACTCC GCCGAAGATTACAGTATGTCACCACCTAAGAAGT TGACATTGGACGAGAGTAGAGTGGTATATTCA
Afi-Runt1	AfiCDS.id407.tr30996	GGTAGATCTGGCAGAGGCAAAAGTTTGACATTAT CCATCATCGTAGCAACCAGTCCTCCTCAGGTAGC CACCTACAACCGTGCAATCAAAGTAACCGTAG
Afi-Rx	AfiCDS.id52378.tr63731	AAACATAGGAGAAATCGCACTACCTTCACAACGT ACCAGTTGCATGAGTTGGAAAGAGCATTTGAAAA ATCACATTATCCGGACGTGTACAGTCGGGAAG
Afi-Sclb	AfiCDS.id29842.tr63729	ACAGTTATGGATACAAAACCAATTGTGCTCACAT CTACGCACGCGCAGTTAAGCGATCTCAAATTTCC CGCCAAAACAGACTCTACCACAGTCCGTACAG
Afi-Serrate	AfiCDS.id91048.tr11324	GATCCCAACCCTTGCACGAATGGTGCTCGTTGTT TTAACGTGCTTGGGGATTACTACTGTGCTTGTGC TGAGAGTTTCCAAGGCAAGAATTGCTCCGAGA
Afi-Six1	AfiCDS.id42235.tr12895	ACCCAGCACCAGCTCCGAGGAAGAATTGGCAGT GAATGGAAAAGAGAATCTTGACTCCGGTGACATG GGGCCGCTTTCCCACCATCAAACCTCTATCATG
Afi-Six3	AfiCDS.id45608.tr3325	AACACAAGTAGGAAATTGGTTCAAGAATAGACGG CAAAGAGACAGAGCAGCGGCAGCTAAAAACAGA ATGCAGTCACACAACCAACCGCCACTGTCTAGT
Afi-Slc4a10	AfiCDS.id61902.tr45342	CACAAGGTGCAGAAGCAGCCAACGTACTAGTTG GTGAAGTAGATTTTCTTGAGAAACCAATCATTGC CTTCGTTAGATTGAGCCAAGGAGTCAACTTGGA
Afi-	AfiCDS.id29974.tr601	GAAAGTAAAACCAAAGACATATTGTCGCATGCAC

Gene	Accession number (Echinonet.eu)	Probe sequence
Scl4a1ap		GTTGGGCACATGTTCAAGTTAGCAGGGAGCACA CGGTTGTATATCTTGCAGGGCCCAGCAGAAGAT
Afi-Snail	AfiCDS.id32534.tr38806	CCAAAGAAAGCAAAAGAATCTGCCTCCAAAAGAC GCAAATCTTCCAAAGGAGATCGCGCCGAAGGTA CAAAATATACCTGCAGTGACTGTACTAAAGTTT
Afi-SoxB1	AfiCDS.id91348.tr60524	CTAACTGAAGAACAGAAGCGGCCATTTATTGATG AAGCTAAGCGTCTGAGAGCTGTTCACATGAAAGA GCATCCCGACTACAAATATCGTCCACGCCGTA
Afi-SoxB2	AfiCDS.id23770.tr24943	CCGTTACGCATTTCCAATCCCATGTATACCAACC AGTTCATACGGACCAGTTTCCTCATCATCGCCGT TGTCACCTAGCGACATCCTAGCATCAGAAAAG
Afi-SoxC	AfiCDS.id33804.tr61034	CTTGGTAGACGCTGGAAAATGCTGAATGAAACGC AGAAGGGACCCTTCGTTGAGGAAGCAGAAAGAC TGCGACTTCTTCACATGCAAGAGTTTCCTGATT
Afi-SoxD1	AfiCDS.id37686.tr6742	TAAGATACAATTATTAACCCAGGCGATACAAACC CAATCTGGTGCCGCTGGCCAATTTTTAAGGCTGG TGCCAATTTATCCCACCGACTATGCACGTGGA
Afi-Tbr	AfiCDS.id43541.tr66231	AAGGGCAAAGACAATGGTCATGTCATCTTACATT CCATGCATCAGTACCAACCACGTATTCATGTTTTA GAGCTAACTGAGAGAAGAACGCTACAGACAC
Afi-Tel	AfiCDS.id20271.tr14217	GGCTGAAACGCAACAAAGATTACCCGATAGAGA CCCGTCTCAATTTATCTTCCATCATCAAACCCGTC AACCCGCTGATTTGCTTGTTCGCAGACACAAT
Afi-Tetraspanin	AfiCDS.id30755.tr5407	TTCTACATCATCGCGAAGGTCCATTTGCAACCTT GCTTCCCAGCTTCCCATTTCTCAACGCAGCGAAT CTGTGCATCGCAGTTGGGGTAGTCATAATGGC
Afi-Tfb1m	AfiCDS.id25258.tr39360	CAGTGAAGAAGGACTGGCATGGAGATCTTCCAG ATGTGCATATCATTGGTAACCTACCATTCAATGTG TCTACACCACTGATAATCCGATGGTTAGCGGC
Afi-Tgif	AfiCDS.id49825.tr1310	TCTTGCCAGCAACAGTACCTATAGCGACATAACC ACCATGGCAGATACTACACCCATTAGTACACCAA

Gene	Accession number (Echinonet.eu)	Probe sequence
		CCAACAGTTCCGGGGGTCCTCCTGCTAAGAAA
Afi-Tie1	AfiCDS.id43567.tr10046	AACGGAATGGACTAACGTTCTATTTTACACCGTA TGGACACAATGGCGACTGGAAGTTTAAGTGTGAT GCCAATGTGGATGGTCATATGTTCAGCTACAC
Afi-Tk8/Cad96a	AfiCDS.id57681.tr3943	CAAAATCTCACTTTTATTAAAGAACTCGGCATGG GCCAATACGGAGTGGTCCACTTAGCCAAAGCCG TAGGAATCTCGGAGAGAAGTCAATGGATTTCAA
Afi-tr10933	AfiCDS.id63133.tr10933	CGCATACACCCAACCTGTTCAAAACACAAGAGTC GTTGGAAAACAAATCGCCATGTTGCTTTCTCACA TTGCAGCTCAGACACAAATCAAACTTGGGACT
Afi-tr12446	AfiCDS.id12966.tr12446	CTCAAACAACCAAGCTTTACCAGATGATGGAGCA TATGGTGCCGCCAATGCAGCAAACAATGCTGGT GCGGGAGGAGTTTCAATTTCAACCAATAATGGC
Afi-tr1291	AfiCDS.id5647.tr1291	TTCGTCAGAAGATGTTGGATACGTTAGACTCCAT CAAGAAAGATCCAGCGGGAGCGGATAAATGGGC ACTCTTCTTTGGCTGGGATCCTGAACTTATCGC
Afi-tr1339	AfiCDS.id43930.tr1339	TTAAGCATGAAGGAAAATGTTGGATGTTTGACTG CGGAGAAGGAACCCAGATACAGCTGATGCGTAG TCAGCTAAAAGCAGCTCGTATCACCAAGATCTT
Afi-tr14406	AfiCDS.id11683.tr14406	TATTTATCAACCAACCAGTTCTAACCAGGGATCC TAGAGGGGTCAGTCGGATCACACACAGTGTAGG GAAATTGGCACAAAGAAGGAAGTGCTGTGCATG
Afi-tr19326	AfiCDS.id75617.tr19326	CATTAGCTATCATGGTTGTCATGGCAGTAGCAGC AGCTTTATGGATGAATCGTAACAAGAACGGAAAT ACGGAAACATTTGGAATGAATCAGCTACCGCG
Afi-tr23254	AfiCDS.id35451.tr23254	GGGTGCACTCTCCATCTCAGTTCAGTGTTCACCA TGTATGGAAGCAGTAAACACTATTTGGAGGCAGT GGTCTCCTCTGCGTACTATGGTAGGAATTATT
Afi-tr31926	AfiCDS.id88683.tr31926	AGATTATCCCAAGTGGAGGTAATGCTGGAGGAG TTTCAAGGCAAACTGGAGGTTCAAACAACCAAGC TGTTGCTGATCCAGTCGCTGCCAATCCGGGAGG

Gene	Accession number (Echinonet.eu)	Probe sequence
Afi-tr26306	AfiCDS.id91903.tr26306	TCTCGACGCATCGAAGCAGAAATGAAGATTCAGC TACAAGACATTGTCATGTTCTTCACAAACAAAAG GGTGTTCGTGACAGAAATAGGCGACTGTGGAG
Afi-tr34323	AfiCDS.id29222.tr34323	GCCTTCGGCACACTCAATGAAACATTTTTCAACT GCAATGGTACAGAAGGACAAAACAACGCCAGAG AAAGTTGTGATCTACGGTGGGGTTTCTTAGCTG
Afi-tr35695	AfiCDS.id66499.tr35695	GGTGAATTGAAGGCTGGTAACAGCAAAGTAAGC GGTCTTGGTATTGCTATTGGAGTCTGTTTACTTGT TGGTGCAACAACAGCAGTAGCCGTATTCGCAA
Afi-tr45279	AfiCDS.id53027.tr45279	TAACTTTATATACCTGGTTTGTACAGGGCCGGGA TGGATATCACGAATACACACAGACGGTAGGAAG GTTTCGTGTCCGACAAGGCGGGAAGAATTTAAA
Afi-tr9107	AfiCDS.id70646.tr9107	GATGCCAACTTCCCACAGTTTGCTGTTGTAGTTG CCGATGGGAATAGGTTCGTCGTCTTCTTCTGGAG CTGCCGAGCGCGCCTGACTCCGTGCTACCTGA
Afi-tr6206	AfiCDS.id7469.tr6206	GGCGCAAGTTCTTCAGATACTCCAACGTCAACAC ATGCAATGTTGTCAAAAATCGTTAGCGATGACCC GCGACAAGGTACCATAACAATCCTCTTCATCG
Afi-tr62663	AfiCDS.id4513.tr62663	GCATTGCTTGCTTATGTGTGCCATCTTAAGCGTG ACAAGAAACGGAGGACATGGAGTGCTCTTCTGA CGCCAACAGTAACTTTAAACGAATCGCCTAAGG
Afi-tr63013	AfiCDS.id59532.tr63013	AGTCGTGGAATATCAATACAGGGGAAGTGTTATG CAAACATTCAGGACACATTGGGGTTGAGGAGATA CTATACAATGCTGAAAAGAAGTACGGAATGCG
Afi-tr65264	AfiCDS.id43938.tr65264	TTCCATTCAAAATGCTGCACTTCTTCACCTTGCAA AACAAAGCTCTGCCACTGGGTGCGTTGTCGGCT CCAAGATGGTGGTTCGCAATCATTGTATGTAG
Afi-tr68751	AfiCDS.id59305.tr68751	TGACGCAGCTGAAAGTGAAGAGGAAGTTGAGCA GGTTGGCGGTGCACTTGGTGGCGTTGTTGGTGG CTCAAGTAGTGTAGAAGCAGGTGCAGGTGCAAC T

Gene	Accession number (Echinonet.eu)	Probe sequence
Afi-Trh	Unigene59995-6-Amphiura-filiformis-TRH-precursor-A	CAGGATCTTATGCACCTAAGAGGCTGTATAGTGC CTCTATTCTTCCTCGTAGCATTAAGTACTGTTTGC TGTTCAGCAGATGCAGAATTTGAAGCCGCAC
Afi-Trim2	AfiCDS.id62800.tr22663	AAAATACCACGAAGTAATGTCAAACAACGAGCCA CAAGAAGGCCTCATAGTGCAGCTGGATCACTCA GATCATATCGTAAAACCAATCCCATTGAAGATG
Afi-Trop1	AfiCDS.id81471.tr38967	AAGATAACAGGTTTAGAGGTTGCATTGAAAAAAG CGAGGGAGCTTGCAGAAGAAAATGACCGTGAAC GAGTGCAGGCTAACCGTAAATTGCAAGTTGCTG
Afi-Twist	AfiCDS.id89079.tr60007	GATACATTGACTTTCTTTACCAAGTGTTAAGAAGC GACGAGGCTGACCAAAAAATGGCCAACAGTTGC AGTTATATGGCACACGAAAGACTGAGCTATGC
Afi-Ubc	AfiCDS.id79379.tr62324	ATAAATAAGGAACTTCAAGACCTTGGTAGAGACC CTCCAGCACAATGTTCAGCAGGTCCAGTAGGTG ATGATTTATTCCATTGGCAAGCAACAATAATGG
Afi-Ubq	AfiCDS.id15709.tr1489	GTGGTGGTATGCAGATATTTGTGAAGACCCTTAC AGGTAAAACCATCACTTTGGAAGTGGAACCAAGT GACACCATTGAGAACGTCAAGGCTAAAATCCA
Afi-Vasa	AfiCDS.id26402.tr21483	CGAACGACAAACGCTCATGTTCAGCGCTACATTC CCAACAGAAGTGCAAGAGAAAGCAGCCGAGTAT CTGAACGACTATGTCTTCCTGACGATTGGTCGT
Afi-Vegf2	AfiCDS.id11730.tr8523	AATATTACCCGCAGTCGTCCAGTCTACATCGTAC CTGAATGTACAACGGTGTTGAGGTGCCAAAATGA TGATTGCTGTGCCCGAGTTAAGCCTTGTATTC
Afi-Vegf3	AfiCDS.id52846.tr38849	AAATAGTCCGGAATAGTTCATATCTCAACACAGG CAAAAAGAGAACGGGCAGAAGAGCCAGCGGTAA ATCAAGATCAGCACTAGCATTTTCTTCAGCGGA
Afi-Vegfr	AfiCDS.id89175.tr20202	GTCGTGTCACCAATCCCGATATACAGGTTGAATT GGATACGAGTAGTGGATACTTAGCCCGCTCCATC TATGGAGGTACCAGCTACTATGATCCAAAAGT

Table A.0.3: Adult arm gene expression time-courses heatmap. *NR – non-regenerating, hpa – hours post amputation, st – stage, prox – proximal segments, dist – distal segments without distal cap.* See bottom for key.

Gene	NR	24hpa	48hpa	72hpa	St 3	St 4	St 5	50% prox	50% dist
Afi-AcSc	35	23	13	35	61	40	38	376	330
Afi-Col2a1	17830	10212	14181	16033	33105	45295	46001	128680	72182
Afi-Alx/Arx	0	2	6	6	12	1	3	6	2
Afi-Alx1	73	92	225	350	668	726	672	806	1049
Afi-Brn1/2/4	11	2	7	6	12	7	9	120	55
Afi-C-lectin	2270	1203	2171	2703	6793	7543	7315	35385	16705
Afi-Cara?	0	2	50	170	2089	2208	1577	214	783
Afi-CycA	11	9	15	41	403	530	476	362	568
Afi-CycB	45	19	38	70	809	768	789	718	1058
Afi-CycE	21	12	41	86	335	434	467	532	741
Afi-Ctchrm-b	31537	28885	55967	58562	40690	41506	39582	45802	45202
Afi-Delta	229	172	251	258	202	166	181	426	313
Afi-Dlx	6	12	3	42	549	369	432	29	93
Afi-Dri	39	28	41	86	146	181	140	279	212
Afi-EgifL2	4	3	1	0	0	0	3	8	0
Afi-Egr	2778	1257	1696	1261	1373	889	659	1756	542
Afi-ElavL	981	674	1855	1329	974	897	691	4133	1151
Afi-Erg	335	503	1130	979	418	450	405	1541	675
Afi-Ese	1881	593	2007	942	277	199	377	803	302
Afi-Ets1	385	300	1139	1024	1081	938	817	704	977
Afi-Fgf6	165	69	124	102	5	13	9	123	7
Afi-Fgf8	33	149	345	322	432	510	636	281	622
Afi-Fgf9/16/20	70	114	254	125	90	80	101	161	165
Afi-Fgfr1	554	432	623	537	948	1065	985	1157	1303
Afi-Fgfr2	23	14	20	30	24	26	27	88	65
Afi-Fn3-Egff-1	131	400	466	356	364	345	295	708	387
Afi-Fos	377	69	114	88	17	26	15	20	19
Afi-FoxA	57	33	71	71	95	106	189	329	359
Afi-FoxB	62	21	45	40	58	101	231	343	504
Afi-FoxJ1	4	3	10	6	24	16	18	18	13
Afi-FoxN2	234	127	275	256	292	321	268	499	338
Afi-FoxQ2	1	0	0	3	5	1	1	2	4
Afi-GataC	462	437	1873	1743	2660	2383	2191	1898	1750
Afi-GataE	1	0	2	4	5	5	4	3	3
Afi-Gcm	4	5	3	4	2	3	6	21	2
Afi-HesC	25	23	45	69	228	204	206	196	272
Afi-Hex	83	173	350	344	143	143	111	309	202
Afi-Hox11/13b	6	3	11	12	5	3	6	17	2
Afi-Jun	4860	2276	3247	3119	2330	1521	1093	3129	1811
Afi-Khdrbh2	687	828	1945	1908	2672	2648	2660	1868	2411
Afi-KirrelL	226	90	150	130	202	250	253	789	419
Afi-Klf4	2123	357	489	343	534	573	483	584	723
Afi-L1	1812	1419	2352	2070	2284	2041	1935	3615	1510
Afi-Lmo	1	9	3	4	7	4	2	12	5
Afi-MhC	2364	3392	4255	3329	2736	2602	2522	3164	2794
Afi-Msp130L	2109	1246	3266	4072	1987	2101	1905	18400	3934
Afi-Msp130r6	11	9	23	32	22	13	6	58	18
Afi-Mt14	793	12257	3351	1799	1144	669	642	556	470
Afi-Musashi	1186	735	1718	2049	3868	4140	3601	4080	3869
Afi-Myc	191	258	857	855	1686	1683	1950	816	1608
Afi-MyoD2	16	9	26	51	51	92	120	145	115
Afi-Ncbp1	141	128	421	483	627	708	779	556	720
Afi-NeuroD	166	88	72	55	12	10	22	280	111
Afi-Ngn	1	0	1	4	36	11	16	149	108
Afi-Nk7	11	23	35	34	73	107	62	120	98
Afi-Nkx2	15	5	13	7	7	6	7	274	173
Afi-Nkx3	4	2	7	3	41	36	44	24	48
Afi-Notch	955	688	882	604	338	258	307	560	341
Afi-Oct1	16	5	18	12	2	9	11	21	22

Gene	NR	24hpa	48hpa	72hpa	St 3	St 4	St 5	50% prox	50% dist
Afi-Orexin1	92	33	48	50	12	2	3	59	8
Afi-Orexin2	1	0	0	2	0	0	1	1	1
Afi-Otx	0	5	2	7	0	3	6	25	11
Afi-P19	885	1094	1256	1007	797	1007	911	2357	1443
Afi-P58a	146	49	154	175	513	667	614	1273	690
Afi-P58b	57	49	87	128	396	428	425	816	519
Afi-Pax2	53	85	102	147	160	110	133	273	168
Afi-Pax6	15	14	12	6	19	15	23	104	19
Afi-Pcna	279	270	1112	1927	8447	9515	10849	5722	8973
Afi-Pea	317	210	331	279	471	496	518	844	665
Afi-Phb1	1	0	1	3	7	2	1	3	2
Afi-Piwi	208	151	562	503	1025	1024	977	843	877
Afi-Pplx	1	2	1	2	5	1	0	4	2
Afi-Prox	263	246	536	494	262	221	224	697	296
Afi-Rreb1	108	62	150	165	248	227	217	258	263
Afi-Runt1	913	4756	12043	9144	5821	4351	4584	1185	3165
Afi-Rx	1	2	4	2	2	1	3	10	5
Afi-Sclb	175	130	260	272	199	305	258	431	425
Afi-Serrate	63	43	75	105	160	179	115	111	93
Afi-Six1/2	75	57	140	105	17	30	73	929	548
Afi-Six3	83	52	106	109	224	194	214	1059	482
Afi-Slc4a10	145	38	142	176	260	358	372	1083	665
Afi-Smad	39	23	51	57	85	91	114	99	120
Afi-Snail	125	130	222	233	102	63	88	519	379
Afi-SoxB1	1465	1770	3755	4538	8032	6498	9308	7951	9771
Afi-SoxB2	486	594	854	1216	1543	1417	1826	1643	1368
Afi-SoxC	150	298	847	801	1113	1017	1021	3411	2758
Afi-SoxD1	304	300	594	650	350	400	285	963	403
Afi-Tbr	4	2	5	5	7	9	5	10	8
Afi-Tel	131	54	63	105	44	26	45	148	16
Afi-Trspn	25	26	28	60	415	373	325	333	343
Afi-Tfb1m	26	28	115	126	216	237	218	99	172
Afi-Tgif	323	534	1449	1312	1154	1018	1043	1037	1091
Afi-Tie1	196	523	946	913	187	86	91	210	45
Afi-Tk8	153	68	89	122	39	86	139	268	180
Afi-tr10933	294	217	430	495	275	343	458	4018	886
Afi-tr12446	1360	499	923	1474	581	765	869	21120	3407
Afi-tr1291	0	0	0	3	0	0	2	1	5
Afi-tr1339	31	9	41	44	87	78	70	76	68
Afi-tr14406	47	14	75	64	75	31	51	86	59
Afi-tr19326	58	29	63	81	49	75	64	231	115
Afi-tr23254	8	2	5	4	5	6	7	21	8
Afi-Tr25409	60	29	78	75	15	35	34	48	21
Afi-tr26306	3	2	3	2	10	4	6	9	5
Afi-tr34323	863	614	765	625	352	358	453	1391	488
Afi-tr35695	830	704	1440	1639	1295	1652	1864	9200	4149
Afi-tr45279	26	33	41	46	19	9	15	38	10
Afi-Tr4886	1	0	1	0	0	1	2	7	2
Afi-tr6206	104	161	406	287	41	40	38	62	23
Afi-tr62663	54	106	190	83	2	9	5	53	11
Afi-tr63013	3	0	0	0	5	0	3	3	2
Afi-tr65264	0	0	0	0	0	0	1	1	5
Afi-tr68751	252	224	410	320	102	104	93	530	139
Afi-Trh	1451	371	936	729	7	4	9	380	11
Afi-Trim2	400	113	245	235	143	137	141	815	306
Afi-Trop1	2024	3484	5300	4425	2643	2442	2210	4599	2597
Afi-Twist	164	113	141	191	126	119	191	783	495
Afi-Ubc	1779	2931	4688	4445	4288	4365	4208	4614	4133
Afi-Ubq	6790	3834	7935	7249	5756	5007	5007	7660	5267
Afi-Vasa	609	1529	2065	1872	2884	3249	3076	1360	2163
Afi-Vegf2	40	29	37	33	5	11	18	65	21
Afi-Vegf3	428	340	480	482	481	470	548	896	681
Afi-Vegfr	151	102	226	196	245	300	219	416	302

Key:

>5001 detected, normalized Nanostring counts/100ng of total RNA
<5000 detected, normalized Nanostring counts/100ng of total RNA
<1001 detected, normalized Nanostring counts/100ng of total RNA
<501 detected, normalized Nanostring counts/100ng of total RNA
<11 detected, normalized Nanostring counts/100ng of total RNA
0 detected, normalized Nanostring counts/100ng of total RNA

Table A.0.4: Embryonic gene expression time-courses heatmap. *hpf – hours post fertilization.* See bottom for key.

Gene	3hpf	6hpf	9hpf	12hpf	15hpf	18hpf	21hpf	24hpf	27hpf	30hpf	33hpf	36hpf
Afi-AcSc	56	33	21	20	27	138	146	104	131	112	80	71
Afi-AlphaCol	82	104	94	147	72	48	1959	407	1210	1599	1925	2958
Afi-Alx/Arx	4	4	5	10	5	3	16	6	2	4	5	5
Afi-Alx1	3	5	54	806	1110	1487	1658	1783	1596	605	380	240
Afi-Brn1/2/4	11	14	7	12	3	12	35	71	227	195	205	197
Afi-C-lectin	2	2	17	169	526	1298	4063	3830	6919	6791	7530	8545
Afi-CaraX	8	7	9	36	72	127	508	351	646	655	859	929
Afi-CycA	12068	12050	12330	16571	9385	3838	1597	1184	1099	691	717	577
Afi-CycB	9058	9102	9007	12656	9632	8519	5412	3689	3462	2016	1724	1452
Afi-CycE	9140	9482	9467	12017	4708	2548	1604	1398	1479	1113	988	818
Afi-Cytochromeb	45874	44727	46531	66298	50303	57814	52287	46661	57767	40373	42955	33831
Afi-Delta	108	117	153	525	508	348	264	239	303	246	268	229
Afi-Dlx	291	266	259	712	1256	2219	2148	1846	1857	1026	727	513
Afi-Dri	77	60	42	81	313	1083	1410	1504	1632	1067	1081	930
Afi-EgifL2	1	4	3	0	0	0	0	0	1	3	0	0
Afi-Egr	90	75	67	49	43	101	609	301	211	109	102	82
Afi-ElavL	163	138	98	68	98	154	303	386	619	483	531	559
Afi-Erg	31	42	36	49	170	560	868	821	919	536	483	482
Afi-Ese	82	68	84	268	359	420	395	388	535	438	507	531
Afi-Ets1	2771	2593	2082	2379	1293	1506	1554	1482	2051	1316	1231	1130
Afi-Fgf6	0	0	3	2	2	1	1	1	2	0	1	1
Afi-Fgf8	4	2	4	27	153	375	363	269	291	165	170	125
Afi-Fgf9/16/20	9	12	5	32	14	16	44	55	111	100	91	91
Afi-Fgfr1	90	93	33	30	69	236	541	651	880	681	712	625
Afi-Fgfr2	0	2	1	0	2	10	35	46	59	51	66	86
Afi-Fn3-Egff-1	4	4	5	14	16	53	221	611	1138	680	491	261
Afi-Fos	3	5	4	7	4	10	60	81	137	103	102	26
Afi-FoxA	8	12	12	20	86	545	1325	1549	2472	2184	2380	2521
Afi-FoxB	2	6	4	10	13	23	63	44	106	83	117	117
Afi-FoxJ1	232	214	226	107	94	212	308	207	236	141	146	168
Afi-FoxN2/3	18	13	4	15	60	139	147	105	122	133	158	164
Afi-FoxQ2	60	47	57	191	213	228	162	118	163	111	137	114
Afi-GataC	0	0	7	14	26	37	173	491	1057	769	538	369
Afi-GataE	5	5	1	8	4	5	66	43	83	103	125	198
Afi-Gcm	3	1	4	3	5	6	14	6	10	3	6	3
Afi-HesC	60	39	24	203	157	196	167	114	109	129	203	214
Afi-Hex	3	2	2	59	134	324	590	717	934	689	587	509
Afi-Hox11/13	0	2	2	15	54	232	446	582	798	594	452	350
Afi-Jun	982	931	623	607	775	1129	2184	1494	1671	1323	1192	952
Afi-Khdrbh2	3280	3361	3254	4208	3094	2602	2138	2048	2499	1795	1665	1524
Afi-KirrelL	0	1	1	5	3	0	30	5	39	127	184	238
Afi-Klf4	473	500	291	525	955	808	943	702	734	440	294	260
Afi-L1	962	981	1049	1288	912	705	405	263	386	305	338	331
Afi-Lmo	5	1	3	8	2	5	8	3	4	1	4	4
Afi-MhC	291	292	247	271	200	252	572	461	671	542	575	633
Afi-Msp130L	2	2	7	5	2	7	777	133	554	1025	1408	2124
Afi-Msp130r6	6	4	4	0	7	6	168	59	203	281	364	499
Afi-Mt14	6	5	2	14	6	11	131	34	113	153	224	243
Afi-Musashi	1861	1806	1736	2411	1973	2036	2663	2264	2739	2047	1969	1940
Afi-Myc	371	397	341	280	168	255	511	507	599	464	471	383
Afi-MyoD2	2	3	4	5	7	2	11	2	6	3	3	7
Afi-Ncbp1	774	781	771	847	661	670	708	607	704	534	470	426
Afi-NeuroD	2	2	2	5	0	2	2	0	5	7	11	18
Afi-Neurogenin	2	2	4	12	14	54	91	79	112	82	72	56
Afi-Nk7	9	3	2	2	17	73	309	431	327	141	93	52
Afi-Nkx2	2148	2034	1971	3143	3179	3878	3117	2236	2729	1594	1881	1431

Gene	3hpf	6hpf	9hpf	12hpf	15hpf	18hpf	21hpf	24hpf	27hpf	30hpf	33hpf	36hpf
Afi-Nkx3	5	3	7	30	15	16	67	25	61	56	58	66
Afi-Notch	1102	1147	980	590	124	93	149	198	215	163	167	147
Afi-Oct1	1081	1039	977	1249	807	587	513	572	684	492	448	355
Afi-Orexin1	2	2	4	5	3	2	1	2	4	2	2	0
Afi-Orexin2	2	0	1	0	0	1	1	0	0	3	0	0
Afi-Otx	263	268	249	347	296	430	465	447	618	403	378	379
Afi-P19	2	4	5	51	106	237	397	488	629	481	455	433
Afi-P58a	2	2	3	12	18	69	267	445	993	918	951	1051
Afi-P58b	0	0	0	3	12	36	183	336	630	666	651	727
Afi-Pax2	31	15	20	53	114	173	179	167	227	190	188	184
Afi-Pax6	10	9	5	10	5	15	20	26	25	27	24	21
Afi-Pcna	1882	1168	588	446	334	407	543	404	559	498	501	465
Afi-Pea	238	219	201	276	190	279	493	482	667	591	665	657
Afi-Phb1	2	5	24	56	73	118	66	47	30	13	14	8
Afi-Piwi	723	676	615	830	722	929	924	922	1337	985	940	915
Afi-Pplx	10	106	601	1130	663	358	109	46	44	19	18	16
Afi-Prox	70	59	52	44	34	29	16	10	30	84	102	131
Afi-Rreb1	18	21	18	152	321	485	384	244	317	222	196	168
Afi-Runt1	1085	962	764	837	1065	1322	1794	1493	2074	1464	1341	988
Afi-Rx	0	3	4	36	90	169	171	177	188	122	136	98
Afi-Sclb	5	2	4	15	48	247	518	632	825	593	540	345
Afi-Serrate	135	124	132	93	46	96	136	124	159	115	130	138
Afi-Six1	4	6	4	7	2	1	1	1	0	2	1	1
Afi-Six3	15	7	8	93	141	375	677	787	1005	787	737	804
Afi-Slc4a10	6	2	3	14	13	39	193	224	595	681	850	1136
Afi-Smad	43	30	23	30	15	24	32	27	43	28	44	47
Afi-Snail	5	7	22	149	166	57	38	62	169	199	167	117
Afi-SoxB1	12366	12330	12223	18989	14496	10543	6931	5264	6935	5921	6498	6854
Afi-SoxB2	217	207	201	925	1907	1986	1328	967	1317	872	665	534
Afi-SoxC	203	172	193	771	1114	1196	1344	1326	1634	1326	1299	1255
Afi-SoxD1	630	707	628	652	280	67	98	145	303	264	201	199
Afi-Tbr	49	48	31	259	686	1276	1787	2053	2501	1669	1290	860
Afi-Tel	202	168	183	229	162	69	30	48	98	84	59	27
Afi-Tetraspanin	0	2	2	2	72	265	559	778	966	591	490	458
Afi-Tfb1m	79	70	54	91	58	58	58	59	70	60	42	33
Afi-Tgif	468	395	458	1061	1357	1360	1572	1714	1929	1563	1384	1365
Afi-Tie1	39	26	27	20	15	20	63	162	318	269	228	219
Afi-Tk8	5	12	3	14	5	2	5	5	13	8	8	6
Afi-tr10933	1	0	1	5	10	9	101	13	32	111	215	396
Afi-tr12446	2	1	1	2	3	2	150	2	4	14	36	75
Afi-tr1291	2	2	3	2	5	16	166	35	111	240	463	815
Afi-tr1339	48	32	33	41	21	28	25	20	45	36	33	26
Afi-tr14406	29	18	9	7	20	33	32	28	48	32	36	41
Afi-tr19326	1	0	0	7	0	5	10	4	23	65	81	95
Afi-tr23254	46	36	41	130	197	277	152	75	77	67	62	63
Afi-Tr25409	0	0	1	0	2	3	185	117	383	491	545	566
Afi-tr26306	3	2	4	7	1	2	4	1	5	2	1	2
Afi-tr34323	0	1	0	3	1	1	47	6	58	149	248	314
Afi-tr35695	1	1	0	3	1	0	191	35	210	397	516	651
Afi-tr45279	3	1	3	5	2	2	13	8	17	30	24	14
Afi-Tr4886	1	2	1	0	3	0	0	0	3	1	0	3
Afi-tr6206	0	0	1	3	2	0	5	2	4	9	12	22
Afi-tr62663	2	1	0	5	2	1	11	2	16	19	22	72
Afi-tr63013	64	66	52	54	37	22	23	9	12	20	16	22
Afi-tr65264	1	0	1	3	3	3	2	1	0	0	1	3
Afi-tr68751	0	1	1	0	1	0	18	2	5	14	23	25
Afi-Trh	2	0	1	3	1	1	4	1	3	0	1	2
Afi-Trim2	20	21	23	12	21	17	12	15	9	17	20	21
Afi-Trop	1450	1382	1363	1842	1305	1553	1654	1604	2102	1509	1408	1290
Afi-Twist	10	2	11	20	20	16	12	7	17	13	12	21

Gene	3hpf	6hpf	9hpf	12hpf	15hpf	18hpf	21hpf	24hpf	27hpf	30hpf	33hpf	36hpf
Afi-Ubc	2068	1988	1569	1255	727	780	951	831	1016	774	718	628
Afi-Ubq	5067	4916	4620	5809	5302	6513	7884	7568	8329	5057	3741	3096
Afi-Vasa	11669	11413	11402	15333	11579	11082	8156	6400	5315	2865	2294	1873
Afi-Vegf2	2	2	1	2	4	1	1	4	7	7	10	16
Afi-Vegf3	47	37	31	47	30	104	296	432	767	570	539	421
Afi-Vegfr	9	6	7	3	46	246	338	358	444	285	299	274

Key:

>5001 detected, normalized Nanostring counts/100ng of total RNA

<5000 detected, normalized Nanostring counts/100ng of total RNA

<2001 detected, normalized Nanostring counts/100ng of total RNA

<1001 detected, normalized Nanostring counts/100ng of total RNA

<101 detected, normalized Nanostring counts/100ng of total RNA

<10 detected, normalized Nanostring counts/100ng of total RNA

Table A.0.5: Summary of Nanostring experiments in embryos and regenerating adult arms of *A. filiformis* treated with SU5402 and Axitinib inhibitors. Values shown are Log2(Inhibitor/DMSO). Threshold of significance is ±1. Positive values indicate upregulation, negative values indicate downregulation. *TB – transcriptome batch, NB – Nanostring batch*. *N/D – not detected*, *Yellow highlight – internal standards, grey highlight – low level genes. Red – significantly upregulated, Blue – significantly downregulated.*

	Embryo SU5402			Adult SU5402			Embryo Axitinib	Adult Axitinib
Gene	**TB**	**NB1**	**NB2**	**NB1**	**NB2**	**NB3**	**NB1**	**NB1**
Afi-AcSc	0.33	0.60	0.80	1.52	2.81	1.35	-0.20	0.35
Afi-Col2a1	-0.31	-0.53	-0.56	-0.38	-0.67	0.03	-0.28	0.26
Afi-Alx/Arx	7.71	3.13	4.06	2.70	-0.40	3.66	-0.32	N/D
Afi-Alx1	0.01	0.09	-0.20	-0.33	-0.40	0.17	-0.38	-0.80
Afi-Brn1/2/4	-0.37	-0.39	-0.25	0.73	1.77	-1.29	-0.13	-1.41
Afi-C-lectin	-0.33	-0.68	-0.56	-0.20	-0.21	-0.14	-0.24	-0.33
Afi-CycA	-0.72	-0.37	-0.33	-0.66	-0.39	-0.49	0.26	0.23
Afi-CycB	-0.03	-0.04	-0.11	-0.23	0.30	0.15	0.39	0.64
Afi-CycE	-0.91	-0.44	-0.50	-0.81	0.03	-0.25	0.03	0.02
Afi-Cytochromeb	0.48	-0.16	0.24	0.45	-0.25	0.56	0.08	0.04
Afi-Delta	-0.33	0.00	0.11	0.21	-0.13	0.71	-0.01	0.07
Afi-Dlx	0.48	0.60	0.80	-1.12	-0.59	-0.88	0.30	-0.16
Afi-Dri	-0.16	0.29	-0.12	-0.93	-0.67	-0.51	0.02	-0.61
Afi-EgifL2	5.57	N/D	N/D	N/D	N/D	N/D	N/D	N/D
Afi-Egr	-2.26	-1.71	-0.90	-2.21	-1.57	-1.49	0.50	-2.86
Afi-ElavL	-0.47	-0.55	-0.28	-0.21	-0.07	0.08	-0.41	-0.06
Afi-Erg	-0.41	0.00	-0.04	-0.78	-0.48	0.24	-0.09	-0.13
Afi-Ese	-0.35	-0.18	0.05	0.26	0.05	0.95	0.42	0.31
Afi-Ets1/2	-0.4	-0.29	0.11	-0.48	0.24	-0.20	0.13	-0.24
Afi-Fgf6		N/D	N/D	-0.03	1.92	0.21	0.49	0.94
Afi-Fgf8	-0.37	0.03	-0.49	-0.31	-0.53	0.62	0.30	0.04
Afi-Fgf9/16/20	-0.27	-0.14	0.49	-1.13	-1.19	-1.15	-0.27	-1.93
Afi-Fgfr1	-0.48	-0.08	0.13	-0.14	0.27	0.17	0.10	0.09
Afi-Fgfr2	-0.34	-0.33	-0.95	-1.03	0.37	-0.21	-0.17	-1.43
Afi-Fn3-Egff-1	-1.47	-1.23	-1.46	-1.69	-0.85	-0.97	-0.68	-0.80
Afi-Fos	-1.36	-1.19	-0.95	3.13	0.05	2.27	0.02	-0.58
Afi-FoxA	0.21	0.17	0.01	0.02	0.69	1.20	0.00	1.74
Afi-FoxB	-0.19	-0.15	0.18	-2.65	0.60	-2.06	0.12	-0.90
Afi-FoxJ1	-0.17	0.06	0.02	0.56	-1.01	0.49	-0.11	0.26
Afi-FoxN2/3	0.06	0.39	-0.02	-0.68	-0.31	-0.35	0.17	-0.39
Afi-FoxQ2	-0.8	-0.81	-1.06	N/D	-1.40	N/D	-0.06	1.35
Afi-GataC	-0.36	-0.48	-0.82	-0.83	-0.53	-0.78	-0.26	-0.38
Afi-GataE	-0.78	-1.04	-0.66	N/D	0.60	-0.01	0.03	N/D
Afi-Gcm	0.5	1.25	-1.14	1.29	-2.40	-0.01	0.75	0.35
Afi-HesC	0.13	0.15	0.50	-0.13	-0.06	-0.02	-0.14	-0.43

	Embryo SU5402			Adult SU5402			Embryo Axitinib	Adult Axitinib
Gene	**TB**	**NB1**	**NB2**	**NB1**	**NB2**	**NB3**	**NB1**	**NB1**
Afi-Hex	-0.41	-0.30	-0.95	-1.30	-0.81	-0.60	0.08	0.23
Afi-Hox11/13b	0.02	-0.27	0.07	-0.18	N/D	-0.01	-0.02	0.09
Afi-Jun	0.07	0.07	0.51	0.53	-0.93	0.54	0.01	-0.24
Afi-Khdrbh2	0.57	0.29	0.10	0.42	0.63	0.45	0.05	0.04
Afi-KirrelL	-4.56	-5.13	-4.41	-2.29	-0.65	-1.80	-2.47	-0.99
Afi-Klf4	0.28	0.41	0.12	-0.83	-0.40	-0.89	0.33	-0.98
Afi-L1	-0.06	0.53	0.17	-0.38	0.12	0.14	0.22	0.12
Afi-Lmo		1.67	1.86	0.56	1.41	0.16	0.07	-0.65
Afi-MhC	-0.33	-0.30	-0.35	-0.90	-0.59	-0.33	0.03	-0.26
Afi-Msp130L	-2.49	-3.09	-2.59	-1.10	-1.13	-0.33	-0.96	-0.46
Afi-Msp130r6	-1.84	-1.97	-1.70	0.33	-0.84	0.31	-0.87	-0.23
Afi-Mt14/mmp7	-3.02	-1.46	-2.74	-2.89	-2.90	-1.76	-0.18	-0.77
Afi-Musashi	0.29	0.12	-0.07	-0.59	-0.52	-0.06	0.05	-0.16
Afi-Myc	0.04	0.15	-0.05	-0.72	-0.79	-0.46	0.06	-0.84
Afi-MyoD2		-2.33	0.44	-1.19	-1.19	-0.55	-0.10	-1.81
Afi-Ncbp1	0.32	-0.14	-0.08	-0.31	0.15	-0.51	0.04	-0.01
Afi-NeuroD	-1.33	-2.14	-0.88	-0.32	0.34	-0.51	0.07	-0.49
Afi-Neurogenin	-0.63	-0.36	-0.36	N/D	-0.66	-1.01	0.34	-0.39
Afi-Nk7	-0.03	-0.21	-0.53	-0.33	0.14	-0.46	-0.17	-1.20
Afi-Nkx2.1	-0.17	0.09	-0.17	-0.76	N/D	-0.75	0.14	-0.97
Afi-Nkx3.2	-0.7	-0.21	-0.05	-1.76	1.69	-0.54	-0.29	1.17
Afi-Notch	-0.18	0.49	0.09	0.05	0.22	0.74	0.83	0.37
Afi-Oct1/2	-0.4	0.24	0.14	-0.12	0.60	-0.30	0.13	-1.11
Afi-Orexin1		-1.92	0.86	-0.44	-1.40	0.58	-1.10	0.94
Afi-Orexin2		0.25	-0.14	-0.44	N/D	-1.01	N/D	0.35
Afi-Otx	0.05	0.03	0.01	N/D	N/D	0.99	0.10	0.35
Afi-P19	-0.59	-0.67	-0.68	0.07	-0.70	-0.07	-0.29	-0.65
Afi-P58a	-1.18	-1.07	-0.92	-0.86	0.20	-0.58	-0.61	-1.12
Afi-P58b	-1.24	-1.22	-1.12	-0.86	0.39	-0.41	-0.70	-0.88
Afi-Pax2/5/8	-0.04	-0.15	-0.26	-0.16	-1.23	-0.82	-0.27	-0.39
Afi-Pax6	-0.34	0.11	0.21	-0.14	0.51	0.77	1.32	-0.87
Afi-Pcna	-1.19	-0.59	-1.09	-0.93	-0.17	-0.98	-0.25	0.08
Afi-Pea	-0.65	-0.33	-0.62	-0.75	-1.11	-1.09	-0.09	-1.15
Afi-Phb1	-0.17	-0.07	0.24	0.56	N/D	N/D	-1.10	0.67
Afi-Piwi	-0.11	-0.09	-0.08	-0.03	0.36	0.14	0.10	0.17
Afi-Pplx		1.10	0.37	0.56	N/D	N/D	0.26	N/D
Afi-Prox	-0.97	-0.76	-0.38	0.17	-0.04	0.03	-0.29	-0.59
Afi-Rreb1	-1.78	-0.79	0.02	-0.56	0.10	0.28	-0.50	-0.13
Afi-Runt1	0.08	0.16	-0.09	-1.64	-0.99	-0.86	0.06	-0.61
Afi-Rx	-0.27	0.20	0.10	N/D	-0.40	N/D	0.26	N/D
Afi-Scl	-0.99	-0.68	-0.60	-0.96	-0.48	-0.40	-0.35	-0.60
Afi-Serrate	0.23	0.27	0.90	2.21	0.34	1.05	0.37	0.06
Afi-Six1/2		-2.33	N/D	0.66	4.62	2.65	N/D	3.39
Afi-Six3	-0.05	0.31	0.04	-0.98	-0.72	-1.53	0.05	-0.11

	Embryo SU5402			Adult SU5402			Embryo Axitinib	Adult Axitinib
Gene	**TB**	**NB1**	**NB2**	**NB1**	**NB2**	**NB3**	**NB1**	**NB1**
Afi-Slc4a10	-1.15	-1.38	-1.29	-1.19	-0.55	-1.34	-0.52	-1.09
Afi-Slc4a1ap	-1.73	-2.08	-2.54	-0.66	-0.48	-1.53	-0.31	0.03
Afi-Snail	-1.25	-0.91	-0.97	-0.05	0.72	-0.02	-0.80	-0.08
Afi-SoxB1	0.2	0.02	-0.28	-0.40	-0.18	0.08	0.02	0.19
Afi-SoxB2	0.09	-0.05	-0.34	-0.33	-0.42	-0.51	-0.01	-0.59
Afi-SoxC	-0.15	0.11	0.23	0.15	0.75	0.34	0.04	0.24
Afi-SoxD1	-1.51	-1.00	-0.94	-0.83	-0.05	-0.32	-0.48	-0.63
Afi-Tbr	-0.13	-0.08	-0.34	2.14	N/D	-0.01	-0.03	-1.23
Afi-Tel	-0.12	0.00	-0.33	-0.09	0.33	1.72	-0.05	0.89
Afi-Tetraspanin	-1.12	-1.15	-1.01	-0.72	-0.42	-0.37	-0.59	-0.86
Afi-Tfb1m	0.53	0.16	-0.02	-1.40	-0.52	-0.56	-0.34	-0.14
Afi-Tgif	-0.07	0.12	0.00	-0.45	-0.60	-0.42	0.12	-0.40
Afi-Tie1/2	-0.33	-0.47	-0.76	-1.54	-0.90	-0.29	-0.05	0.21
Afi-Tk8/Cad96a	4.02	3.19	3.27	1.92	1.37	1.29	0.81	0.67
Afi-tr10933	-2.17	-2.55	-2.77	-1.21	-0.13	-0.25	-0.10	-0.51
Afi-tr12446	-2.5	-2.33	-0.26	-0.91	0.20	-0.20	0.81	0.22
Afi-tr1291	-3.50	-3.00	-3.71	0.56	N/D	1.58	0.43	N/D
Afi-tr1339	-3.67	-0.97	-0.46	-2.03	-0.43	-1.26	-0.07	0.51
Afi-tr14406	-2.62	-1.52	-0.02	-0.88	0.34	-0.33	-0.38	-0.18
Afi-tr19326	-2.76	-2.04	-2.14	-0.61	-0.36	0.50	-1.00	-0.34
Afi-tr23254	-2.01	-1.31	-0.17	1.73	0.19	0.35	0.20	-0.13
Afi-tr31926	-3.29	-2.93	-2.41	N/D	0.45	-0.59	-1.43	0.64
Afi-tr26306	-2.39	-1.92	0.27	N/D	0.92	0.58	-1.51	2.16
Afi-tr34323	-3.29	-3.08	-2.71	-0.76	0.15	0.05	-3.18	-0.42
Afi-tr35695	-1.98	-2.02	-1.37	-1.62	-0.53	-1.28	-1.20	-0.75
Afi-tr45279	-2.10	-0.48	-1.60	-3.14	-1.05	-1.40	-0.17	0.05
Afi-tr9107	-3.41	-0.33	N/D	0.56	N/D	-1.01	N/D	N/D
Afi-tr6206	-2.39	-2.33	N/D	-2.33	0.02	-1.99	N/D	0.02
Afi-tr62663	-2.58	-1.07	-3.95	-3.23	-1.21	0.25	N/D	-1.97
Afi-tr63013	-2.58	-1.17	0.86	N/D	N/D	N/D	-0.51	N/D
Afi-tr65264	-2.5	0.67	-0.73	0.56	N/D	2.80	N/D	1.35
Afi-tr68751	-2.00	-2.33	-0.56	-0.38	-0.49	0.26	-0.51	-0.67
Afi-Trh		N/D	-0.14	-0.44	-0.72	3.45	1.49	0.77
Afi-Trim2	2.58	3.53	2.23	-0.52	1.01	0.29	-0.51	0.04
Afi-Trop1	0.03	0.09	-0.22	-0.29	-0.19	0.25	0.20	-0.03
Afi-Twist	0.5	0.15	-0.43	-0.68	0.01	0.57	-0.21	0.46
Afi-Ubc	-0.29	-0.04	-0.17	-0.11	-0.14	0.08	0.12	0.01
Afi-Ubq	-0.38	-0.09	-0.05	-0.50	-0.36	-0.60	0.02	-0.08
Afi-Vasa	0.5	1.02	0.67	-0.24	-0.18	-0.04	0.17	-0.17
Afi-Vegf2	5.38	2.40	2.42	1.18	2.30	3.41	0.22	-0.23
Afi-Vegf3	-0.33	0.40	0.36	0.20	0.15	1.35	0.08	0.00
Afi-Vegfr	-1	-0.65	0.14	-1.45	-0.50	-0.94	-0.21	-1.02

Table A.0.6: List of experiments performed in *A. filiformis* but not discussed in the thesis.

Experiment type	Result	Problems to troubleshoot
Microinjection of vital dye into arm	Successful injection of DiI label into arm without causing autotomy or regeneration defects	Difficulty in piercing through thick cuticle makes it troublesome to inject the inner layers (radial water canal, nerve cord)
Arm electroporation	Could electroporate arms without causing autotomy, sometimes regenerative defects were observed.	Without successfully electroporation of fluorescent constructs it is difficult to assess if method works.
Electroporation of morpholinos/ vivo MOs	Only once was fluorescent signal observed when control lissamine-tagged morpholino was electroporated. Very localized signal. Sometimes autotomy and regenerative defects were observed	Only one time did an arm show the signal, thus the general conditions for electroporations are still not known.
Electroporation of DNA constructs	Never was any fluorescent signal detected, however lower toxicity then morpholino injections.	No signal means general conditions for electroporations are still not known.
Small molecule inhibitors in explants	Successfully tested small molecule inhibitors of other signalling pathways not mentioned in thesis (DAPT for Delta/Notch, UO126 for MAPK, C59 for Wnt etc).	Many of the inhibitors had small or not noticeable effects on regeneration in early stages. Incubation at different time-points would elucidate effects at different stages of regeneration.
Apoptotic cell detection assay (TUNEL assay)	Successfully visualized nuclei with fluorescent label.	Difficult to assess if only apoptotic nuclei were specifically labelled. More experiments would be required to confirm (for example antibodies)
Senescent cell detection assay (SA-B-gal assay)	Did not show any specifically labelled blue cells.	Technique might require to be optimized (for example by use on sections) or tested with UV-damaged samples to exclude if no senescent cells are present.

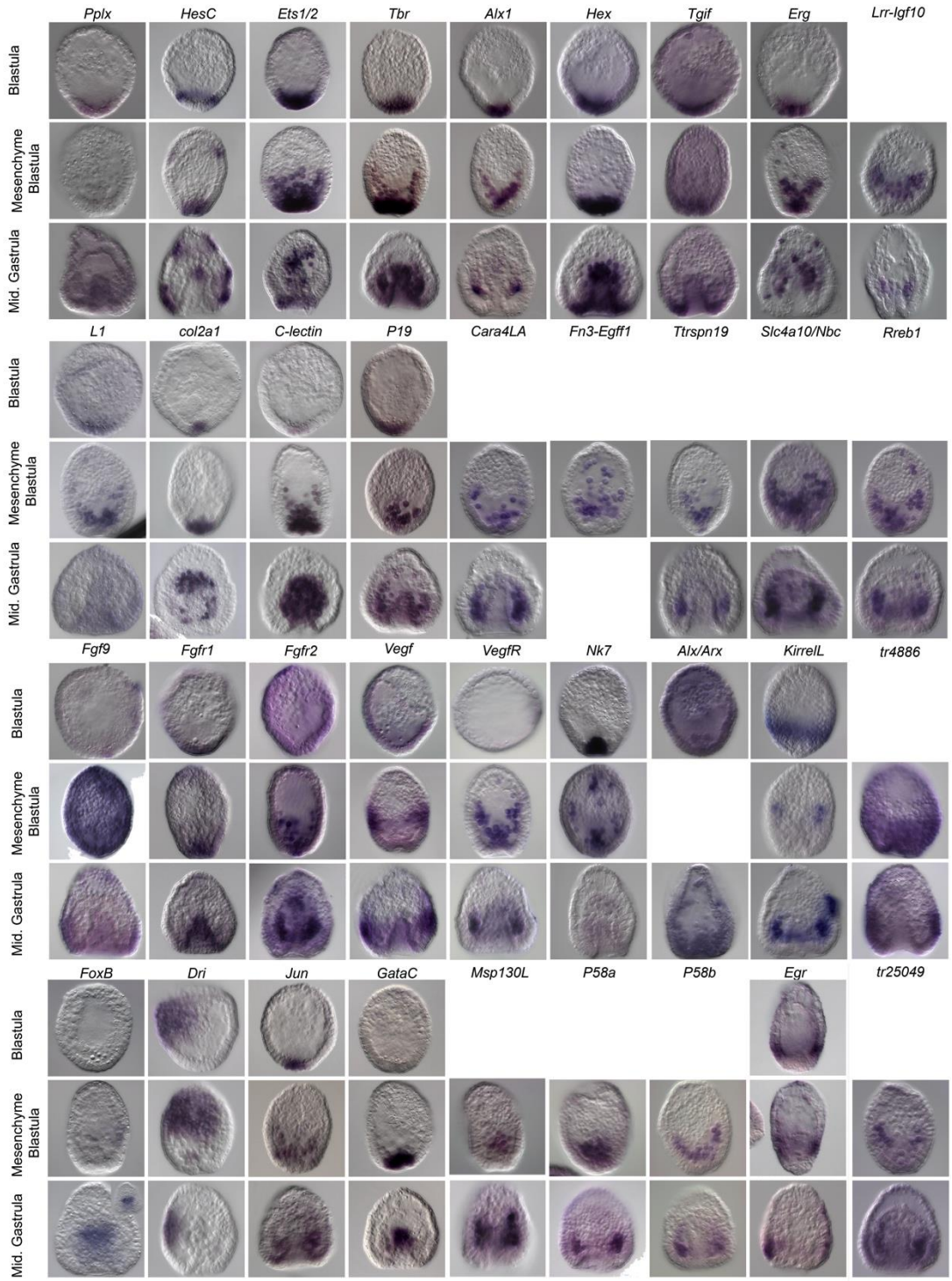

Figure A.0.1: Summary of embryonic WMISH experiments in *A. filiformis* (courtesy of David Dylus).

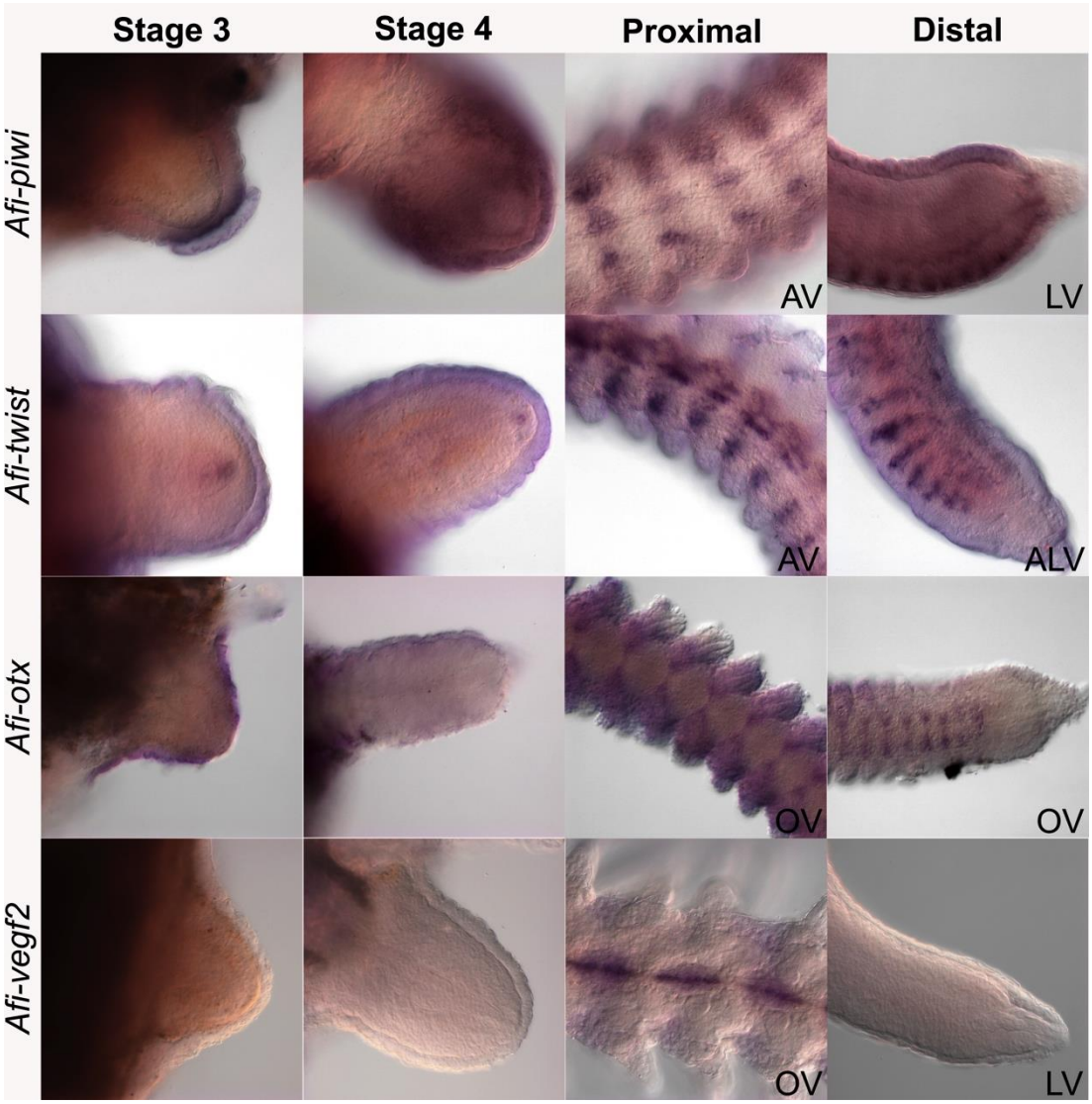

Figure A.0.2: WMISH on additional genes not discussed in thesis – *Afi-piwi, Afi-twist, Afi-otx* and *Afi-vegf2*. *Afi-piwi* can first be detected by ISH around stage 4 in the epidermis, aboral coelomic epithelium and radial nerve. In proximal segments of 50% DI regenerates expression can be detected primarily in the aboral coelomic epithelium, and in two adjacent bilateral patches. In the distal end the expression resembles early stages, namely *Afi-piwi* is expressed in the epidermis, radial nerve and aboral coelomic epithelium. *Afi-twist* is only detected as a small patch of expression at the tip of the aboral coelomic epithelium and radial water canal. In proximal segments of late stages it is expressed in the developing vertebrae and at the base of the lateral shields and spines. In the distal region *Afi-twist* is found around the aboral coelomic epithelium and in stripes corresponding to the newly forming lateral shields. *Afi-otx* is only faintly expressed in the epidermis at early stages and then shows a consistent patterned expression of stripes at the oral side of the late regenerate. *Afi-vegf2* is not detected in early stages or the distal part of late regenerates, but is expressed in the radial water canal of proximal segments of 50% DI arms.

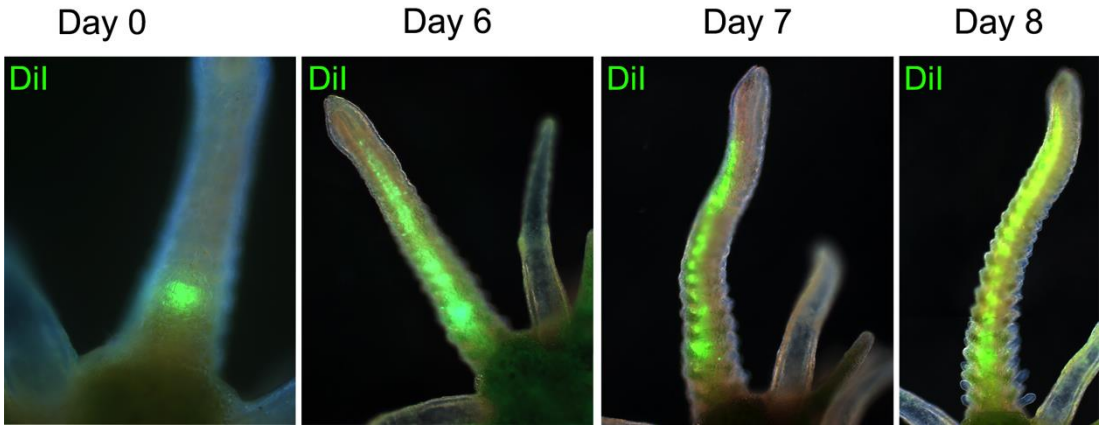

Figure A.0.3: Preliminary data showing DiI labelling of cells in the radial water canal observed for eight days. Aboral view of cells in the radial water canal labelled by microinjection of the vital dye DiI at a late stage of regeneration (Day 0). The labelled cells were then observed at days 6, 7, and 8 after injection. Labelled cells were confined strictly to the radial water canal and did not spread into other tissues, not even the podia. This result suggests the contribution of cells from the radial water canal to other structures (like the skeleton, nerve or the distal tip) is minimal to none.